Genetic mapping of novel mutation, *UV90*, and its effects on the *Neurospora crassa* circadian system

Elizabeth Kafes

A Thesis Submitted to the Faculty of Graduate Studies in Partial Fulfillment of the Requirements for the Degree of

Master of Science

Graduate Program in Biology

York University, Toronto, Ontario, Canada

August, 2013

ABSTRACT

Neurospora crassa is a model organism for circadian rhythm research. The FRQ-WCC feedback loop is the main mechanism driving rhythms in *Neurospora*. Recent evidence revealed a second oscillator in the absence of the FRQ-WCC loop, the FRQ-less oscillator (FLO). The purpose of this study was to identify the components and mechanism of the FLO. One mutation, *UV90*, disrupts the rhythmic conidiation of the FLO, and locating this gene will lead to better understanding of the FLO mechanism.

Mapping of the *UV90* gene location was performed using Cleaved Amplified Polymorphic Sequence (CAPS) markers and gene knockout screens. DNA sequencing and complementation tests were performed to characterize the nature of the mutation and confirm the restoration of the *UV90* phenotype.

Sequencing and complementation tests failed to reveal the exact nature of the mutation; however mapping and gene knockout studies confirmed the *UV90* gene is represented by locus NCU05950 on Linkage Group VI.

ACKNOWLEDGEMENTS

TABLE OF CONTENTS

LIST OF TABLES

LIST OF FIGURES

LIST OF ABBREVIATIONS

ACTH: adrenocorticotropic hormone

AMPK: AMP kinase

ATX2: ataxin-2

bd: band mutation

BMAL1: brain and muscle ARNT-like 1

CAMK1: Calcium/calmodulin dependent kinase

CAPS: cleaved amplified polymorphic sequence

CCA1: circadian clock associated 1

ccg: clock controlled gene

chol-1: choline mutation

CK: casein kinase

CLK: clock

CRH: corticotropin releasing hormone

CRY: cryptochrome

csp-1: conidial separation mutation

cwo: clockwork orange

CYC: cycle

DBT: doubletime

DD: constant darkness

FLO: FRQ-less oscillator

FRH: FRQ interacting RNA helicase

FRQ: frequency

*frq*¹⁰: frequency null mutation

GFP: green fluorescent protein

GI: gigantea

his-3: histidine mutation

hyg: Hygromycin B resistance gene

LHY: late elongated hypocotyl

LL: constant light

LRE: light response element

MA: maltose-arginine

MV: Mauriceville

OR: Oak Ridge

PER: period

PP: protein phosphatase

prd: period mutation

PRR: pseudo response regulator

SCN: suprachiasmatic nucleus

sg #: silica gel number

SNPs: single nucleotide polymorphisms

TAP: tandem affinity purification

TIM: timeless

TOC1: timing of cab expression 1

TTFL: transcription-translation feedback loop

TYF: twenty-four

UV90: *UV90* mutant

vri: vrille

WC: white collar

WCC: white collar complex

ZTL: zeitlupe

CHAPTER 1

INTRODUCTION

1.1 Circadian rhythms

Circadian rhythms control many physiological processes and are found in nearly all organisms including mammals, fungi, bacteria, and plants (Liu and Bell-Pedersen, 2006; Harmer, 2009; Brunner and Schafmeier, 2006). Circadian clocks affect physiological processes such as the sleep-wake cycle in humans, plant flowering, and even behavioural activities such as hibernation in mammals and migration patterns in butterflies and birds (Harmer, 2009). In order for a rhythm to be classified as circadian, it needs to exhibit 3 criteria: it has a period length of approximately 24 hours under constant conditions (free-running period), it is entrained by environmental factors (i.e. light and temperature), and it can compensate for fluctuations in temperature with little effect on the period length (Liu and Bell-Pedersen, 2006; Harmer, 2009; Brunner and Schafmeier, 2006; Johnson et al., 2008; O'Neill and Reddy, 2011; Lakin-Thomas, 2006a). Daily rhythms in organisms are generally thought to arise from internal biological (genetic) clocks that are entrained by environmental factors such as light and temperature (Ellman et al., 1984; Harmer, 2009; Nagel and Kay, 2012). It is believed circadian rhythms can allow an organism to anticipate environmental changes and adjust physiological processes accordingly (Harmer, 2009; Mohawk et al., 2012). Free-running rhythms are seen in the absence of cycles of light and temperature, yet often do not fall into 24-hour periods (Ellman et al., 1984; Harmer, 2009). It is thought that external,

1

environmental factors adjust these internal cellular and genetic rhythms to a 24-hour cycle (Ellman et al., 1984; Harmer, 2009; Nagel and Kay, 2012). Rhythms have been seen in gene transcription in individual cells with no coupling of clocks between neighbouring cells (Harmer, 2009). However, rhythms have also been seen in cyanobacteria proteins *in vitro*, and even in red blood cells which do not contain DNA, indicating that gene transcription is not the sole component that can produce a rhythm (Harmer, 2009; Johnson et al., 2008; Mohawk et al., 2012; O'Neill and Reddy, 2011; Lakin-Thomas, 2006a; Lakin-Thomas, 2006b; Nakajima et al., 2005).

In the past, some argued that environmental factors were the only force driving rhythms in organisms, using cues from the Earth's daily rotation on its axis (Ellman et al., 1984). A clear endogenous rhythm was seen in *Neurospora crassa* cultures that were sent to outer space and kept in the dark, proving that a rhythm can still be seen without the effect of environmental factors (Ellman et al., 1984). The amplitude of this endogenous rhythm in outer space was reduced, thus indicating that the environment does play an important role, yet again, it is not the only factor that controls circadian rhythms (Ellman et al., 1984).

There is some debate as to whether or not there is one main oscillator controlling circadian rhythms in organisms. Evidence of multiple oscillators has been observed in several organisms (Swann and Turek, 1985; Harmer, 2009; Johnson et al., 2008; Mohawk et al., 2012; Zhang and Kay, 2010). In constant exposure to light, rodents can experience a splitting of the locomotor activity into two circadian rhythms occurring 12 hours apart,

2

as opposed to every 24 hours (Swann and Turek, 1985; Pickard et al., 1984; Pickard and Turek, 1982). The 12 hour circadian rhythms initially have different free-running periods, but then become synchronized with each other, indicating that there are multiple oscillators involved (Swann and Turek, 1985; Pickard et al., 1984; Pickard and Turek, 1982). Different free-running periods are often a strong indicator of multiple oscillators (Harmer, 2009; Pickard et al., 1984; Pickard and Turek, 1982). It is also common for individual components of the clock to have multiple functions. For example, glucocorticoid release from the adrenal cortex in mammals is regulated by the suprachiasmatic nucleus (SCN) in the brain, as well as rhythmic levels of corticotropin releasing hormone (CRH) and adrenocorticotropic hormone (ACTH) (Mohawk et al., 2012). Multiple interactions between clock components make circadian systems more complex to study (Harmer, 2009; Mohawk et al., 2012). Given the wide range of organisms in which circadian rhythms are found, the important physiological processes they control, and the high conservation between organisms, it is important to understand how these circadian systems function (Liu and Bell-Pedersen, 2006; Hardin, 2009).

1.2 Circadian rhythms in *Drosophila*

The fruit fly, *Drosophila melanogaster* has long been used in genetic studies and has a well-studied circadian rhythm system (Hardin, 2009). *Drosophila* produced the first genetic model of circadian rhythms: the transcription-translation feedback loop (TTFL) (Hardin, 2009). Gene transcription results in the translation of a protein product, which in turn will feedback once its levels are high enough and represses its own gene

transcription (usually by repressing other proteins). After the protein levels drop, the repression is lifted and gene transcription and translation begins again. This rhythm occurs in many organisms on a 24 hour cycle, with protein levels peaking at specific times each day (Hardin, 2009). Molecular studies using *Drosophila* have increased the knowledge of TTFLs not only in insects but other organisms as well.

In *Drosophila*, the central pacemaker cells are found in the lateral neurons in the brain (Cashmore et al., 1999). Pigment-dispersing factor-expressing neurons in the brain control the locomotor rhythms in *Drosophila* (Lim and Allada, 2013; Plautz et al., 1997). The *Drosophila* circadian system is shown in Figure 1 (Hardin, 2009). Phosphorylated CLOCK (CLK) protein forms a heterodimer with CYCLE (CYC) to activate gene transcription of *period* (*per*), *timeless* (*tim*), and *vrille* (*vri*), and *clockwork orange* (*cwo*) (Fig. 1) (Hardin, 2009; Ceriani et al., 1999; Van Gelder et al., 2003). CLK-CYC will bind to the E-box (CACGTG sequence) on the *per*, *tim*, *vri* and *cwo* gene promoters (Hardin, 2009; Ceriani et al., 1999; Avivi et al., 2001). The mRNA and protein levels of *per* and *tim* cycle approximately every 24 hours (Ceriani et al., 1999; Plautz et al., 1997; Leloup et al., 1999). A complex with PER and DOUBLETIME (DBT) kinase (and sometimes TIM) will in turn feedback and repress transcription by CLK-CYC (Hardin, 2009; Avivi et al., 2001; Van Gelder et al., 2003). VRI has also been seen to repress activation of *clk* and *tim* (Zhang and Kay, 2010; Van Gelder et al., 2003). TIM may also be involved in repressing transcription by the CLK-CYC complex (Hardin, 2009).

4

Increased phosphorylation of CLK causes the release of CLK-CYC from the *per* and *tim* genes (Hardin, 2009).

PER and TIM are phosphorylated by casein kinase 2 (CK2) and Shaggy (SGG), respectively, and dephosphorylated by protein phosphatases 1 and 2a (PP1, PP2a) (Hardin, 2009; Zhang and Kay, 2010; Van Gelder et al., 2003). PER-DBT-TIM complex will bind to CLK in the nucleus and increase phosphorylation, causing CLK-CYC complex to release from the gene promoters, forming a negative feedback loop to repress their own transcription (Hardin, 2009; Ceriani et al., 1999; Leloup et al., 1999). Phosphorylation of PER causes its degradation, and allows CLK-CYC to positively regulate and activate transcription once PER and TIM levels drop (Hardin, 2009). The *vri* gene, which is also activated by CLK-CYC, feeds back and negatively regulates by repressing *Clk* transcription (Hardin, 2009; Van Gelder et al., 2003). It is unknown how the CWO protein affects the circadian rhythm, yet is it believed to be important in the clock system, since *cwo* knockouts have reduced CLK-CYC activated transcription (Hardin, 2009).

Another protein, CRYPTOCHROME (CRY) acts as a photoreceptor and has been shown to repress function of PER-TIM complex in response to light (Fig. 1) (Ceriani et al., 1999; Cashmore et al., 1999). Light also regulates TIM protein levels, and CRY protein has been shown to interact with TIM to stop the PER-TIM complex from repressing transcription (Ceriani et al., 1999; Leloup et al., 1999; Cashmore et al., 1999).

per is expressed in cells in the head, thorax and abdominal tissues in *Drosophila*, indicating that individual cells are capable of running rhythms autonomously (Plautz et al., 1997; Levine et al., 2002). It is possible that individual cells are photoreceptive and capable of running their own rhythms, and receive their cues and entrainment from light in the environment as opposed to the main oscillator in the brain (Plautz et al., 1997). The circadian rhythms of locomotor activity in *Drosophila* that were housed together in total darkness for 2 weeks were more synchronized than flies that were isolated (Levine et al., 2002). This was also observed in honey bees, where the circadian system developed faster in bees that were housed together as opposed to isolated (Eban-Rothschild et al., 2012). This is further evidence that circadian rhythms take cues from the environment, and possibly even from other organisms (Levine et al., 2002; Eban-Rothschild et al., 2012).

It was recently found that another protein, ATAXIN-2 (ATX2), activated PER translation (Lim and Allada, 2013). ATX2 interacts with TWENTY-FOUR (TYF), which activates translation of PER (Lim and Allada, 2013). ATX2 in humans has been implicated in diseases such as amyotrophic lateral sclerosis and Parkinson's disease (Lim and Allada, 2013). This indicates that there are many other important components of the *Drosophila* system that have not yet been discovered that can also be related to diseases in other organisms (Lim and Allada, 2013).

1.3 Circadian rhythms in plants

Circadian rhythms in plants control many processes such as leaf movement, timing of flowering, plant growth, photosynthesis, and scent release (Harmer, 2009; Nagel and Kay, 2012). Not as much is known about the circadian system in plants as compared to other organisms such as *Drosophila* and *Neurospora* (Salomé and McClung, 2004; Green and Tobin, 1999). One of the most studied plants in circadian rhythm research is *Arabidopsis thaliana* (Salomé and McClung, 2004). The current model of the circadian system in *Arabidopsis* is shown in Figure 2.

In *Arabidopsis*, red light photoreceptors cause the transcription of the *LHCB* gene, which shows a circadian rhythm of gene expression (Harmer, 2009; Salomé and McClung, 2004). CIRCADIAN CLOCK ASSOCIATED 1 (CCA1) protein was found to bind to the light response element on the *LHCB* promoter. A similar protein called LATE ELONGATED HYPOCOTYL (LHY) was also discovered (Salomé and McClung, 2004). Overexpression of CCA1 and LHY cause similar disruptions in plant rhythms: arrhythmic leaf movement and *LHCB* gene expression, long hypocotyls and late flowering (Salomé and McClung, 2004; Nagel and Kay, 2012). *cca1* or *lhy* null mutants produce a shorter period in leaf movement and *LHCB* expression, yet double mutants are arrhythmic (Salomé and McClung, 2004; Green and Tobin, 1999). Either *cca1* or *lhy* null mutants do not produce completely arrhythmic oscillations, suggesting that they may be able to compensate for each other (Salomé and McClung, 2004; Green and Tobin, 1999).

CCA1 and LHY bind to and repress expression of the TIMING OF CAB

EXPRESSION 1 (*TOC1*) gene promoter when their levels are higher (Fig. 2, Loop A)

(Salomé and McClung, 2004; Harmer, 2009; Nagel and Kay, 2012). *CCA1* and *LHY*

expression is also induced by light (Harmer, 2009; Green and Tobin, 1999). CCA1 also

represses expression of the *LHY* gene (Green and Tobin, 1999). TOC1 in turn will

positively regulate expression of *CCA1* and *LHY* genes when their protein levels are low

(Fig. 2, Loop A) (Salomé and McClung, 2004; Harmer, 2009). It is unknown whether or

not TOC1 regulates *CCA1* and *LHY* directly or through another factor (Salomé and

McClung, 2004; Harmer, 2009). Some studies have shown that TOC1 may repress

expression of *CCA1* and *LHY*, indicating that more studies need to be done and that the

circadian system in *Arabidopsis* is likely more complex than initially believed (Nagel and

Kay, 2012).

An unknown component Y may also positively regulate *TOC1* expresson (Fig. 2,

Loop B) (Harmer, 2009). ZEITLUPE (ZTL) protein is responsible for TOC1

degradation, and it is regulated by GIGANTEA (GI) protein (Fig. 2, Loop D) (Salomé

and McClung, 2004; Harmer, 2009). Pseudo Response Regulators 7 and 9 (PRR7 and

PRR9) are thought to form another feedback loop with CCA1 and LHY (Fig. 2, Loop C)

(Harmer, 2009; Nagel and Kay, 2012). CCA1 and LHY promote expression of *PRR7*

and *PRR9* genes, and these proteins in turn repress expression of *CCA1* and *LHY*

(Harmer, 2009; Nagel and Kay, 2012).

These multiple feedback loops indicate that there are likely multiple oscillators controlling various processes in plants (Harmer, 2009). It is unclear how multiple oscillators are interacting and coordinating with each other, however environmental cues may be responsible for coupling oscillators together (Harmer, 2009). Blue-light photoreceptor proteins called CRYPTOCHROMES (CRY1, CRY2) have been discovered in *Arabidopsis* and are thought to help regulate the circadian rhythm (Cashmore et al., 1999). CRY1 has been seen to cause shortening of the *Arabidopsis* hypocotyl and cotyledon expansion under blue light (Cashmore et al., 1999). Mutations in *cry1* cause an increase in the period of gene expression by approximately 4 hours, and *cry2* mutants exhibit late flowering (Cashmore et al., 1999).

There is recent evidence that melatonin in plants may play a role in the circadian rhythm in the same manner as it does in mammals (Paredes et al., 2009). In *Eichhornia crassipes* (Common Water Hyacinth), melatonin exhibits a daily circadian rhythm with levels peaking at sunset (Paredes et al., 2009). In *Chenopodium rubrum* (Red Goosefoot), melatonin also exhibits a daily rhythm but with levels peaking at night (Paredes et al., 2009). Melatonin was seen to represses flowering in *C. rubrum* and *Arabidopsis thaliana* (Paredes et al., 2009). Further studies are needed on melatonin in other plants and the exact role it plays in circadian rhythms (Paredes et al., 2009).

1.4 Circadian rhythms in bacteria

Cyanobacteria are one of the oldest groups of organisms on earth and currently the only prokaryotes that show evidence of a circadian rhythm mechanism (Dong et al.,

2010; Tomita et al., 2005; Dvornyk et al., 2003). The most commonly studied is

Synechococcus elongatus, a unicellular cyanobacterium which possesses a circadian

clock mechanism (Dong et al., 2010; Johnson et al., 2008). Cyanobacteria are unique in

the fact that they have a rhythm of phosphorylation and dephosphorylation of proteins,

which does not require a TTFL typical of circadian systems (Brunner and Schafmeier,

2006; Zhang and Kay, 2010).

The main clock mechanism is made up of 3 proteins: KaiA, KaiB, and KaiC and

is shown in Figure 3 (Dong et al., 2010; Brunner and Schafmeier, 2006; Tomita et al.,

2005; Johnson et al., 2008; Dvornyk et al., 2003). These 3 proteins along with ATP

produce cyclic phosphorylation of KaiC with an approximate 24 hour period (Dong et al.,

2010; Brunner and Schafmeier, 2006). In constant darkness, KaiC will continue to

produce rhythmic phosphorylation and dephosphorylation (Brunner and Schafmeier,

2006). Disruption of the *Kai* genes results in a loss of the rhythm (Brunner and

Schafmeier, 2006). This cycling will synchronize itself with the environment through

light input sensed by the cyanobacteria (Dong et al., 2010).

KaiC, upon stimulation by KaiA, will autophosphorylate itself, and will then

undergo spontaneous dephosphorylation (Dong et al., 2010; Brunner and Schafmeier,

2006). KaiB will bind to dephosphorylated KaiC, which inactivates KaiA, causing

further dephosphorylation of KaiC (Dong et al., 2010; Brunner and Schafmeier, 2006).

Mutations to residues in KaiC can abolish the circadian rhythm, and mutated forms of

KaiA cause changes in phosphorylation levels of KaiC and a shorter period (Dong et al.,

2010; Brunner and Schafmeier, 2006; Tomita et al., 2005). The phosphorylation cycle causes changes to the conformation of KaiC protein, yet the exact role and purpose of this conformational change is unknown (Dong et al., 2010)

Clock proteins SasA and RpaA act downstream of KaiC to control the timing of cell division (Fig. 3) (Dong et al., 2010; Johnson et al., 2008). The rate of cell division does not have an effect on the clock as the circadian rhythm maintains an approximate 24 hour rhythm regardless of the rate of cell division (Dong et al., 2010; Kondo et al., 1997; Johnson et al., 2008). Gene transcription levels are also affected by KaiC, yet the mechanism is currently unknown (Dong et al., 2010; Brunner and Schafmeier, 2006).

Input protein CikA binds quinone and represses KaiC activity (Fig. 3) (Dong et al., 2010). The *pex* gene, which encodes a repressor of the *KaiA* gene, is repressed by light input (Dong et al., 2010). Oxidized quinone also destabilizes KaiA by directly binding to it, but not in the reduced form, suggesting that the cyanobacteria sense light by changes in the oxidation or reduction states of quinone (Dong et al., 2010).

Because *Synechococcus elongatus* is a photoautotroph, it was expected that in constant darkness (DD) gene expression and protein synthesis would halt, causing a disruption in the rhythm of Kai proteins (Tomita et al., 2005). KaiA, KaiB and KaiC proteins levels were constant and exhibited no rhythm after transfer to DD (Tomita et al., 2005). However, KaiC phosphorylation showed a temperature-compensated rhythm in DD (Tomita et al., 2005). KaiA, KaiB, and KaiC proteins were incubated *in vitro* along with adenosine triphosphate (ATP) (Nakajima et al., 2005). KaiC exhibited rhythmic

phosphorylation with a period of approximately 24 hours (Nakajima et al., 2005). In addition, the period of phosphorylation rhythm was temperature compensated, ranging from 20-22 hours over a temperature of 25-35°C (Nakajima et al., 2005). This provided strong evidence that the KaiA, KaiB, and KaiC phosphorylation oscillator can run independently of any gene transcription and is the basis for circadian rhythms in cyanobacteria (Tomita et al., 2005; Johnson et al., 2008; Lakin-Thomas, 2006a; Lakin-Thomas, 2006b; Nakajima et al., 2005).

It has also been seen that if KaiC is halted at a particular phosphorylation state, rhythmic gene expression is still observed in the cyanobacteria, suggesting a TTFL may exist independently of the Kai-protein phosphorylation oscillator (Dong et al., 2010; Lakin-Thomas, 2006b). However, other researchers have noticed when KaiC phosphorylation is halted, a dampening of the gene expression rhythm is observed, suggesting that another oscillator may be involved and may interact in some way with the Kai protein oscillator (Dong et al., 2010; Tomita et al., 2005; Johnson et al., 2008).

Other cyanobacteria such as *Synechocystis*, *Cyanothece*, and *Thermosynechococcus elongatus* all have the *KaiA*, *KaiB* and *KaiC* genes (Dong et al., 2010). Although the main circadian mechanism in cyanobacteria possibly does not directly involve a TTFL, regulation of circadian rhythm proteins by phosphorylation has been seen in many other organisms (Dong et al., 2010; Brunner and Schafmeier, 2006). The cyanobacteria system brings up the possibility that circadian systems outside of the

TTFL may exist in other organisms such as eukaryotes (Johnson et al., 2008; Lakin-Thomas, 2006a; Lakin-Thomas, 2006b).

1.5 Circadian rhythms in mammals

Circadian rhythms in mammals are generally seen as being quite complex. It is believed that, like other organisms, there are multiple oscillators that control circadian rhythms in mammals (Swann and Turek, 1985; Mohawk et al., 2012; Zhang and Kay, 2010). The circadian system controls activities such as feeding, rest, metabolism, body temperature, and hormone secretion (Mohawk et al., 2012; Reddy and O'Neill, 2010). The suprachiasmatic nucleus (SCN) in the brain hypothalamus is important for controlling circadian rhythms in mammals (Plautz et al., 1997; Mohawk et al., 2012; Reddy and O'Neill, 2010). It is made up of approximately 20,000 neurons which each have individual circadian oscillators that couple together to form a synchronous circadian rhythm (Mohawk et al., 2012; Zhang and Kay, 2010). The peripheral oscillators found in the fibroblasts, liver, kidneys, lungs and other tissues, are not as robust, and can be easily entrained by low-amplitude temperature cycles, whereas the SCN is more resistant to this type of entrainment (Mohawk et al., 2012). Mutations in rhythms seen in individual cells and tissues can be rescued by the SCN network, indicating that the SCN likely is coupled with individual peripheral oscillators to control and synchronize their rhythmicity (Mohawk et al., 2012; Zhang and Kay, 2010).

It has been observed in rodents that food-anticipatory behaviour is rhythmically regulated and the circadian rhythm phase will adjust in accordance with the presence of

food (Mohawk et al., 2012; Fuller et al., 2008). In humans that are kept in isolation chambers, the body temperature and sleep-wake cycles have been observed to split and become out of phase with each other, running with different periods (Pickard et al., 1984). This provides evidence that circadian rhythms controlling various physiological processes may be controlled by separate oscillators (Pickard et al., 1984; Pickard and Turek, 1982). In hamsters, unilateral ablation of the bilateral SCN was performed, and this resulted in the abolishment of the splitting phenomenon and single activity rhythms (Pickard and Turek, 1982). This indicated that each side of the bilaterial SCN may function as a separate oscillator, and is likely coupled with the other side to control circadian rhythms (Pickard and Turek, 1982).

The circadian system of mammals is shown in Figure 4 (Mohawk et al., 2012). The core oscillator in the clock is a TTFL made up of proteins CLOCK (CLK) and Brain and Muscle ARNT-like 1 (BMAL1) that bind to the E-box and activate transcription of *period* (*per1, per2*) and *cryptochrome* (*cry1, cry2*) genes (Fig. 4) (Mohawk et al., 2012; Avivi et al., 2001; Zhang and Kay, 2010; Tsuchiya et al., 2009). PER and CRY in turn repress transcription of *clk* and *bmal1* genes, as well repressing their own gene transcription (Mohawk et al., 2012; Avivi et al., 2001; Zhang and Kay, 2010; Tsuchiya et al., 2009). Another protein called REV-ERBα activated by CLK and BMAL1 forms a negative feedback loop and represses *bmal1* transcription (Mohawk et al., 2012; Zhang and Kay, 2010; Tsuchiya et al., 2009).

PER and CRY are phosphorylated by casein kinase 1 and 2 (CK1, CK2) and

AMP kinase (AMPK), respectively, which targets them for degradation by the

proteasome by ubiquitin ligases (Mohawk et al., 2012; Tsuchiya et al., 2009). As PER

and CRY are degraded, their protein levels drop which repeats the cycle of their

activation by CLK and BMAL1 (Zhang and Kay, 2010). It is believed that BMAL1 is

responsible for entrainment of food-anticipatory behaviour (Fuller et al., 2008).

Photoreceptors in the retinal ganglions, along with rods and cones, feed back into

the SCN to provide input to the circadian rhythm for entrainment (Mohawk et al., 2012;

Avivi et al., 2001). In completely blind mammals, such as the subterranean mole rat, the

retina is seen to still function in entraining locomotor activity and thermoregulation

(Avivi et al., 2001).

1.5.1 Circadian rhythms and human health

The cells and tissues in the body produce rhythmic outputs of glucose and

hormone production, and fat storage, which feed back into the SCN (Mohawk et al.,

2012). Disruption of these rhythms may therefore affect metabolic activity. Circadian

rhythm disruption in humans, seen often in shift workers, can produce serious long-term

health risks such as increased risk of cancer, strokes and cardiovascular disease (O'Neill

and Reddy, 2011; Reddy and O'Neill, 2010; Portaluppi et al., 2012). Disruptions to the

cardiovascular system, such as cardiac arrhythmias, also follow a clear rhythmic pattern,

occurring more often in the morning and daytime than at night (Portaluppi et al., 2012).

In shift workers, there are higher risks of breast, colorectal, endometrial and prostate

cancers (Reddy and O'Neill, 2010). In addition, diabetes and obesity have also been linked to rotational shift work (Reddy and O'Neill, 2010).

Disrupted sleep patterns in humans has been associated with Alzheimer's, Huntington's disease and dementia (Reddy and O'Neill, 2010). In mouse models, it was noticed that the disruption of the circadian rhythm via phase shifts produced retrograde amnesia, indicating that rhythms may play a role in memory loss and function (Tapp and Holloway, 1981). Children with autism have also exhibited severely disrupted sleep-wake cycles, which may help in diagnosis and treatment of this disease (Glickman, 2010).

Sleep disorders have also been linked to substance abuse and addiction, which in turn can cause a disruption of the circadian rhythm (Hasler et al., 2012). Substance abuse may cause desynchrony in the circadian system, which can possibly lead to continual relapses of addictive behaviour (Hasler et al., 2012). Therapy involving sleep-wake cycles and light-dark entrainment of the circadian system may aid in treatment of addictions (Hasler et al., 2012).

Increased cancer risks have been seen in humans and rodents that have rhythms which are not synchronized with the external environment (Reddy and O'Neill, 2010). The circadian system regulates cell division, and arrythmicity may be a factor in producing uncontrolled cell division in cancer (Reddy and O'Neill, 2010). In addition, many core clock genes such as CLK, BMAL1, PER1 and PER2 have been shown to have tumour suppressing abilities and provide protection against DNA damage by chemicals

16

and radiation (Reddy and O'Neill, 2010). Mice with CLK and BMAL1 mutations were more sensitive to treatment from anticancer drugs and exhibited greater body weight loss than those with wild type CLK and BMAL1 (Reddy and O'Neill, 2010). The reduction in the number of lymphocytes and neutrophils was also greater in CLK mutant mice (Reddy and O'Neill, 2010). Implanted tumours have been seen to grow more rapidly in animals that have disrupted rhythms via conditions that simulate jet-lag or shift work (Reddy and O'Neill, 2010).

Peroxiredoxins (proteins in red blood cells) have been found to exhibit a free-running, 24-hour circadian rhythm in constant conditions that is temperature compensated (O'Neill and Reddy, 2011). Levels of NADH and NADPH in the red blood cells were also found to exhibit a 24-hour rhythm, indicating that the rhythmic activity of metabolic pathways may be important to their optimal function (O'Neill and Reddy, 2011). Circadian rhythms of calcium and phosphate levels have also been found in the blood of healthy human adults (Markowitz et al., 1981). Children with hypoparathyroidism that are treated with daily Vitamin D doses exhibit blood calcium levels that do not follow a circadian rhythm or have a calcium rhythm with a lower amplitude (Markowitz et al., 1981). Deviations from these rhythmic levels at various stages of diseases may therefore be a target for treatment and prevention (Markowitz et al., 1981). Observing blood calcium levels may be important for detecting abnormalities in hormonal and mineral metabolism (Markowitz et al., 1981).

Circadian rhythm knowledge is now being used in cancer therapy, where the timing of drug dosage is controlled to specific times of day (Reddy and O'Neill, 2010). The toxic effect of several anticancer drugs has been seen to depend on the time of day it is administered (Reddy and O'Neill, 2010). In the case of Huntington's disease in mice, a daily sleep cycle has been shown to improve survival and cognitive abilities, leading to the possibility of controlling and improving disease symptoms via circadian rhythm restoration (Reddy and O'Neill, 2010).

1.6 Circadian rhythms in *Neurospora*

1.6.1 *Neurospora* as a model organism and life cycle

Neurospora as a model organism

Neurospora crassa is a bread mold first reported in Paris in the late 1800s by Payen (cited in Galagan et al., 2003). It is non-pathogenic and typically feeds on dead or decaying matter (Galagan et al., 2003). It is now extensively used as a model organism in genetic studies, specifically circadian rhythm research (Galagan et al., 2003; Liu and Bell-Pedersen, 2006). *Neurospora* provides an advantage since it can be used to easily study eukaryotic genetics as compared to using mammals or prokaryotic organisms (Galagan et al., 2003). It is a haploid organism which is very easy to grow and exhibits a rhythmic asexual spore formation (conidiation) on petri dishes or long cylindrical glass tubes (race tubes) (Liu and Bell-Pedersen, 2006; Lakin-Thomas et al., 2011). Its genome consists of 7 chromosomes (or Linkage Groups) and approximately 10,000 genes (Galagan et al., 2003). Haploid genetics make *Neurospora* easier to study since

mutations can be observed without the complementation of other alleles as seen in diploids (Lakin-Thomas et al., 2011).

Neurospora life cycle

The life cycle of *Neurospora* includes an asexual and sexual cycle (Griffiths et al., 1993; Metzenberg and Glass, 1990). The asexual cycle involves mitosis of haploid nuclei, and the formation of conidia from hyphae (long cellular threads) (Griffiths et al., 1993). Multinucleate hyphae grow and produce multinucleate asexual spores, which germinate to form new mycelia (Griffiths et al., 1993).

In the sexual cycle, protoperithecia are fertilized by the opposite mating type, designated either *A* or *a* (Metzenberg and Glass, 1990). Nuclear fusion of the haploid nuclei occurs, followed by meiosis and mitosis to produce asci inside the perithecia (Griffiths et al., 1993; Metzenberg and Glass, 1990; Lindegren, 1932). Each ascus contains 8 haploid ascospores (sexual spores), each containing a single nucleus (Griffiths et al., 1993; Metzenberg and Glass, 1990; Lindegren, 1932).

The *Neurospora* clock

Neurospora has been seen to have an endogenous rhythm of approximately 22 hours in constant dark conditions (Ellman et al., 1984; Lakin-Thomas et al., 2011). The *Neurospora* circadian clock exhibits the standard traits of circadian rhythms: it has a rhythm close to 24 hours under constant conditions (i.e. constant darkness, DD), the period is temperature compensated between 16-30°C, and entrainable by light (Lakin-Thomas et al., 2011). There is high conservation of function between *Neurospora* clock

genes and clocks in other organisms which allows research on *Neurospora* to be related to other circadian systems (Liu and Bell-Pedersen, 2006; Lakin-Thomas et al., 2011).

On a genetic level, the main circadian systems in *Neurospora*, *Drosophila*, and mammals typically function using positive and negative regulation in a transcription-translation feedback loop (Liu and Bell-Pedersen, 2006; Brunner and Schafmeier, 2006; Hardin, 2009). WC-1 and WC-2 proteins in *Neurospora*, dCLOCK (dCLK) and CYCLE (CYC) proteins in *Drosophila*, and BMAL1 and CLOCK (CLK) proteins in mammals all positively regulate transcription of the FRQ protein in *Neurospora*, PERIOD (PER) and TIMELESS (TIM) proteins in *Drosophila*, and PERIOD (PER) and CRYPTOCHROME (CRY) proteins in mammals, respectively (Liu and Bell-Pedersen, 2006; Salomé and McClung, 2004; Brunner and Schafmeier, 2006; Mohawk et al., 2012; Zhang and Kay, 2010). These proteins in turn are negative regulators of the initial activating proteins, forming a positive-negative feedback loop (Liu and Bell-Pedersen, 2006; Brunner and Schafmeier, 2006). Proteins in the *Neurospora, Drosophila, Arabidopsis* and mammalian circadian rhythm loops are all regulated by phosphorylation and in some cases, even phosphorylated by the same kinases (Liu and Bell-Pedersen, 2006; Nagel and Kay, 2012; Brunner and Schafmeier, 2006). Therefore studying the circadian rhythms in *Neurospora* can shed light on the circadian rhythms and TTFLs occurring in other organisms.

1.6.2 FRQ-WCC TTFL in *Neurospora*

The main circadian system driving rhythms in *Neurospora* is the frequency-white collar complex (FRQ-WCC) transcription-translation feedback loop (TTFL) shown in

Figure 5 (Liu and Bell-Pedersen, 2006; Brunner and Schafmeier, 2006; Lakin-Thomas et al., 2011; Dunlap and Loros, 2006; Cheng et al., 2001). White collar proteins 1 and 2 (WC-1, WC-2) are the positive regulators and will bind together to form the white collar complex (WCC) (Liu and Bell-Pedersen, 2006; Brunner and Schafmeier, 2006; Lakin-Thomas et al., 2011; Dunlap and Loros, 2006; Cheng et al., 2001). WCC rhythmically binds to the clock box (C-box) or light response element (LRE) on the frequency (*frq*) gene promoter and initiates transcription, which in turn creates mRNA and FRQ protein (Liu and Bell-Pedersen, 2006; Brunner and Schafmeier, 2006; Lakin-Thomas et al., 2011; Dunlap and Loros, 2006; Cheng et al., 2001; Froehlich et al., 2003).

FRQ protein binds to the FRH (FRQ interacting RNA helicase) which becomes the negative regulator and supresses WCC binding to the *frq* gene (Liu and Bell-Pedersen, 2006; Brunner and Schafmeier, 2006; Leloup et al., 1999; Lakin-Thomas et al., 2011; Aronson et al., 1994a; Dunlap and Loros, 2006; Dunlap and Loros, 2004). FRH is responsible for the interaction of FRQ and WCC, and without this, FRQ is unable to repress WCC binding to the *frq* gene (Liu and Bell-Pedersen, 2006; Brunner and Schafmeier, 2006; Dunlap and Loros, 2006).

FRQ protein repression is caused by phosphorylated WCC, which in turn is kept in an inactive state and will not bind to the *frq* gene (Brunner and Schafmeier, 2006; Lakin-Thomas et al., 2011; Dunlap and Loros, 2006). This causes FRQ protein levels to drop and WCC suppression to be lifted via dephosphorylation (Liu and Bell-Pedersen, 2006; Brunner and Schafmeier, 2006; Lakin-Thomas et al., 2011; Dunlap and Loros,

2006). FRQ protein, however, also increases expression of WC-1 and WC-2 themselves at either a post-transcriptional or post-translational level (Liu and Bell-Pedersen, 2006; Brunner and Schafmeier, 2006; Lakin-Thomas et al., 2011; Cheng et al., 2001).

The levels of FRQ RNA and protein exhibit a circadian rhythm (Brunner and Schafmeier, 2006; Lakin-Thomas et al., 2011; Aronson et al., 1994a; Froehlich et al., 2003). FRQ becomes phosphorylated and attached to FWD-1 (a component of ubiquitin ligase), which signals FRQ protein degradation by the proteasome (Liu and Bell-Pedersen, 2006; Brunner and Schafmeier, 2006; Lakin-Thomas et al., 2011; Dunlap and Loros, 2004). Proteins responsible for phosphorylation in the FRQ-WCC TTFL are Calcium/calmodulin dependent kinase (CAMK1), casein kinase 1a and II (CK-1a, CKII) (Liu and Bell-Pedersen, 2006; Brunner and Schafmeier, 2006; Lakin-Thomas et al., 2011; Dunlap and Loros, 2006; Dunlap and Loros, 2004). Dephosphorylation is achieved by protein phosphatases 1 and 2a (PP1, PP2a) (Liu and Bell-Pedersen, 2006; Brunner and Schafmeier, 2006; Lakin-Thomas et al., 2011). WC-1 levels are found to be rhythmic, in an antiphase rhythm to FRQ (Brunner and Schafmeier, 2006; Lakin-Thomas et al., 2011). Deletion or mutation of *frq*, *wc-1* or *wc-2* genes will cause an abolishment of the rhythm, indicating that the FRQ-WCC loop is the main mechanism driving the circadian rhythm (Liu and Bell-Pedersen, 2006; Lakin-Thomas et al., 2011).

WC-1 also serves as a blue light photoreceptor which allows the fungus to sense the environment and reset the daily rhythm based on light cues (Liu and Bell-Pedersen, 2006; Brunner and Schafmeier, 2006; Lakin-Thomas et al., 2011; Correa et al., 2003;

Crosthwaite et al., 1997; Dunlap and Loros, 2004; Froehlich et al., 2002). Light causes

the WCC to bind to the light response element on the *frq* promoter and activates

transcription (Liu and Bell-Pedersen, 2006; Brunner and Schafmeier, 2006; Leloup et al.,

1999; Lakin-Thomas et al., 2011; Crosthwaite et al., 1997; Dunlap and Loros, 2004).

Constant or long-term exposure to light increases WCC phosphorylation which in turn

will decrease binding to the *frq* promoter (Liu and Bell-Pedersen, 2006; Brunner and

Schafmeier, 2006; Lakin-Thomas et al., 2011; Froehlich et al., 2002).

1.6.3 FRQ-Less Oscillator (FLO)

Although *frq*, *wc-1*, and *wc-2* mutants are generally observed to be arrhythmic,

some rhythms can be seen in these null mutants under certain conditions (Lakin-Thomas

et al., 2011; Aronson et al., 1994b; Dunlap and Loros, 2004). This oscillator has been

dubbed the *frq*-less oscillator (FLO) (Lakin-Thomas et al., 2011; Correa et al., 2003;

Dunlap and Loros, 2004; Granshaw et al., 2003; Christensen et al., 2004; de Paula et al.,

2006).

Some frequency null mutants (*frq^9* and *frq^{10}*) were seen to produce a rhythm on

long race tubes (Lakin-Thomas et al., 2011; Loros and Feldman, 1986; Aronson et al.,

1994b). The period varies to a greater degree in these rhythmic mutants and the

temperature compensation of the period is abolished (Lakin-Thomas et al., 2011;

Granshaw et al., 2003). *frq^{10}* strains are entrainable to high temperature pulses, which is

a characteristic of circadian rhythms, and indicates the presence of a second oscillator (Li

et al., 2011). Adding farnesol, geraniol, or menadione to the media was also seen to

23

produce a rhythm in *frq*, *wc-1* and *wc-2* null mutants (Lakin-Thomas et al., 2011; Granshaw et al., 2003).

Rhythmic oscillations of nitrate reductase activity were also seen in *frq^9* and *wc-1* knockouts, indicating these rhythms are driven by something other than the FRQ-WCC loop (Christensen et al., 2004). Some clock-controlled genes (ccgs) such as *ccg-16*, have been seen to produce rhythmic mRNA levels in a *frq* knockout, indicating the presence of an alternate oscillator (Lakin-Thomas et al., 2011; Correa et al., 2003; de Paula et al., 2006). *ccg-16* rhythmic activity required WC-1 and WC-2, indicating that these proteins may be linked to, and possibly even regulate, the FLO (de Paula et al., 2006). Three other ccgs were discovered to have short-period rhythms in the mutated, long-period *frq^7* strain (Correa et al., 2003).

In addition, double mutants containing both the choline (*chol-1*) and *frq^{10}* mutations exhibit clear, long period rhythms with low choline concentrations in the media (Lakin-Thomas et al., 2011; Lakin-Thomas and Brody, 2000). Strains with a *chol-1* mutation are unable to produce normal levels of phosphatidylcholine and require choline in the media for normal growth (Lakin-Thomas, 1996; Lakin-Thomas and Brody, 2000). Other double mutants, such as *ult; frq^{10}*, *vvd; frq^{10}* and *sod-1; frq^{10}* also produced rhythms in the *frq* null strains (Lakin-Thomas et al., 2011).

Two period mutants (*prd-1* and *prd-2*) were also tested in a *chol-1; frq^{10}* strain and were discovered to disrupt the circadian rhythm on media containing low choline

(Lakin-Thomas et al., 2011; Li and Lakin-Thomas, 2010). *prd-1* and *prd-2* also greatly

affected the heat entrainment seen in the *frq^{10}* strain (Li and Lakin-Thomas, 2010).

Several genes and proteins have been discovered which appear to be a part of the

FLO.

However, the exact nature and all components of the FLO is not fully understood, nor is

the nature of the relationship between the FLO and the FRQ-WCC loop (Lakin-Thomas

et al., 2011; de Paula et al., 2006). Due to the overwhelming evidence that circadian

rhythms are complex in other organisms, it stands to reason that the *Neurospora* clock is

similarly complex and does not only involve the FRQ-WCC feedback loop. Discovering

the function of multiple oscillators in *Neurospora* can shed light on similar mechanisms

in other organisms.

1.6.4 Novel mutation in the FLO (*UV90*):

In order to determine the components of the FLO, a new mutation was introduced

into a *chol-1; frq^{10}* strain which displays a circadian rhythm without choline in the media

(Li et al., 2011). A new mutant was created by subjecting ~600 conidiospores from a

chol-1; frq^{10} strain to ultraviolet light (Li et al., 2011). Spores were tested on race tubes

and viable progeny that exhibited rhythm mutations were arbitrarily numbered. The 90th

mutated spore, dubbed *UV90*, produced arrhythmic progeny in the typically rhythmic

chol-1; frq^{10} strain on low choline (Fig. 6A) (Li et al., 2011; Lakin-Thomas et al., 2011).

In the absence of the choline mutation, *UV+* and *UV90* both appear arrhythmic in *frq^{10}*

strains (Fig. 6B). This is an indication that *UV90* is likely a part of, or affects the FLO (Li et al., 2011).

The *UV90* mutant was then crossed to *frq+* to test the phenotype of the *UV90* mutation in the presence of functional *frq* gene (Li et al., 2011). In *chol-1; frq+* strains, *UV90* exhibited a low amplitude rhythm with the addition of choline, and an arrhythmic pattern on media without choline (Fig. 6C). In *frq+* strains without the choline mutation, similar results were seen, as *UV90* created a low amplitude rhythm (Fig. 6D).

The FLO is possibly acting downstream of the FRQ-WCC feedback loop, as rhythms (perhaps from the same oscillator) were seen in both *frq+* and *frq* null strains (Lakin-Thomas et al., 2011). In addition to effects on the circadian rhythm, *UV90* also exhibited a slightly slower growth rate than wild type and altered the temperature compensation of the period in the *frq+* strains (Li et al., 2011). The heat-entrained rhythm present in the *frq^{10}* strain was altered by the *UV90* mutation more strongly in *frq^{10}* than the *frq+* strains, again indicating that *UV90* affects the FLO (Li et al., 2011). *UV90* also lowered the amplitude of FRQ protein levels (Li et al., 2011; Lakin-Thomas et al., 2011). The FLO and *UV90* may therefore have an interaction with the FRQ-WCC loop (Li et al., 2011; Lakin-Thomas et al., 2011).

The *UV90* gene was mapped to a region on Linkage Group VI by crossing it with strains with known mutations (Li et al., 2011). In the backcross to the band (*bd*) strain, *UV90* was seen to have 50% recombination with *frq* (Linkage Group (LG) VII), and 48.9% recombination with *chol-1* (LG IV) (Li et al., 2011). Recombination rates of

26

nearly 50% are an indication of genes that are located on separate chromosomes and therefore unlinked (Griffiths et al., 1993).

In a cross to the *alcoy* tester strain which contains multiple mutations on known chromosomes, *UV90* was 51.9% recombinant with *cot-1* (LG IVL/VR), 40.7% with *al-1* (LG IR/IIL), and 16.7% with *ylo-1* (LG IIIR/VIR) (Li et al., 2011).

Bulked segregant analysis was performed according to the methods of Jin et al. (2007) and *UV90* was found to be unlinked to marker 3-52 on LG III (Li et al., 2011). *UV90* was determined to be linked (less than 10% recombination) to markers 6-39 and 6-68, which are located on the left and right of the centromere on LG VI, respectively (Li et al., 2011).

The conclusion was made that *UV90* is likely located on LG VI, possibly on either side of the centromere.

1.7 Purpose of this study

The long term goal of this project is to discover the components and mechanism of the *frq*-less oscillator (FLO), specifically, what interaction the FLO may be having with the FRQ-WCC oscillator, and what roles FLO components such as *prd-1*, *prd-2* and *UV90* play in controlling the *Neurospora* circadian rhythm. Locating the *UV90* gene will lead to a better understanding of one component of the FLO and how this specific mutation affects the circadian rhythm.

The purpose of this study is to map the location of the gene causing the *UV90* phenotype, and to characterize the *UV90* gene mutation. Cleaved Amplified

27

Polymorphic Sequence (CAPS) marker analysis and gene knockout screens will be used

to map the location of the gene on LG VI, along with DNA sequencing to characterize

the nature of the *UV90* mutation. Complementation tests will also be performed on the

UV90 strain to confirm the restoration of the *UV90* phenotype with the wild type copy of

the putative gene.
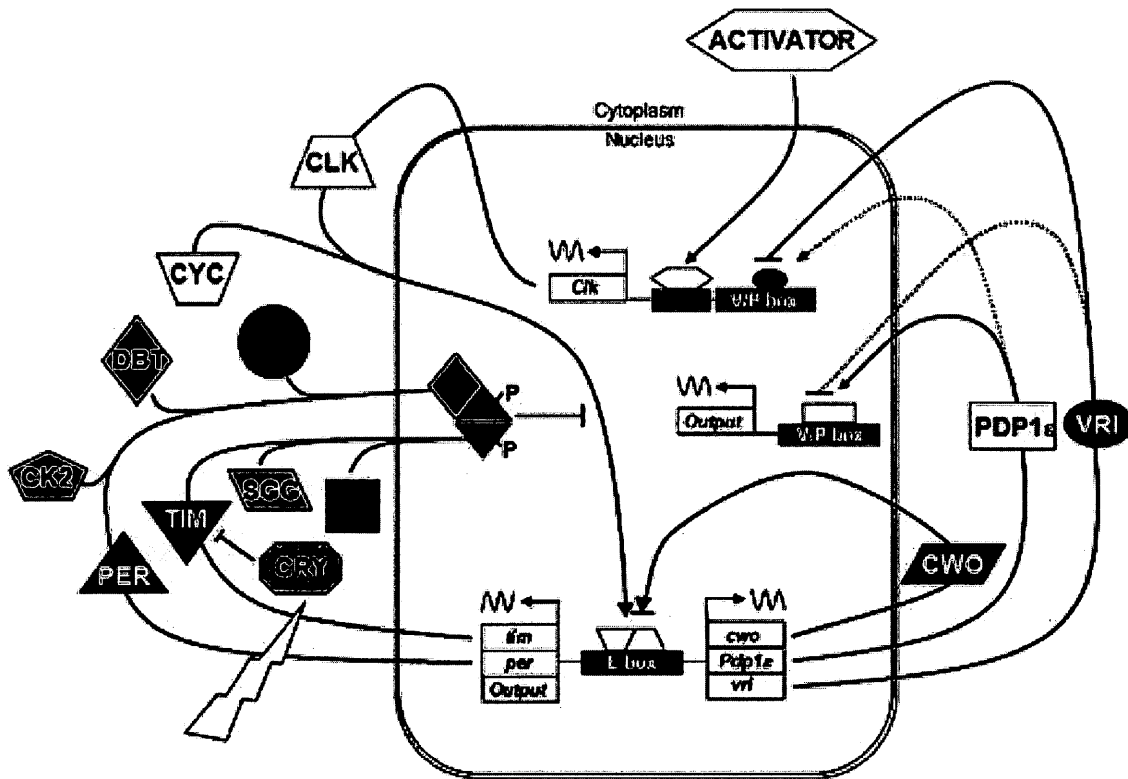
Figure 1. The circadian system of *Drosophila melanogaster*.

Obtained from Hardin (2009). See Introduction, Section 1.2 for detailed description.
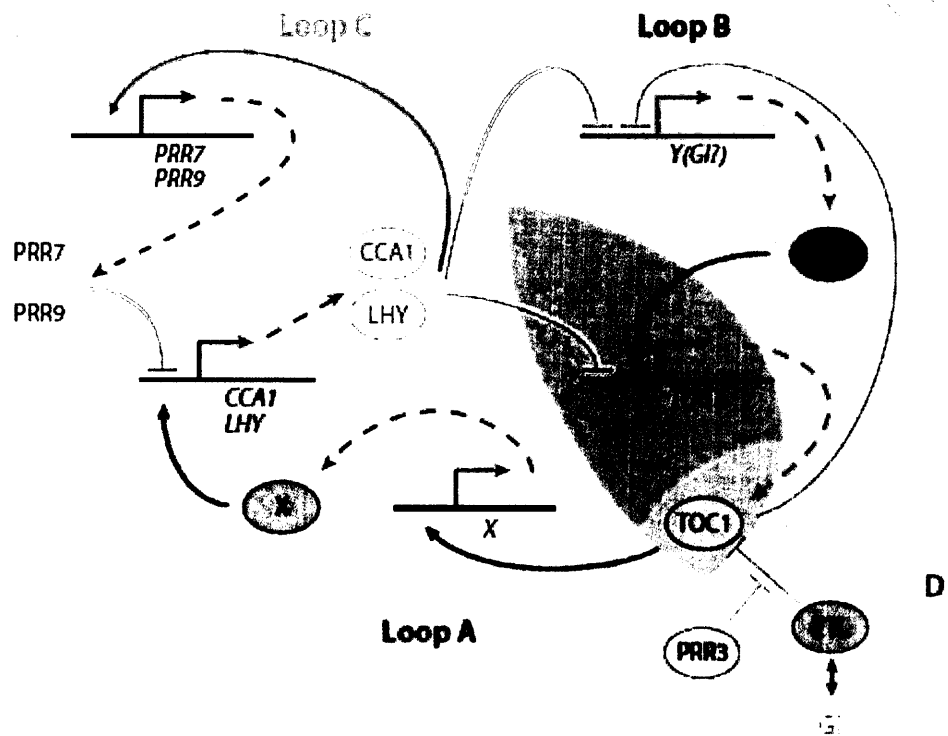
Figure 2. The plant circadian system in *Arabidopsis thaliana*.

Obtained from Harmer (2009). See Introduction, Section 1.3 for detailed description.
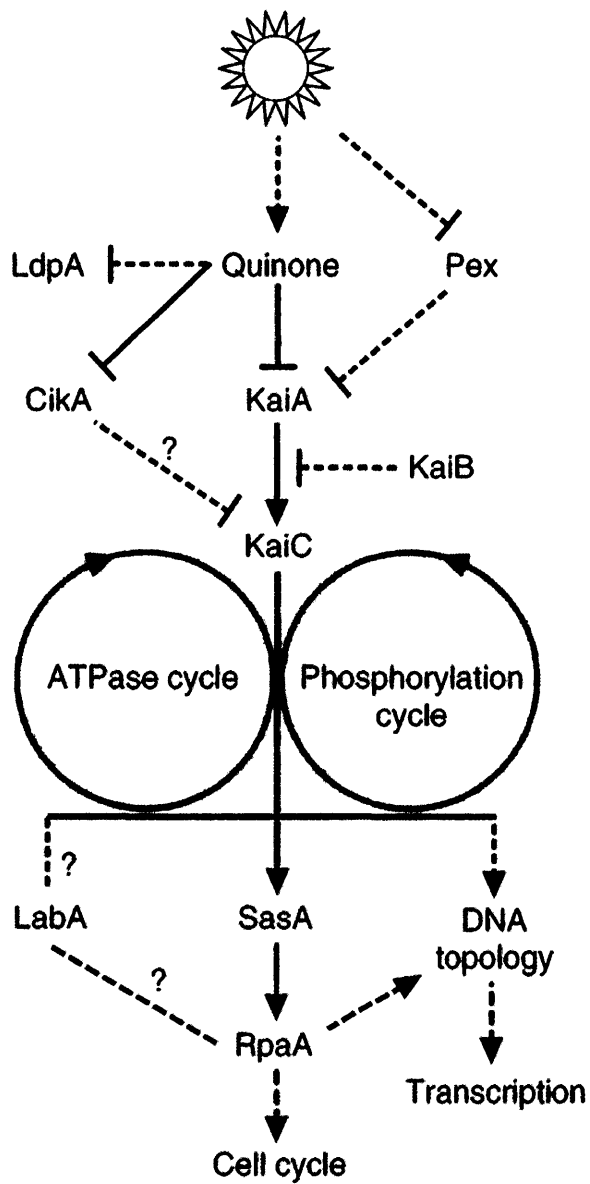
Figure 3. The cyanobacteria circadian system in *Synechococcus elongatus*

Obtained from Dong et al. (2010). See Introduction, Section 1.4 for detailed description.

31
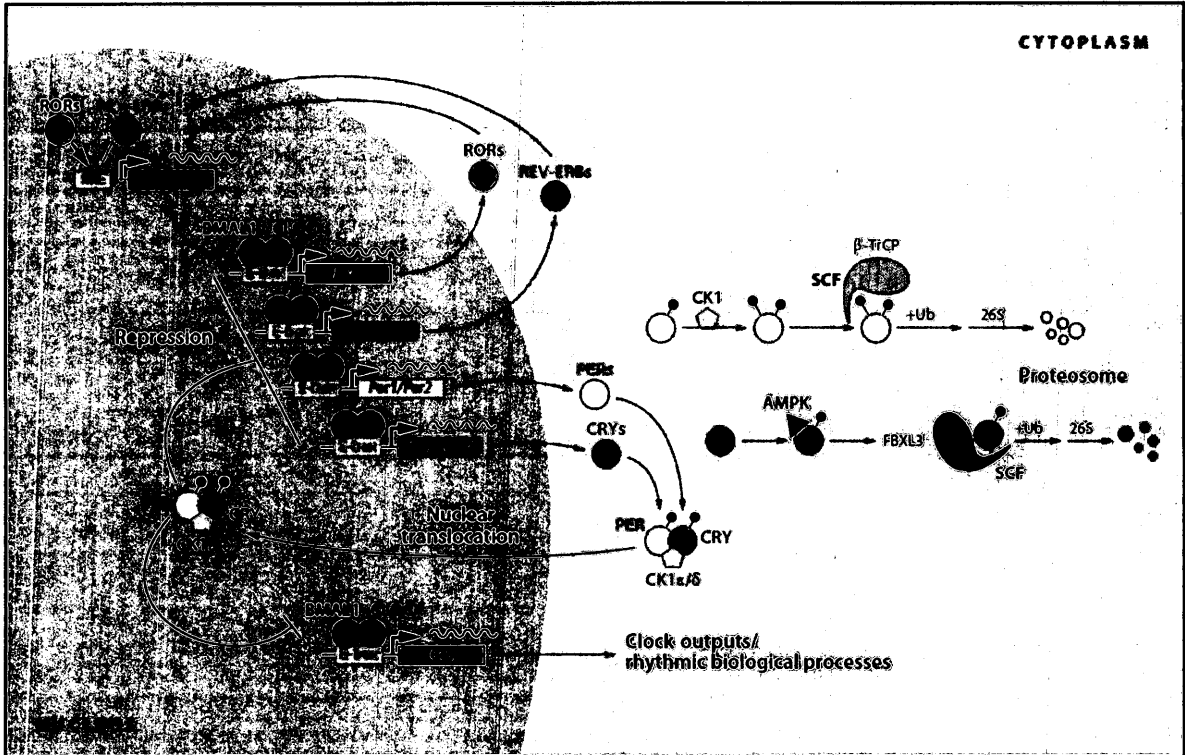
Figure 4. The mammalian circadian system

Obtained from Mohawk et al. (2012). See Introduction, Section 1.5 for detailed

description.
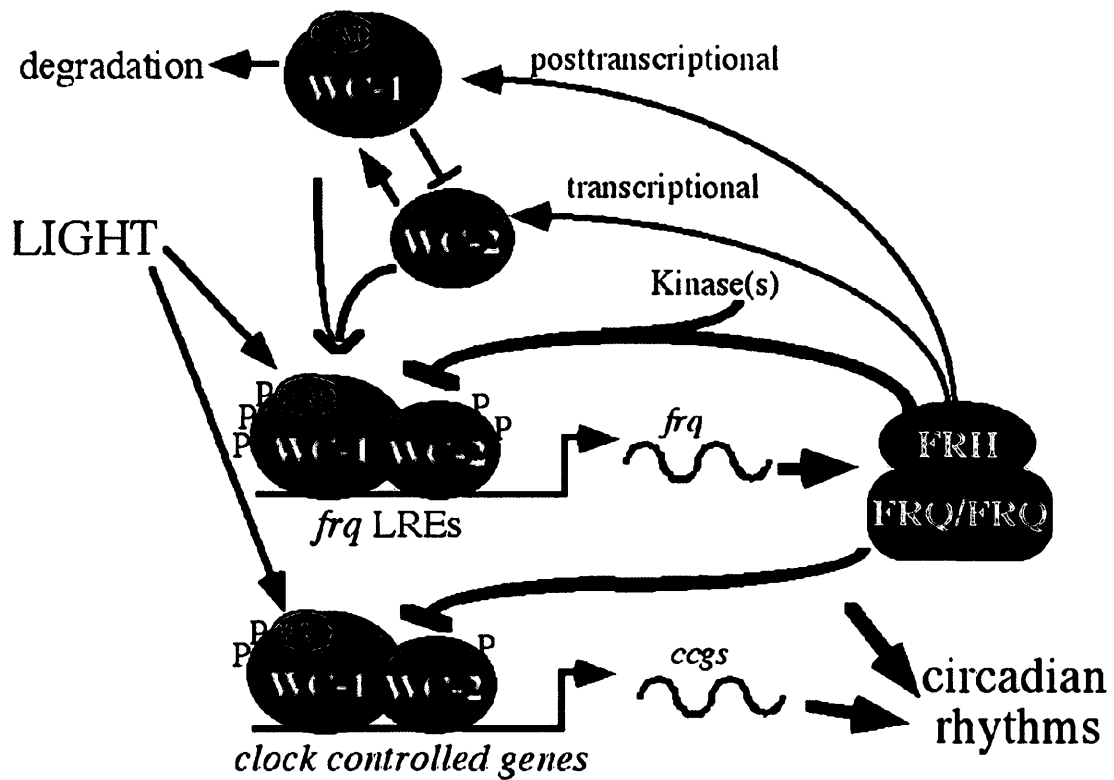
Figure 5. The FRQ-WCC transcription translation feedback loop in *Neurospora crassa*

Adapted from Liu and Bell-Pedersen (2006). See Introduction, Section 1.6.2 for detailed

description.
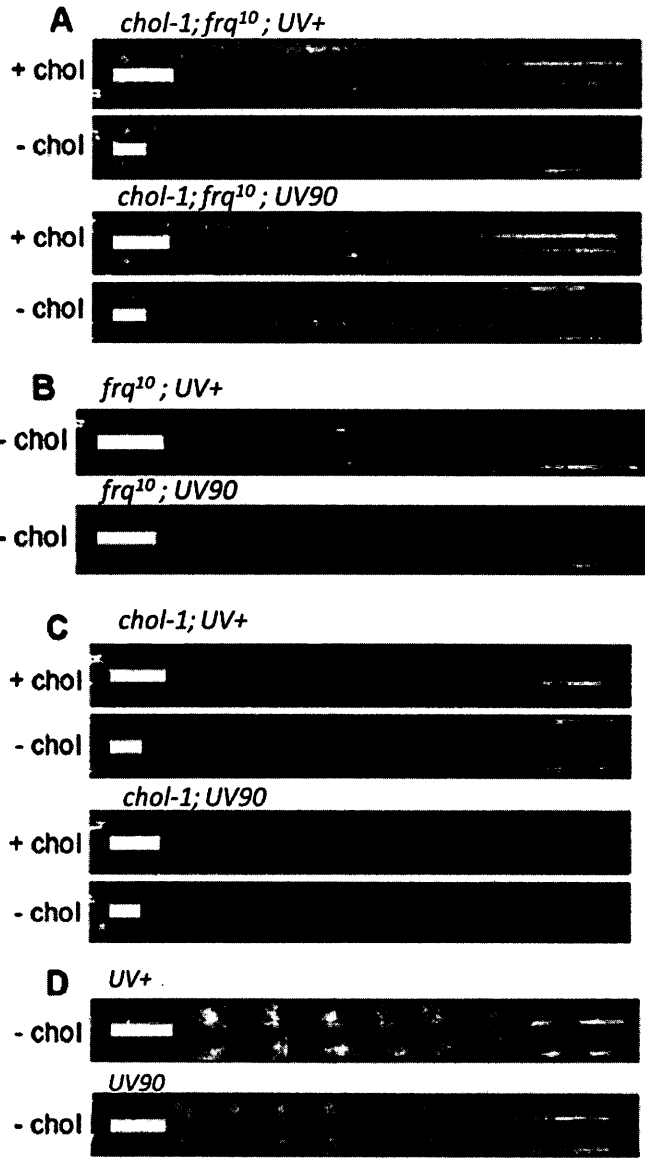
Figure 6. *UV90* phenotype in *chol-1/chol+* and *frq+/frq*^{10} backgrounds. Adapted from Li et al. (2011). + chol = the addition of 100 μM choline to the growth media. – chol = no choline added to the media. Growth is from left to right. White bars indicate average distance of 24 hr growth. Two replicates of each genotype are shown. All strains carry conidial separation (*csp-1*) and band (*bd*) mutations.

CHAPTER 2

MATERIALS AND METHODS

2.1 *Neurospora* strains used

All *Neurospora crassa* strains used were either Mauriceville (MV) or Oak Ridge (OR). *Neurospora* mating types are designated either *A* or *a* (Fincham et al., 1979). Strains kept in the laboratory are labelled with a silica gel number (sg #) corresponding to the order in which they were stored. To obtain progeny for genetic mapping, a cross was performed (previously by Dr. Kamyar Motavaze) between *csp-1; bd; UV90 a* (OR, sg #227) and *csp+; bd+; UV+ A* (wild type MV, sg #258). The band (*bd*) mutation is used to reduce carbon dioxide sensitivity and observe conidiation (spore formation) in closed areas such as test tubes, since carbon dioxide inhibits the appearance of rhythmic band formation (Granshaw et al., 2003; Lakin-Thomas and Brody, 2000). The conidial separation (*csp-1*) mutation is used to prevent spore separation from hyphae and prevents cross-contamination (Granshaw et al., 2003; Lakin-Thomas and Brody, 2000). Both *bd* and *csp-1* mutations have no effect on the circadian rhythm.

Other strains used either for polymerase chain reaction (PCR) or in race tube analyses were: *csp+; bd+; UV+* (wild type OR, sg #259), *csp-1; bd* (OR, sg #1), *csp-1; bd+; UV90* (OR; progeny #131), *csp-1; chol-1 bd; frq^{10}* (OR, sg #80) and *csp-1; chol-1 bd; UV90; frq^{10}* (OR, sg #213). Strains with a choline mutation (*chol-1*) are unable to produce normal levels of the phospholipid phosphatidylcholine and require choline in the medium for normal growth (Lakin-Thomas, 1996). The frequency gene (*frq*) in

Neurospora is an important part of the circadian clock mechanism (Aronson et al.,

1994a). Strains which lack the *frq* gene (*frq^{10}*) are arrhythmic under some conditions

(Aronson et al., 1994b).

DNA from progeny from a cross between *csp-1; prd-1; bd* (OR, sg #250) and MV

(sg #258) was previously prepared by Nardin Nano. *csp-1; prd-1; bd* and *csp-1; prd+;*

bd progeny were used for PCR. *Neurospora* strains that have a period (*prd-1*) mutation

exhibit a disruption of the rhythm in the *csp-1; chol-1 bd; frq^{10}* strain (Li and Lakin-

Thomas, 2010).

Strains used in transformation of *Neurospora* were *csp-1; chol-1 bd* (OR, sg #26)

and *csp-1; chol-1 bd; UV90* (OR, sg #224). The wild type copy of the putative *UV90*

gene used for transformation was taken from *csp-1; chol-1 bd; frq^{10}* (OR, sg #80). The

Fungal Genetics Stock Center (FGSC) knockout strains used are listed in Table 1.

2.2 Genetic Mapping of *UV90* gene

2.2.1 Genetic cross & spore picking

To obtain *UV90* progeny, a cross between *csp-1; bd; UV90 a* (OR, sg #227) and

csp+; bd+; UV+ A (MV, sg #258) was performed using standard genetics techniques and

spores were picked after approximately one month (Davis, 2000). A flame-sterilized

scalpel was used to cut a piece of 4% agar (Appendix I) to fit a microscope slide. Half of

the agar was scored into ~100 squares and the other half was unscored and covered with

1-2 drops of 10% bleach solution. Perithecia from the cross were picked using a flame-

sterilized wire and the spores were spread onto the agar containing bleach. Under a

dissecting microscope, 100 spores were picked and placed on individual agar squares. Care was taken to ensure only mature spores, which appear black and shiny, were picked. Each agar square was placed into a "baby" (10 x 75 mm) test tube containing 1 mL of minimal agar medium (Appendix I). The tubes were placed in a 58 °C water bath for 30 min to heat-shock the spores and left at room temperature to germinate for approximately one week.

2.2.2 *csp-1* "tap test" & race tube analysis

Progeny were tested for the presence of the *csp-1* mutation by the "tap test". Baby tubes were "tapped" on a hard surface and the presence of flying spores appearing as a fine powder indicated the *csp+* phenotype. Progeny that were determined to be *csp-1* were numbered and kept for race tube analyses.

Progeny from baby tubes along with controls were inoculated on either short (30 cm) or long (40 cm) race tubes (cylindrical glass tubes open at both ends) containing maltose-arginine (MA) medium (Appendix I). Race tubes were placed in constant light (LL) for 24 hours at 30 °C and then moved to constant darkness (DD) at 22 °C until growth finished. The growth front was marked on the race tubes daily under red light. For use in genetic mapping, progeny were determined to be either *bd* or *bd+* and *UV+* or *UV90* through visual inspection of the race tubes. Growth rates and periods of progeny were determined through a mathematical program ("MacTau", developed by Dr. Patricia Lakin-Thomas) which compares growth front distances on scanned race tube pictures with daily marking times.

2.2.3 DNA extraction

DNA extraction protocol from Jin et al. (2007) was performed on progeny from the aforementioned genetic cross. DNA extraction was also performed on the parental strains,

csp-1; bd; UV90 (OR, sg #227) and *csp+; bd+; UV+* (MV, sg #258). Progeny were inoculated into 24-well microtiter plates containing 1 mL each of liquid minimal medium (Appendix II) and left to grow at room temperature for 2-3 days. Progeny were also inoculated at the same time onto stock tubes containing minimal agar medium (Appendix I) and left to germinate for approximately one week before freezing.

Mycelia from microtiter wells were rinsed in a vacuum filtration system with double distilled water (dd H_2O) using Whatman P8, 3.5 cm filter papers. Samples were placed into 1.5 mL eppendorf tubes, frozen in liquid nitrogen, and stored at -80 °C until DNA extraction was performed.

Each sample was ground in a separate mortar and pestle pre-cooled with liquid nitrogen and the fungal powder was placed in a 1.5 mL tube. To each sample, 600 μL of DNA extraction buffer with 1% SDS (Appendix II) and 3 μL Proteinase K (20 mg/mL in 20 mM Tris-HCl, 1 mM $CaCl_2$, 50% glycerol, pH 7.5, obtained from New England Biolabs (NEB)) were added, mixed thoroughly and incubated at 65 °C for 1 hour. Samples were vortexed and 200 μL of 7.5 M ammonium acetate was added, mixed thoroughly and left on ice for 5 minutes. Samples were centrifuged at 16,000*g*, 4 °C for 3

minutes, supernatant was removed into a fresh 1.5 mL tube, and RNase A (Appendix II) was added. Samples were vortexed and incubated at 37 °C for 1 hour.

DNA was extracted from each sample with 500 μL chloroform followed by centrifugation at 14,000g, 4 °C for 5 minutes. Supernatant was again removed into a fresh 1.5 mL tube and DNA was precipitated with 650 μL isopropanol followed by centrifugation at 14,000g, 4 °C for 15 minutes. Isopropanol was removed and DNA pellet washed with 70% ethanol followed by centrifugation at 7,500g, 4 °C for 5 minutes. DNA pellet was dissolved in 100 μL TE Buffer (Appendix II).

Each sample was diluted 1/10 (10 μL stock DNA + 90 μL dd H$_2$O) and DNA concentrations were determined using Beckman Coulter DU800 UV/Visible spectrophotometer. Concentrations were read in μg/mL and each sample was diluted to a final concentration of 50 ng/μL, 50 μL total volume, for use in PCR. DNA concentrations (in ng/μL) for some undiluted samples were also determined using Thermo-Fisher Scientific Nanodrop2000 UV/Visible spectrophotometer.

2.2.4 CAPS markers & primer design

Single nucleotide polymorphisms (SNPs) between the *Neurospora crassa* Oak Ridge and Mauriceville strains were used to map the location of the *UV90* gene. The cleaved amplified polymorphic sequence (CAPS) marker method uses specific SNPs that either remove or create an enzyme restriction (or cleavage) site in either the OR or MV strain (Lambreghts et al., 2009). In this study, CAPS markers were used to map the location of the *UV90* gene as in Jin et al. (2007).

39

Locations of SNPs that create specific restriction enzyme cleavage sites in the OR

strain are available on the FGSC website (Pomraning et al., 2010). To create CAPS

markers approximately 500 base pairs (bp) in length, DNA sequences approximately 250

bp upstream and downstream of individual SNP locations were retrieved from the Broad

Institute *Neurospora crassa* database

(www.broadinstitute.org/annotation/genome/neurospora/Regions.html). The DNA

sequence was checked to detect the location of multiple restriction enzyme sites. If

multiple sites appeared for one particular restriction enzyme, another SNP and DNA

sequence was chosen. Forward primers were designed to have GC contents of 50-55%,

melting temperatures (Tm) of 58-65 °C, and lengths of 20-22 nucleotides (nt) using

Thermo-Fisher Scientific "Tm Calculator"

(www.thermoscientificbio.com/webtools/tmc/). Tm's of primers received from

Invitrogen and Integrated DNA Technologies (IDT) were approximately 5 and 10 °C

lower than the calculated Tm's, respectively. Reverse primers were designed with the

above criteria with the following additions: the reverse primer Tm was within 2 °C of the

forward primer, length was within 1 nt of the forward primer, and the reverse and

complement of the DNA sequence was determined using Attotron Biosensor Corporation

"Nucleic Acid Sequence Massager" (www.attotron.com/cybertory/analysis/

seqMassager.htm). Primers were BLASTED against the Broad Institute *Neurospora*

crassa OR genome to ensure there was only one match per primer

(www.broadinstitute.org/annotation/genome/neurospora/Blast.html). An example of a

designed CAPS marker is shown in Appendix III. A complete list of primers, CAPS

markers and SNPs designed for *UV90* mapping are given in Tables 2 and 3.

2.2.5 PCR, restriction enzyme digestion & gel electrophoresis

For genetic mapping of *UV90*, polymerase chain reaction (PCR) was performed

on all progeny from the cross between *bd csp-1 UV90* x MV that underwent DNA

extraction as described in Methods 2.2.3 (see Appendix IV, PCR). *Taq* DNA polymerase

with ThermoPol Buffer (NEB) was used for genetic mapping. The lengths of CAPS

markers are given in Table 3.

Restriction enzyme digestion was performed on all PCR products based on the

enzyme associated with each SNP and CAPS marker given in Table 3 (see Appendix IV,

Restriction Enzymes). All restriction enzymes were obtained from NEB.

Gel electrophoresis was performed on all undigested and digested PCR products

(see Appendix IV, Gel Electrophoresis). A 1.5% agarose gel was used for PCR products

less than 1,000 bp in size and 1.0% for all larger samples. Pictures of gels were taken

using a UV light box at the York University Core Facility. Gel imaging system and

software used was Alpha Innotech Corporation Alpha Ease FluorChem FC2 AIC.

2.2.6 Sequencing putative *UV90* gene

For sequencing the suspected *UV90* gene, PCR and gel electrophoresis were

performed using sequencing primers listed in Table 4 and as described in Methods 2.2.5.

Takara LA Taq DNA polymerase (Takara Bio Inc.) was used instead of *Taq* DNA

polymerase (NEB) due to increased fidelity and improved PCR results with DNA

sequences larger than 1 kb (see Appendix IV, PCR). Number of cycles in PCR Step #2 (Appendix IV, Table A4) was increased to 35 to increase the amount of product. Sizes of DNA sequences were determined based on the locations of sequencing primers used in Table 4.

After gel electrophoresis, any successful PCR products were excised from the gel over a UV light using a scalpel and purified using QIAquick Gel Extraction Kit (QIAGEN). Purified PCR samples were given to the York University Core Facility for sequencing.

PCR products obtained from Integrated DNA Technologies (IDT) primers (see Table 4) were sent to The Centre for Applied Genomics (Hospital for Sick Children, Toronto, Canada). DNA concentrations of these purified samples were determined using NanoDrop2000 UV/Vis spectrophotometer. PCR products under 1 kb in size were diluted to 50 ng in 7 μL. Products under 500 bp were diluted to 20 ng in 7 μL. Primers were diluted to 5 pmol in 0.7 μL and single primers added to individual PCR products. 2-3 replicates of each sample were prepared. Sequences were compared to the *Neurospora crassa* OR genome using BLAST searches at the Broad Institute *Neurospora* database (www.broadinstitute.org/annotation/genome/neurospora/ Blast.html) and the online Swiss Institute of Bioinformatics LALIGN program (http://embnet.vital-it.ch/software/LALIGN_form.html).

2.3 FGSC Knockouts

2.3.1 Knockout *UV90* screening

FGSC knockout strains (shown in Table 1) to screen for the presence of the *UV90*

mutation were ordered using gene loci searches in the FGSC Database

(http://www.fgsc.net/ scripts/StrainSearchForm.asp). Gene loci (given as NCU#####)

were discovered through a gene search between 3.29 and 3.37 Mbp on Linkage Group VI

at the Broad Institute *Neurospora* database

(www.broadinstitute.org/annotation/genome/neurospora/FeatureSearch.html). Knockout

strains were created as described in Colot et al. (2006).

FGSC knockout strains were inoculated onto race tubes containing MA medium

(Appendix I) as described in Methods 2.2.2 along with controls *csp-1; bd+; UV90* (OR,

progeny #131) and OR wild type (sg #259). 2-3 replicates of each strain were inoculated.

Knockouts were compared by visual inspection of the race tubes and therefore period and

growth rate data were not calculated.

2.3.2 Cross between putative *UV90* KO x #80

FGSC knockout strain #18029 (gene NCU05950, Table 1) was chosen as a

putative *UV90* candidate. A cross was performed (previously by Dr. Patricia Lakin-

Thomas) between FGSC #18029 and *csp-1; chol-1 bd; frq^{10}* (OR, sg #80) to check for the

UV90 phenotype in the knockout strain. Spores were picked as described in Methods

2.2.1, and *csp-1* "tap test" was performed as described in Methods 2.2.2. *csp-1* progeny

were inoculated onto race tubes containing MA medium both with and without 100 μM

choline (Appendix I) as described in Methods 2.2.2. Controls on "high choline" (with choline) were *csp-1; chol-1 bd; frq^{10}* (OR, sg #80) and *csp-1; chol-1 bd; UV90; frq^{10}* (OR, sg #213). Controls on "low choline" (without choline) were *csp-1; chol-1 bd* (OR, sg #26), *csp-1; chol-1 bd; UV90* (OR, sg #224), *csp-1; chol-1 bd; frq^{10}* (OR, sg #80) and *csp-1; chol-1 bd; UV90; frq^{10}* (OR, sg #213).

2.4 *Neurospora* transformation

2.4.1 Creation of "AD" CAPS marker & Hygromycin B gene

Transformation of *Neurospora crassa* was performed to test the complementation of *UV90* candidate gene NCU05950 (FGSC #18029, Table 1) in the *UV90* mutant strain. Some *Neurospora* transformation procedures were repeated by Sareh Ahmadi.

A wild type copy of the NCU05950 gene was amplified from *csp-1; chol-1 bd; frq^{10}* (OR, sg #80) with PCR and gel electrophoresis (as described in Methods 2.2.5) using *Takara LA Taq* DNA polymerase (Takara Bio Inc.). Primers used are listed in Appendix V and Tables 4 and 5. This was labelled as CAPS marker "AD". In addition, an EcoRI restriction enzyme site was created in the "AD" CAPS marker based on the overlapping-PCR procedure by Heckman and Pease (2007) to create a method of ensuring the gene is transformed into *Neurospora*. The CAPS marker and primers designed to create the EcoRI restriction site are shown in Appendix V.

Smaller "AB" and "CD" PCR products (Appendix V) were purified using QIAquick Gel Extraction Kit (QIAGEN) and DNA concentrations checked using NanoDrop2000 UV/Vis spectrophotometer. Concentration of final "AD" piece was

estimated by visual inspection of the gel by comparison to NEB values given for PCR

ladders. Restriction enzyme digestion was also performed on "AD" using EcoRI to

ensure the overlapping PCR method produced a second restriction site (Appendix IV,

Restriction Enzymes).

To screen for transformants, the Hygromycin resistance gene (*hyg*) was also

amplified by Dr. Keyur Adhvaryu from the pCSN44 plasmid (obtained from FGSC).

Methods for using Hygromycin B in *Neurospora* transformation were derived from

Staben et al. (1989).

2.4.2 Harvesting & washing conidia

For harvesting conidia (spores), *csp-1; chol-1 bd* (OR, sg #26) and *csp-1; chol-1*

bd; UV90 (OR, sg #224) were previously prepared on stock tubes with minimal medium

(Appendix I) and left to grow at 30 °C, LL for 3-7 days. 10 flasks for *csp-1; chol-1 bd;*

UV90 were prepared with minimal medium for transformation (Appendix VI), inoculated

from the stock tubes and placed in 30 °C, LL for 3-7 days. *csp-1; chol-1 bd* flasks were

prepared and harvested by Sareh Ahmadi.

50 mL of cold 1M sorbitol (Appendix VI) was added to each flask and conidia

were scraped vigorously using a sterile loop. Contents of one flask were combined with a

second and strained into a beaker covered with 3 layers of sterile cheesecloth. This was

repeated for the remaining flasks (5 beakers total). Strained liquid from each beaker was

poured into two sterile 50 mL conical tubes and kept on ice. Tubes were centrifuged at

3,000 rpm, 4 °C for 10 min.

Supernatant was discarded and 10 mL 1M sorbitol was added to one pellet and resuspended. Resuspended pellet was added to a second tube, shaken, and repeated with all conical tubes to concentrate all ten pellets into a single tube. Final pellet was centrifuged, washed and resuspended with 10 mL sorbital two more times. After final wash and centrifugation, conidia pellet was suspended in 500 µL 1M sorbitol and transferred to 1.5 mL screw-cap tubes and stored at -80 °C.

To prepare the spores for transformation, 100 µL of each strain was transferred to 1.5 mL tubes. 1 mL 1M sorbitol was added and mixed. Samples were centrifuged at 5,000 rpm, 4 °C for 5 min. Supernatant was removed and 40 µL 1M sorbitol was added and mixed gently.

2.4.3 DNA precipitation, electroporation and plating

DNA for use in transformation was precipitated. Concentrations of PCR products "AD" and hygromycin resistance gene (*hyg*) were estimated by visual inspection after gel electrophoresis. My "AD" PCR products were combined with Sareh Ahmadi's for a total amount of 2500 ng (in 125 µL). This was divided into two equal 1.5 mL tubes and 1.6 µL of *hyg* (750 ng/µL) was added to each for a 1:1 ratio of AD:*hyg* DNA. Water was added to each sample for a total of 100 µL. To precipitate the DNA, 10 µL of 3.0 M sodium acetate pH 8.0 was added followed by 200 µL absolute (100%) ethanol. Samples were stored at -80 °C overnight. DNA was centrifuged at 13,000 rpm, 4 °C for 5 min. Supernatant was removed, DNA washed with 300 µL of 75% ethanol, and centrifuged

again. Supernatant was removed and pellet air dried for 15-20 min at room temperature.

Final DNA pellet was dissolved in 15 μL dd H₂O.

For the transformation, electroporation cuvettes were pre-cooled on ice. DNA was added

to prepared conidia, mixed gently and left on ice for 5 min. Conidia was transferred to

the cuvette and placed into BioRAD Gene Pulser II (conditions: 1.5 kV, 7.5 kV/cm,

capacitance: 25 μF; resistance: 600 ohms). *UV+* strain was electroporated for 13.4

milliseconds, *UV90* for 10.3 milliseconds. 1 mL recovery medium (Appendix VI) was

immediately added to each strain, gently mixed and transferred into 1.5 mL tubes. Tubes

were placed horizontally on a shaker platform for 1 hour at 150 rpm to recover.

After recovery, 1/10 (100 μL spores + 900 μL recovery medium) and 1/100 (100

μL of 1/10 dilution + 900 μL recovery medium) dilutions were prepared for each strain.

1 mL of each dilution (including original, undiluted transformed spores) was placed into

15 mL top agar and poured into three plates (5 mL each) containing bottom agar with

hygromycin (Appendix VI). Plates were incubated face up at 30 °C, LL for 3-7 days.

2.4.4 Race tube & PCR analysis of transformants

Transformants from the petri plates were inoculated onto minimal agar stock

tubes (Appendix I) with the addition of 1.5 mL choline (2 mg/mL) and 0.4 mL

hygromycin (50 mg/mL) per 100 mL added after autoclaving, and incubated at 30 °C,

LL. They were also tested for the ability to grow on hygromycin using liquid minimal

medium in microtiter wells (Appendix II). 1 mL choline (10 mM) and 0.4 mL

47

hygromycin (50 mg/mL) per 100 mL were added after autoclaving. Wells were inoculated and placed in 30 °C, LL.

Transformants were grown on race tubes containing MA medium with choline as described in Methods 2.2.2, with the addition of 0.4 mL hygromycin (50 mg/mL) per 100 mL added after autoclaving. Parental controls (*csp-1; chol-1 bd* and *csp-1; chol-1 bd; UV90*) did not receive the addition of hygromycin.

DNA was extracted from transformants as described in Methods 2.2.3. PCR, restriction enzyme digestion with EcoRI, and gel electrophoresis was performed as described in Methods 2.2.5 using *Takara LA Taq* polymerase. PCR was performed with F4, R4, F1 and R1 primers (Table 4) on transformants as well as *csp-1; chol-1 bd; frq^{10}* (OR, sg #80), *csp-1; chol-1 bd; UV90; frq^{10}* (OR, sg #213), and *csp-1; bd; UV90* (OR, sg #227).

Table 1.
Fungal Genetics Stock Center (FGSC) knockout strains used to screen for the *UV90* mutation

FGSC #*	Mating Type	Genotype (gene locus)**	Linkage Group (chromosome) #	Race Tube #
17842	A	NCU05958.2	VI	1
13721	A	NCU05957.2	VI	2
17841	A	NCU05954.2	VI	3
17839	A	NCU05952.2	VI	4
18085	a	NCU05951.2	VI	5
17845	A	NCU05962.2	VI	6
11909	A	NCU05961.2	VI	7
11310	A	NCU05956.2	VI	8
13535	A	NCU05955.2	VI	9
18029	A	NCU05950.2	VI	10
17838	A	NCU05949.2	VI	11
18213	A	NCU05948.2	VI	12
18028	A	NCU05947.2	VI	13
17836	A	NCU05946.2	VI	14
17835	A	NCU05945.2	VI	15
13533	A	NCU05944.2	VI	16

*FGSC numbers were determined through the FGSC Strain Database (http://www.fgsc.net/scripts/StrainSearchForm.asp)
**Genotypes were determined through gene searches at the Broad Institute *Neurospora crassa* database
(http://www.broadinstitute.org/annotation/genome/neurospora/FeatureSearch.html)

Table 2.

Primers designed for CAPS markers and genetic mapping of the *UV90* gene on Linkage Group VI

Primer Name	Sequence 5' -> 3'	Location (bp) and strand (+/-)	Length (nt)*	GC content (%)*	Tm (°C)*
F3**	ACCTACTTGCGACAGCGTGCTTG	2,059,068-090 (-)	23	56.52	71.6
R3**	TTGTCCACTTACACTCGGCACG	2,057,830-851 (+)	22	54.55	69.6
F6**	TTCACGAGTGTCCCGGATGTG	2,141,366-386 (-)	21	57.14	70.9
R6**	GCATTGTCATCTCGTTGGTGC	2,140,152-172 (+)	21	52.38	68.2
F9**	AAGGTCGGGTTGTTAGACGA	2,410,071-090 (-)	20	50	63.8
R9**	GGCTGAGGGTGGATAGCTAGA	2,409,630-650 (+)	21	57.14	64.8
LCF1	CGGCCGTGTAGCAGAATACA	2,726,641-660 (+)	20	55	66.32
LCR1	ATAATGGCGATGGCGATGTG	2,727,065-084 (-)	20	50	68.10
LCF2	GGGCGCCATCAATTTCACTT	2,734,610-629 (+)	20	50	68.36
LCR2	TTTGAGCTCGGGATTTGCTG	2,735,067-086 (-)	20	50	67.72
RCF3	CTTTTCGGAGCTGGTCAGCA	3,127,818-837 (+)	20	55	68.06
RCR3	ACCCAGGACATGCAAGGGTT	3,128,243-262 (-)	20	55	68.09
RCF4	ATCCAGTACCCGTCCCCAAA	3,153,328-347 (+)	20	55	67.71
RCR4	CAACCCAAGCTCAACTGCCA	3,153,772-791 (-)	20	55	68.85
F10	TCATCGAGTTACCTGCCAAGC	2,547,480-500 (+)	21	52.38	66.68
R10	TTGGGTGTTCGTTGGACTCC	2,547,877-896 (-)	20	55	67.55

Primer Name	Sequence 5' -> 3'	Location (bp) and strand (+/-)	Length (nt)*	GC content (%)*	Tm (°C)*
F11	GGTAACTATGTACATGCCCCGTG	2,559,077-099 (+)	23	52.17	66.26
R11	CGATACGATTCTTGGCATCAGC	2,559,500-521 (-)	22	50	67.9
RCF5	GCGAATTGGAAATCTCCAAGGG	3,102,391-412 (+)	22	50	69.62
RCR5	ATCTCCCACGTAGCCTTGGCTT	3,102,900-921 (-)	22	54.55	69.08
RCF6	TTTGGCCTGGGCTCATGTTAGT	3,133,754-775 (+)	22	50	68.82
RCR6	CTCACCATGATGGGGGAAGAT	3,134,286-306 (-)	21	52.38	67.44
668F ***	ATGTCTTGGGTGTTTGGCAT	3,293,478-497 (+)	20	45	64.57
668R ***	TCCTCAAGATCGTCACTCAGC	3,294,181-201 (-)	21	52.38	64.98
F15	TCCAGCAGCACTAGCACAACGT	3,476,119-140 (+)	22	54.55	69.49
R15	GAAATGGACGTAGCAACCGAGG	3,476,554-575 (-)	22	54.55	68.82
F16	ATCCAATCTCTTCCCGGTGTG	3,483,486-506 (+)	21	52.38	67.52
R16	TCTTGGTTAGTGTAGCCGCACC	3,483,923-944 (-)	22	54.55	67.45
3317F	CTCGGACGACAAGTCACCAACA	3,317,357-378 (+)	22	54.55	69.88
3317R	CGTCCCTCTGATGCCCAAAGTA	3,317,838-859 (-)	22	54.55	69.45
3346F	CTTGAACGAGTTCCAGCCCTGA	3,346,503-524 (+)	22	54.55	69.91
3346R	CAGTGGTTGATCACCCAACCAA	3,346,963-984 (-)	22	50	69.30
3368F	GAAATACCGGGCGCATTACCA	3,368,165-185 (+)	21	52.38	69.67
3368R	TGTTGATTGGCTGTCGGTGG	3,368,673-692 (-)	20	55	69.72

Primer Name	Sequence 5' -> 3'	Location (bp) and strand (+/-)	Length (nt)*	GC content (%)*	Tm (°C)*
3395F	TTGCTTGCTTTGTCTCGGACG	3,395,402-422 (+)	21	52.38	69.87
3395R	ACAGAGTTGGGTGTTCACGTGG	3,395,890-911 (-)	22	54.55	68.69
3436F	GGACAGCTTCTCCGAGCGATTT	3,436,787-808 (+)	22	54.55	69.91
3436R	CGTTGACGGACTCTGAATGAGG	3,437,239-260 (-)	22	54.55	68.33
3451F	TCCCGCCAGTAGTGAAACCTTC	3,451,512-533 (+)	22	54.55	68.54
3451R	CGTCAGCTTCGTCCTCATCAAC	3,451,989-3,452,010 (-)	22	54.55	68.47
3333F	CGACCACCATACTTGCGGTTGT	3,332,973-994 (+)	22	54.55	70.18
3333R	TGGGCATTGTCCTCACTCCTGA	3,333,417-438 (-)	22	54.55	71.47
3352F	TTCTTACCTTTGCCTGTCGCCG	3,352,740-761 (+)	22	54.55	71.19
3352R	ACTGGGGCAAAGAGAAAAGCGC	3,353,183-204 (-)	22	54.55	71.43

*Calculated using "Tm calculator" (http://www.thermoscientificbio.com/webtools/tmc/);
All primers ordered from Invitrogen
**Designed by Dr. Kamyar Motavaze
***Sequence obtained from Jin et al. (2007)

Table 3.

Linkage Group VI CAPS markers, single nucleotide polymorphisms (SNPs) and restriction enzymes for mapping of *UV90* gene

CAPS marker (see Table 2 for primers)	Total size (bp)	SNP location	Base pair (bp) change in OR -> MV	SNP restriction enzyme
F6-R6	1,235	Unknown*	Cut in OR Uncut in MV	EcoRI
F9-R9	461	Unknown*	Cut in OR Uncut in MV	Taqα1
LCF1-LCR1	444	2,726,773	T -> A	Taqα1
LCF2-LCR2	477	2,734,761	C -> T	HaeIII
RCF3-RCR3	445	3,127,958	G -> A	HaeIII
RCF4-RCR4	464	3,153,461	C -> T	Taqα1
F10-R10	417	2,547,621	C -> A	HaeIII
F11-R11	445	2,559,175	G -> A	Taqα1
RCF5-RCR5	531	3,102,537	G -> A	Taqα1
RCF6-RCR6	553	3,133,969	C -> T	MspI
668F-668R	724	Unknown**	Uncut in OR Cut in MV	MspI
F15-R15	457	3,476,241	G -> T	Taqα1
F16-R16	459	3,483,592	G -> A	HaeIII
3317F-3317R	503	3,317,544	A -> G	Taqα1
3346F-3346R	482	3,346,642	C -> T	Taqα1
3368F-3368R	528	3,368,360	T -> C	MseI
3395F-3395R	510	3,395,716	G -> A	Taqα1
3436F-3436R	474	3,436,987	T -> C	Taqα1
3451F-3451R	499	3,451,692	A -> G	MseI
3333F-3333R	466	3,333,091	C -> G	HaeIII
3352F-3352R	465	3,352,908	T -> C	Taqα1

*Designed by Dr. Kamyar Motavaze; SNP is unknown
**Sequence obtained from Jin et al. (2007); SNP is unknown

Table 4.

Primers designed for sequencing of Broad Institute gene "NCU05950" (*UV90* gene candidate) on Linkage Group VI

Primer Name	Sequence 5' -> 3'	Location (bp) and strand (+/-)	Length (nt)*	GC content (%)*	Tm (°C)*
F6	GACATTGGCCGCAGATGGAT	3,345,920-939 (+)	20	55	69.68
F5	GGAACCTCCGAAGAAAGGAAGG	3,346,404-425 (+)	22	54.55	68.17
F4	CCGGATGACTTCATCTTCCCTG	3,346,862-883 (+)	22	54.55	69.11
F3	CTTGGAACCGCGCAGTAACAT	3,348,428-448 (+)	21	52.38	68.38
F2	TACTTCGACGACGTCTGGCTTC	3,347,890-911 (+)	22	54.55	67.90
F1	CCGTGACACATTTGTTGCTGC	3,347,371-391 (+)	21	52.38	69.08
R1	TCCGGAACAGCATCAGGAAAG	3,348,966-986 (-)	21	52.38	68.76
R2	CATGGGTTTATCATGCGGGAC	3,348,468-488 (-)	21	52.38	68.44
R3	CCGTCGCGAAGAGATGAAACTC	3,347,852-873 (-)	22	54.55	69.39
R4	AAATGGCTGTGGTCGCATCTC	3,349,471-491 (-)	21	52.38	68.73
R5	ATGAGGAAGCCGAGAGCATCTC	3,349,938-959 (-)	22	54.55	68.25
R6	CCGGTATGAGCGTCGGAATTT	3,350,451-471 (-)	21	52.38	69.12
R7	GCCCGGATGTTTGTTTCGTTC	3,350,986-3,351,006 (-)	21	52.38	69.70
R8	TCAGTCTTTTTGGTCACGGACG	3,351,543-564 (-)	22	50	68.6
R9	ACTCGCACATGCATACTCGCA	3,352,122-142 (-)	21	52.38	69.33
UV90A For **	ACGTGGACTGTTGCGTGACAC	3,348,179-199 (+)	21	57.14	69.0

54

Primer Name	Sequence 5' -> 3'	Location (bp) and strand (+/-)	Length (nt)*	GC content (%)*	Tm (°C)*
UV90A Rev **	GTGTCACGCAACAGTCCACGT	3,348,179-199 (-)	21	57.14	69.0
UV90B For **	AACTTTACCGATGCCGCTGC	3,348,687-706 (+)	20	55	68.5
UV90B Rev **	GCAGCGGCATCGGTAAAGTT	3,348,687-706 (-)	20	55	68.5
FlipR1 For **	CTTTCCTGATGCTGTTCCGGA	3,348,966-986 (+)	21	52.38	68.8
FlipR4 For **	GAGATGCGACCACAGCCATTT	3,349,471-491 (+)	21	52.38	68.7

*Calculated using "Tm calculator" (http://www.thermoscientificbio.com/webtools/tmc/)
**Primers ordered from Integrated DNA Technologies (IDT); all others ordered from Invitrogen

Table 5.
Mutagenic primers designed for PCR-driven overlap extension in the transformation of
Neurospora crassa

Primer Name	Sequence 5' -> 3'	Length (nt)*	GC content (%)*	Tm (°C)*
ForC-NCU5950	GCGTTCAGCGAATTCGATAGGT	21	52.38	67.6
RevB-NCU5950	ACCTATCGAATTCGCTGAACGC	21	52.38	67.6
For2C-NCU5950	TCAGCGAATTCGATAGGTCTGCGGCCAG	27	59.26	79.48
Rev2B-NCU5950	CTGGCCGCAGACCTATCGAATTCGCTGA	27	59.26	79.48
For3C-NCU5950	CTTTCCTGATGCTGAATTCCGGA	21	52.38	68.76
Rev3B-NCU5950	TCCGGAATTCAGCATCAGGAAAG	21	52.38	68.76
AD-Rp	ACCGGACAAGATGGCTTGGTA	21	52.38	67.91

*Calculated using "Tm calculator" (http://www.thermoscientificbio.com/webtools/tmc/);
Criteria for mutagenic primers were calculated for correctly matched sequences only

CHAPTER 3

RESULTS

3.1 Genetic Mapping of *UV90* gene

3.1.1 Genetic mapping using CAPS markers

Progeny from the *csp-1; bd; UV90* x Mauriceville cross were initially sorted via race tube analyses into *UV90* or *UV+* phenotypes, and therefore contained either *UV90* or *UV+* DNA at the mutated gene. However, progeny may contain either Oak Ridge (OR) or Mauriceville (MV) DNA sequences at other random locations in the genome. Genes farther away from the *UV90* gene have greater rates of recombination (chromosomal crossover events between OR and MV parental strains), whereas genes next to *UV90* will exhibit very few recombination events. Genes closer together are linked and experience fewer recombination rates between them due to the close physical distance (Griffiths et al., 1993). Recombinant progeny will exhibit the *UV90* (OR) or *UV+* (MV) phenotype on the race tubes but show opposing parental DNA at other locations on the genome, indicating a crossover event between *UV90* and the other location. Recombination rates between the *UV90* gene and specific DNA sequences, called Cleaved Amplified Polymorphic Sequence (CAPS) markers will be used to determine the *UV90* gene location through PCR and restriction enzyme digestion. Left-right mapping will be performed to map the specific location of the UV90 gene between CAPS markers. The CAPS markers contain single nucleotide polymorphisms (SNPs) between the OR and

MV strains to distinguish which parental DNA each progeny has at a particular location, and therefore determines which progeny are recombinant.

3.1.2 CAPS markers F6-R6, F9-R9 and *prd-1* progeny

Classification of progeny:

To determine the location of the *UV90* gene, genetic mapping was performed using PCR and restriction enzyme digestion on progeny resulting from the cross between *csp-1; bd; UV90* (Oak Ridge (OR), sg #227) and Mauriceville (MV) wild type (sg #258). This cross was previously performed by Dr. Kamyar Motavaze. 192 spores were picked and placed in test tubes with minimal agar medium and allowed to germinate, as described in Methods 2.2.1. Progeny cultures were visually inspected for the *csp*+ or *csp-1* phenotype by the "tap" test (Methods 2.2.2). 87 progeny were found to be *csp-1*, 93 were *csp*+, and 12 did not germinate (Table 6).

csp-1 progeny were numbered and inoculated onto maltose-arginine medium in race tubes as described in Methods 2.2.2. The first growth mark on the race tubes (Fig. 7) denotes the moment the tubes were transferred from constant light (LL) to constant darkness (DD). Replicate tubes of the following controls were also inoculated: *csp-1; bd* (sg #1), *csp-1; bd; UV90* (sg #227) and *csp*+; *bd*+; *UV*+ (MV, sg #258). Through visual inspection, 44 out of 87 were determined to be *csp-1; bd; UV*+ or *UV90* by resembling either sg #1 or sg #227 (Fig. 7; Table 7). *bd* strains have slower growth rates than *bd*+ which is seen by the growth fronts marked daily on the tubes (Fig. 7). 42 progeny were

classified as *csp-1; bd+* by having faster rates of growth and resembling sg #258 (Fig. 8; Table 7). One race tube was unclassifiable as either *bd+* or *bd* (Fig. 8; Table 7).

25 *csp-1; bd* progeny were visually determined to be *csp-1; bd; UV90* due to weak, low amplitude rhythms (Fig. 9; Table 8). 14 showed clear, strong rhythms and were determined to be *csp-1; bd; UV+* (Fig. 10; Table 8), and 5 were unclassifiable as either *UV+* or *UV90* (Table 8). Only *csp-1; bd* progeny were kept for further use in PCR and restriction enzyme analysis.

A few unclassifiable progeny are typically seen in a genetic cross due to minor genetic variations between the parental strains. Also, a few mutations may collect in the nuclei in the parental strains which show up in the progeny after being put through a cross. There is the possibility that recombination events occurred in some progeny bringing together variant genes that can cause slow growth rates and unusual phenotypes on the race tubes. The low numbers of unclassifiable progeny in the cross suggest that this is merely a chance occurrence and not related to the *UV90* gene.

Out of 44 *csp-1; bd* progeny, 25 (56.8%) exhibited the *UV90* phenotype and 14 (31%) were *UV+* (Table 8). The approximate 50% segregation of *UV90* from *UV+* follows Mendelian genetic ratios and confirms the presence of a single gene mutation (Griffiths et al., 1993). However, since fewer than 50% *UV+* progeny were observed, a chi-square test was performed to determine if the observed values fall within chance deviations. For Table 8, the *p* value was determined to be non-significant ($p = 0.0685$),

59

indicating that the slightly lower *UV+* values observed are likely due to chance deviations, and not linked genes (Appendix X).

The periods and growth rates of the final 39 *UV+* and *UV90* progeny were determined through a mathematical program ("MacTau", developed by Dr. Patricia Lakin-Thomas) which compares growth front distances on scanned pictures with daily marking times to determine the period lengths and growth rates (Table 9). The mean growth rate for the *csp-1; bd; UV90* progeny was 0.99 (± 0.014) mm/hr, while *csp-1; bd; UV+* progeny had a mean growth rate of 1.09 (± 0.036) mm/hr and a period of 23.19 (± 0.486) hr (Table 9). Although both the *csp-1; bd; UV90* and *UV+* growth rates are lower than the previously reported values of 1.16 and 1.29 mm/hr, respectively, and the *UV+* period is slightly slower than the reported 21.2 hrs., results confirm that *UV90* is slower growing than the wild type (Li et al., 2011).

<u>CAPS markers F6-R6 and F9-R9:</u>

DNA extraction was performed on the 39 *csp-1; bd; UV+* and *UV90* progeny along with parental strains *csp-1; bd; UV90* and MV wild type as described in Methods 2.2.3. The DNA concentrations ranged from 193-712 µg/mL (data not shown). CAPS markers F6-R6 and F9-R9 were designed and obtained by Dr. Kamyar Motavaze (Tables 2 and 3, Materials and Methods). PCR, restriction enzyme digestion and gel electrophoresis were performed on the parental strains and 39 *UV+* and *UV90* progeny as described in Methods 2.2.5.

PCR and restriction enzyme digestion was performed on the *UV+* and *UV90* progeny using CAPS markers F9-R9 and F6-R6. F9-R9 produced 2 *UV+* recombinants (Fig. 11) and 5 *UV90* recombinants (Fig. 12). Additional *UV90* progeny for F9-R9 are shown in Appendix VII (Fig. A1). F6-R6 produced identical recombinant progeny, 2 for *UV+* and 5 for *UV90* (Figs. 13 and 14). Additional *UV90* progeny for F6-R6 are shown in Appendix VII (Fig. A2).

A list of the PCR results for F6-R6 and F9-R9 CAPS markers are listed in Table 10. 7 out of 39 progeny were recombinant for both CAPS markers (Table 10). Primers F6, R6, F9 and R9 were re-ordered from Invitrogen and PCR was repeated for all progeny. Identical results were obtained (data not shown). To re-test the phenotypes, all 39 progeny were re-inoculated onto race tubes containing maltose-arginine medium as described above along with controls *csp-1; bd* (sg #1) and *csp-1; bd; UV90* (sg #227). 5 *UV+* and 5 *UV90* progeny produced unclear phenotypes (Fig. 15) and were removed from further analyses, reducing the number of recombinants to 3 out of 29 (Table 10).

prd-1 progeny:

Due to the identical recombinant progeny and zero recombination seen between markers F6-R6 and F9-R9, it was suspected that the markers were possibly binding to an incorrect location, or that there possibly was an inversion between those markers. Therefore, the CAPS markers were tested using another Oak Ridge strain with a period mutation (*prd-1*) on a different chromosome than *UV90*.

DNA from progeny from a cross between *csp-1; prd-1; bd* (OR, sg #250) and MV

(sg #258) was previously prepared by Nardin Nano. PCR and restriction enzyme

digestion on *csp-1; prd-1; bd* and *prd+* progeny were performed with F6-R6 and F9-R9

CAPS markers. Gel electrophoresis of *csp-1; prd-1; bd* progeny #1-64A with F9-R9

primers is shown in Fig. 16. *csp-1; prd-1; bd* progeny #1-64A with F6-R6 primers is

shown in Fig. 17. Gels from remaining *csp-1; prd-1; bd* and *prd+* progeny are not

shown. A complete list of PCR results for *prd-1* and *prd+* progeny using F6-R6 and F9-

R9 CAPS markers is given in Table 11. 12 out of 25 *prd-1*, and 9 out of 20 *prd+*

progeny were recombinant for F6-R6 and F9-R9 (Table 11). The *prd-1* gene is located

on Linkage Group III (Li and Lakin-Thomas, 2010), and therefore high recombination

values were expected with CAPS markers F6-R6 and F9-R9 which are located on

Linkage Group VI. Unlinked genes should produce recombination rates close to 50%

(Griffiths et al., 1993), which was observed with the *prd-1/prd+* progeny with both

markers. This confirmed that the primers were binding to the correct locations and that

there is reduced recombination between markers F6-R6 and F9-R9.

Figure 18 shows a schematic of Linkage Group VI with primers F3, F6, F9 and

668F. Dr. Kamyar Motavaze also performed genetic mapping on a different set of *UV+*

and *UV90* progeny from the cross between *csp-1; bd; UV90* (OR, sg #227) and MV wild

type (sg #258). CAPS marker F3-R3 produced 10 out of 49 recombinants, while F6-R6

and F9-R9 produced 7 out of 49 recombinants (data from Dr. Kamyar Motavaze). My

UV90 progeny produced 3 out of 29 recombinants with F6-R6 and F9-R9. No

recombination was seen between F6-R6 and F9-R9 CAPS markers in either case.

Genetic mapping of progeny from the same cross by Daniel Rubinger produced 4 out of

54 recombinants with 668F-668R. The decreasing numbers of recombinants moving

from marker F3-R3 to F9-R9 suggest that *UV90* is further downstream to the right of F9-

R9, yet its exact location on either side of the centromere is unknown (Fig. 18).

Table 6. *csp+* and *csp-1* progeny from cross between *csp-1; bd; UV90* (OR, sg #227) and *csp+; bd+; UV+* (MV, sg #258)

Total spores picked	*csp-1* progeny	*csp+* progeny*	Non-germinating progeny*
192	87/192 (45.3%)	93/192 (48.4%)	12/192 (6.3%)

*csp+ and non-germinating progeny were excluded from further analysis

Table 7. *csp-1* progeny from cross between *csp-1; bd; UV90* (OR, sg #227) and *csp+; bd+; UV+* (MV, sg #258)

Total *csp-1* progeny analyzed	*csp-1; bd* progeny	*csp-1; bd+* progeny*	Unclassifiable progeny*
87	44/87 (50.6%)	42/87 (48.3%)	1/87 (1.1%)
	(progeny #: 3, 5, 6, 8, 9, 12, 13, 15, 17, 19, 21, 23, 27-29, 31, 32, 35, 36, 41, 44, 47-51, 53, 55, 57, 58, 61, 65, 67, 68, 70, 71, 74, 75, 78-81, 83, 87)	(progeny #: 1, 2, 4, 7, 10, 11, 14, 16, 18, 20, 22, 24-26, 30, 33, 34, 37-40, 42, 43, 45, 46, 52, 56, 59, 60, 62-64, 66, 69, 72, 73, 76, 77, 82, 84-86)	(progeny #54)

*bd+ and unclassifiable progeny were excluded from further analysis

Table 8. *csp-1; bd; UV90* and *UV+* progeny from cross between *csp-1; bd; UV90* (OR, sg #227) and *csp+; bd+; UV+* (MV, sg #258)

Total *csp-1; bd* progeny analyzed	*csp-1; bd; UV90* progeny	*csp-1; bd; UV+* progeny	Unclassifiable progeny*
44	25/44 (56.8%)	14/44 (31%)	5/44 (11.4%)
	(progeny #: 3, 5, 6, 8, 15, 23, 28, 29, 31, 32, 35, 36, 41, 48, 50, 51, 57, 67, 68, 71, 74, 78, 81, 83, 87)	(progeny #: 9, 12, 13, 17, 21, 27, 53, 55, 58, 61, 70, 75, 79, 80)	(progeny #: 19, 44, 47, 49, 65)

*Unclassifiable progeny were excluded from PCR and restriction enzyme analysis

Table 9. Periods and growth rates of *csp-1; bd; UV90* and *csp-1; bd; UV+* progeny

csp-1; bd; UV90 progeny			csp-1; bd; UV+ progeny		
Progeny #	Growth Rate (mm/hr)	Period (hr)	Progeny #	Period (hr)	Growth Rate (mm/hr)
csp-1; bd; UV90 (control)	1.12	N/A*	*csp-1; bd* (control)	21.95	1.26
3	0.92		9	22.07	1.04
5	1.07		12	21.85	1.19
6	1.06		13	26.01	1.18
8	1.06		17	21.38	1.08
15	0.97		21	20.97	1.18
23	1.04		27	25.80	1.05
28	0.94		53	25.20	1.10
29	0.95		55	23.63	1.11
31	0.95		58	21.92	0.86
32	0.93		61	21.16	1.20
35	1.05		70	23.22	0.95
36	1.03		75	22.02	1.30
41	1.11		79	24.20	0.84
48	1.06		80	25.33	1.20
50	1.05			**Mean Period: 23.19 ± 0.486 (S.E.M.)**	**Mean Growth Rate: 1.09 ± 0.036 (S.E.M.)**
51	1.13				
57	1.01				
67	0.95				
68	1.00				
71	0.98				
74	0.86				
78	0.88				
81	0.94				
83	1.05				
87	0.94				
	Mean Growth Rate: 0.99 ± 0.014 (S.E.M)				

*Not applicable: progeny showed low amplitude, unclear rhythms; period was not calculated
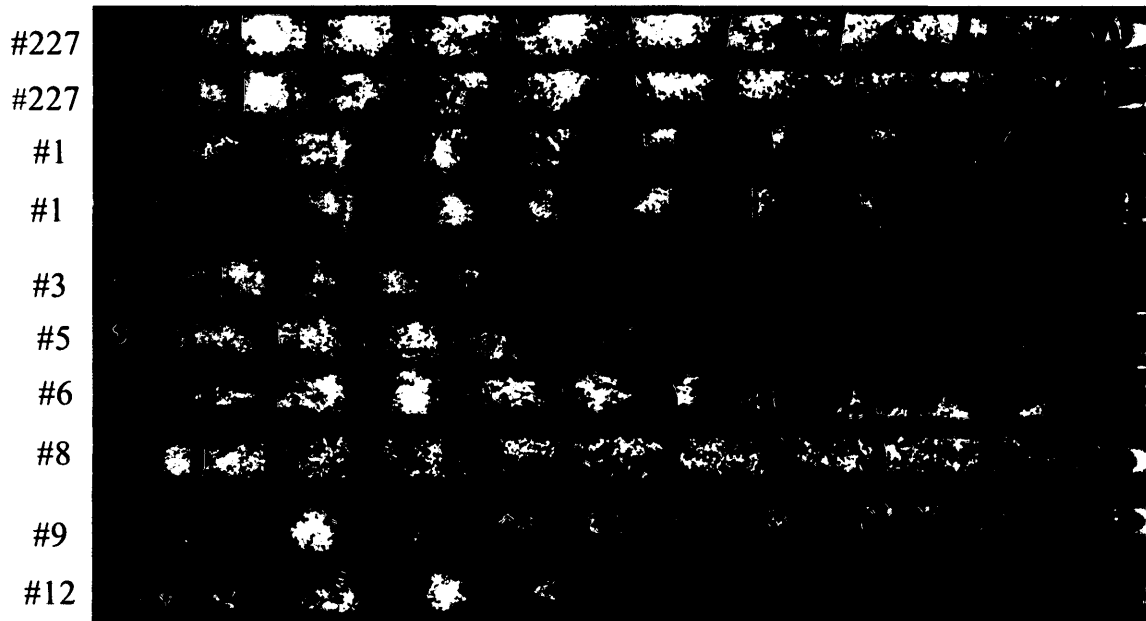
Figure 7. Examples of *csp-1; bd; UV90* or *UV+* progeny obtained from *csp-1; bd; UV90*

x *csp+; bd; UV+* (Mauriceville wild type) cross.

#1 (*csp-1; bd*) and #227 (*csp-1; bd; UV90*) served as controls. Progeny #3 through #12

were placed first into the *bd* category. Progeny showed similar band patterns, growth

rates (marked growth fronts) and physical appearance when compared to either of the *bd*

controls.

Growth on all race tubes is from left to right. Vertical marks show the position of the

growth front at daily intervals.
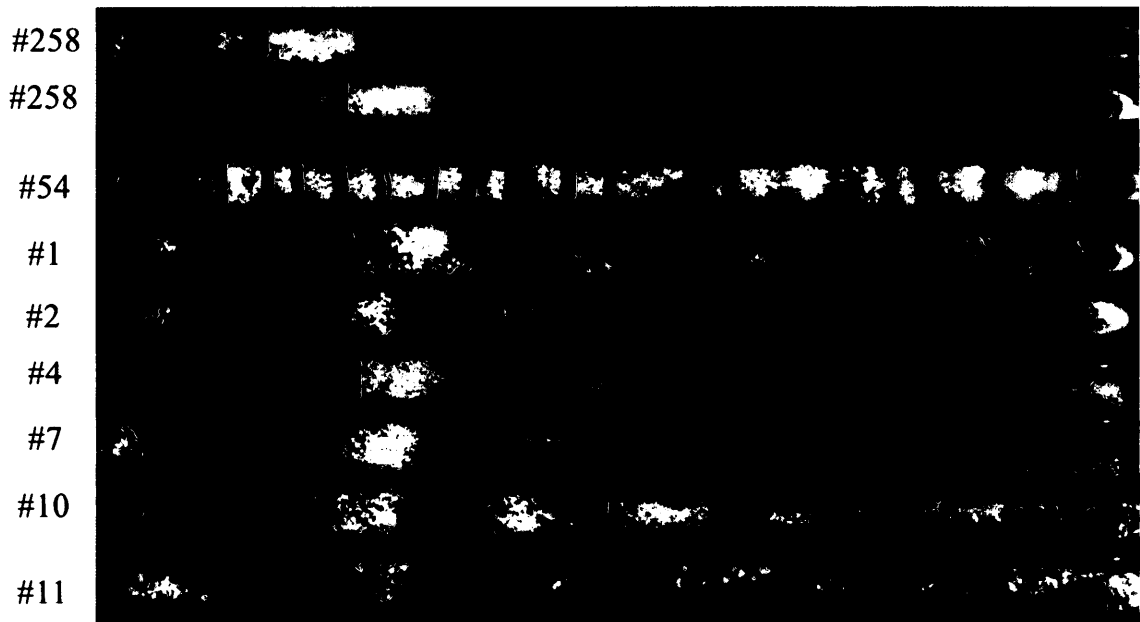
Figure 8. Examples of *csp-1; bd+; UV90* or *UV+* progeny obtained from *csp-1; bd;*

UV90 x *csp+; bd+; UV+* (Mauriceville wild type) cross.

#258 (Mauriceville wild type) served as a control. Progeny #1 through #11 were placed

into the *bd+* category first. Progeny showed similar band patterns, growth rates (marked

growth fronts) and physical appearance in comparison to *bd+* control. #54 was

unclassifiable due to abnormal growth rate and physical appearance.

A

#48
#41
#36
#35
#32
#29
#28
#23
#15
#8
#227
#227

B

#48
#41
#36
#35
#32
#29
#28
#23
#15
#8
#227
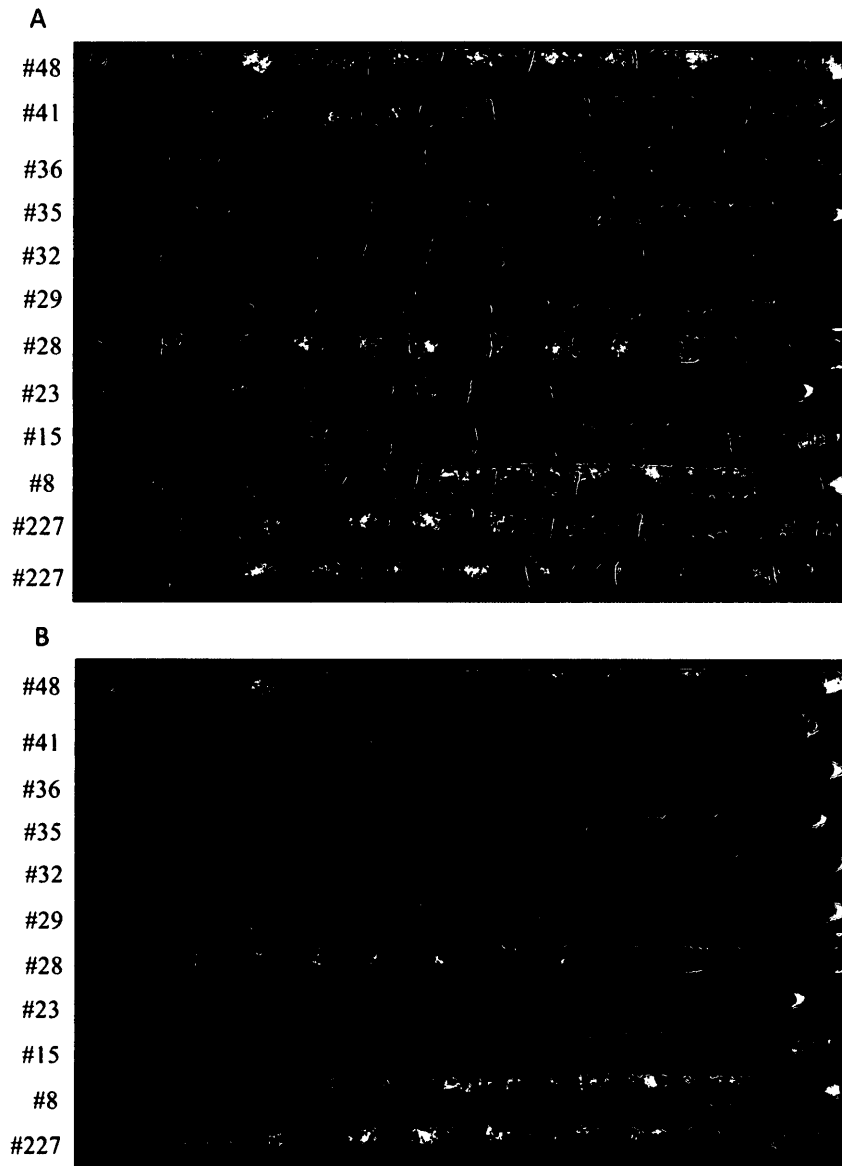
Figure 9. Examples of *csp-1; bd; UV90* progeny with (A) and without (B) marked

growth fronts, obtained from *csp-1; bd; UV90* x *csp+; bd+; UV+* (Mauriceville wild

type) cross. #227 (*csp-1; bd; UV90*) served as a control. Progeny #8 through #48

showed either low amplitude rhythms or constant conidiation, and similar physical

appearance as the control.
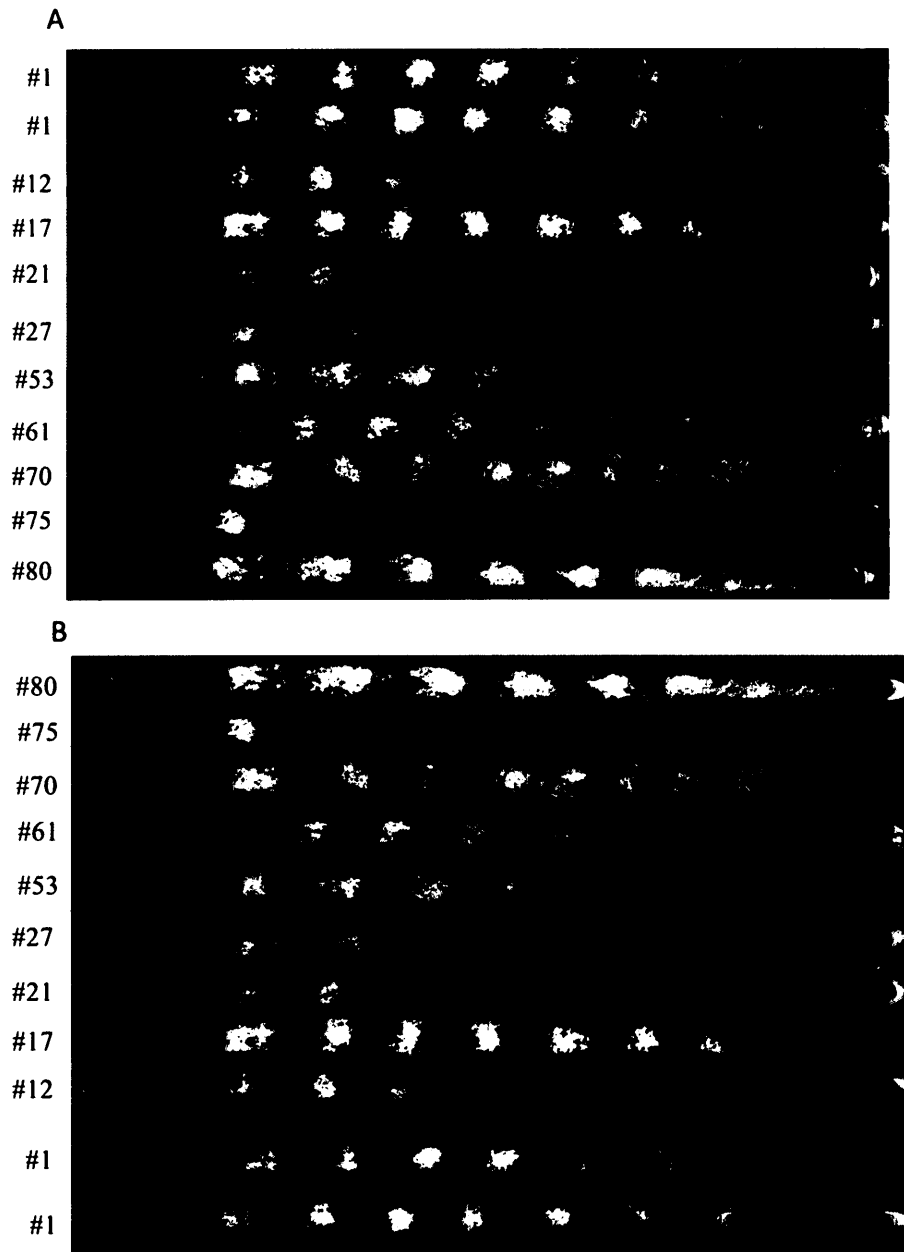
Figure 10. Examples of *csp-1; bd; UV+* progeny with (A) and without (B) marked

growth fronts, obtained from *csp-1; bd; UV90* x *csp+; bd+; UV+* (Mauriceville wild

type) cross. #1 (*csp-1; bd*) served as a control. Progeny #12 through #80 showed strong

rhythmic conidiation and similar physical appearance as the control.
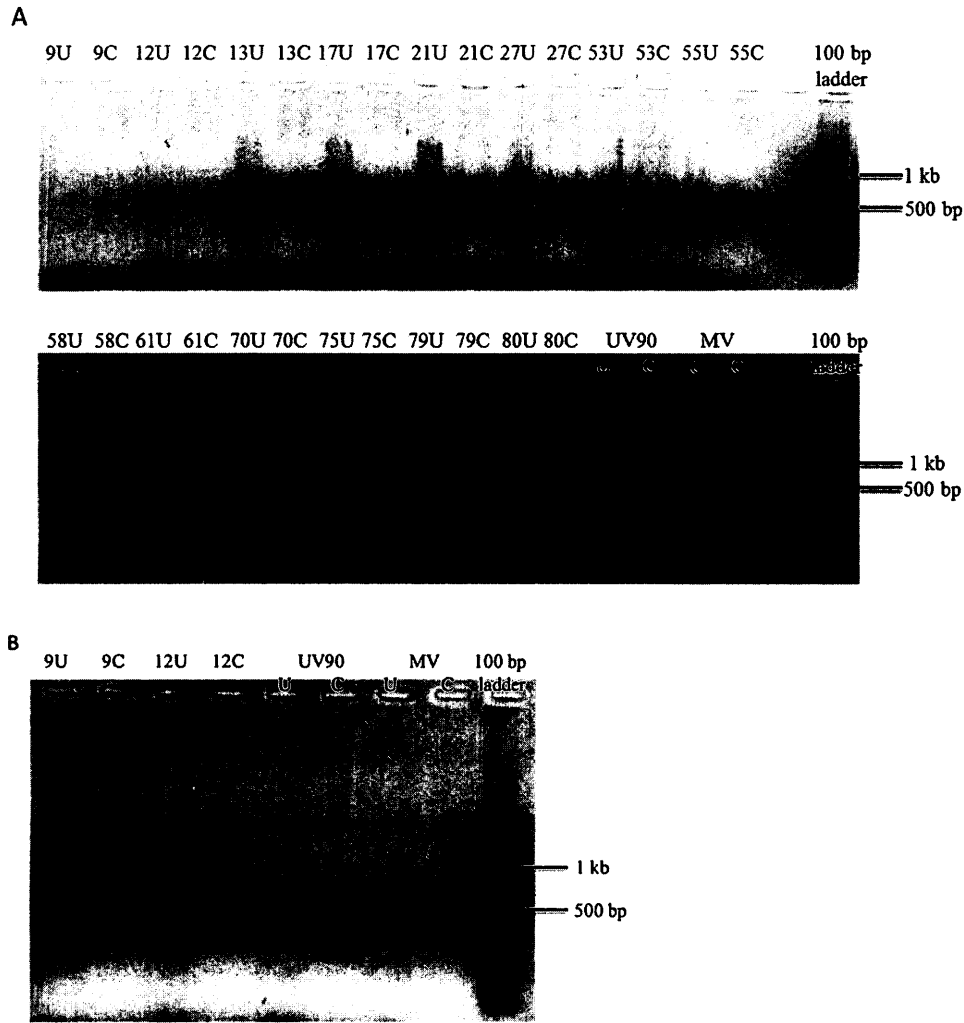
Figure 11. PCR results from *csp-1; bd; UV+* progeny using F9-R9 primers.

U = "uncut", undigested DNA; C = "cut", DNA digested with Taqα1 restriction enzyme.

"Cut" OR DNA exhibits two overlapping bands, each ~250 bp in size. *UV90 (csp-1; bd;*

UV90) and MV (Mauriceville, *csp+; bd+; UV+*) served as controls. Progeny #9 and #12

were repeated in (B). Most *UV+* progeny resembled MV after digestion with the

exception of #17 and #75 which resembled *UV90*, and thus were determined to be

recombinants.

70
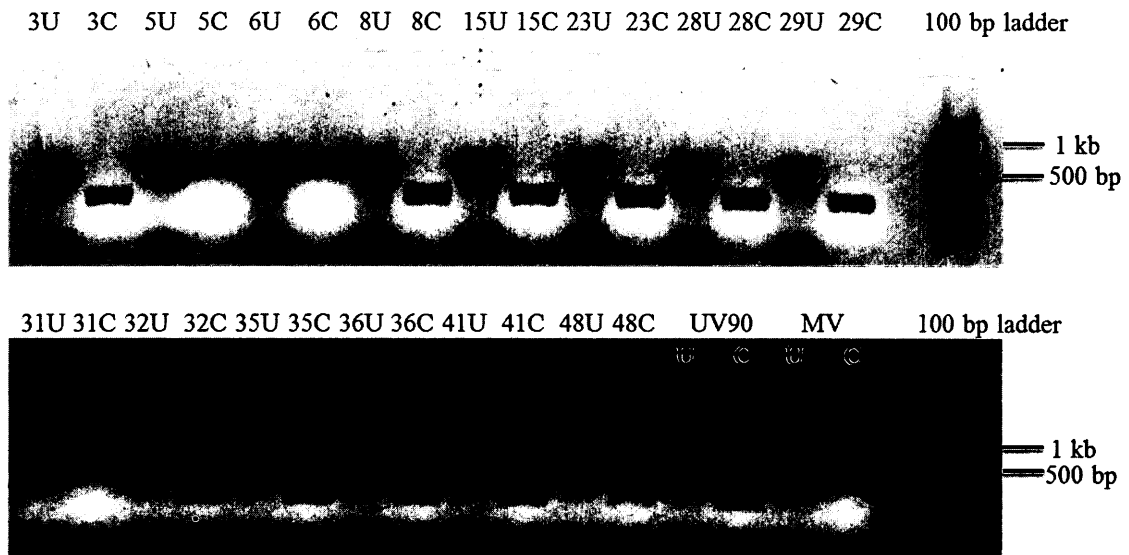
Figure 12. PCR results from *csp-1; bd; UV90* progeny #3-48 using F9-R9 primers.

U = "uncut", undigested DNA; C = "cut", DNA digested with Taqα1 restriction enzyme.

"Cut" OR DNA exhibits two overlapping bands, each ~250 bp in size. *UV90 (csp-1; bd;*

UV90) and MV (Mauriceville, *csp+; bd+; UV+*) served as controls.

Most *UV90* progeny resembled *UV90* control after digestion with the exception of #5, #6

and #31 which resembled MV, and thus were determined to be recombinants. Progeny

#50 through #87 are shown in Appendix VII, Fig. A1.
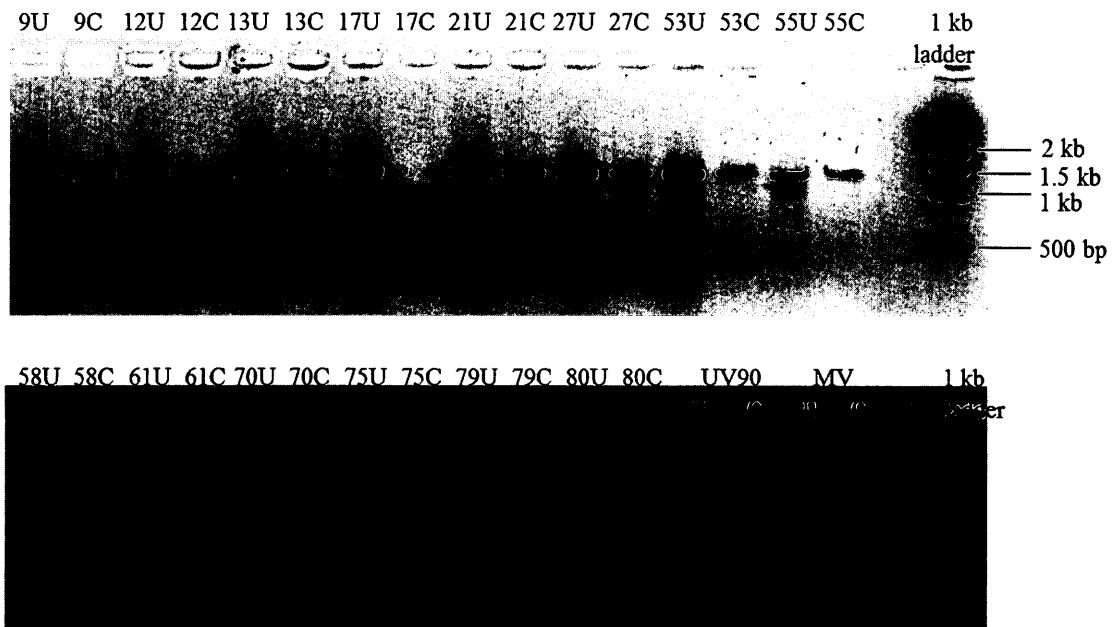
Figure 13. PCR results from *csp-1; bd; UV+* progeny using F6-R6 primers.

U = "uncut", undigested DNA; C = "cut", DNA digested with EcoRI restriction enzyme.

UV90 (csp-1; bd; UV90) and MV (Mauriceville, *csp+; bd+; UV+*) served as controls.

Most *UV+* progeny resembled MV control after digestion with the exception of #17 and

#75 which resembled *UV90*, and thus were determined to be recombinants.
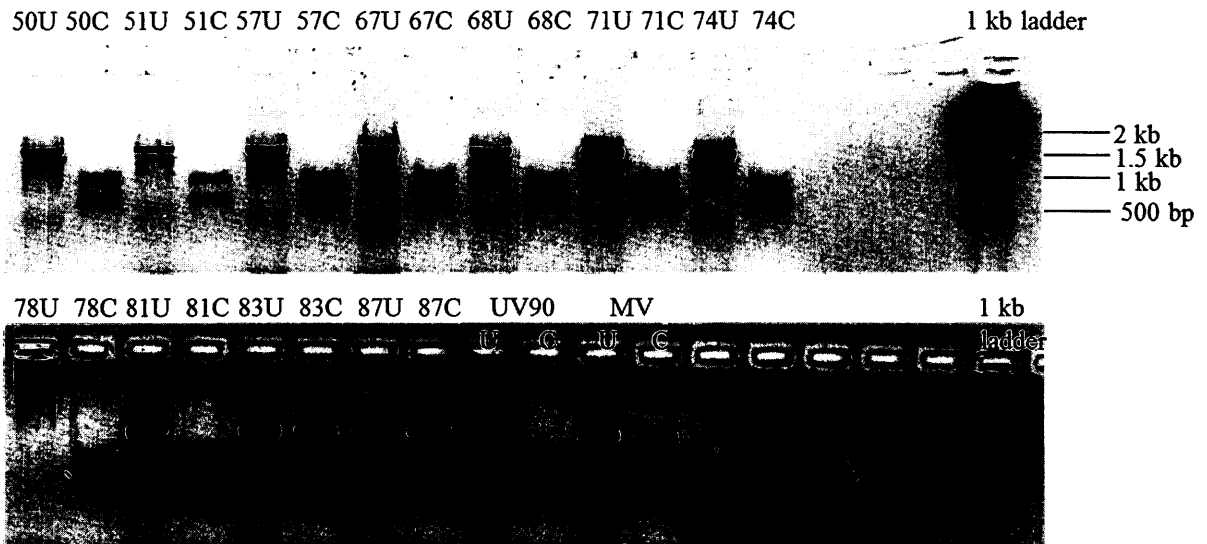
Figure 14. PCR results from *csp-1; bd; UV90* progeny using F6-R6 primers.

U = "uncut", undigested DNA; C = "cut", DNA digested with EcoRI restriction enzyme.

UV90 (*csp-1; bd; UV90*) and MV (Mauriceville, *csp+; bd+; UV+*) served as controls.

Most progeny resembled *UV90* control after digestion with the exception of #83 and #87

which resembled MV, and thus were determined to be recombinants. Progeny #3

through #48 are shown in Appendix VII, Fig. A2.

Table 10. Recombination frequencies of *csp-1; bd; UV90* and *csp-1; bd; UV+* progeny with F6-R6 and F9-R9 CAPS markers

Progeny tested with F6 & R6 primers				Progeny tested with F9 & R9 primers			
csp-1; bd; UV90		*csp-1; bd; UV+*		*csp-1; bd; UV90*		*csp-1; bd; UV+*	
Progeny #	Recom. (Yes/Y, No/N)*	Progeny #	Recom. (Yes/Y, No/N)*	Progeny #	Recom. (Yes/Y, No/N)*	Progeny #	Recom. (Yes/Y, No/N)*
3**	N	9**	N	3**	N	9**	N
5**	Y	12	N	5**	Y	12	N
6**	Y	13**	N	6**	Y	13**	N
8	N	17	Y	8	N	17	Y
15	N	21	N	15	N	21	N
23	N	27	N	23	N	27	N
28	N	53	N	28	N	53	N
29	N	55**	N	29	N	55**	N
31**	Y	58**	N	31**	Y	58**	N
32	N	61	N	32	N	61	N
35	N	70	N	35	N	70	N
36	N	75	Y	36	N	75	Y
41	N	79**	N	41	N	79**	N
48	N	80	N	48	N	80	N
50	N			50	N		
51	N			51	N		
57	N			57	N		
67	N			67	N		
68	N			68	N		
71	N			71	N		
74	N			74	N		
78	N			78	N		
81	N			81	N		
83	Y			83	Y		
87**	Y			87**	Y		
	Total UV90: 5/25		Total UV+: 2/14		Total UV90: 5/25		Total UV+: 2/14
Total recombinant progeny: 7/39 (17.9%) Adjusted total: 3/29 (10.3%)**				Total recombinant progeny: 7/39 (17.9%) Adjusted total: 3/29 (10.3%)**			

*Recom. = recombinant. Recombinant progeny are highlighted in red
**10 progeny were disregarded due to unclassifiable race tube phenotypes (see Fig. 15)
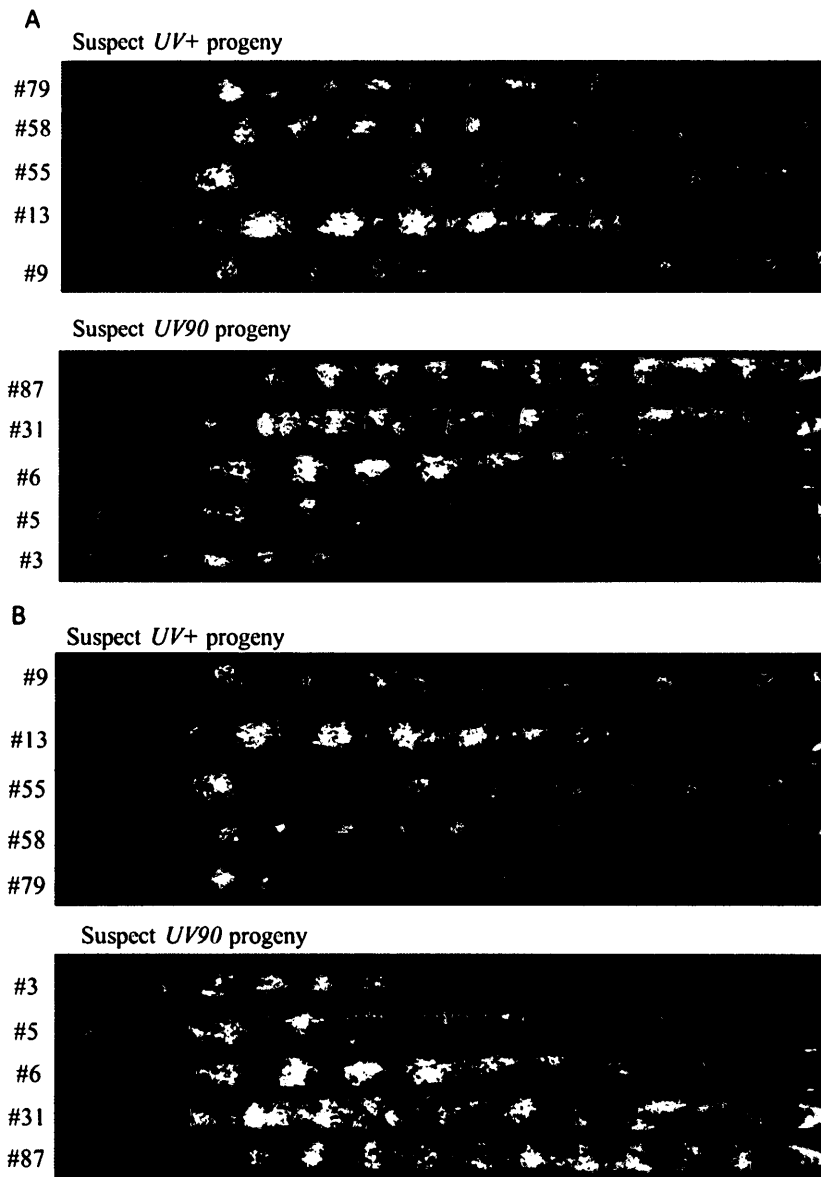
Figure 15. Unclassifiable *csp-1; bd; UV+* and *UV90* progeny obtained from *csp-1; bd;*

UV90 x *csp+; bd+; UV+* (Mauriceville wild type) cross. Shown with (A) and without

(B) marked growth fronts. Progeny did not show clear *UV+* or *UV90* phenotypes when

compared to other progeny and controls (Figs. 9 & 10) and were excluded from further

analyses (Tables 10 & 12).
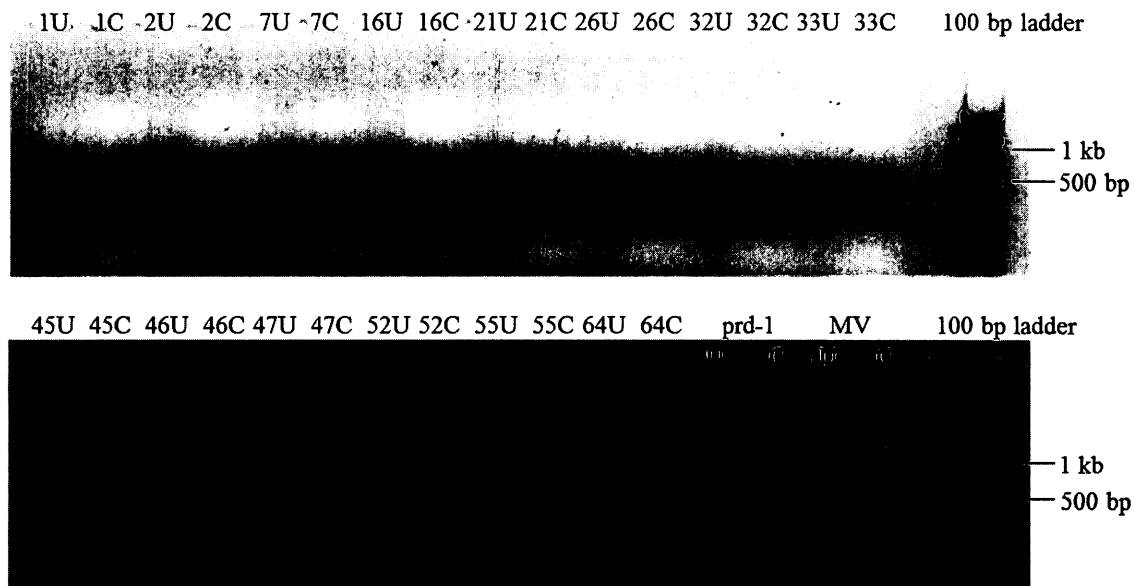
Figure 16. PCR results from *csp-1; prd-1; bd* progeny #1-64A using F9-R9 primers.

U = "uncut", undigested DNA; C = "cut", DNA digested with Taqα1 restriction enzyme.

"Cut" OR DNA exhibits two overlapping bands, each ~250 bp in size.

prd-1 (*csp-1; prd-1; bd*) and MV (Mauriceville wild type, *csp+; prd+; bd+*) served as

controls.

Progeny #1, 7, 21, 33, 45 and 46 showed no DNA cleavage after digestion, resembling

the MV control, and were therefore determined to be recombinants.
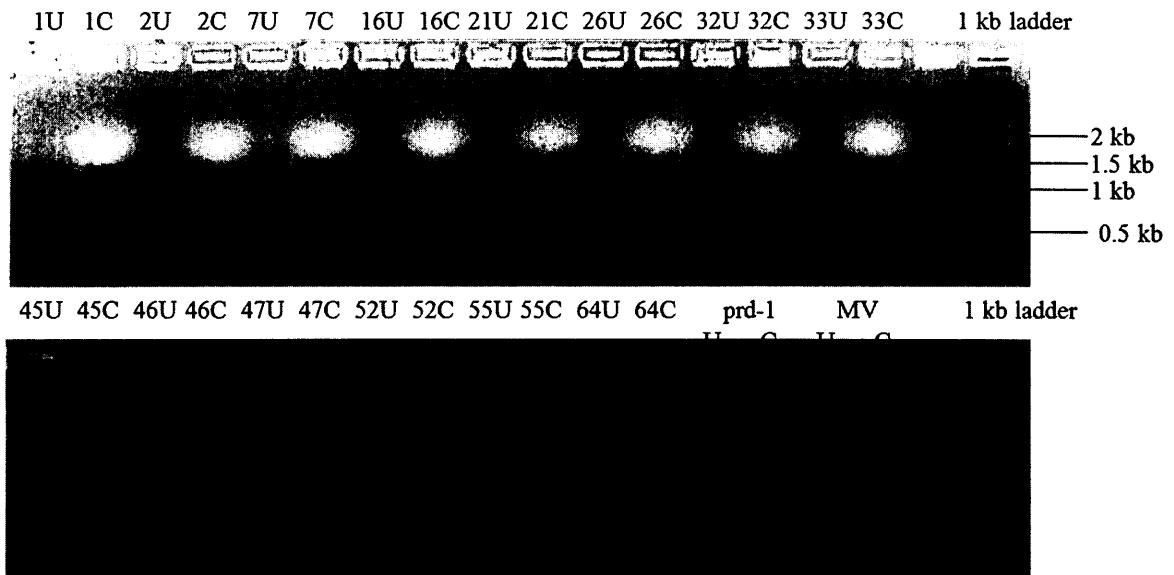
Figure 17. PCR results from *csp-1; prd-1; bd* progeny #1-64A using F6-R6 primers.

U = "uncut", undigested DNA; C = "cut", DNA digested with EcoRI restriction enzyme.

prd-1 (*csp-1; prd-1; bd*) and MV (Mauriceville wild type, *csp+; prd+; bd+*) served as

controls.

Progeny #1, 7, 21, 33, 45 and 46 showed no DNA cleavage after digestion, resembling

the MV control, and were therefore determined to be recombinants.

Table 11. Recombination frequencies of *csp-1; prd-1; bd* and *csp-1; prd+; bd* progeny with F6-R6 and F9-R9 CAPS markers

Progeny tested with F6 & R6 primers				Progeny tested with F9 & R9 primers			
csp-1; prd-1; bd		*csp-1; prd+; bd*		*csp-1; prd-1; bd*		*csp-1; prd+; bd*	
Progeny #	Recom. (Yes/Y, No/N)*	Progeny #	Recom. (Yes/Y, No/N)*	Progeny #	Recom. (Yes/Y, No/N)*	Progeny #	Recom. (Yes/Y, No/N)*
1A	Y	17A	Y	1A	Y	17A	Y
2A	N	19A	N	2A	N	19A	N
7A	Y	28A	N	7A	Y	28A	N
16A	N	29A	N	16A	N	29A	N
21A	Y	30A	Y	21A	Y	30A	Y
26A	N	34A	N	26A	N	34A	N
32A	N	35A	Y	32A	N	35A	Y
33A	Y	41A	Y	33A	Y	41A	Y
45A	Y	44A	Y	45A	Y	44A	Y
46A	Y	49A	Y	46A	Y	49A	Y
47A	N	50A	N	47A	N	50A	N
52A	N	54A	Y	52A	N	54A	Y
55A	N	34B	N	55A	N	34B	N
64A	N	36B	Y	64A	N	36B	Y
2B	N	41B	N	2B	N	41B	N
3B	N	55B	N	3B	N	55B	N
11B	Y	56B	Y	11B	Y	56B	Y
12B	Y	57B	N	12B	Y	57B	N
13B	Y	59B	N	13B	Y	59B	N
14B	Y	64B	N	14B	Y	64B	N
15B	Y			15B	Y		
16B	N			16B	N		
19B	Y			19B	Y		
23B	N			23B	N		
26B	N			26B	N		
	Total *prd-1*: 12/25		Total *prd+*: 9/20		Total *prd-1*: 12/25		Total *prd+*: 9/20
Total recombinant progeny: 21/45 (46.7%)				Total recombinant progeny: 21/45 (46.7%)			

*Recom. = recombinant. Recombinant progeny are highlighted in red
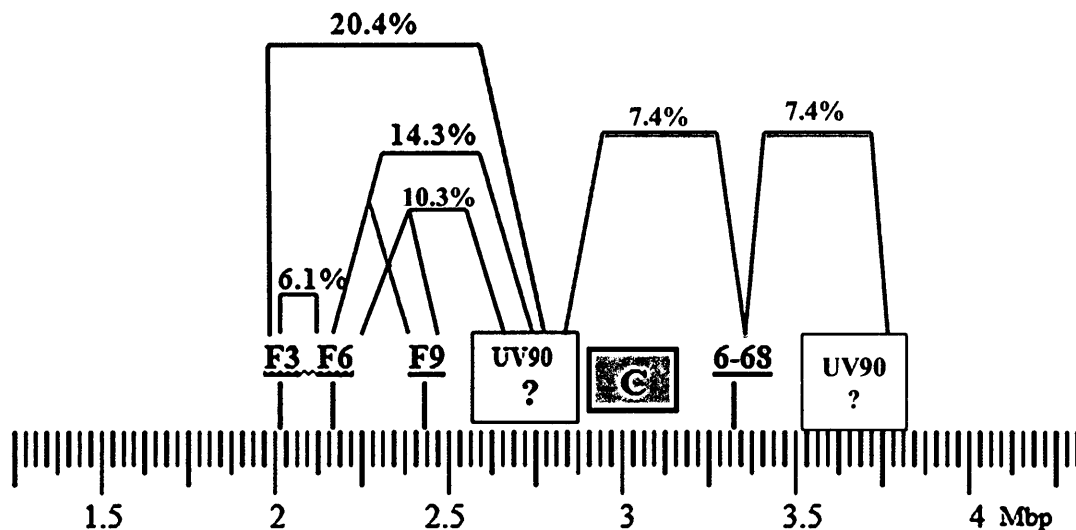
Figure 18. Schematic of *Neurospora crassa* Linkage Group VI displaying primer

locations, *UV90* progeny recombination and suspected location of *UV90* mutation.

Scale is in Mega basepairs (Mbp). Primers **F3, F6, F9** and **6-68** are located at 2.06, 2.14,

2.41, and 3.29 Mbp, respectively.

| C | = centromere, located at 2.8 – 3.1 Mbp. | UV90 ? | = potential location of *UV90*

gene.

Primer F3 showed 10/49 **(20.4%)** recombinant progeny. F6 and F9 primers produced

7/49 **(14.3%)** and 3/29 (10.3%) identical recombinant progeny. Recombination between

F6 and F9 primers was zero. Recombination between F3 and F6 primers was 3/49

progeny **(6.1%)**. Primer 6-68 showed 4/54 **(7.4%)** recombinant progeny. Data in red

obtained from Dr. Kamyar Motavaze. Data in green obtained from Daniel Rubinger.

3.1.3 Left centromere CAPS markers: LCF2-LCR2 and F11-R11

Six CAPS markers were designed as described in Methods 2.2.4: LCF1-LCR1, LCF2-LCR2, RCF3-RCR3, RCF4-RCR4, F10-R10, F11-R11 (Tables 2 and 3, Materials and Methods). New 50 ng/μL dilutions of all 39 *UV90* progeny and parental strains (*csp-1; bd; UV90* and MV) were made from extracted stock DNA. PCR, restriction enzyme digestion and gel electrophoresis was performed on the parental strains as described in Methods 2.2.5 (Fig. 19). CAPS markers LCF1-LCR1 and F10-R10 were not used further due to undesirable or no results with the parental strains. RCF3-RCR3 and RCF4-RCR4 produced identical banding patterns for both parents due to multiple restriction enzyme locations which were not checked for during primer design. LCF2-LCR2 and F11-R11 produced distinct bands for OR and MV and were used to perform PCR on the *UV90* progeny. PCR on parental strains was repeated with CAPS markers LCF1-LCR1, LCF2-LCR2, F10-R10 and F11-R11 and identical results were obtained (data not shown).

PCR was performed using LCF2 and LCR2 primers on all 39 *UV90* and *UV+* progeny. Two recombinants were seen with *UV+* progeny (Fig. 20). Four recombinants were seen with *UV90* progeny (Fig. 21). Only *UV90* progeny #50-87 are shown in Figure 21. PCR was performed using primers F11 and R11. Identical results were obtained as with LCF2 and LCR2. Two recombinants were seen with *UV+* progeny and four with *UV90* progeny (Figs. 22 and 23). Only *UV90* progeny #50-87 are shown in Figure 23.

PCR results with CAPS markers LCF2-LCR2 and F11-R11 are listed in Table 12. Six out of 39 progeny were recombinant with both CAPS markers (Table 12). Disregarding the unclassifiable race tubes (Fig. 15) resulted in 2 out of 29 recombinants (Table 12). The decreasing number of recombinants with LCF2-LCR2 and F11-R11 (2 out of 29) as compared to F6-R6 and F9-R9 (3 out of 29) suggest that *UV90* is further downstream and possibly to the right of the centromere.
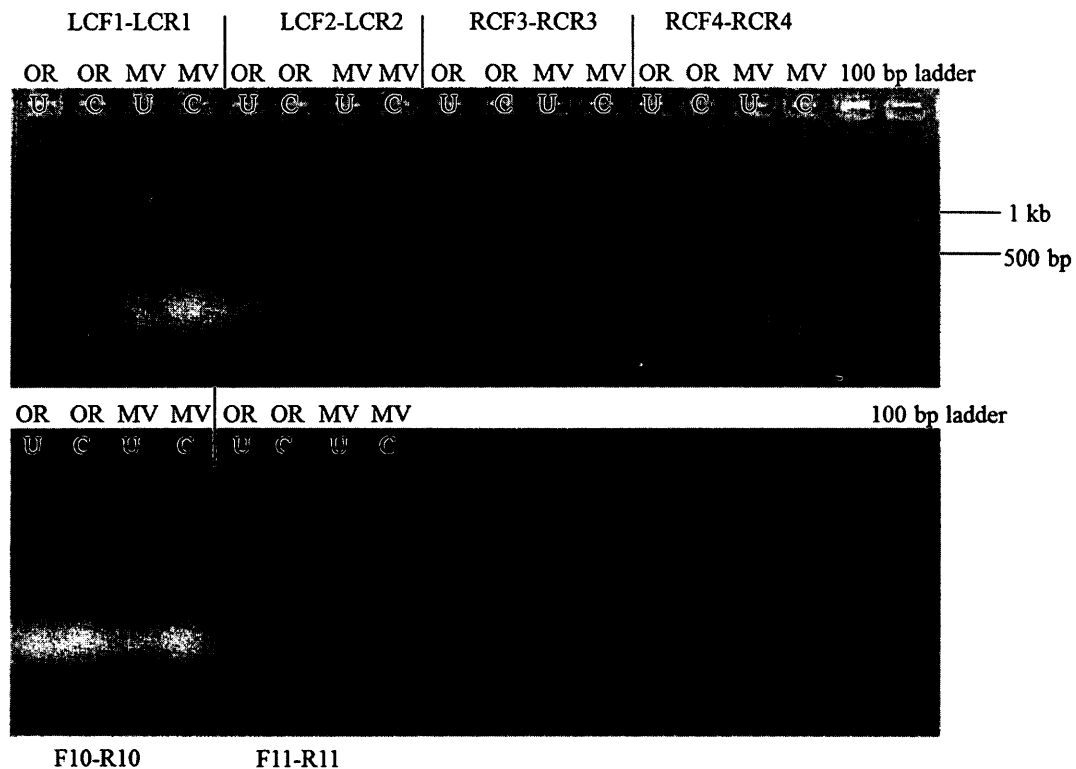
Figure 19. PCR results from *UV90* parental strains using CAPS marker pairs: LCF1-R1,

LCF2-R2, RCF3-R3, RCF4-R4, F10-R11 and F11-R11.

U = "uncut", undigested DNA; C = "cut", DNA digested with Taqα1 (LCF1-R1; RCF4-

R4; F11-R11), and HaeIII (LCF2-R2; RCF3-R3; F10-R10) restriction enzymes. OR =

Oak Ridge *csp-1; bd; UV90* parent; MV = Mauriceville wild type, *csp+; bd+; UV+*

parent.
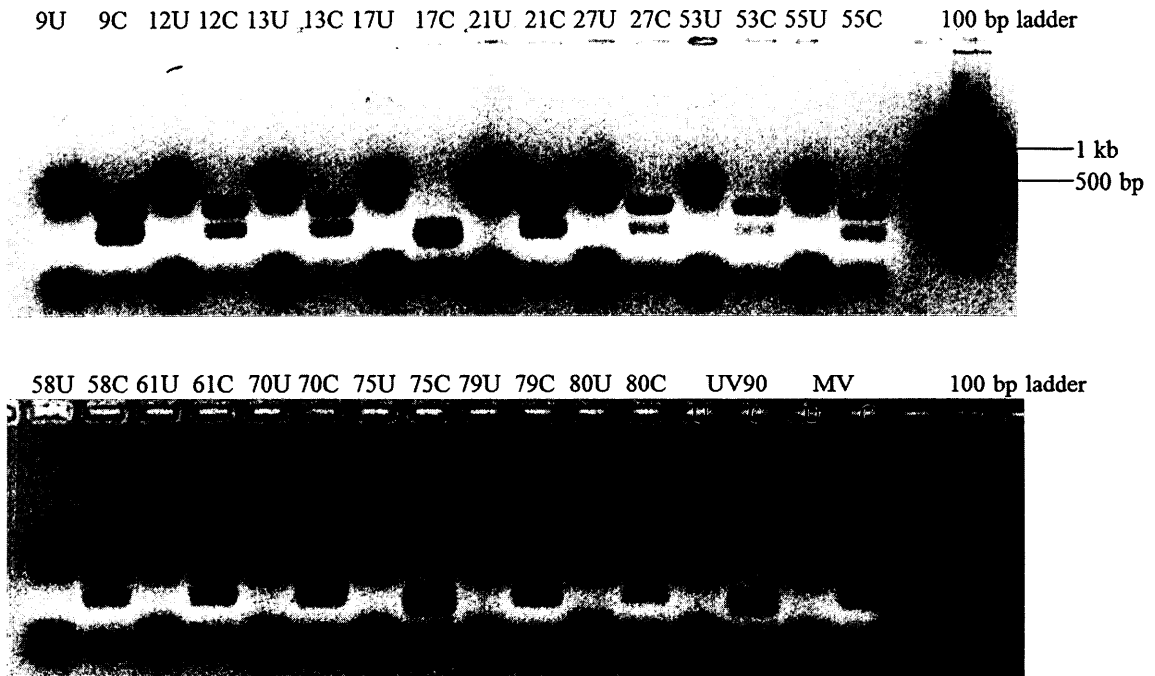
Figure 20. PCR results showing *csp-1; bd; UV+* progeny using LCF2-LCR2 primers.

U = "uncut", undigested DNA; C = "cut", DNA digested with HaeIII restriction enzyme.

"Cut" OR DNA exhibits two overlapping bands, each ~250 bp in size.

UV90 (csp-1; bd; UV90) and MV (Mauriceville wild type, *csp+; bd+; UV+*) served as controls.

Most *UV+* progeny resembled MV after digestion with the exception of #17 and #75 which resembled *UV90* and were determined to be recombinants.
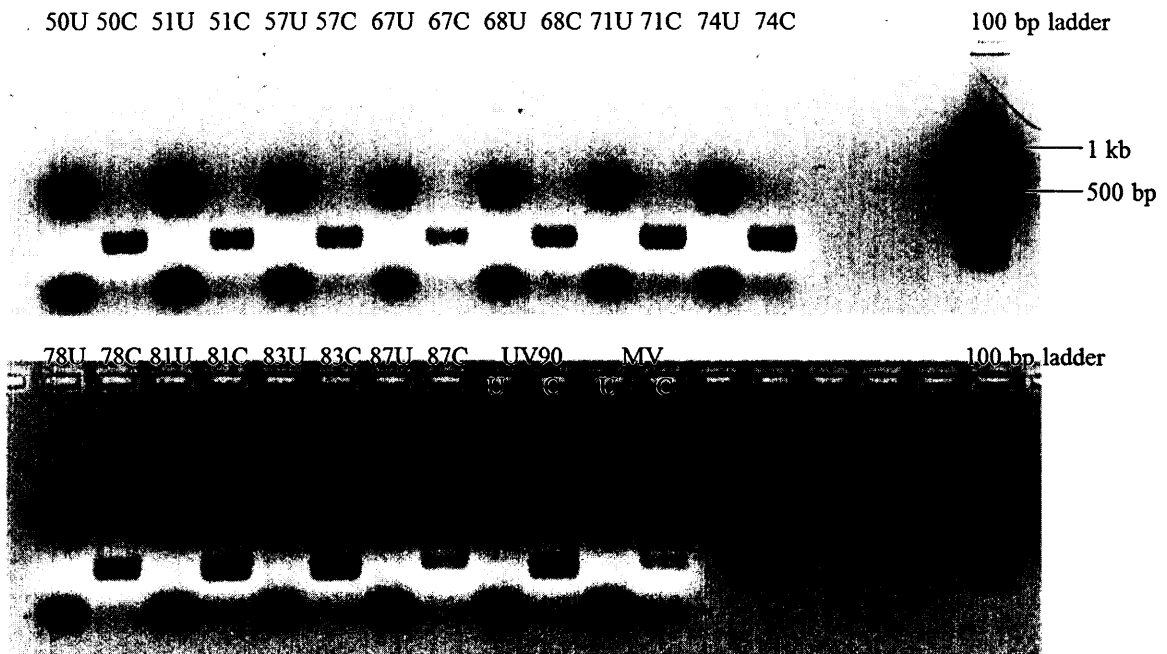
Figure 21. PCR results showing *csp-1; bd; UV90* progeny using LCF2-LCR2 primers.

U = "uncut", undigested DNA; C = "cut", DNA digested with HaeIII restriction enzyme.

"Cut" OR DNA exhibits two overlapping bands, each ~250 bp in size.

UV90 (*csp-1; bd; UV90*) and MV (Mauriceville wild type, *csp+; bd+; UV+*) served as controls.

Most progeny resembled *UV90* control after digestion with the exception of #87 which resembled MV and was determined to be recombinant.
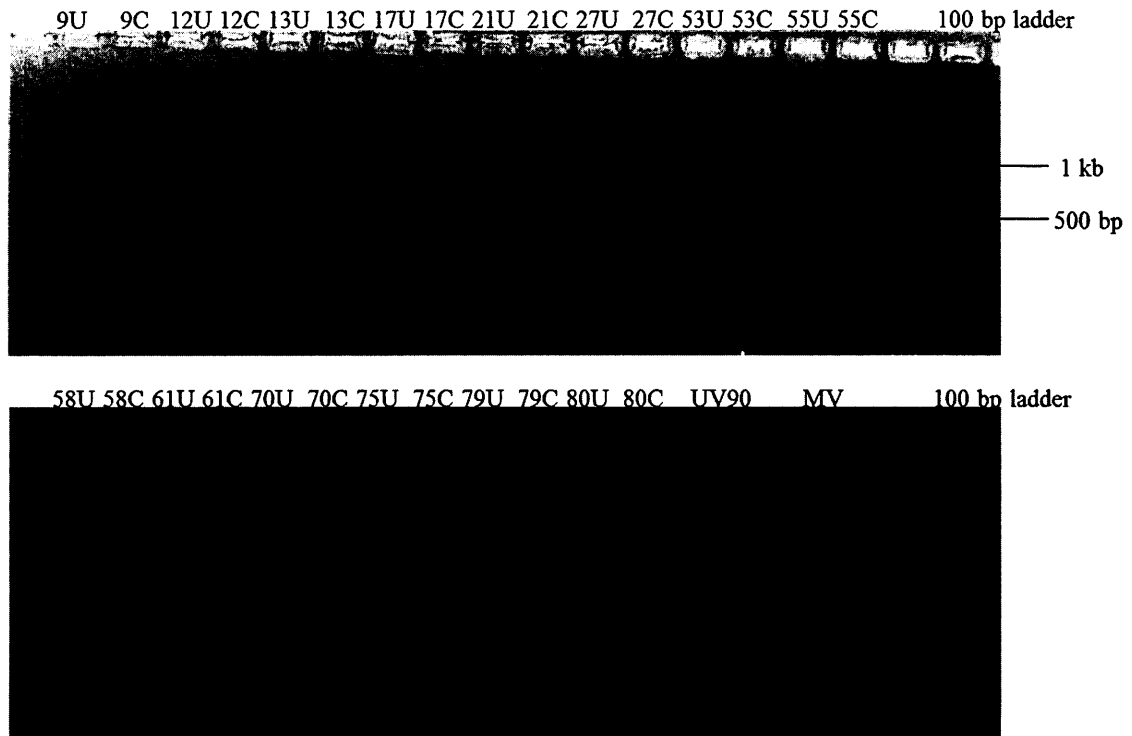
Figure 22. PCR results showing *csp-1; bd; UV+* progeny using F11-R11 primers.

U = "uncut", undigested DNA; C = "cut", DNA digested with Taqα1 restriction enzyme.

UV90 (csp-1; bd; UV90) and MV (Mauriceville wild type, *csp+; bd+; UV+*) served as controls.

Most progeny resembled MV after digestion with the exception of #17 and #75 which resembled *UV90* and were determined to be recombinants. Progeny #55 was repeated and resembled MV (data not shown).
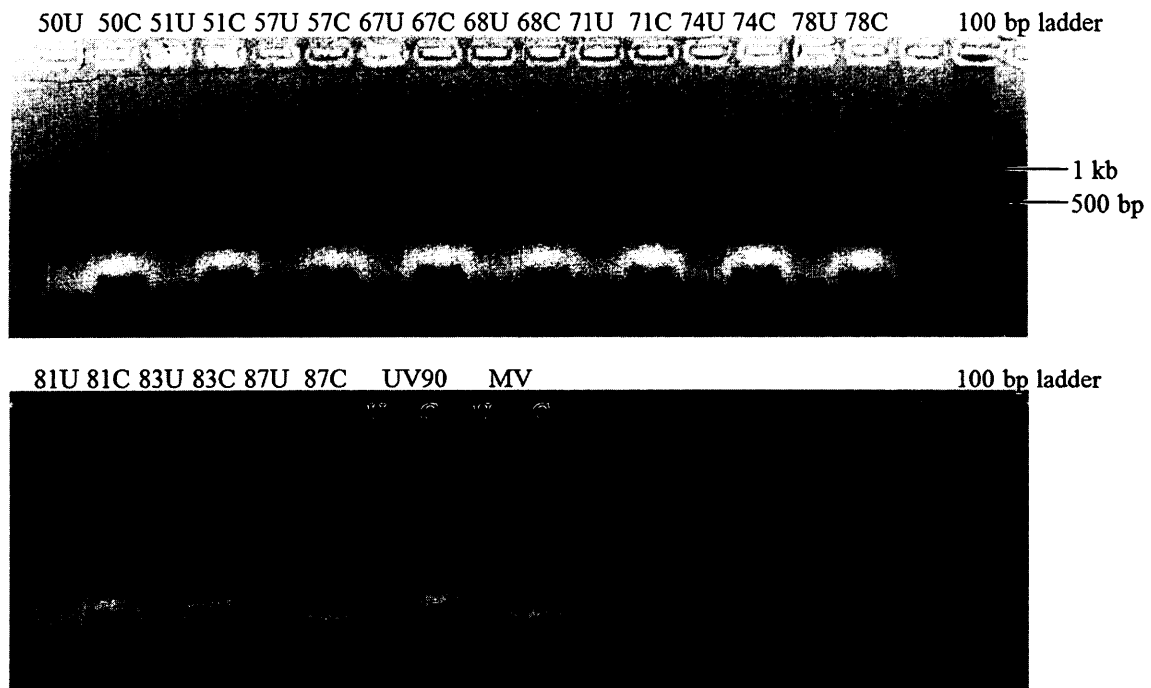
Figure 23. PCR results showing *csp-1; bd; UV90* progeny using F11-R11 primers.

U = "uncut", undigested DNA; C = "cut", DNA digested with Taqα1 restriction enzyme.

UV90 (csp-1; bd; UV90) and MV (Mauriceville wild type, *csp+; bd+; UV+*) served as

controls.

Most progeny resembled *UV90* after digestion with the exception of #87 which

resembled MV and was determined to be recombinant.

Table 12. Recombination frequencies of *csp-1; bd; UV90* and *csp-1; bd; UV+* progeny with LCF2-LCR2 and F11-R11 CAPS markers

| Progeny tested with LCF2 & LCR2 primers				Progeny tested with F11 & R11 primers			
csp-1; bd; UV90		*csp-1; bd; UV+*		*csp-1; bd; UV90*		*csp-1; bd; UV+*	
Progeny #	Recom. (Yes/Y, No/N)*	Progeny #	Recom. (Yes/Y, No/N)*	Progeny #	Recom. (Yes/Y, No/N)*	Progeny #	Recom. (Yes/Y, No/N)*
3**	N	9**	N	3**	N	9**	N
5**	Y	12	N	5**	Y	12	N
6**	Y	13**	N	6**	Y	13**	N
8	N	17	Y	8	N	17	Y
15	N	21	N	15	N	21	N
23	N	27	N	23	N	27	N
28	N	53	N	28	N	53	N
29	N	55**	N	29	N	55**	N
31**	Y	58**	N	31**	Y	58**	N
32	N	61	N	32	N	61	N
35	N	70	N	35	N	70	N
36	N	75	Y	36	N	75	Y
41	N	79**	N	41	N	79**	N
48	N	80	N	48	N	80	N
50	N			50	N		
51	N			51	N		
57	N			57	N		
67	N			67	N		
68	N			68	N		
71	N			71	N		
74	N			74	N		
78	N			78	N		
81	N			81	N		
83	N			83	N		
87**	Y			87**	Y		
	Total *UV90*: 4/25		Total *UV+*: 2/14		Total *UV90*: 4/25		Total *UV+*: 2/14
Total recombinant progeny: 6/39 (15.38%) Adjusted total: 2/29 (6.9%)**				Total recombinant progeny: 6/39 (15.38%) Adjusted total: 2/29 (6.9%)**			

*Recom. = recombinant. Recombinant progeny are highlighted in red
**10 progeny were disregarded due to unclassifiable race tube phenotypes (see Fig. 15)

3.1.4 New *UV90* progeny and right centromere CAPS markers: RCF5-RCR5, 668F-668R and F16-R16

New *UV90* progeny:

To increase the number of *UV90* progeny for PCR, approximately 400 spores were picked from the cross between *csp-1; bd; UV90* (OR, sg #227) and MV wild type (sg #258) as described in Methods 2.2.1. The "tap test" was performed on the baby tubes to visually check for *csp-1* and *csp+* progeny as described in Methods 2.2.2. 194 were found to be *csp-1*, 165 were *csp+* and 41 did not germinate (Table 13).

100 *csp-1* progeny were numbered and inoculated onto maltose-arginine medium in race tubes as described in Methods 2.2.2. Replicate tubes of the following controls were also inoculated: *csp-1; bd* (sg #1), *csp-1; bd; UV90* (sg #227) and *csp+; bd+; UV+* (MV, sg #258). Progeny were visually separated into *bd+* or *bd* phenotypes based on growth fronts marked daily on the tubes in comparison to controls *csp-1; bd* (sg #1) and MV wild type (sg #258) (Figs. 24 and 26). *bd* tubes were then sorted into *UV+* by the presence of clear, rhythmic bands (Fig. 24) or *UV90* by exhibiting a low amplitude rhythm (Fig. 25). *bd+* tubes were sorted into *UV+* by exhibiting bands as in the MV wild type control (Fig. 26) or *UV90* by the presence of constant, arrhythmic conidiation (Fig. 27).

21 progeny were found to be *csp-1; bd; UV90*, 19 were *csp-1; bd; UV+*, 25 were *csp-1; bd+; UV90*, 21 were *csp-1; bd+; UV+* and 14 were unclassifiable (Table 14). Unclassifiable progeny were not used further in DNA extraction or PCR. Progeny

88

generally fall into a 1:1:1:1 ratio for all 4 classes (Table 14), which indicates again that a single gene is responsible for the *UV90* phenotype and is segregating independently (Griffiths et al., 1993). A chi-square test was performed and the *p* value was determined to be non-significant ($p = 0.4368$), which confirms that the slight variations observed in the number of progeny were due to chance deviations (Table 14, Appendix X).

Periods and growth rates of all progeny are listed in Tables 15 and 16. *csp-1; bd+; UV+* progeny exhibited a mean growth rate of 2.12 (± 0.088) mm/hr and a period of 22 (± 0.444) hr (Table 15). *csp-1; bd+; UV90* progeny had a mean growth rate of 1.65 (± 0.027) mm/hr (Table 15). These values match the previously reported values for *bd+* progeny (Li et al., 2011). Although the mean growth rate matches the reported values, there appears to be a larger variation among the growth rates for *bd+* progeny (Table 15). This is likely due to small nucleotide polymorphisms (SNPs) between the parental OR and MV strains as well as the *bd+* strains being faster growing than *bd* strains. *csp-1; bd; UV+* progeny had a mean growth rate of 1.28 (± 0.020) mm/hr and a period of 21.86 (± 0.139) hr (Table 16). *csp-1; bd; UV90* progeny had a mean growth rate of 1.09 (± 0.013) mm/hr (Table 16). The previously reported growth rate for *csp-1; bd; UV90* is slightly higher at 1.16 mm/hr, yet it confirms again that the *UV90* phenotype is slower growing than the wild type (Li et al., 2011). The *csp-1; bd; UV+* growth rate and period were very close to the reported rates of 1.29 mm/hr and 21.2 hr (Li et al., 2011).

DNA extraction was performed on the 86 *UV+* and *UV90* progeny along with parental strains *csp-1; bd; UV90* and MV wild type as described in Methods 2.2.3. The

DNA concentrations ranged from 90-418 µg/mL for *UV+* progeny and 79-288 µg/mL for *UV90* progeny (data not shown). *csp-1; bd; UV90* progeny #198 did not produce a DNA pellet, leaving 85 progeny. CAPS markers RCF5-RCR5, RCF6-RCR6, F15-R15 and F16-R16 were designed as described in Methods 2.2.4. Primer sequences for 668F and 668R were obtained from Jin et al. (2007) (Tables 2 and 3, Materials and Methods). PCR, restriction enzyme digestion and gel electrophoresis were performed on the parental strains and all *UV+* and *UV90* progeny as described in Methods 2.2.5.

<u>CAPS markers RCF5-RCR5, 668F-668R and F16-R16:</u>

PCR was performed on the parental strains *csp-1; bd; UV90* (sg #227) and MV wild type with CAPS markers RCF5-RCR5, RCF6-RCR6 and 668F-668R (Fig. 28). RCF6-RCR6 did not produce any PCR product when repeated twice (Fig. 28, A and B). RCF5-RCR5 and 668F-668R both produced distinct bands for each parent after digestion (Fig. 28) and were used for PCR. PCR was performed on the previous 39 *UV+* and *UV90* progeny with RCF5-RCR5 primers and no PCR products were obtained. It is believed the DNA had degraded due to multiple freezing and thawing during use. PCR was then continued with the new 85 *UV+* and *UV90* progeny.

6 out of 40 *UV+* progeny and 2 out of 45 *UV90* progeny were recombinant with RCF5-RCR5 (Figs. 29 and 30). Only digested *csp-1; bd+; UV+* and *csp-1; bd+; UV90* progeny are shown in Figs. 29 and 30. 2 out of 40 *UV+* and 1 out of 45 *UV90* progeny were recombinant with 668F-668R (Figs. 31 and 32). Only digested *csp-1; bd; UV+* and *csp-1; bd+; UV90* progeny are shown in Figs. 31 and 32. A complete list of PCR results

with RCF5-RCR5 and 668F-668R is shown in Table 17. 8 out of 85 total progeny were recombinant with RCF5-RCR5 and 3 out of 85 total progeny were recombinant with 668F-668R (Table 17).

PCR was performed on the parental strains *csp-1; bd; UV90* (sg #227) and MV wild type with CAPS markers F15-R15 and F16-R16 (Fig. 33). F16-R16 was chosen for the progeny. 4 out of 40 *UV+* progeny and 4 out of 45 *UV90* progeny were recombinant with F16-R16 (Figs. 34 and 35). Only digested *csp-1; bd+; UV+* and *csp-1; bd+; UV90* progeny are shown in Figs. 34 and 35. A complete list of PCR results with F16-R16 primers is shown in Table 18. 8 out of 85 total progeny were recombinant with F16-R16 (Table 18).

A map showing the number of recombinants and locations of primers F6 through F16 is shown in Fig. 36. The number of recombinant progeny decreased to its lowest amount, 3 out of 85 (3.53%) at CAPS marker 668F-668R, suggesting that the 668F-668R marker is closer to *UV90*. The progeny that were recombinant with marker 668F-668R (#143, 184, and 122) were also recombinant with RCF5-RCR5 (Table 17; Fig. 41). This indicates that the crossover event which caused these progeny to appear recombinant with both markers occurred to the right of 668F-668R, but prior to the *UV90* gene. The number of recombinants increased to 8 out of 85 (9.41%) at F16-R16, which indicates the marker is farther away from *UV90*. This suggests the *UV90* gene is located between markers 668F-668R and F16-R16 (Fig. 36; Fig. 41).

Table 13. Second group of *csp+* and *csp-1* progeny from cross between *csp-1; bd; UV90* (OR, sg #227) and *csp+; bd+; UV+* (MV, sg #258)

Total spores picked	*csp-1* progeny	*csp+* progeny*	Non-germinating progeny*
400	194/400** (48.5%)	165/400 (41.25%)	41/400 (10.25%)

*csp+ and non-germinating progeny were excluded from further testing
**Four *csp-1* test tubes were broken, only 190 *csp-1* progeny remained for race tube analysis

Table 14. Second group of *csp-1; bd; UV+/UV90*, and *csp-1; bd+; UV+/UV90* progeny from cross between *csp-1; bd; UV90* (OR, sg #227) and *csp+; bd+; UV+* (MV, sg #258)

Number of *csp-1* progeny	*csp-1; bd; UV90* progeny	*csp-1; bd; UV+* progeny	*csp-1; bd+; UV90* progeny	*csp-1; bd+; UV+* progeny	Unclassifiable progeny*
100**	21/100 (21%) (strains: #100, 103, 111, 118, 119, 120, 127, 129, 140, 146, 151, 158, 159, 160, 162, 164, 176, 187, 189, 197, 198)	19/100 (19%) (strains: #104, 110, 117, 121, 122, 128, 136, 137, 141, 149, 153, 155, 156, 161, 165, 171, 181, 183, 196)	25/100 (25%) (strains: #106, 109, 116, 125, 130, 131, 133, 134, 135, 139, 144, 145, 150, 166, 168, 170, 173, 175, 179, 184, 186, 188, 190, 192, 195)	21/100 (21%) (strains: #105, 108, 112, 113, 115, 123, 126, 132, 138, 143, 147, 163, 167, 169, 174, 182, 185, 191, 193, 194, 199)	14/100 (14%) (strains: #101, 102, 107, 114, 124, 142, 148, 152, 154, 157, 172, 177, 178, 180)

*Unclassifiable progeny were excluded from further analysis
**100 out of 190 *csp-1* progeny were tested on race tubes and used for DNA extraction & PCR
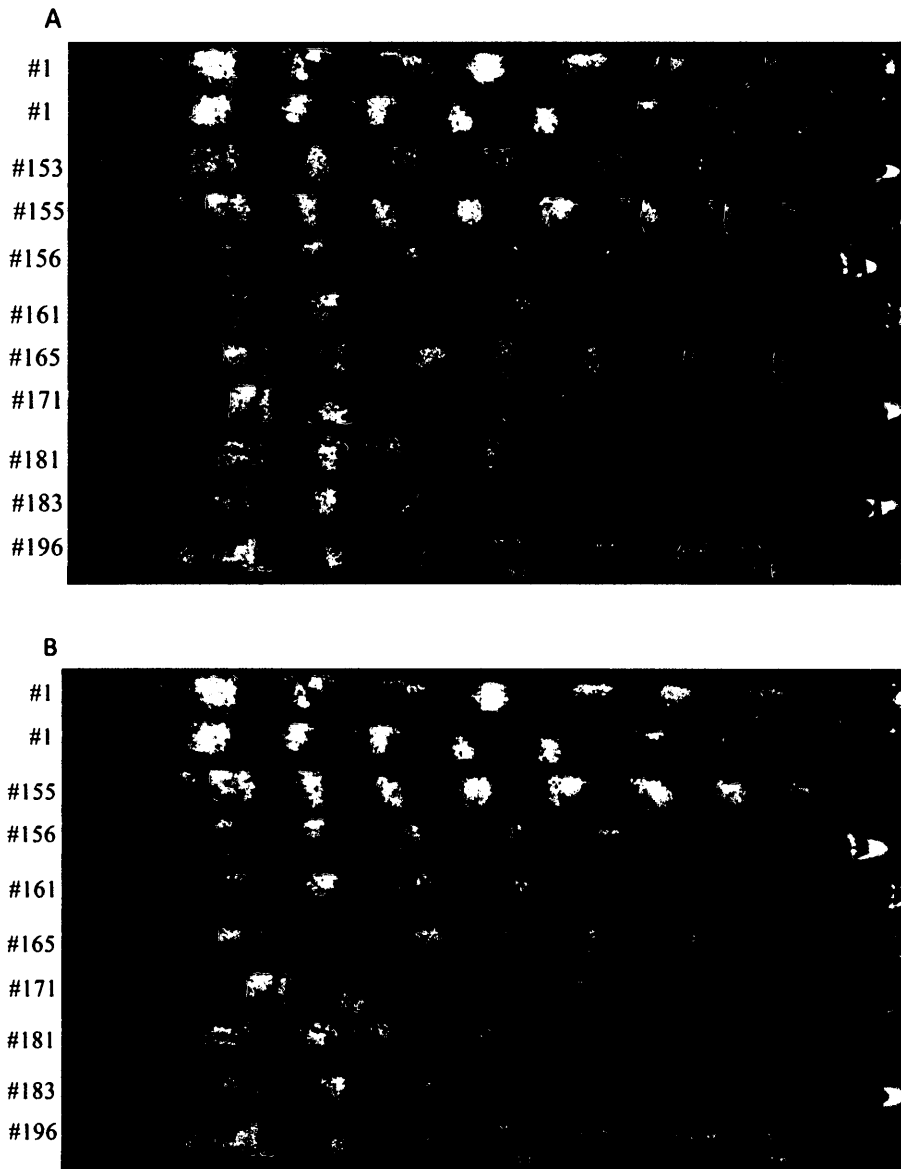
Figure 24. Examples of *csp-1; bd; UV*+ progeny with (A) and without (B) marked

growth fronts, obtained from *csp-1; bd; UV90* x *csp+; bd+; UV*+ (Mauriceville wild

type) cross. #1 (*csp-1; bd*) served as a control. Progeny were classified as *bd* phenotype

based on marked growth rates in (A), and classified as *UV*+ in (B) based on strong,

rhythmic conidiation.
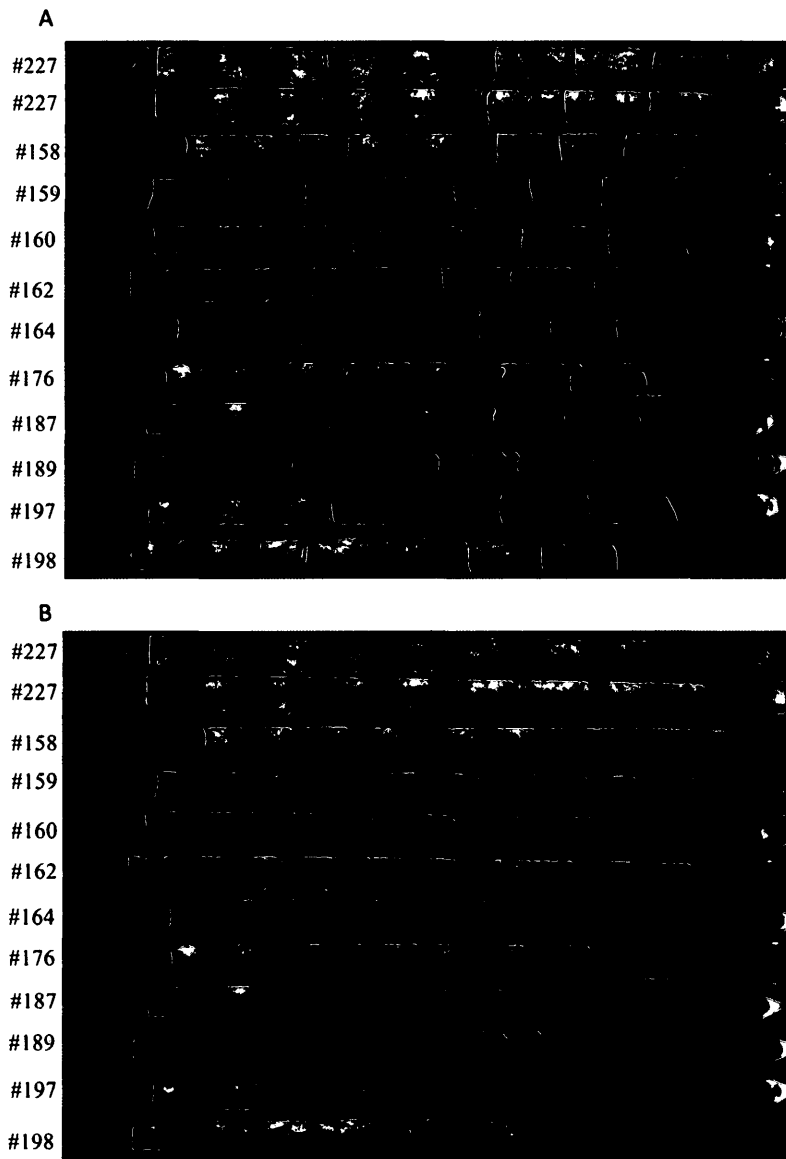
Figure 25. Examples of *csp-1; bd; UV90* progeny with (A) and without (B) marked

growth fronts, obtained from *csp-1; bd; UV90* x *csp+; bd+; UV+* (Mauriceville wild

type) cross. #227 (*csp-1; bd; UV90*) served as a control. Progeny were classified as *bd*

phenotype based on marked growth rates in (A), and classified as *UV90* in (B) based on

low amplitude rhythms.
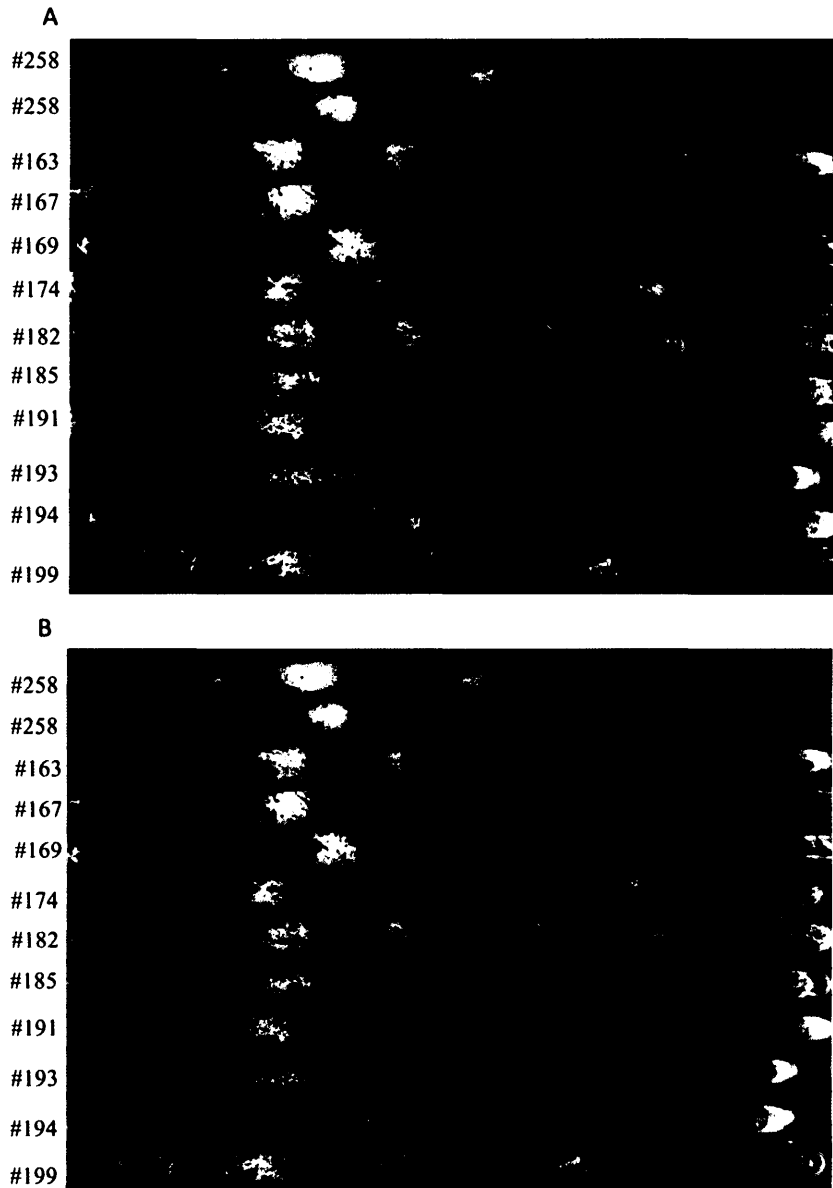
Figure 26. Examples of *csp-1; bd+; UV+* progeny with (A) and without (B) marked

growth fronts, obtained from *csp-1; bd; UV90* x *csp+; bd+; UV+* (Mauriceville wild

type) cross. #258 (*csp+; bd+; UV+*) served as a control. Progeny were classified as *bd+*

phenotype based on marked growth rates in (A), and classified as *UV+* in (B) based on

similar conidiation as control.

95

A

#258
#258
#106
#109
#116
#125
#130
#131
#133
#134

B

#258
#258
#184
#186
#188
#190
#192
#195
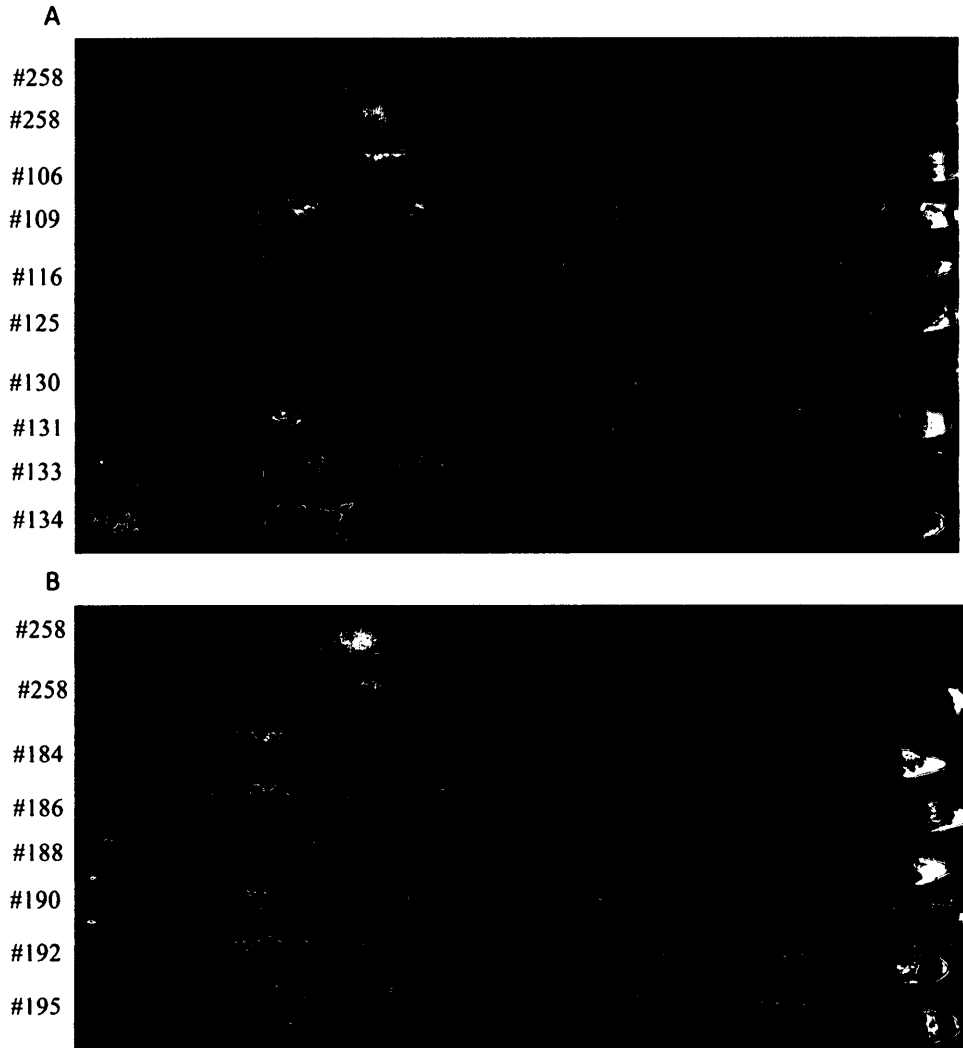
Figure 27. Examples of *csp-1; bd+; UV90* progeny with (A) and without (B) marked growth fronts, obtained from *csp-1; bd; UV90* x *csp+; bd+; UV+* (Mauriceville wild type) cross. #258 (*csp+; bd+; UV+*) served as a control. Progeny were classified as *bd+* phenotype based on marked growth rates in (A), and classified as *UV90* in (B) based on arrhythmic conidiation.

Table 15. Growth rates and periods of second group of *csp-1; bd+; UV+* and *UV90* progeny

csp-1; bd+; UV+			csp-1; bd+; UV90		
Progeny #	Growth Rate (mm/hr)	Period (hr)	Progeny #	Growth Rate (mm/hr)	Period (hr)
csp+; bd+; UV+ (control)	1.72	22.52	--	--	N/A**
csp+; bd+; UV+ (control)	1.69	21.24	--	--	
105	1.64	27.54	106	1.58	
108	2.79	20.14	109	1.59	
112	1.66	22.21	116	1.55	
113	2.24	21.52	125	1.54	
115	1.66	20.06	130	1.68	
123	2.32	20.50	131	1.70	
126	1.66	24.40	133	1.74	
132	2.77	18.40	134	1.75	
138	2.29	21.00	135	1.56	
143	1.61	25.02	139	1.52	
147	2.14	22.48	144	1.79	
163	1.77	22.52	145	1.81	
167	2.30	N/A*	150	1.67	
169	2.43	20.41	166	1.80	
174	1.78	22.54	168	1.70	
182	1.75	22.73	170	1.37	
185	2.23	21.38	173	1.70	
191	1.83	21.86	175	1.72	
193	2.54	22.64	179	1.69	
194	2.58	21.22	184	1.76	
199	2.52	21.46	186	1.28	
			188	1.76	
	Mean Growth Rate: 2.12 ± 0.088 (S.E.M.)	**Mean Period:** 22.00 ± 0.444 (S.E.M.)	190	1.75	
			192	1.77	
			195	1.55	
				Mean Growth Rate: 1.65 ± 0.027 (S.E.M.)	

*Progeny #167 showed only one large band, making a period calculation unattainable
**Not applicable: *bd+; UV90* progeny were arrhythmic; period was not calculated

Table 16. Growth Rates and periods of second group of *csp-1; bd; UV+* and *UV90* progeny

csp-1; bd; UV+			csp-1; bd; UV90		
Progeny #	Growth Rate (mm/hr)	Period (hr)	Progeny #	Growth Rate (mm/hr)	Period (hr)
csp-1; bd; UV+ (control)	1.31	21.62	*csp-1; bd; UV90* (control)	1.11	N/A*
csp-1; bd; UV+ (control)	1.25	21.44	*csp-1; bd; UV90* (control)	1.11	
104	1.25	21.63	100	1.13	
110	1.21	21.89	103	1.09	
117	1.07	22.12	111	1.11	
121	1.36	21.73	118	1.14	
122	1.28	22.38	119	1.12	
128	1.33	22.63	120	1.14	
136	1.34	21.64	127	1.10	
137	1.32	22.50	129	0.97	
141	1.34	21.22	140	1.14	
149	1.37	19.91	146	1.11	
153	1.33	22.38	151	1.10	
155	1.18	22.25	158	0.98	
156	1.33	22.31	159	1.02	
161	1.44	21.88	160	1.17	
165	1.30	21.54	162	1.03	
171	1.15	22.06	164	0.99	
181	1.21	22.23	176	1.06	
183	1.34	21.66	187	1.07	
196	1.26	22.13	189	1.05	
			197	1.17	
			198	1.07	
	Mean Growth Rate: 1.28 ± 0.020 (S.E.M.)	Mean Period: 21.86 ± 0.139 (S.E.M.)		Mean Growth Rate: 1.09 ± 0.013 (S.E.M.)	

*Not applicable: *bd; UV90* progeny showed low amplitude rhythms; period was not calculated

98
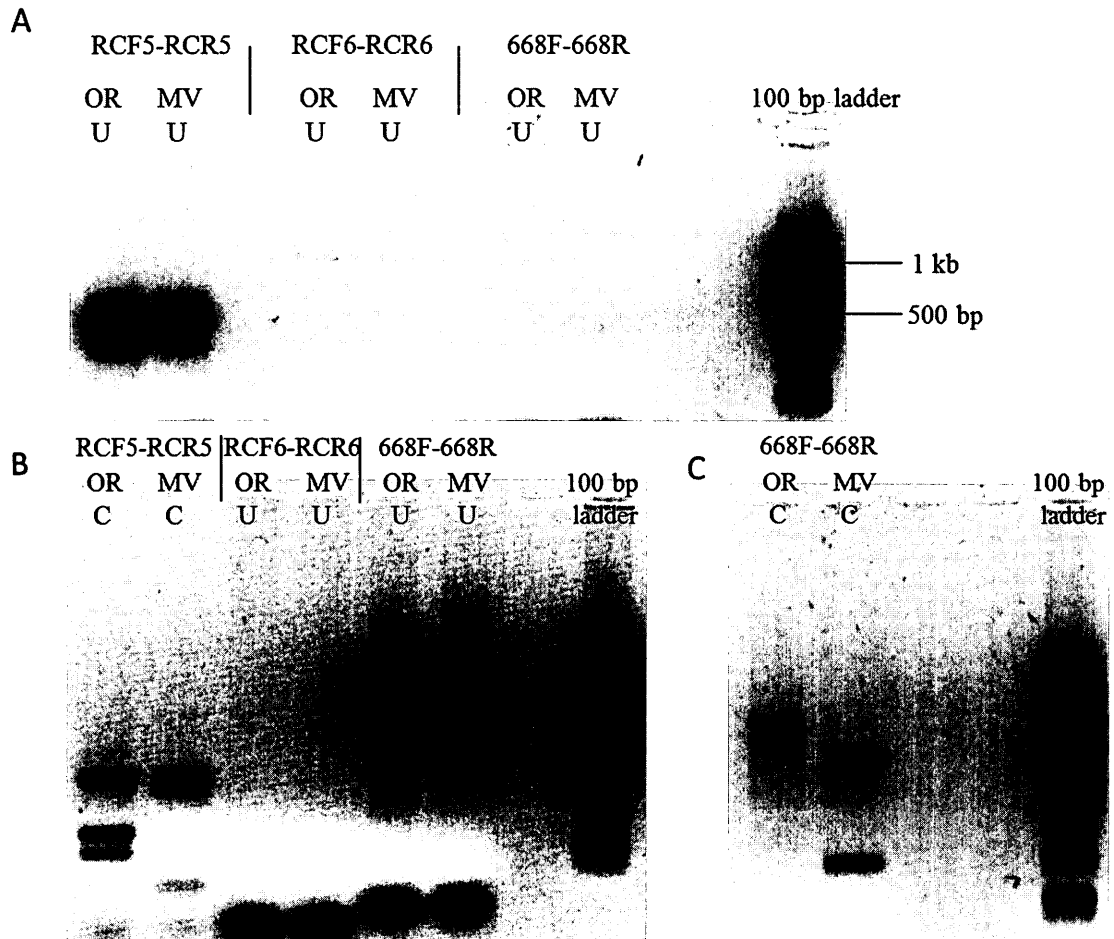
Figure 28. PCR results from *UV90* parental strains using CAPS marker pairs: RCF5-RCR5, RCF6-RCR6 and 668F-668R.

U = "uncut", undigested DNA; C = "cut", DNA digested with Taqα1 (RCF5-RCR5) or MspI (RCF6-RCR6, 668F-668R) restriction enzymes. OR = Oak Ridge *csp-1; bd; UV90* parent; MV = Mauriceville wild type, *csp+; bd+; UV+* parent.

(A) shows parents with all CAPS markers. (B) shows digested RCF5-RCR5 and repeated RCF6-RCR6 and 668F-668R. (C) shows digested 668F-668R.
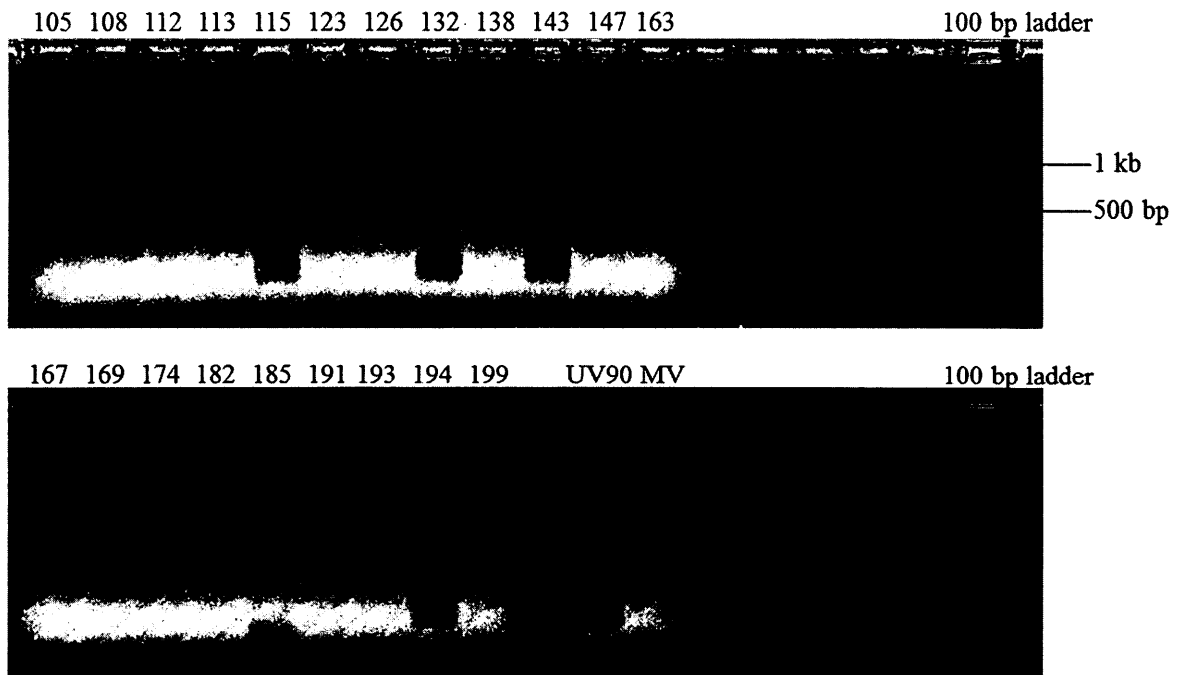
Figure 29. PCR results showing digested *csp-1; bd+; UV+* progeny using RCF5-RCR5

primers. All progeny digested with Taqα1 restriction enzyme. Digested OR DNA

exhibits two overlapping bands, each ~100 bp in size. *UV90 (csp-1; bd; UV90)* and MV

(Mauriceville wild type, *csp+; bd+; UV+*) served as controls.

Most progeny resembled MV after digestion with the exception of #115, 132, 143 and

194 which resembled *UV90* and were determined to be recombinant.
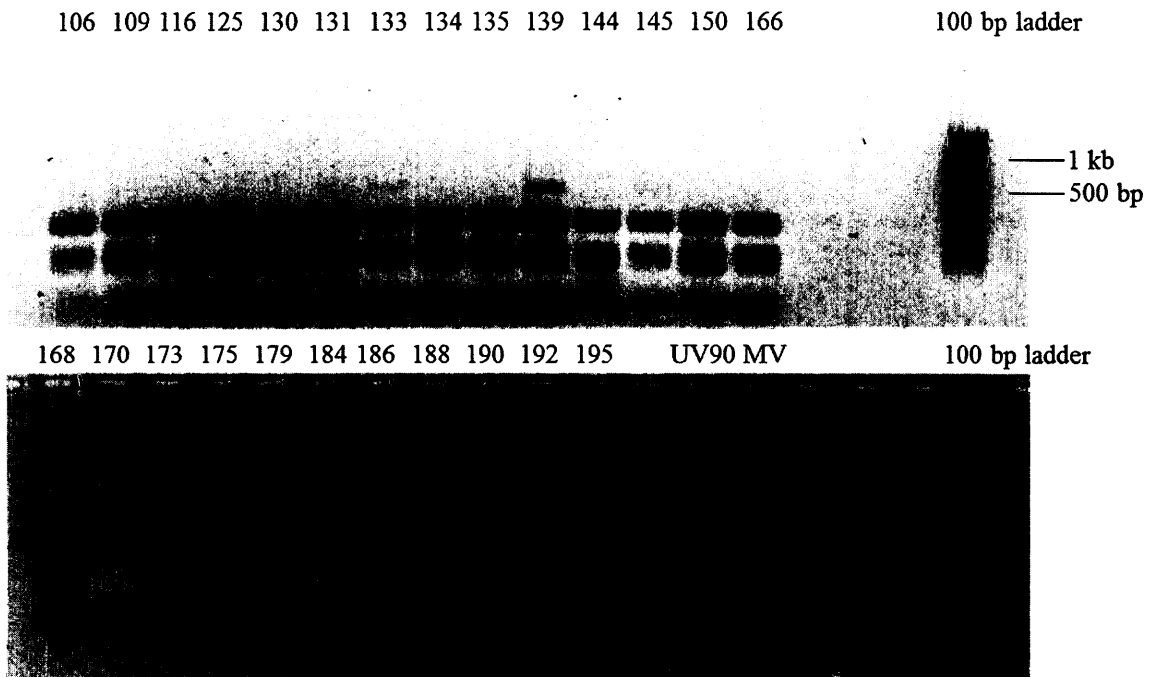
Figure 30. PCR results showing digested *csp-1; bd+; UV90* progeny using RCF5-RCR5

primers. All progeny digested with Taqα1 restriction enzyme. Digested OR DNA

exhibits two overlapping bands, each ~100 bp in size. *UV90 (csp-1; bd; UV90)* and MV

(Mauriceville wild type, *csp+; bd+; UV+*) served as controls.

Most progeny resembled *UV90* after digestion with the exception of #170 and #184

which resembled MV and were determined to be recombinant.
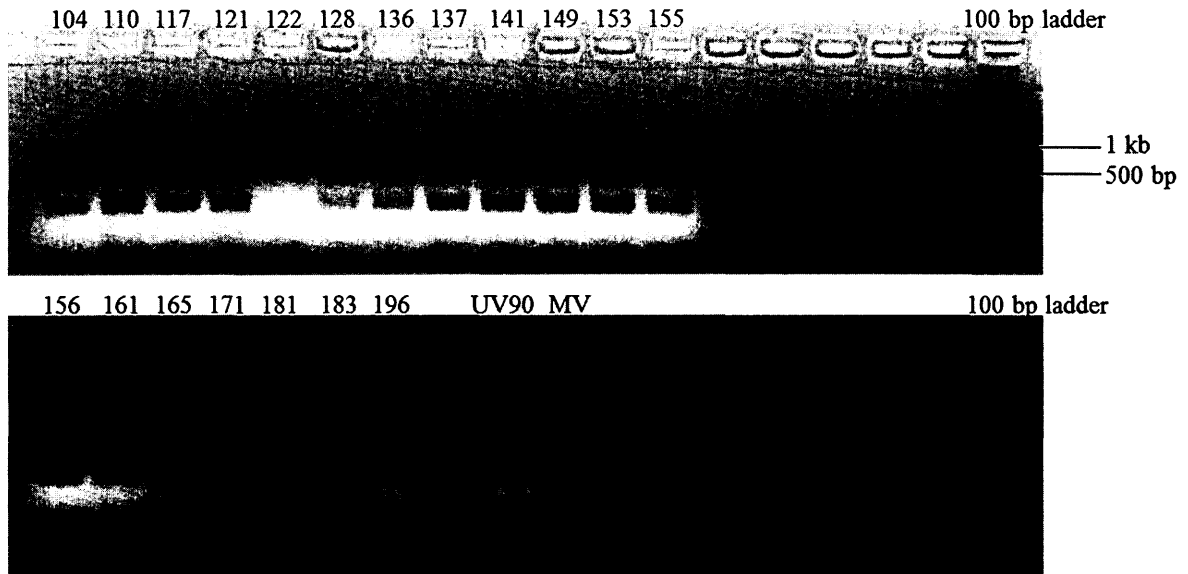
Figure 31. PCR results showing digested *csp-1; bd; UV*+ progeny using 668F-668R

primers.

All progeny digested with MspI restriction enzyme. *UV90 (csp-1; bd; UV90)* and MV

(Mauriceville wild type, *csp+; bd+; UV+*) served as controls.

Most progeny resembled MV after digestion with the exception of #122 which resembled

UV90 and was determined to be recombinant.
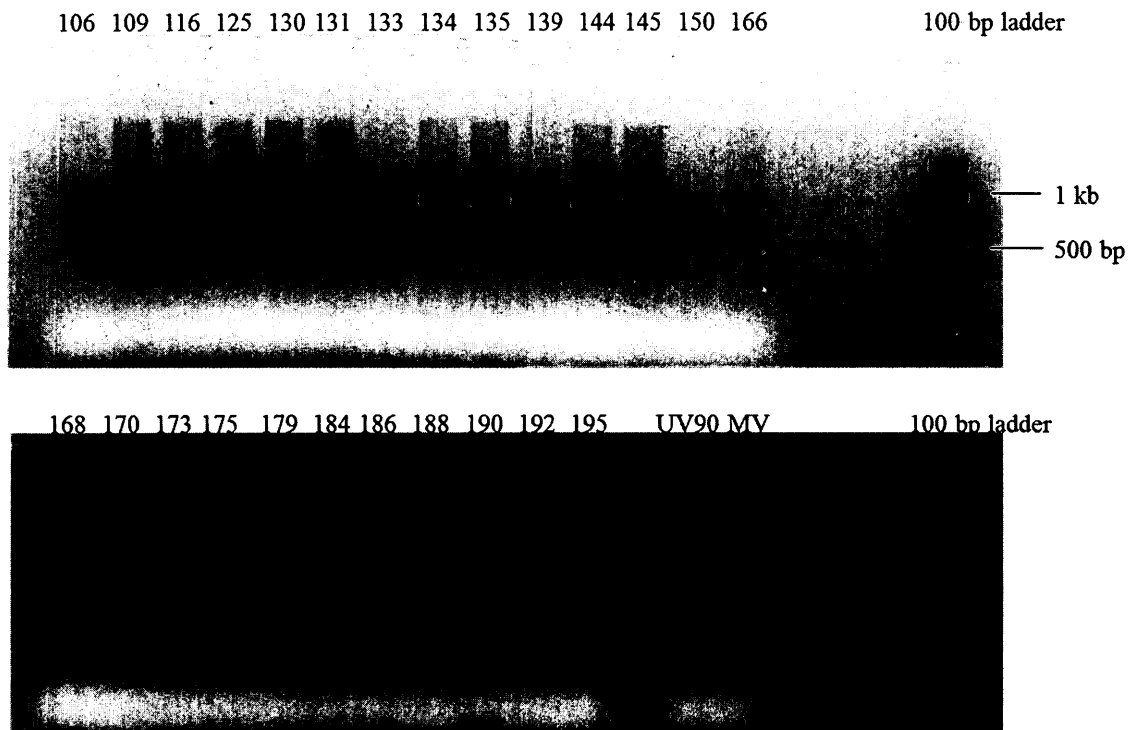
Figure 32. PCR results showing digested *csp-1; bd+; UV90* progeny using 668F-668R

primers.

All progeny digested with MspI restriction enzyme. *UV90 (csp-1; bd; UV90)* and MV

(Mauriceville wild type, *csp+; bd+; UV+*) served as controls.

Most progeny resembled *UV90* after digestion with the exception of #184 which

resembled MV and was determined to be recombinant.

Table 17. Recombination frequencies of *csp-1; bd+; UV+/UV90* and *csp-1; bd; UV+/UV90* progeny with RCF5-RCR5 and 668F-668R CAPS markers

Progeny tested with RCF5 & RCR5 primers				Progeny tested with 668F & 668R primers			
csp-1; bd+; UV90		*csp-1; bd+; UV+*		*csp-1; bd+; UV90*		*csp-1; bd+; UV+*	
Progeny #	Recom. (Yes/Y, No/N)*	Progeny #	Recom. (Yes/Y, No/N)*	Progeny #	Recom. (Yes/Y, No/N)*	Progeny	Recom. (Yes/Y, No/N)*
106	N	105	N	106	N	105	N
109	N	108	N	109	N	108	N
116	N	112	N	116	N	112	N
125	N	113	N	125	N	113	N
130	N	115	Y	130	N	115	N
131	N	123	N	131	N	123	N
133	N	126	N	133	N	126	N
134	N	132	Y	134	N	132	N
135	N	138	N	135	N	138	N
139	N	143	Y	139	N	143	Y
144	N	147	N	144	N	147	N
145	N	163	N	145	N	163	N
150	N	167	N	150	N	167	N
166	N	169	N	166	N	169	N
168	N	174	N	168	N	174	N
170	Y	182	N	170	N	182	N
173	N	185	N	173	N	185	N
175	N	191	N	175	N	191	N
179	N	193	N	179	N	193	N
184	Y	194	Y	184	Y	194	N
186	N	199	N	186	N	199	N
188	N			188	N		
190	N			190	N		
192	N			192	N		
195	N			195	N		
csp-1; bd; UV90		*csp-1; bd; UV+*		*csp-1; bd; UV90*		*csp-1; bd; UV+*	
100	N	104	N	100	N	104	N
103	N	110	N	103	N	110	N
111	N	117	N	111	N	117	N
118	N	121	N	118	N	121	N
119	N	122	Y	119	N	122	Y

Progeny tested with RCF5 & RCR5 primers				Progeny tested with 668F & 668R primers			
120	N	128	N	120	N	128	N
127	N	136	N	127	N	136	N
129	N	137	N	129	N	137	N
140	N	141	N	140	N	141	N
146	N	149	N	146	N	149	N
151	N	153	N	151	N	153	N
158	N	155	Y	158	N	155	N
159	N	156	N	159	N	156	N
160	N	161	N	160	N	161	N
162	N	165	N	162	N	165	N
164	N	171	N	164	N	171	N
176	N	181	N	176	N	181	N
187	N	183	N	187	N	183	N
189	N	196	N	189	N	196	N
197	N			197	N		
	Total *UV90*: 2/45		Total *UV+*: 6/40		Total *UV90*: 1/45		Total *UV+*: 2/40
Total recombinant progeny: 8/85 (9.41%)				Total recombinant progeny: 3/85 (3.53%)			

*Recom. = recombinant. Recombinant progeny are shown in red
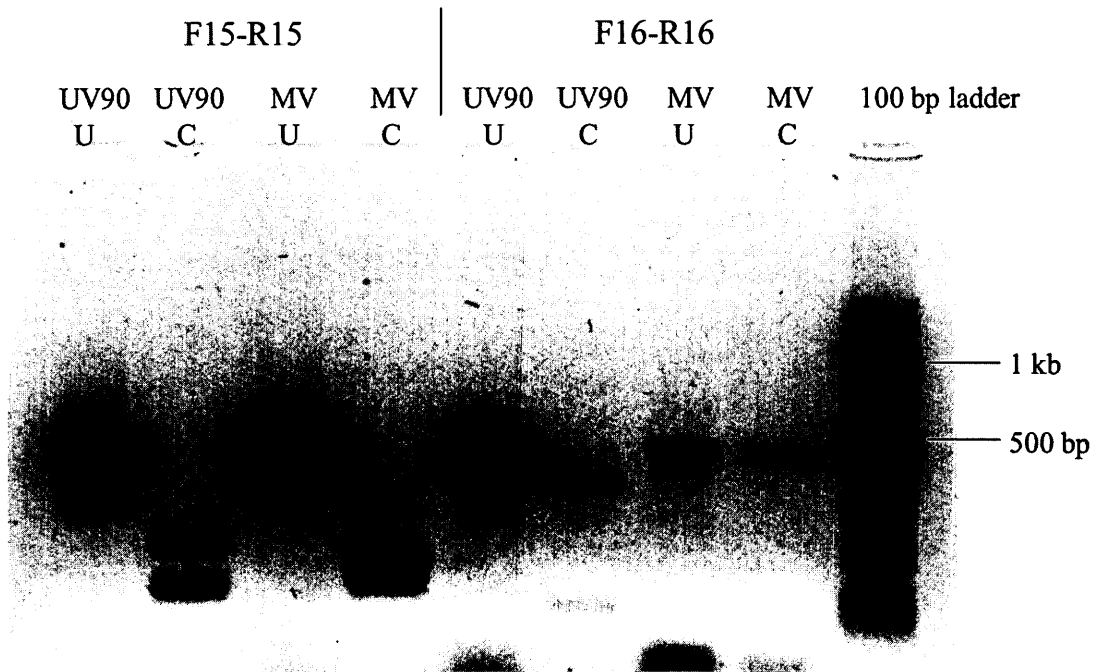
Figure 33. PCR results from *UV90* parental strains using CAPS markers F15-R15 and

F16-R16.

U = "uncut", undigested DNA; C = "cut", DNA digested with Taqα1 (F15-R15) or

HaeIII (F16-R16) restriction enzymes. Digested MV DNA (F15-R15) exhibits two

overlapping bands, each ~250 bp in size. *UV90* = *csp-1; bd; UV90* parent; MV =

Mauriceville wild type, *csp+; bd+; UV+* parent.
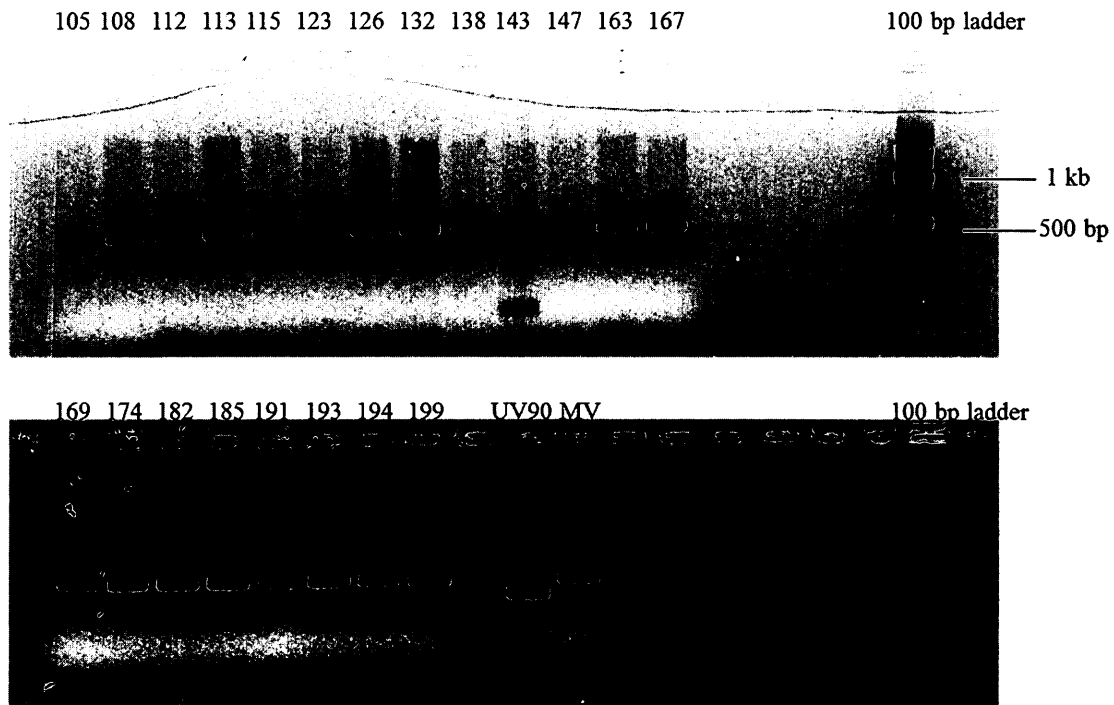
Figure 34. PCR results showing digested *csp-1; bd+; UV+* progeny using F16-R16

primers.

All progeny digested with HaeIII restriction enzyme. *UV90 (csp-1; bd; UV90)* and MV

(Mauriceville wild type, *csp+; bd+; UV+*) served as controls.

Most progeny resembled MV after digestion with the exception of #143 which resembled

UV90 and was determined to be recombinant.

106 109 116 125 130 131 134 135 139 144 145 150 166 168   100 bp ladder

— 1 kb

— 500 bp

173 175 179 184 186 188 192 195   UV90 MV   100 bp ladder
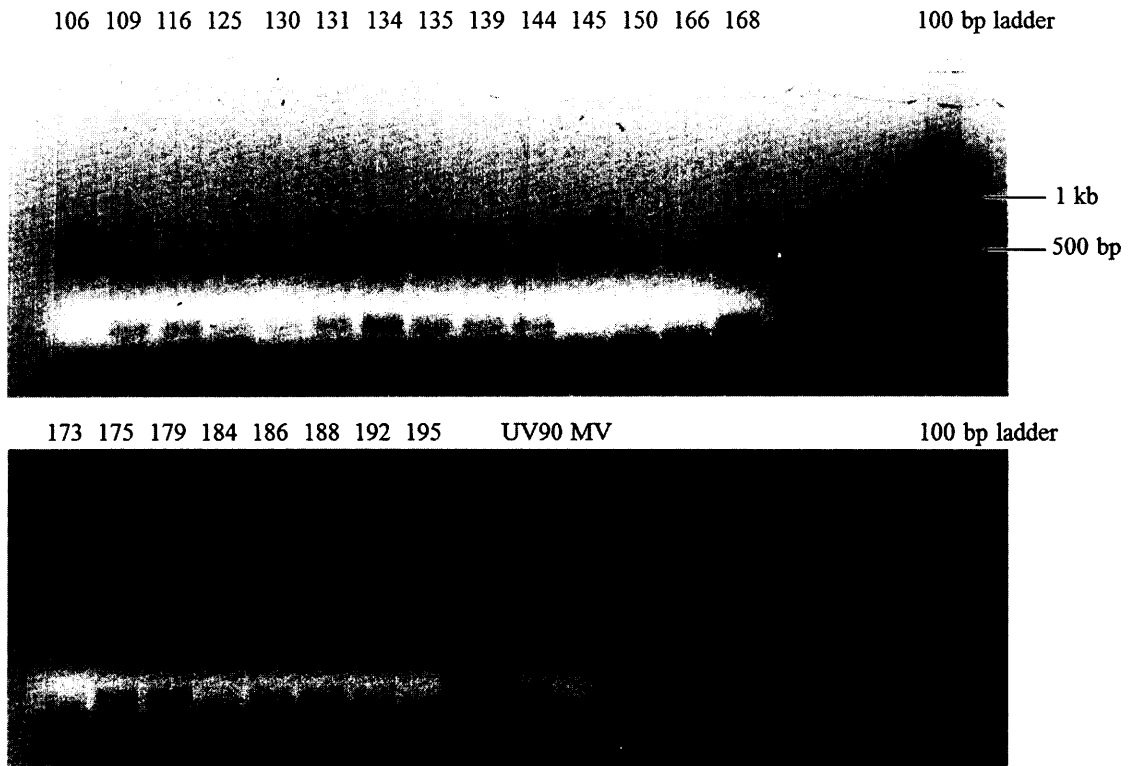
Figure 35. PCR results showing digested *csp-1; bd+; UV90* progeny using F16-R16

primers.

All progeny digested with HaeIII restriction enzyme. *UV90 (csp-1; bd; UV90)* and MV

(Mauriceville wild type, *csp+; bd+; UV+*) served as controls.

Most progeny resembled *UV90* after digestion with the exception of #106 and #145

which resembled MV and were determined to be recombinant.

Table 18. Recombination frequencies of *csp-1; bd+; UV+/UV90* and *csp-1; bd; UV+/UV90* progeny with F16-R16 CAPS marker

Progeny tested with F16 & R16 primers							
csp-1; bd+; UV90		*csp-1; bd; UV90*		*csp-1; bd+; UV+*		*csp-1; bd; UV+*	
Progeny #	Recom. (Yes/Y, No/N)*	Progeny #	Recom. (Yes/Y, No/N)*	Progeny #	Recom. (Yes/Y, No/N)*	Progeny	Recom. (Yes/Y, No/N)*
106	Y	100	N	105	N	104	N
109	N	103	N	108	N	110	Y
116	N	111	N	112	N	117	N
125	N	118	N	113	N	121	N
130	N	119	N	115	N	122	N
131	N	120	N	123	N	128	N
133	N	127	N	126	N	136	N
134	N	129	N	132	N	137	N
135	N	140	Y	138	N	141	Y
139	N	146	N	143	Y	149	N
144	N	151	N	147	N	153	N
145	Y	158	N	163	N	155	N
150	N	159	N	167	N	156	N
166	N	160	Y	169	N	161	N
168	N	162	N	174	N	165	N
170	N	164	N	182	N	171	N
173	N	176	N	185	N	181	N
175	N	187	N	191	N	183	Y
179	N	189	N	193	N	196	N
184	N	197	N	194	N		
186	N			199	N		
188	N						
190	N						
192	N						
195	N						
Total *UV90*: 4/45				Total *UV+*: 4/40			
Total recombinant progeny: 8/85 (9.41%)							

*Recom. = recombinant. Recombinant progeny are shown in red
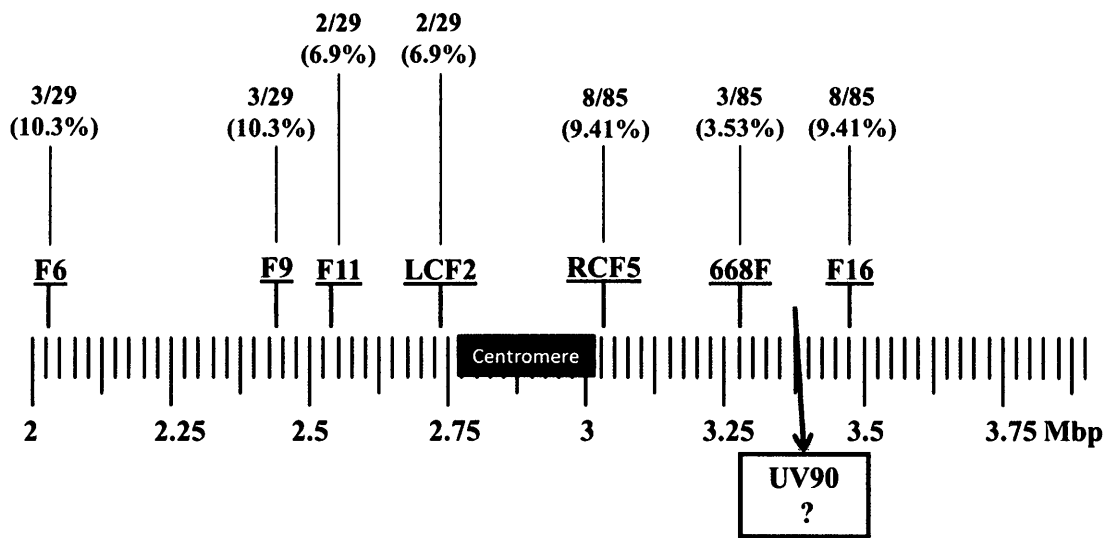
Figure 36. Schematic of *Neurospora crassa* Linkage Group VI displaying primers F6

through F16, *UV90* progeny recombination and suspected location of *UV90* mutation.

Scale is in Mega basepairs (Mbp). Primers **F6, F9, F11, LCF2, RCF5, 668F** and **F16**

are located at 2.14, 2.41, 2.56, 2.73, 3.10, 3.29 and 3.48 Mbp, respectively.

UV90 ? = potential location of *UV90* gene.

3.1.5 CAPS markers between 668F-668R and F16-R16 and potential *UV90* genes

To further narrow down the location of the *UV90* gene, 8 pairs of CAPS markers were designed between 668F-668R and F16-R16 as described in Methods 2.2.4: 3317F through 3352R (Tables 2 and 3, Materials and Methods). Primers were named based on their Mega basepair locations on Linkage Group VI. PCR and restriction enzyme digestion were performed on the parental strains *csp-1; bd; UV90* (sg #227) and MV wild type as described in Methods 2.2.5 (Fig. 37). CAPS markers 3317F-3317R, 3395F-3395R, 3436F-3436R, 3368F-3368R and 3451F-3451R produced different patterns after digestion for *UV90* and MV and were chosen for PCR (Fig. 37, A and B). CAPS markers 3346F-3346R, 3333F-3333R and 3352F-3352R did not produce any PCR product for *UV90* and were disregarded for further use (Fig. 37, A and C). PCR was repeated twice more on the parental strains with the disregarded CAPS markers and identical results were obtained (data not shown).

PCR was performed using the new CAPS markers only on progeny which were recombinant with markers 668F-668R and F16-R16 (Tables 17 and 18). Those progeny were chosen since only the recombinants have a crossover event between markers 668F-668R and F16-R16 and can be used for mapping. The recombinants are as follows: *UV90* progeny #106, 140, 145, 160 and 184; *UV+* progeny #110, 122, 141, 143, 183. CAPS marker 3317F-3317R produced 1 recombinant (Fig. 38). CAPS marker 3395F-3395R produced 4 recombinants (Figs. 38 and 39). CAPS marker 3436F-3436R

produced 6 recombinants (Fig. 39). CAPS marker 3368F-3368R produced 2

recombinants (Fig. 40). A list of CAPS markers between 668F-668R and F16-R16 and

recombinant progeny is shown in Table 19 & Figure 41. CAPS marker 3451F-3451R

was not used due to obtaining sufficient data with the other markers. The number of

recombinant progeny decreased from 3 to 1 at markers 668F-668R and 3317F-3317R,

and increased to 2 at marker 3368F-3368R, suggesting *UV90* is likely somewhere in

between 668F-668R and 3368F-3368R (Fig. 41).

It was noted on the Broad Institute *Neurospora crassa* database in March 2013

(http://www.broadinstitute.org/annotation/genome/neurospora/News.html) that a

correction to the DNA sequence was made to a region on Linkage Group VI. A new

BLAST search of all primers

(http://www.broadinstitute.org/annotation/genome/neurospora/Blast.html) revealed new

locations for primers to the left of the centromere. All affected primers with their

previous and new locations are listed in Table 20. Other primers used for genetic

mapping to the right of *UV90* were not affected by the sequence change. The primers

used for mapping on the left of the centromere were in reverse order than previously

thought, and were moving away from the centromere as opposed to towards it. This

indicates that the recombination rates were decreasing as the primers were moving away

from the centromere. It is unknown why the recombination rates decreased as the

markers moved farther away from *UV90*.

A list of candidate *UV90* genes between CAPS markers 668F-668R and 3368F-3368R were determined through a gene search at the Broad Institute *Neurospora crassa* database (http://www.broadinstitute.org/annotation/genome/neurospora/FeatureSearch.html) and are shown in Table 21. Knockouts of each candidate gene were ordered from the Fungal Genetic Stock Center (FGSC) (see Table 1, Materials and Methods). These were screened to check for the presence of the *UV90* gene phenotype.
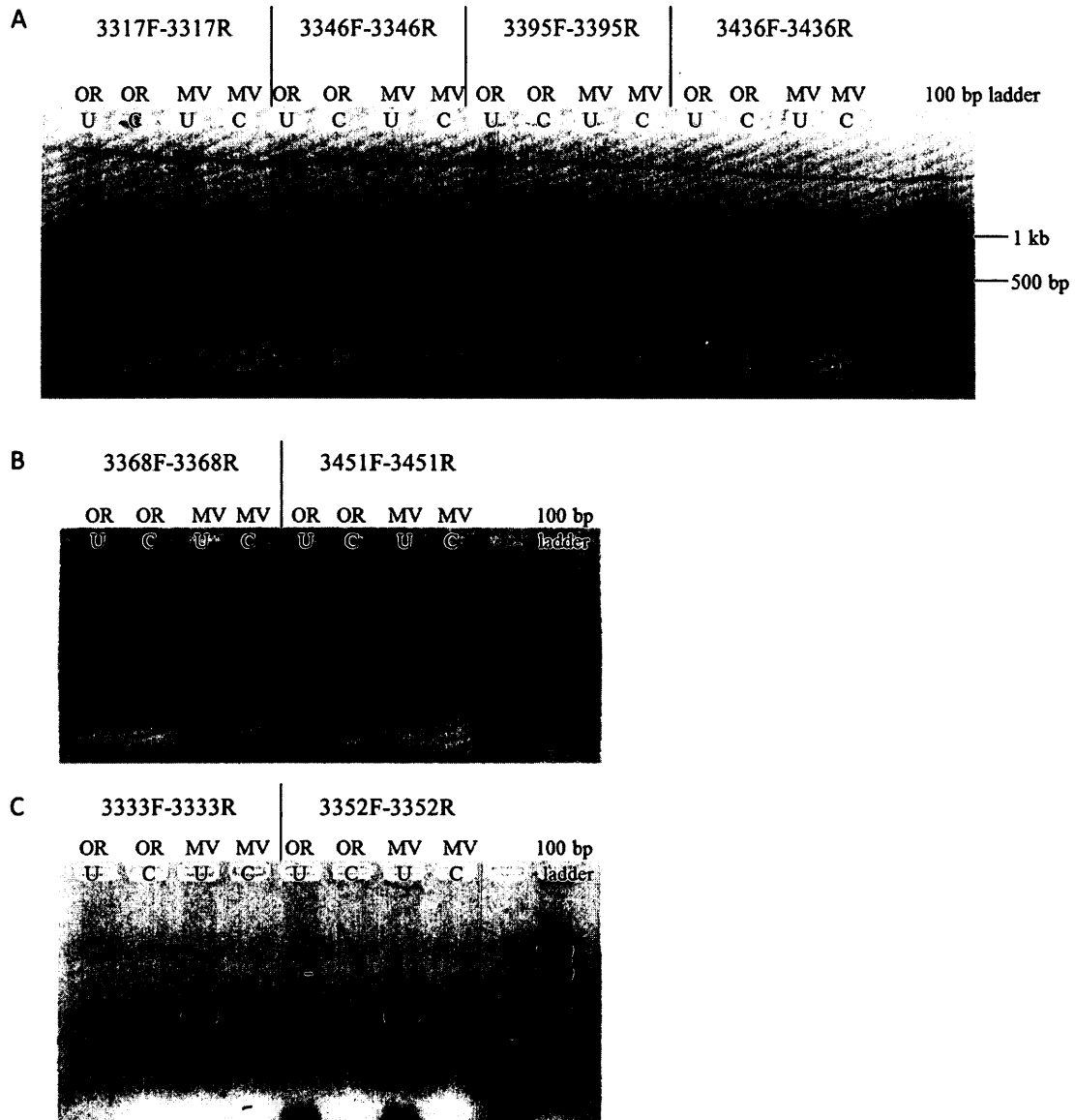
Figure 37. PCR results from *UV90* parental strains using CAPS marker pairs: 3317F-3317R through 3352F-3352R. U = "uncut", undigested DNA; C = "cut", DNA digested with Taqα1 (3317F-R, 3346F-R, 3395F-R, 3436F-R, 3352F-R), MseI (3368F-R, 3451F-R) or HaeIII (3333F-R) restriction enzymes. OR = Oak Ridge *csp-1; bd; UV90* parent; MV = Mauriceville wild type, *csp+; bd+; UV+* parent.
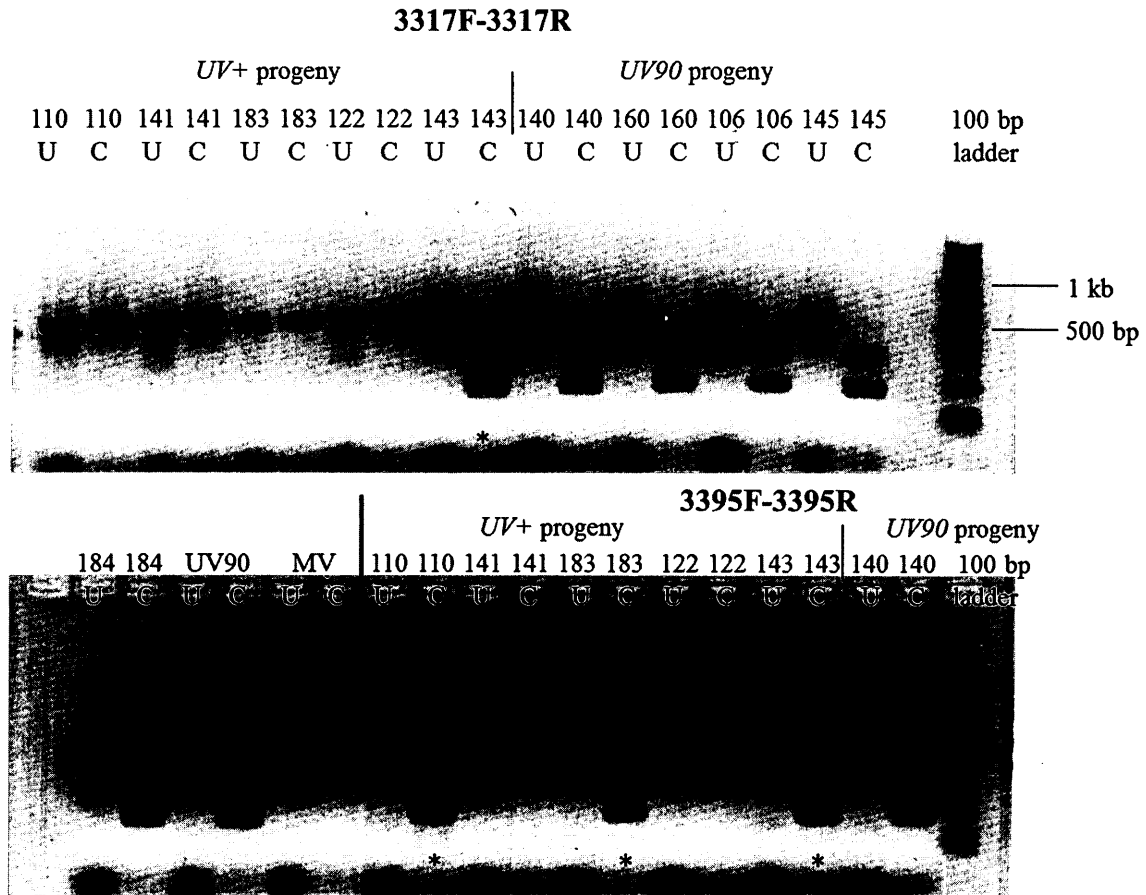
3317F-3317R

Figure 38. PCR results showing 668F-668R and F16-R16 *UV*+ and *UV90* recombinants

using 3317F-3317R and 3395F-3395R CAPS markers.

U = "uncut", undigested DNA; C = "cut", DNA digested with Taqα1 restriction enzyme.

UV90 (*csp-1; bd; UV90*) and MV (Mauriceville wild type, *csp+; bd+; UV+*) served as

controls.

* = denotes recombinant progeny.

3395F-3395R   **3436F-3436R**

UV90 progeny

160 160 106 106 145 145 184 184 UV90   MV |110 110 141 141 183 183   100 bp
U C U C U C U C U C   U* C   U C U C   U C   ladder

—— 1 kb

—— 500 bp

UV+ progeny   *UV90* progeny

122 122 143 143|140 140 160 160 106 106 145 145 184 184 UV90   MV   100 bp
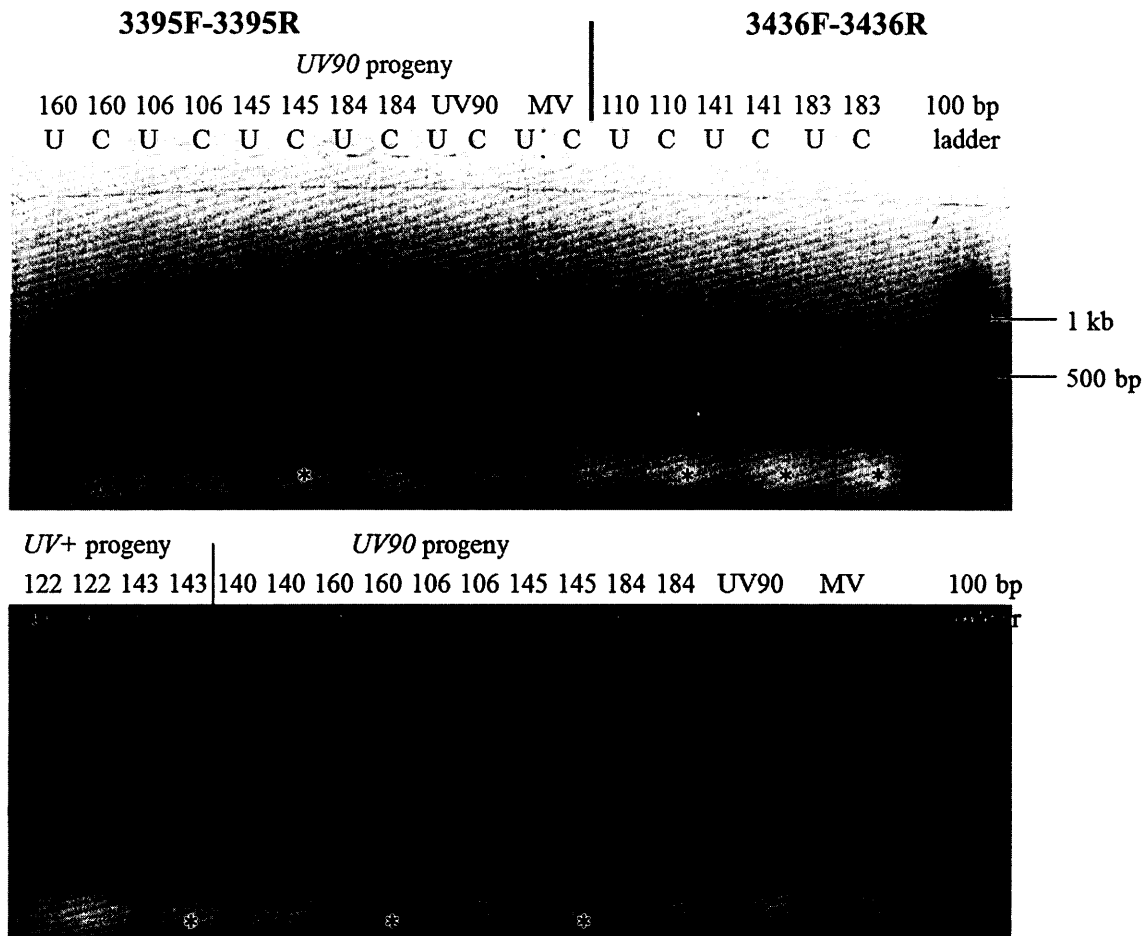
Figure 39. PCR results showing 668F-668R and F16-R16 *UV+* and *UV90* recombinants

using 3395F-3395R and 3436F-3436R CAPS markers.

U = "uncut", undigested DNA;   C = "cut", DNA digested with Taqα1 restriction enzyme.

UV90 (*csp-1; bd; UV90*) and MV (Mauriceville wild type, *csp+; bd+; UV+*) served as

controls.

* = denotes recombinant progeny.

116
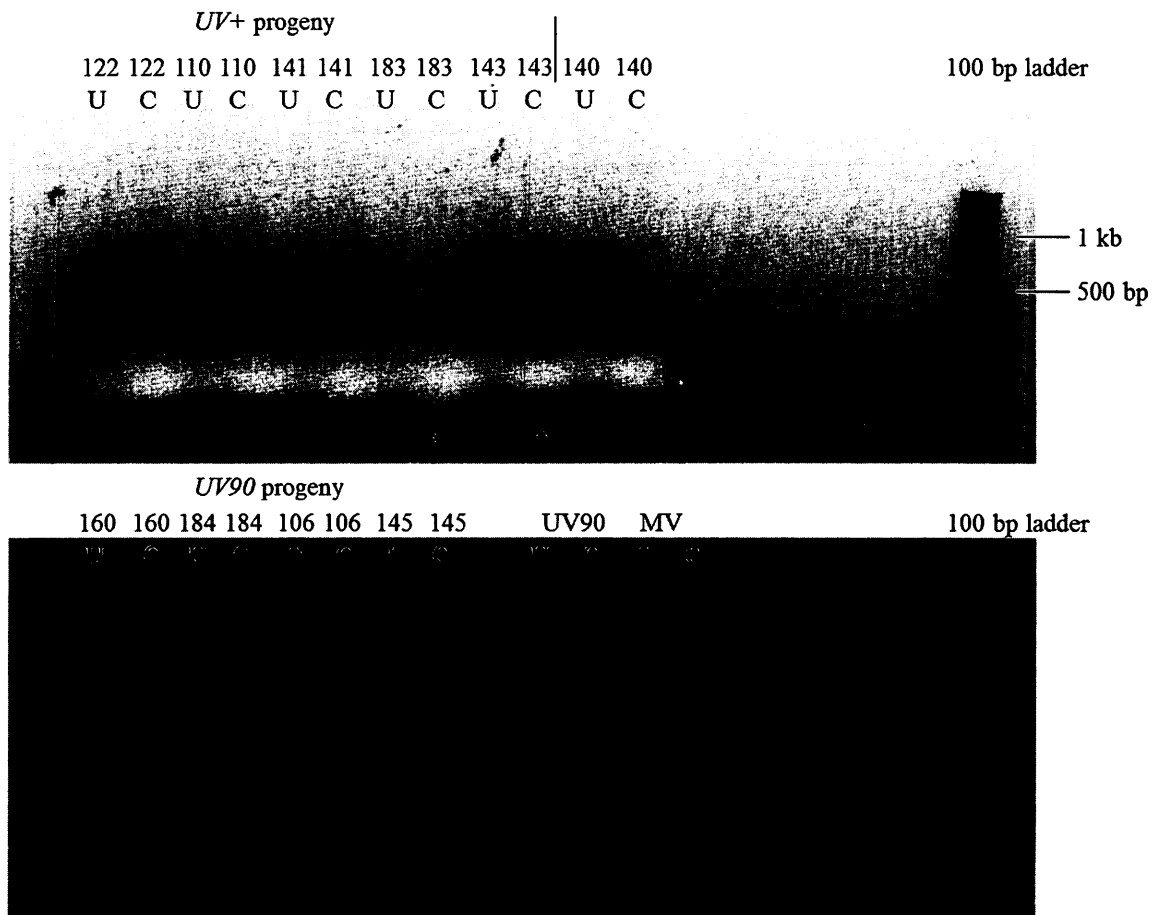
Figure 40. PCR results showing 668F-668R and F16-R16 *UV+* and *UV90* recombinants using 3368F-3368R CAPS markers.

U = "uncut", undigested DNA; C = "cut", DNA digested with MseI restriction enzyme.

UV90 (*csp-1; bd; UV90*) and MV (Mauriceville wild type, *csp+; bd+; UV+*) served as controls. *UV+* progeny #183 was repeated and resembled *UV90*, and was determined to be recombinant (data not shown).

* = denotes recombinant progeny.
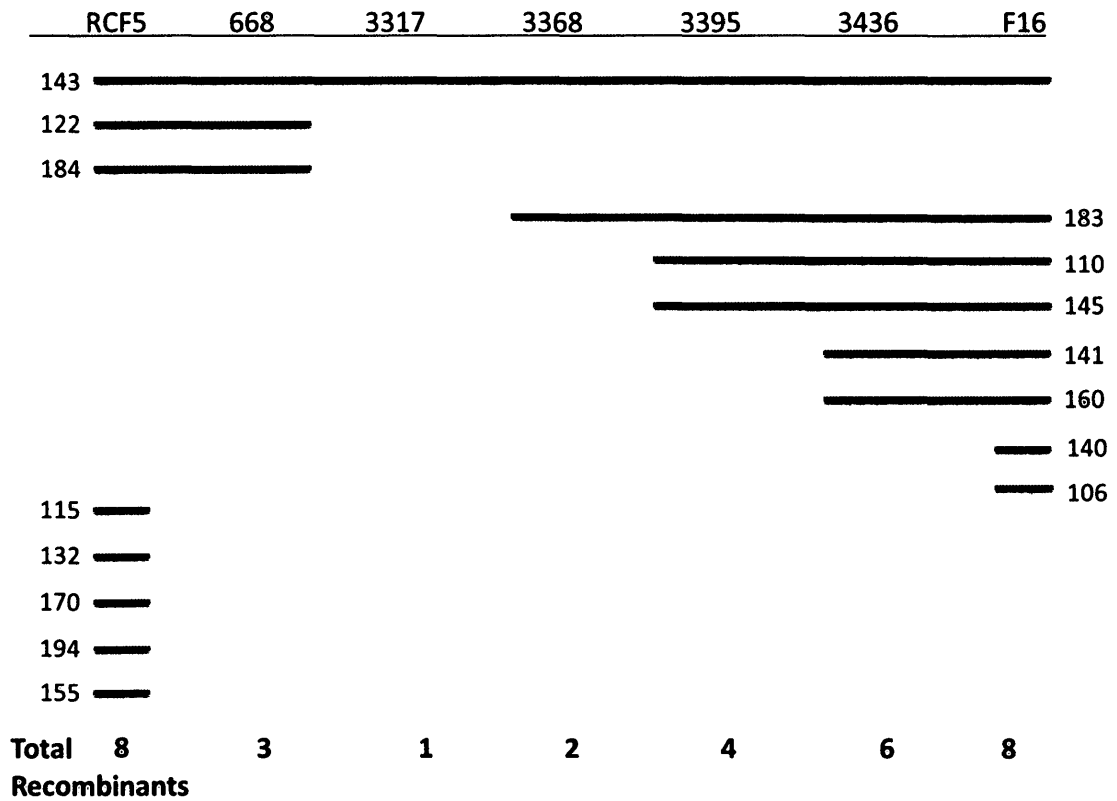
Figure 41. Recombinant progeny with primers RCF5 through F16.

All primers between RCF5 and F16 are shown on the top row. Left and right values are recombinant progeny. Red lines denote which primers the progeny were recombinant with. Total number of recombinants are listed at the bottom row.

Number of recombinant progeny decreases to the right of 668 and increases towards 3368.

Table 19. Number of recombinant progeny with CAPS markers between 668F-668R and F16-R16

CAPS marker	668F-668R	3317F-3317R	3368F-3368R	3395F-3395R	3436F-3436R	F16-R16
Marker location*	3.293	3.317	3.368	3.395	3.436	3.483
Number of recombinant progeny	3 (#122, 143, 184)	1 (#143)	2 (#143, 183)	4 (#110, 143, 145, 183)	6 (#110, 141, 143, 145, 160, 183)	8 (#106, 110, 140, 141, 143, 145, 160, 183)

*In Mega base pairs, Linkage Group VI

Table 20. Previous and new locations of Linkage Group VI primers to the left of the centromere

Primer Name	Sequence 5' -> 3'	Previous location (bp) and strand (+/-)	New Location (bp) and strand (+/-)
F3*	ACCTACTTGCGACAGCGTGCTTG	2,059,068-090 (-)	2,576,160-182 (+)
R3*	TTGTCCACTTACACTCGGCACG	2,057,830-851 (+)	2,577,399-420 (-)
F6*	TTCACGAGTGTCCCGGATGTG	2,141,366-386 (-)	2,493,864-884 (+)
R6*	GCATTGTCATCTCGTTGGTGC	2,140,152-172 (+)	2,495,078-098 (-)
F9*	AAGGTCGGGTTGTTAGACGA	2,410,071-090 (-)	2,225,160-179 (+)
R9*	GGCTGAGGGTGGATAGCTAGA	2,409,630-650 (+)	2,225,600-620 (-)
F10	TCATCGAGTTACCTGCCAAGC	2,547,480-500 (+)	2,087,750-770 (-)
R10	TTGGGTGTTCGTTGGACTCC	2,547,877-896 (-)	2,087,354-373 (+)
F11	GGTAACTATGTACATGCCCCGTG	2,559,077-099 (+)	2,076,151-173 (-)
R11	CGATACGATTCTTGGCATCAGC	2,559,500-521 (-)	2,075,729-750 (+)
LCF1	CGGCCGTGTAGCAGAATACA	2,726,641-660 (+)	1,908,590-609 (-)
LCR1	ATAATGGCGATGGCGATGTG	2,727,065-084 (-)	1,908,166-185 (+)
LCF2	GGGCGCCATCAATTTCACTT	2,734,610-629 (+)	1,900,621-640 (-)
LCR2	TTTGAGCTCGGGATTTGCTG	2,735,067-086 (-)	1,900,164-183 (+)

*Designed by Dr. Kamyar Motavaze

Table 21. List of 21 *Neurospora crassa* candidate *UV90* genes located on Linkage Group (chromosome) VI, from 3.293 to 3.369 Mbp.

Locus	Gene Name	Location (Mbp, Oak Ridge strain, Supercontig 6)	Length (bp)
NCU17127.7*	hypothetical protein	3294468-3295683 +	1216
NCU05962.7	hypothetical protein	3303139-3303378 -	240
NCU05961.7	DUF572 domain-containing protein	3304910-3306530 +	1621
NCU05960.7*	GPI mannosyltransferase 2	3306630-3309661 -	3032
NCU05959.7*	vesicle transport V-SNARE protein VTI1	3311937-3313502 -	1566
NCU05958.7	hypothetical protein	3315098-3318376 +	3279
NCU05957.7	hypothetical protein	3319864-3322467 +	2604
NCU05956.7	glycosylhydrolase family 2-2	3322517-3326426 -	3910
NCU05955.7	Cel74a	3326807-3330420 +	3614
NCU05954.7	hypothetical protein	3332004-3334639 -	2636
NCU05953.7*	hypothetical protein	3339700-3340998 -	1299
NCU05952.7	hypothetical protein	3341267-3343308 -	2042
NCU05951.7	hypothetical protein	3344579-3346273 +	1695
NCU05950.7	hypothetical protein	3347867-3348756 +	890
NCU05949.7	hypothetical protein	3349464-3350054 +	591
NCU05948.7	hypothetical protein	3353034-3355088 -	2055
NCU05947.7	hypothetical protein	3355960-3356454 -	495
NCU12130.7*	hypothetical protein	3362030-3364815 +	2786
NCU05946.7	hypothetical protein	3364883-3365627 -	745
NCU05945.7	hypothetical protein	3366104-3367798 -	1695
NCU05944.7	hypothetical protein	3368035-3369538 +	1504

*Knockout strains of these genes are currently unavailable

3.2 FGSC Knockouts

3.2.1 Knockout screening for *UV90*

FGSC knockout strains (see Table 1) were ordered as described in Methods 2.3.1. Knockout strains were inoculated onto race tubes containing maltose-arginine medium as described in Methods 2.2.2. 2-3 replicates of each knockout along with controls *csp-1; bd+; UV90* (OR, progeny #131) and OR wild type (sg #259) were inoculated. Race tubes are shown in Figures 42-44. All knockouts resembled the OR wild type with the exception of race tube #10 which resembled the *UV90* control (Fig. 43). Race tube #10 corresponded to FGSC strain #18029 and gene NCU05950 (Table 1). It was confirmed in the lab by Amanda Mohabeer through PCR that NCU05950 was indeed the correct gene which was knocked out (data not shown).

3.2.2 Cross between putative *UV90* KO x #80 (*csp-1; chol-1 bd; frq^{10}*)

FGSC knockout strain #18029 (gene NCU05950) was chosen as a potential *UV90* gene candidate. A cross was performed (previously by Dr. Patricia Lakin-Thomas) between #18029 and *csp-1; chol-1 bd; frq^{10}* (OR, sg #80) to determine if the FGSC knockout behaves as *UV90* does in a genetic cross, and affects the rhythm in the *chol-1; frq^{10}* double mutant. The knockout was also crossed with sg #80 to place it into the same genetic background with other strains that contain the *csp-1*, *chol-1*, *bd* and *frq^{10}* mutations.

186 spores were picked as described in Methods 2.2.1, and *csp-1* "tap test" was performed as described in Methods 2.2.2. 105 were determined to be *csp-1*, 49 were

121

csp+ and 32 did not germinate (Table 22). *csp-1* progeny were numbered and inoculated

onto race tubes containing maltose-arginine medium both with and without 100 μM

choline (labelled as high and low choline) as described in Methods 2.2.2. The controls on

high choline were *csp-1; chol-1 bd; frq^{10}* (OR, sg #80) and *csp-1; chol-1 bd; UV90; frq^{10}*

(OR, sg #213). Controls on low choline were *csp-1; chol-1 bd* (OR, sg #26), *csp-1; chol-*

1 bd; UV90 (OR, sg #224), *csp-1; chol-1 bd; frq^{10}* (OR, sg #80) and *csp-1; chol-1 bd;*

UV90; frq^{10} (OR, sg #213).

Progeny were separated into *bd* and *bd+* through visual inspection. The *bd* strains are

slower growing than *bd+* as detected by the marked growth fronts (Fig. 45). 50 were

found to be *bd+* and 55 were *bd* (Table 23).

The *bd* race tubes were further separated into the following groups based on

visual comparisons to the controls: 18 were found to be *csp-1; bd*, 8 were *csp-1; bd;*

UV90, 16 were *csp-1; bd; frq^{10}*, 7 were *csp-1; bd; UV90; frq^{10}* and 6 were unclassifiable

(Figs. 46-47, Table 24).

The number of *UV90* progeny was fewer than expected, and did not fall into a 1:1:1:1

ratio for all 4 classes (Table 24). A chi-square test was performed and the *p* value was

non-significant ($p = 0.0601$) (Table 24, Appendix X). Since the knockout and *frq^{10}* genes

are located on separate chromosomes, this test showed normal segregation of the

knockout when placed through a genetic cross. Only 7 out of 55 progeny were *chol+*

(Table 24), which was expected due to the fact that the *chol-1* and *bd* genes are on the

same chromosome and therefore are linked (http://www.broadinstitute.org/annotation/ genome/neurospora/FeatureSearch.html).

The periods and growth rates of the 55 *csp-1; bd* progeny on high choline are shown in Tables 25 and 26. The growth rate and period of *csp-1; bd* progeny was 1.18 (± 0.023) mm/hr and 21.6 (± 0.152) hr (Table 25). *csp-1; bd; frq^{10}* progeny had a growth rate of 1.26 (± 0.020) mm/hr (Table 25). These values were very close to reported growth rates and periods: 1.18 mm/hr and 21.2 hr for *csp-1; chol-1 bd*, and 1.28 mm/hr for *csp-1; chol-1 bd; frq^{10}* (Li et al., 2011). Reported values of *chol-1* strains were used for comparison since most progeny carried the *chol-1* mutation, and growth rates and periods were calculated on media supplied with 100 μM choline. *csp-1; bd; UV90* growth rate was 1.06 (± 0.041) mm/hr, and 1.10 (± 0.014) mm/hr for *csp-1; bd; UV90; frq^{10}* (Table 26). These values were also close to reported growth rates: 1.07 mm/hr for *csp-1; chol-1 bd; UV90* and 1.19 for *csp-1; chol-1 bd; UV90; frq^{10}* (Li et al., 2011). These data confirm that FGSC knockout #18029 has similar growth rates and periods in a cross with *csp-1; chol-1 bd; frq^{10}* (sg #80).

Figure 46 shows the *csp-1; bd; UV+* and *UV90* progeny on high choline. The *UV+* progeny show a clear, robust rhythm of conidiation, while the *UV90* progeny show a dampened, low amplitude rhythm, consistent with the *UV90* phenotype (Li et al., 2011). Figure 47 shows *csp-1; bd; frq^{10}; UV+* and *UV90* progeny on high choline. *UV+; frq^{10}* progeny show arrhythmic conidiation and a fluffy appearance. *UV90; frq^{10}* progeny also

show arrhythmic conidiation, yet the physical appearance is grainy and not fluffy as in *UV+* strains.

Figure 48 shows *csp-1; bd; UV+* and *UV90* progeny on low choline. *UV+* progeny have a weak, but clear rhythm of conidiation, and *UV90* progeny appear arrhythmic. Figure 49 shows *csp-1; bd; frq^{10}; UV+* and *UV90* progeny on low choline. In the *chol-1; frq^{10}* background, *UV+* progeny appear to have rhythmic conidiation, whereas *UV90* progeny appear arrhythmic. Abolishing the rhythm in a *chol-1; frq^{10}* strain on low choline is a characteristic of the *UV90* mutation (Li et al., 2011). This is a strong indicator that the knocked out gene in FGSC #18029 is *UV90,* as it appears and behaves identical to *UV90* when placed through a cross.

Marked growth fronts were used to distinguish *chol+* from *chol-1* strains, as *chol+* strains have fast growth rates on both high and low choline media (data not shown). *csp-1; bd; UV90* progeny #58, 83, 97 and *csp-1; bd* progeny #13, 63, 72, 98 were determined to be *chol+* (Table 24).
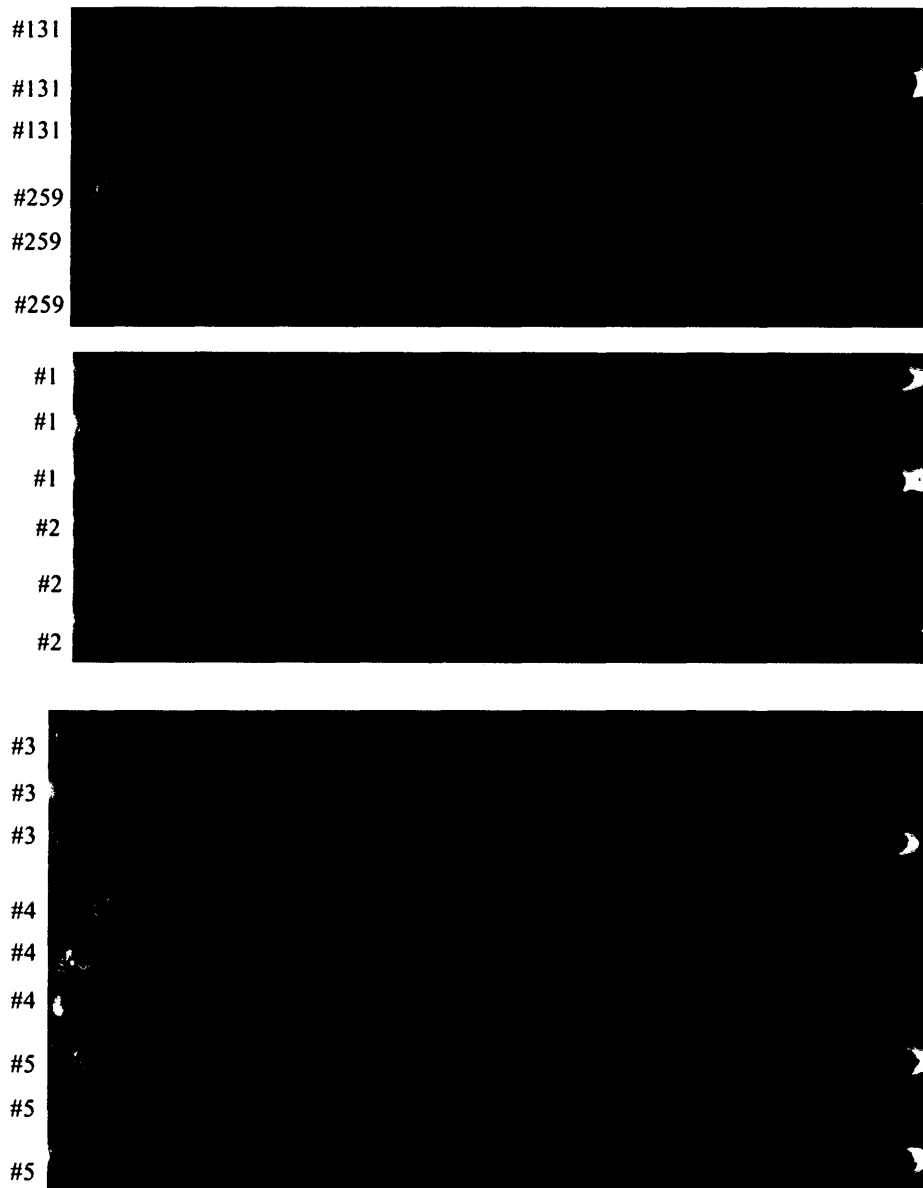
Figure 42. FGSC knockout strains #1-5 and controls *csp-1; bd+; UV90* and Oak Ridge

wild type.

#131 (*csp-1; bd+; UV90*) and #259 (Oak Ridge wild type, *csp+; bd+; UV+*) served as

controls. #1 = FGSC 17842; #2 = FGSC 13721; #3 = FGSC 17841; #4 = FGSC 17839;

#5 = FGSC 18085.
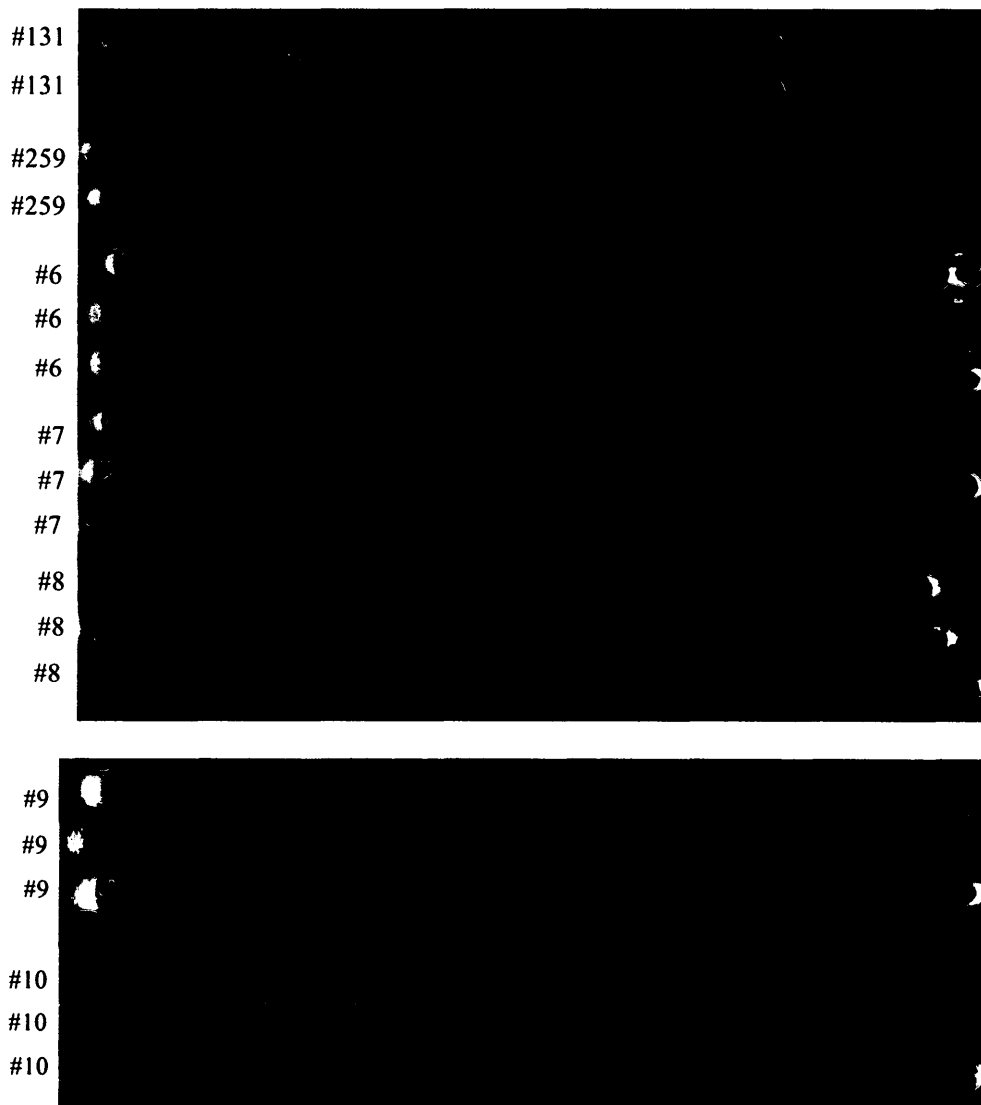
Figure 43. FGSC knockout strains #6-10 and controls *csp-1; bd+; UV90* and Oak Ridge

wild type.

#131 (*csp-1; bd+; UV90*) and #259 (Oak Ridge wild type, *csp+; bd+; UV+*) served as

controls. #6 = FGSC 17845; #7 = FGSC 11909; #8 = FGSC 11310; #9 = FGSC 13535;

#10 = FGSC 18029.

#131

#131

#259

#259

#11

#11

#11

#12

#12

#12

#13

#13

#13

#14

#14

#14

#15

#15

#15

#16

#16

#16
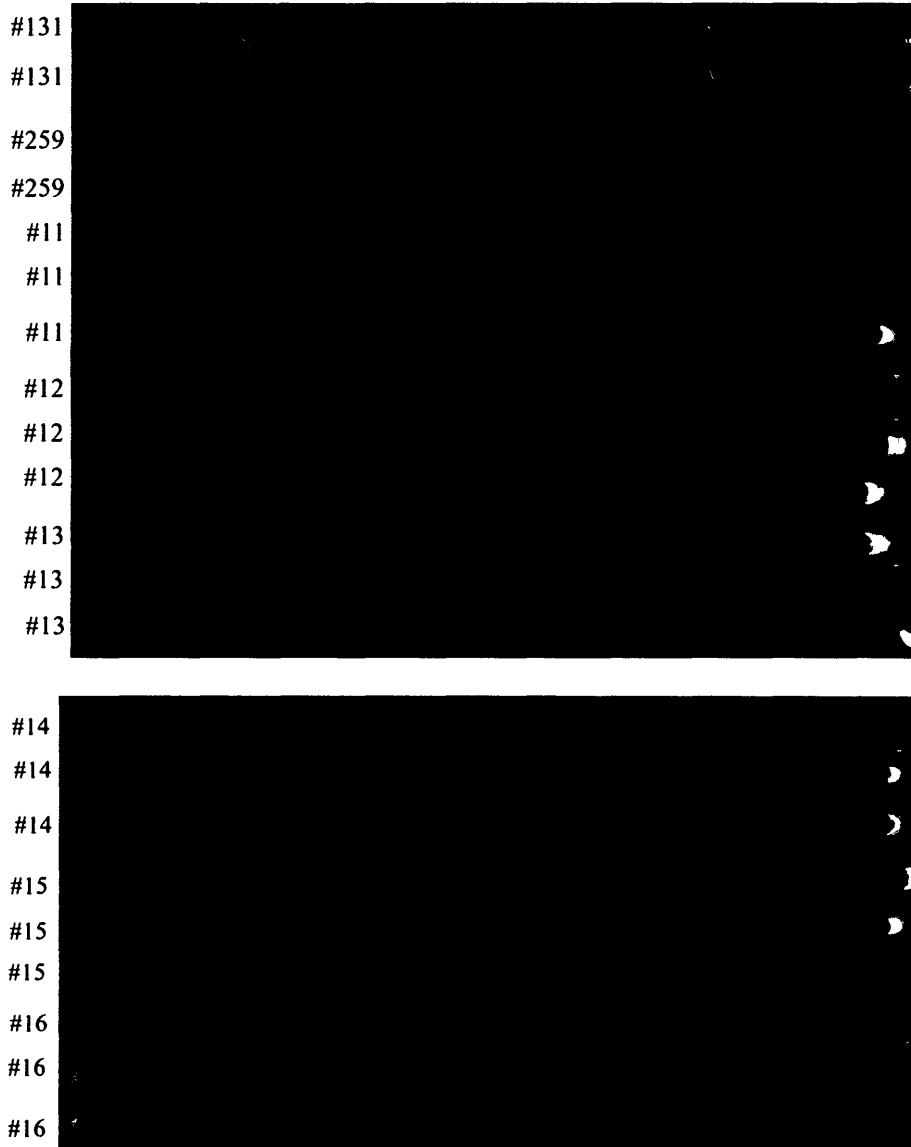
Figure 44. FGSC knockout strains #11-6 and controls *csp-1; bd+; UV90* and Oak Ridge

wild type.

#131 (*csp-1; bd+; UV90*) and #259 (Oak Ridge wild type, *csp+; bd+; UV+*) served as

controls. #11 = FGSC 17838; #12 = FGSC 18213; #13 = FGSC 18028; #14 = FGSC

17836; #15 = FGSC 17835; #16 = FGSC 13533.

Table 22. *csp+* and *csp-1* progeny from cross between FGSC #18029 and *csp-1; chol-1 bd; frq^{10}* (OR, sg #80)

Total spores picked	*csp-1* progeny	*csp+* progeny*	Non-germinating progeny*
186	105 (56.45%)	49 (26.34%)	32 (17.2%)

*csp+ and non-germinating progeny were excluded from further analysis

Table 23. *csp-1* progeny from cross between FGSC #18029 and *csp-1; chol-1 bd; frq^{10}* (OR, sg #80) tested on 100 μM choline

Total *csp-1* progeny analyzed	*csp-1; bd* progeny	*csp-1; bd+* progeny*
105	55 (52.4%)	50 (47.6%)
	#1,4,5,6,7,8,9,11,12,13,15,17,1 8,19,20,21,22,23,25,27,28,29,3 1,32,35,38,39,42,52,54,55, 58,63,64,65,67,68,71,72,73,75 76,82,83,86,87,88,90,91,97,98 100,103, 104,105	#2,3,10,14,16,24,26,30,33,34,3 6,37,40,41,43,44,45,46,47,484 9,50,51,53,56,57,59,60,61,626 6,69,70,74,77-81,84,85,89, 92,93,94,95,96,99,101,102

*bd+ progeny were excluded from further analysis

Table 24. *csp-1; bd* progeny from cross between FGSC #18029 and *csp-1; chol-1 bd; frq^{10}* (OR, sg #80) tested on 100 μM choline

Total *csp-1; bd* progeny analyzed	*csp-1; bd* progeny	*csp-1; bd; UV90* progeny	*csp-1; bd; frq^{10}* progeny	*csp-1; bd; UV90; frq^{10}* progeny	Unclassifiable
55	18 (32.7%)	8 (14.5%)	16 (29.0%)	7 (12.7%)	6 (10.9%)
	(progeny #4,6,7,8,9,**13***,19, 20,28,54,55,**63***, 65,**72***,88,**98***, 104, 105)	(progeny #22,52,**58***,64, **83***,87,91,**97***)	(progeny # 1, 5,17,21,31,35 , 38,39,42,67, 68,71,73,76, 82,90)	(progeny # 15,18,23, 25,29,32, 75)	(progeny # 11, 12,27,86,100, 103)

**all progeny contain *chol-1* mutation except *csp-1; bd; UV90* #58,83,97 and *csp-1; bd* #13,63,72,98 which were determined to be *chol+* by fast growth on both high & low choline

Table 25. Periods and growth rates of *csp-1; bd* and *csp-1; bd; frq^{10}* progeny from cross between FGSC #18029 and *csp-1; chol-1 bd; frq^{10}* (OR, sg #80) tested on 100 µM choline

csp-1; bd progeny			*csp-1; bd; frq^{10}* progeny		
Progeny #	Growth Rate (mm/hr)	Period (hr)	Progeny #	Growth Rate (mm/hr)	Period (hr)
4	1.23	21.13	*csp-1; bd; frq^{10}* (control)	1.23	N/A*
6	1.25	21.27	*csp-1; bd; frq^{10}* (control)	1.26	
7	1.31	21.31	1	1.35	
8	1.28	21.62	5	1.39	
9	1.14	22.03	17	1.37	
13	1.25	21.07	21	1.26	
19	1.19	21.34	31	1.22	
20	1.24	21.25	35	1.32	
28	1.22	21.40	38	1.37	
54	0.95	21.73	39	1.16	
55	1.19	21.79	42	1.16	
63	1.21	23.74	67	1.15	
65	1.15	21.88	68	1.31	
72	1.20	21.55	71	1.24	
88	1.18	21.95	73	1.31	
98	1.21	21.67	76	1.23	
104	1.02	20.56	82	1.18	
105	0.99	21.51	90	1.22	
	Mean Growth Rate: 1.18 ± 0.023 (S.E.M.)	Mean Period: 21.60 ± 0.152 (S.E.M.)		Mean Growth Rate: 1.26 ± 0.020 (S.E.M.)	

*Not applicable: *frq^{10}* progeny were arrhythmic; period was not calculated

129

Table 26. Periods and growth rates of *csp-1; bd; UV90* and *csp-1; bd; UV90; frq^{10}* progeny from cross between FGSC #18029 and *csp-1; chol-1 bd; frq^{10}* (OR, sg #80) tested on 100 μM choline

csp-1; bd; UV90 progeny			*csp-1; bd; UV90; frq^{10}* progeny		
Progeny #	**Growth Rate (mm/hr)**	**Period (hr)**	**Progeny #**	**Growth Rate (mm/hr)**	**Period (hr)**
22	1.11	N/A*	*csp-1; bd; UV90; frq^{10}* (control)	1.19	N/A*
52	0.96		*csp-1; bd; UV90; frq^{10}* (control)	1.12	
58	1.20		15	1.09	
64	1.10		18	1.07	
83	1.13		23	1.07	
87	0.84		25	1.18	
91	1.12		29	1.08	
97	0.99		32	1.09	
	Mean Growth Rate: 1.06 ± 0.041 (S.E.M.)		75	1.10	
				Mean Growth Rate: 1.10 ± 0.014 (S.E.M.)	

*Not applicable: progeny exhibited either low amplitude rhythms or were arrhythmic; period was not calculated
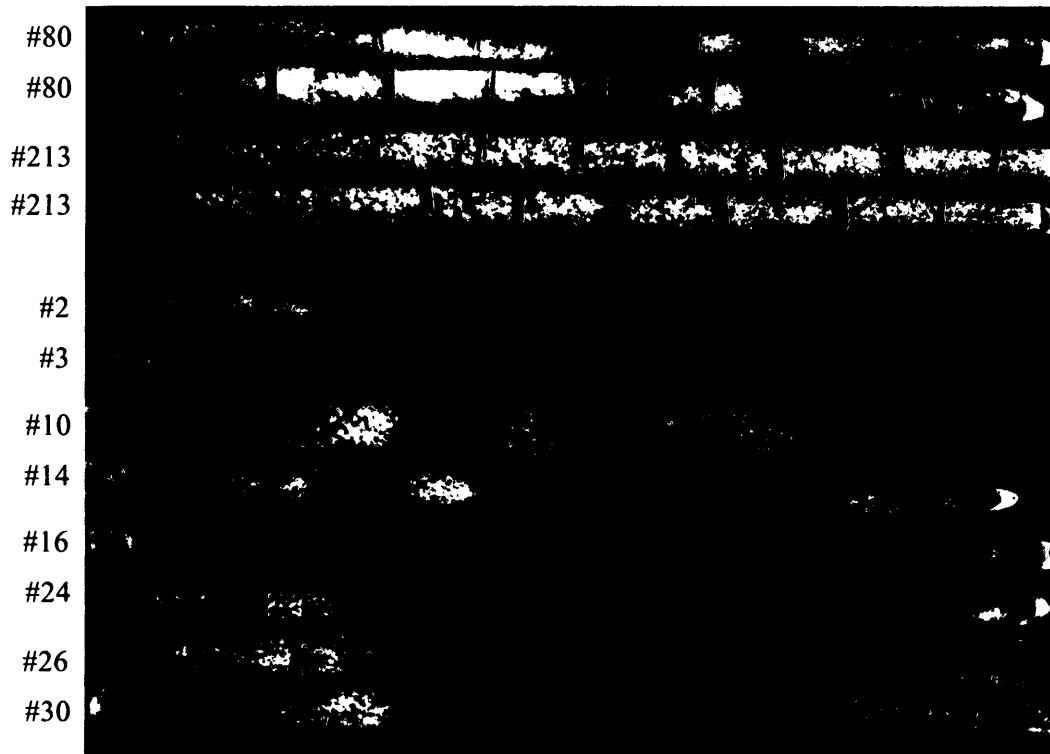
Figure 45. Examples of *csp-1; bd+* progeny obtained from cross between FGSC #18029

and *csp-1; chol-1 bd; frq^{10}* (OR, sg #80) on 100 μM choline.

#80 (*csp-1; chol-1 bd; frq^{10}*) and #213 (*csp-1; chol-1 bd; UV90; frq^{10}*) served as controls.

bd+ progeny #2 through #30 showed faster growth rates than *bd* controls as seen by the

marked growth fronts.
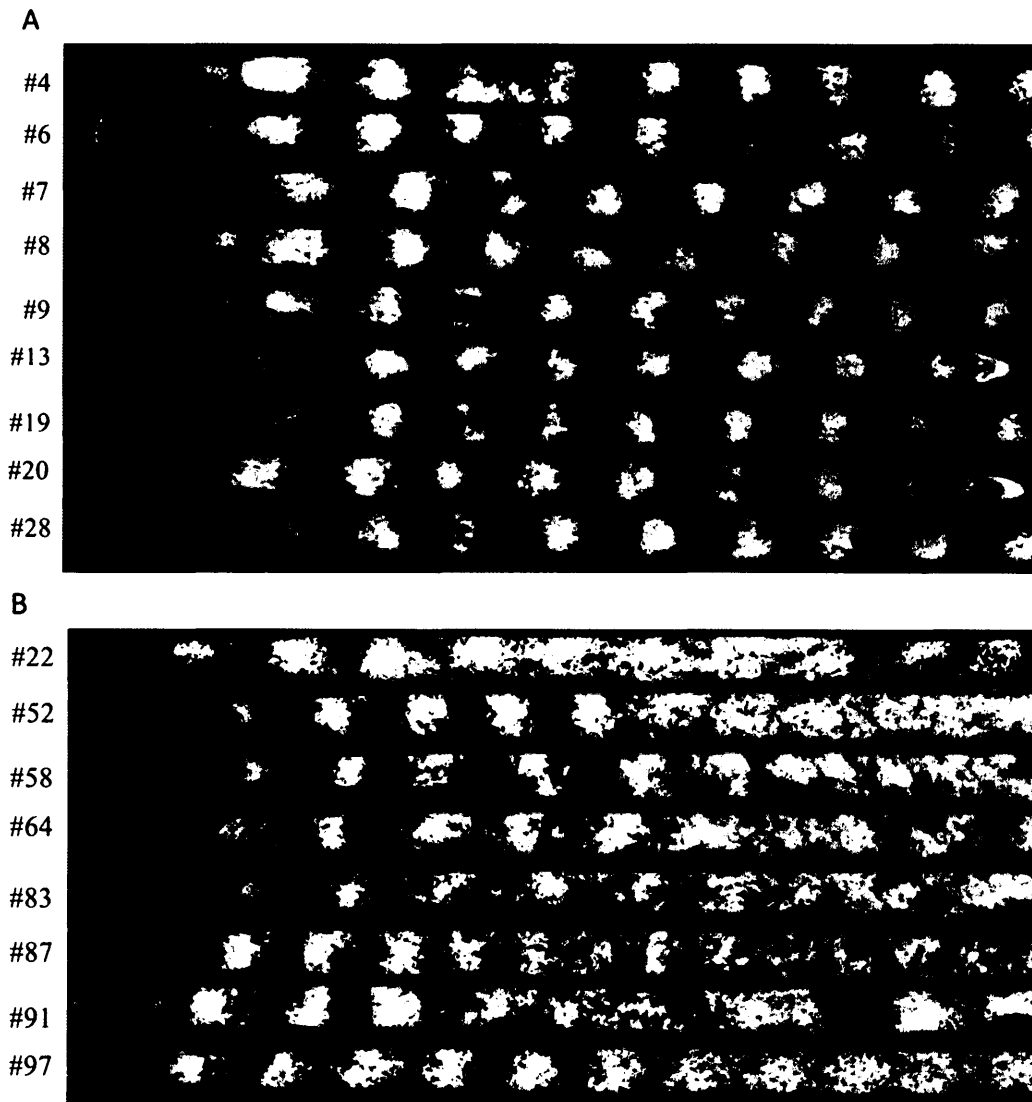
Figure 46. Examples of *csp-1; bd; UV+* and *UV90* progeny obtained from cross

between FGSC #18029 and *csp-1; chol-1 bd; frq^{10}* (OR, sg #80) on 100 μM choline. (A)

csp-1; bd; UV+ progeny showed strong rhythmic conidiation, similar growth rates and

appearance. (B) *csp-1; bd; UV90* progeny showed low amplitude rhythms and similar

physical appearance.

A

B
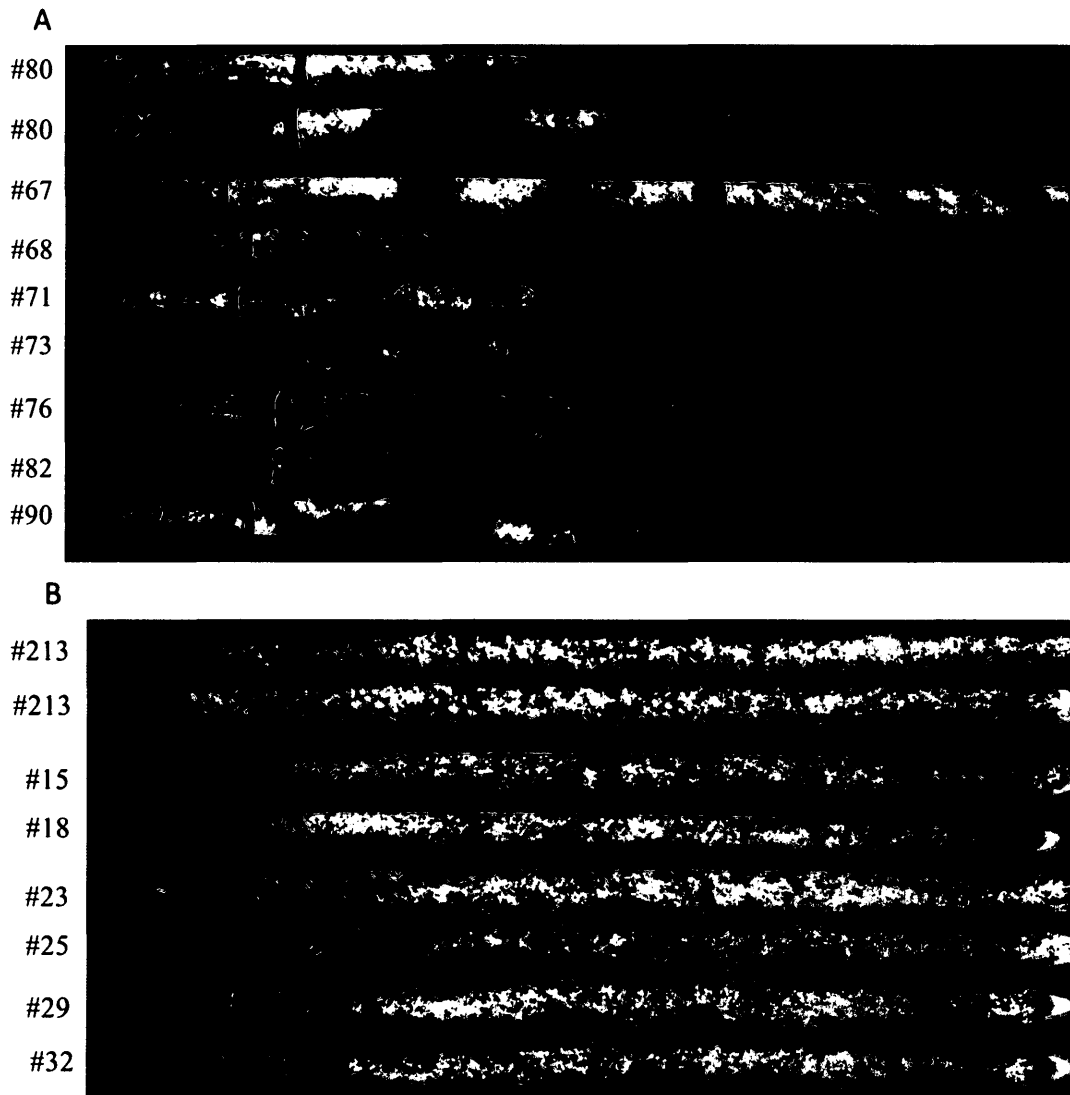
Figure 47. Examples of *csp-1; bd; frq^{10}; UV+* and *UV90* progeny obtained from cross

between FGSC #18029 and *csp-1; chol-1 bd; frq^{10}* (OR, sg #80) on 100 μM choline. #80

(*csp-1; chol-1 bd; frq^{10}*) and #213 (*csp-1; chol-1 bd; UV90; frq^{10}*) served as controls. (A)

csp-1; bd; UV+; frq^{10} progeny showed arrhythmic conidiation and similar physical

appearance as the control. (B) *csp-1; bd; UV90; frq^{10}* showed arrhythmic conidiation and

similar appearance to control.

133

A

#26

#26

#4

#6

#7

#8

#9

#13
#19

#20

B

#224

#224

#22

#52

#64

#87

#91
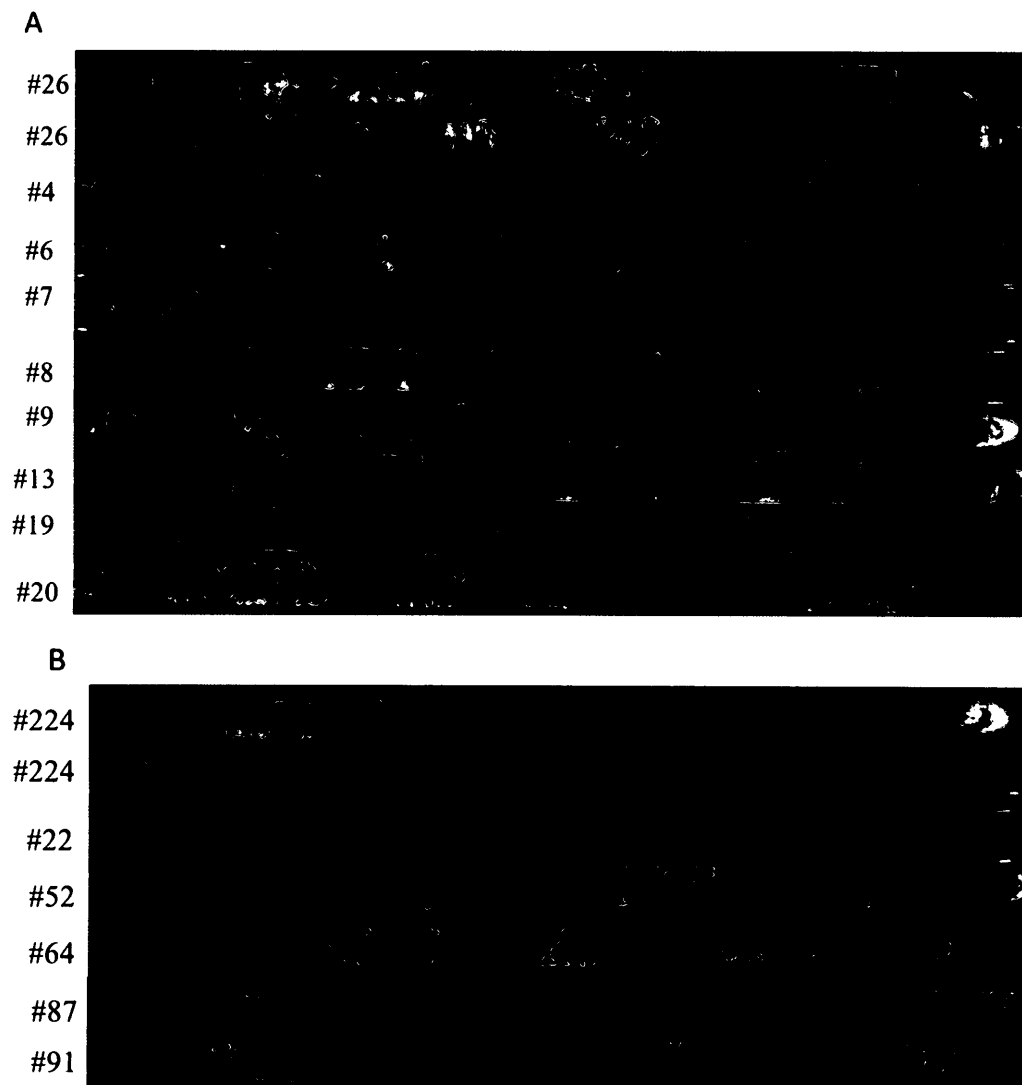
Figure 48. Examples of *csp-1; bd; UV+* and *UV90* progeny obtained from cross

between FGSC #18029 and *csp-1; chol-1 bd; frq^{10}* (OR, sg #80) on low choline. #26

(*csp-1; chol-1 bd*) and #224 (*csp-1; chol-1 bd; UV90*) served as controls. (A) *csp-1; bd;*

UV+ progeny showed rhythmic conidiation and similar appearance as the control. (B)

csp-1; bd; UV90 progeny showed arrhythmic conidiation and similar appearance as the

control. Only *UV90* progeny that were determined to be *chol-1* are displayed.

A

#80
#80
#1
#5
#17
#21
#31
#35
#38
#39
#42
#67

B

#213
#213
#15
#18
#23
#25
#29
#32
#75
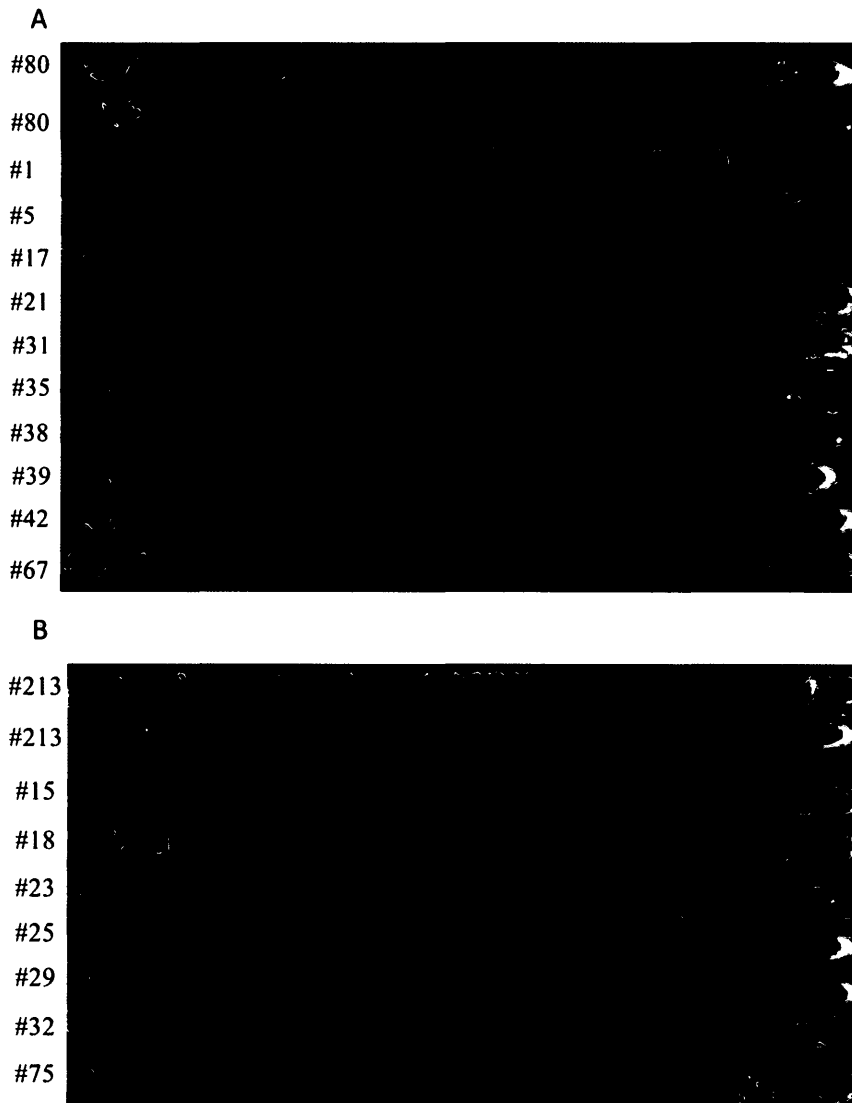
Figure 49. Examples of *csp-1; bd; frq^{10}; UV+* and *UV90* progeny obtained from cross

between FGSC #18029 and *csp-1; chol-1 bd; frq^{10}* (OR, sg #80) on low choline. #80

(*csp-1; chol-1 bd; frq^{10}*) and #213 (*csp-1; chol-1 bd; UV90; frq^{10}*) served as controls. (A)

csp-1; bd; UV+; frq^{10} progeny showed rhythmic conidiation and similar appearance as

the control. (B) *csp-1; bd; UV90; frq^{10}* progeny showed arrhythmic conidiation and

similar appearance as the control.

3.3 Transformation of *Neurospora crassa*

3.3.1 "AD" CAPS marker and Hygromycin B gene

Transformation was performed in order to test the complementation of *UV90*

candidate gene NCU05950 (FGSC #18029, Table 1) in the *UV90* mutant strain. The wild

type NCU05950 gene along with the Hygromycin B resistance gene (*hyg*) were

transformed into both *UV90* and *UV+ Neurospora* strains. It is believed that if

Neurospora was transformed with the NCU05950 gene, it would have taken up the *hyg*

gene as well. The *hyg* gene was therefore used as a marker to detect transformants. The

UV90 strain was used to determine if the NCU05950 gene could restore the wild type

phenotype, and the *UV+* strain was used to determine if there were any effects of having

multiple copies of the wild type gene.

A PCR product labelled "AD" was created using genomic DNA from the *csp-1;*

chol-1 bd; frq^{10} (OR, sg #80) strain as described in Methods 2.4.1. In order to ensure the

AD fragment was received by the transformed *Neurospora* strain, an extra EcoRI

restriction enzyme site (GAATTC) was inserted into the AD sequence based on the

overlapping-PCR procedure by Heckman and Pease (2007) (Appendix V) to create a

CAPS marker in the AD product. To achieve this, mutagenic primers were designed as

described in Methods 2.2.4 with the addition of extra nucleotides to create an EcoRI

restriction enzyme site (Table 5, Materials and Methods; Appendix V). PCR was

performed as described in Methods 2.2.5 on #80 (*csp-1; chol-1 bd; frq^{10}*) using

mutagenic overlapping primers Rev2B and For2C along with primers F4 and R4 (Tables

4 and 5, Materials and Methods) to create two DNA fragments, "AB" and "CD" (Fig. 50 A). PCR was performed using F4 and R4 primers with overlapping fragments "AB" and "CD" as DNA templates to create the final AD product containing a CAPS marker (Fig. 50 B). Only "AB" and "CD" fragments obtained using primers Rev2B and For2C created the final AD product (Fig. 50 B). To confirm that the AD sequence contained the extra EcoRI restriction enzyme site, digestion was performed as described in Methods 2.2.5 on the final AD fragment as well as the fragment from #80 (*csp-1; chol-1 bd; frq^{10}*) with F4 and R4 primers (Fig. 50 C). #80 showed fragments that were 1.0 and 1.5kb in size, while product AD showed fragments 1.0 and 0.5 kb in size, indicating the presence of a second EcoRI restriction enzyme site. Sareh Ahmadi repeated the above PCR and restriction enzyme procedures to obtain her own AD product for transformation. The Hygromycin resistance gene (*hyg*) was amplified by Dr. Keyur Adhvaryu from the pCSN44 plasmid (obtained from FGSC). The above DNA samples were precipitated and prepared as described in Methods 2.4.3.

3.3.2 Race tube and PCR analysis of transformants

Transformation:

Conidia (spores) from strain *csp-1; chol-1 bd; UV90* (sg #224) were harvested as described in Methods 2.4.2. Strain *csp-1; chol-1 bd* (sg #26) was harvested by Sareh Ahmadi. Strains *csp-1; chol-1 bd; UV90; frq^{10}* (sg #213) and *csp-1; chol-1 bd; frq^{10}* (sg #80) were not used in this transformation due to the presence of the *frq^{10}* mutation. This mutation is created by replacing the *frq* gene with a cassette containing the Hygromycin

137

resistance gene (Colot et al., 2006), making it impossible to detect if the transformed

strains contained our inserted *hyg* gene.

Transformation and plating of spores was performed on both strains as described

in Methods 2.4.3. Sareh Ahmadi repeated the transformation procedure with both strains.

One transformant was seen with *csp-1; chol-1 bd; UV90* and 13 transformants with *csp-*

1; chol-1 bd (1 from the 1/10 spore dilution, and 12 from the undiluted spores; data not

shown). Sareh Ahmadi had 3 transformants with *csp-1; chol-1 bd* (with undiluted spores)

and none with *UV90* (data not shown). These transformants indicated the presence of the

hyg gene.

<u>Race tube analysis:</u>

Transformants from the petri plates were inoculated onto minimal agar stock

tubes and microtiter wells containing choline and Hygromycin as described in Methods

2.4.4. All transformants grew in the microtiter wells, confirming further the resistance to

Hygromycin. Replicates of all transformants were inoculated from the stock tubes onto

maltose-arginine race tubes containing choline and Hygromycin as described in Methods

2.4.4. Controls *csp-1; chol-1 bd* and *csp-1; chol-1 bd; UV90* were also inoculated onto

race tubes but did not receive the addition of Hygromycin. Sareh Ahmadi also inoculated

my single *UV90* transformant as well as her *csp-1; chol-1 bd* transformants onto race

tubes.

Race tubes are shown in Fig. 51-53. *UV90* transformant (Fig. 51) did not grow

well on the race tube and appeared arrhythmic. *csp-1; chol-1 bd* transformants (Fig. 51-

53) appeared to grow initially with rhythmic conidiation and healthy growth rates, yet lost the rhythm and displayed a very slow growth rate after several days. *csp-1; chol-1 bd* transformant 26-6 appeared to have a healthy rhythm and growth rate throughout the length of the tube (Fig. 52). The periods and growth rates of the transformants are shown in Table 27. *UV90* transformant had a mean growth rate of 0.32 (± 0.015) mm/hr, which was much slower than the control mean of 1.10 mm/hr. *csp-1; chol-1 bd* transformants had a mean growth rate and period of 0.675 (± 0.035) mm/hr and 25.07 (± 0.943) hr, respectively. The growth rate is much slower than the control mean of 1.12 mm/hr, and the period is longer than the control mean of 22.23 hr. Sareh Ahmadi obtained similar results with her transformants (data not shown).

PCR analysis:

DNA was extracted from the transformants as described in Methods 2.2.3. PCR and restriction enzyme digestion was performed as described in Methods 2.4.4 using primers F4, R4, F1 and R1 (Table 4) on the transformants as well as strains *csp-1; chol-1 bd; frq^{10}* (sg #80), *csp-1; chol-1 bd; UV90; frq^{10}* (sg #213), and *csp-1; bd; UV90* (sg #227).

Figure 54 shows the PCR results on the transformants using F4-R4 primers. *csp-1; chol-1 bd; UV90* transformant, as well as *csp-1; chol-1 bd* transformant #26-8 did not produce a PCR product. PCR products were expected in the *csp-1; chol-1 bd* transformants, as they carry the wild type copy of the *UV90* candidate gene.

Figure 55 shows the transformants cleaved with EcoRI restriction enzyme as well as PCR on *csp-1; chol-1 bd; frq^{10}* (sg #80) and the *csp-1; chol-1 bd; UV90* transformant with F1-R1 primers. Most #26 transformants resembled the control (#80) with the exception of 26-6, 26-7, 27-11 and 26-12 which showed a PCR fragment of 0.5 kb in size, suggesting these transformants have picked up the AD CAPS marker (see Fig. 50 C). F1-R1 primers were tested on #80 as well as the *UV90* transformant to detect for the presence of any copies of the wild type NCU05950 gene. A PCR product the same size as the control appears, however this result was unrepeatable when PCR was attempted again (Fig. 56).

Figure 56 shows the *UV90* transformant as well as controls #80 (*csp-1; chol-1 bd; frq^{10}*), #213 (*csp-1; chol-1 bd; UV90; frq^{10}*) and *UV90* (*csp-1; bd; UV90*) with F1-R1 and F4-R4 primers. F1-R1 primers failed to produce a band similar to #80, 1.5 kb in size, in any of the *UV90* controls or transformant, whereas F4-R4 primers produced faint bands of 2.5 kb in size (Fig. 56 A). Products from the F4-R4 primers were digested with EcoRI restriction enzyme (Fig. 56 B). Control #80 showed the expected cleavage and produced bands that were 1.5 and 1.0 kb in size. *UV90* controls and transformant did not show any cleavage in the PCR product, suggesting that the F4-R4 primers likely did not amplify the correct region and the *UV90* transformant also did not receive the AD CAPS marker.
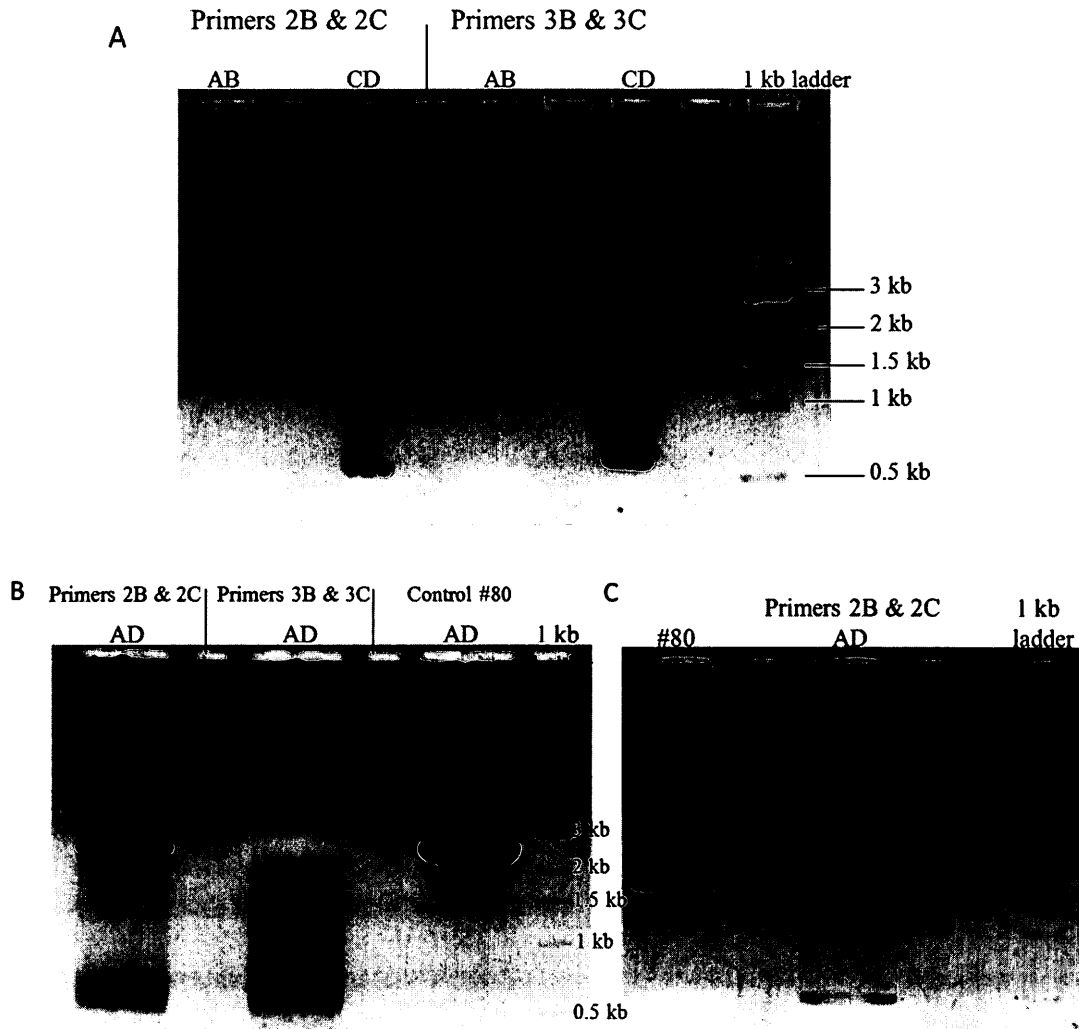
Figure 50. PCR showing creation and EcoRI digestion of AD product from *csp-1; chol-1 bd; frq^{10}* (#80) strain.

(A) shows "AB" and "CD" DNA fragments created by primers F4-Rev2B and R4-For2C (Primers 2B & 2C), and primers F4-Rev3B and R4-For3C (Primers 3B & 3C). (B) shows the AD product using AB & CD pieces from (A) along with primers F4-R4 on control #80 (*csp-1; chol-1 bd; frq^{10}*). (C) shows EcoRI digestion of DNA from (B).
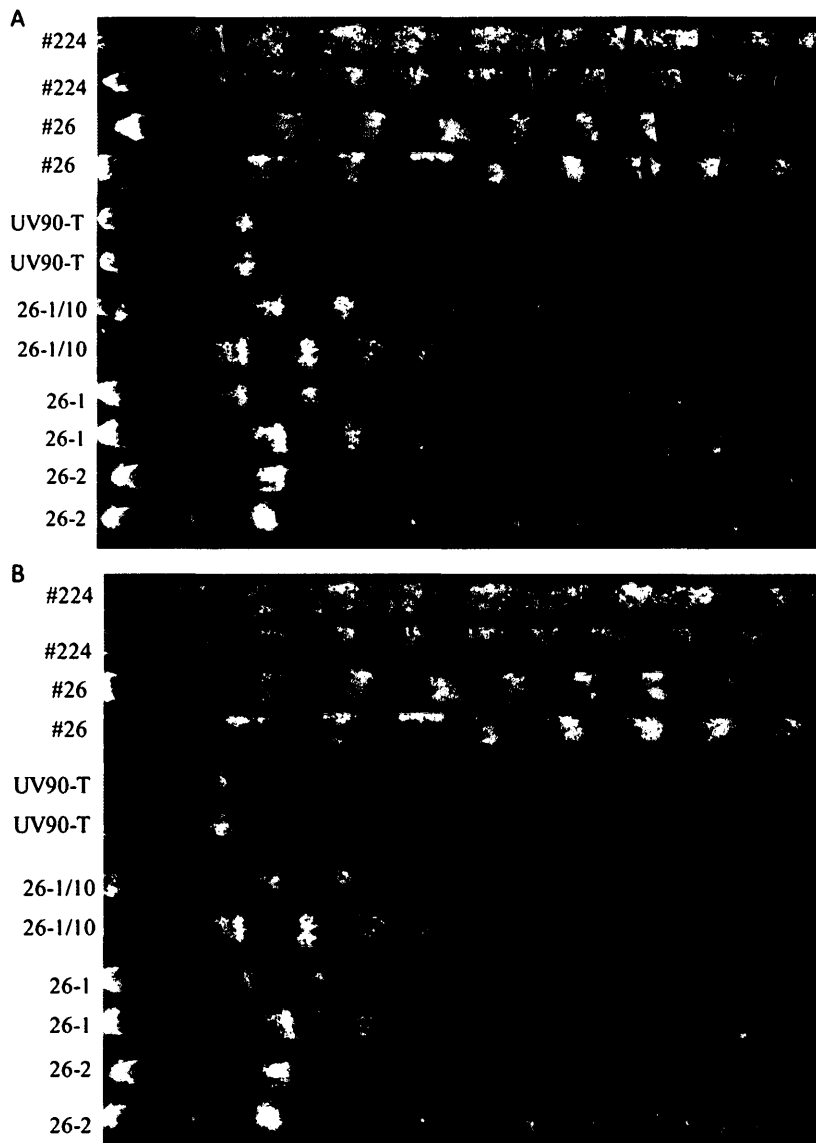
Figure 51. *UV90* and #26 transformants from the transformation of *Neurospora crassa*

with (A) and without (B) marked growth fronts. #224 (*csp-1; chol-1 bd; UV90*) and #26

(*csp-1; chol-1 bd*) served as controls. UV90-T = *csp-1; chol-1 bd; UV90* transformant.

26-1/10 = *csp-1; chol-1 bd* transformant from 1/10 spore dilution. 26-1 and 26-2 are *csp-1; chol-1 bd* transformants from undiluted spores.
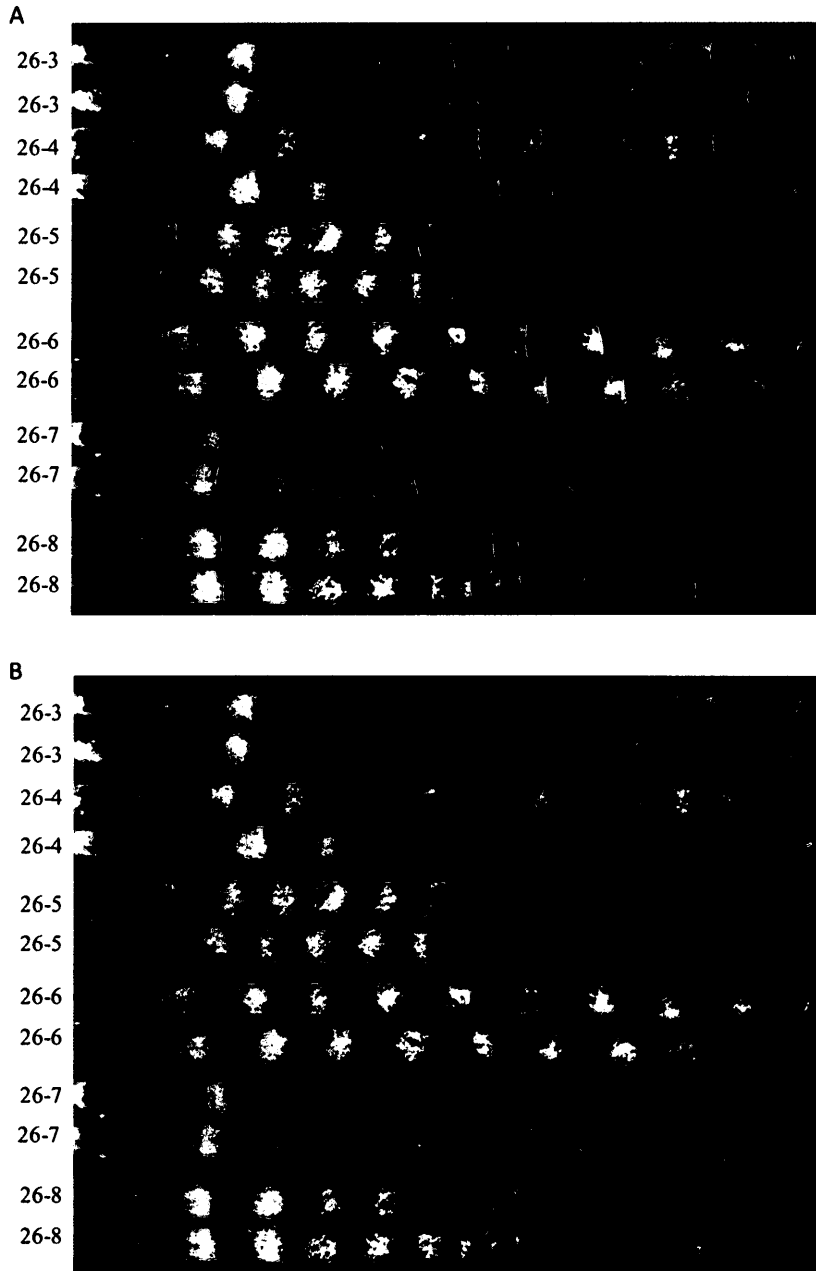
Figure 52. *UV90* and #26 transformants from the transformation of *Neurospora crassa* with (A) and without (B) marked growth fronts. 26-3 through 26-8 are *csp-1; chol-1 bd* transformants from undiluted spores.
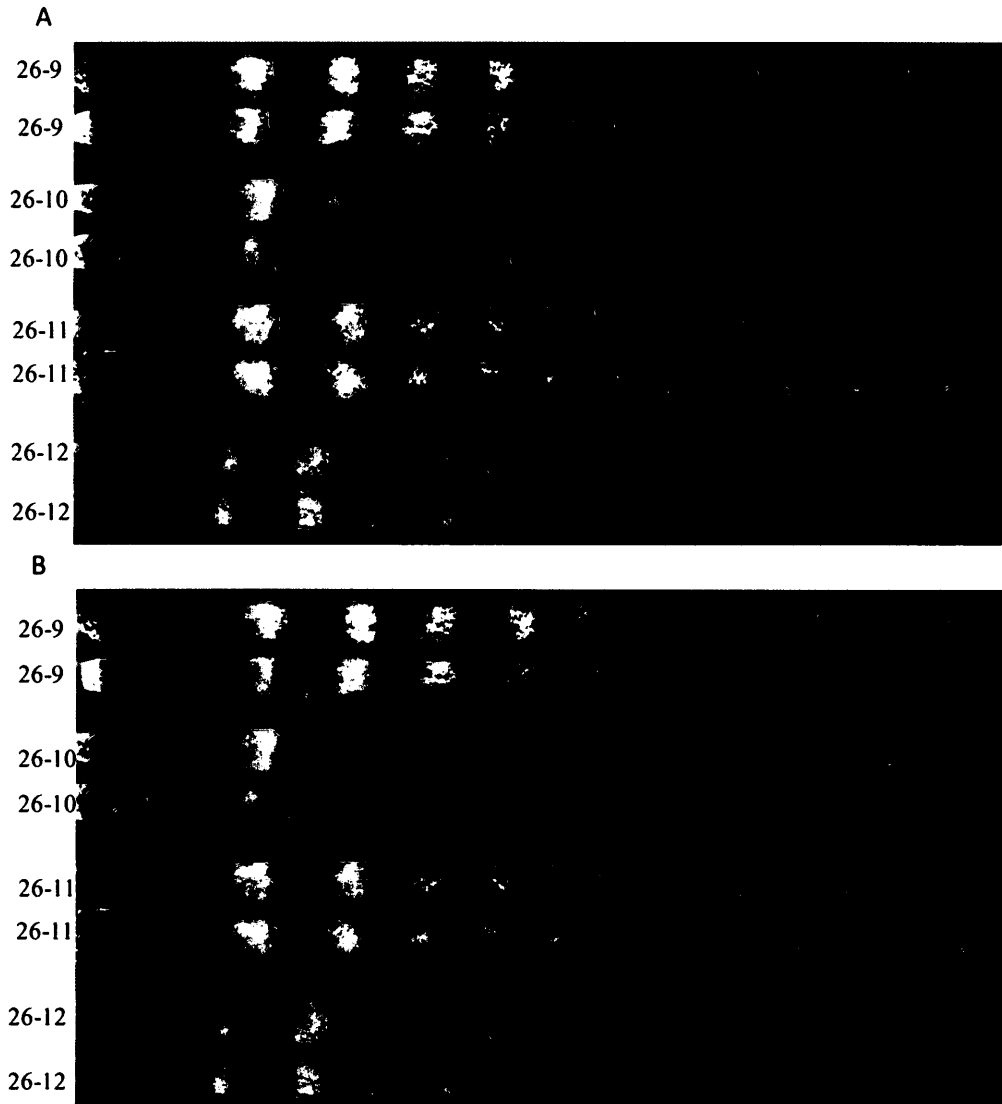
Figure 53. *UV90* and #26 transformants from the transformation of *Neurospora crassa* with (A) and without (B) marked growth fronts. 26-9 through 26-12 are *csp-1; chol-1 bd* transformants from undiluted spores.

Table 27. Periods and growth rates from *csp-1; chol-1 bd; UV90* and *csp-1; chol-1 bd* transformants

csp-1; chol-1 bd; UV90 transformants			csp-1; chol-1 bd transformants		
Progeny #	Growth Rate (mm/hr)	Period (hr)	Progeny #	Growth Rate (mm/hr)	Period (hr)
csp-1; chol-1 bd; UV90 (control)	1.10	N/A*	*csp-1; chol-1 bd* (control)	1.18	22.0
csp-1; chol-1 bd; UV90 (control)	1.10		*csp-1; chol-1 bd* (control)	1.13	22.46
UV90-T	0.30		26-1/10	0.70	28.6
UV90-T	0.33		26-1/10	0.52	24.84
	Mean Growth Rate: 0.32 ± 0.015 (S.E.M.)		26-1	0.83	22.19
			26-1	0.89	22.41
			26-2	0.74	N/A*
			26-2	0.65	N/A*
			26-3	0.55	N/A*
			26-3	0.57	N/A*
			26-4	0.86	25.86
			26-4	0.78	34.42
			26-5	0.77	22.47
			26-5	0.78	22.75
			26-6	1.08	21.97
			26-6	1.14	21.91
			26-7	0.48	N/A*
			26-7	0.57	N/A*
			26-8	0.64	26.13
			26-8	0.61	35.14
			26-9	0.54	24.31
			26-9	0.52	22.16
			26-10	0.60	N/A*
			26-10	0.56	N/A*
			26-11	0.62	25.21
			26-11	0.63	24.98
			26-12	0.47	24.25
			26-12	0.45	21.57

				Mean Growth Rate: 0.675 ± 0.035 (S.E.M.)	Mean Period: 25.07 ± 0.943 (S.E.M.)

*Not applicable: transformants were arrhythmic; the period was not calculated
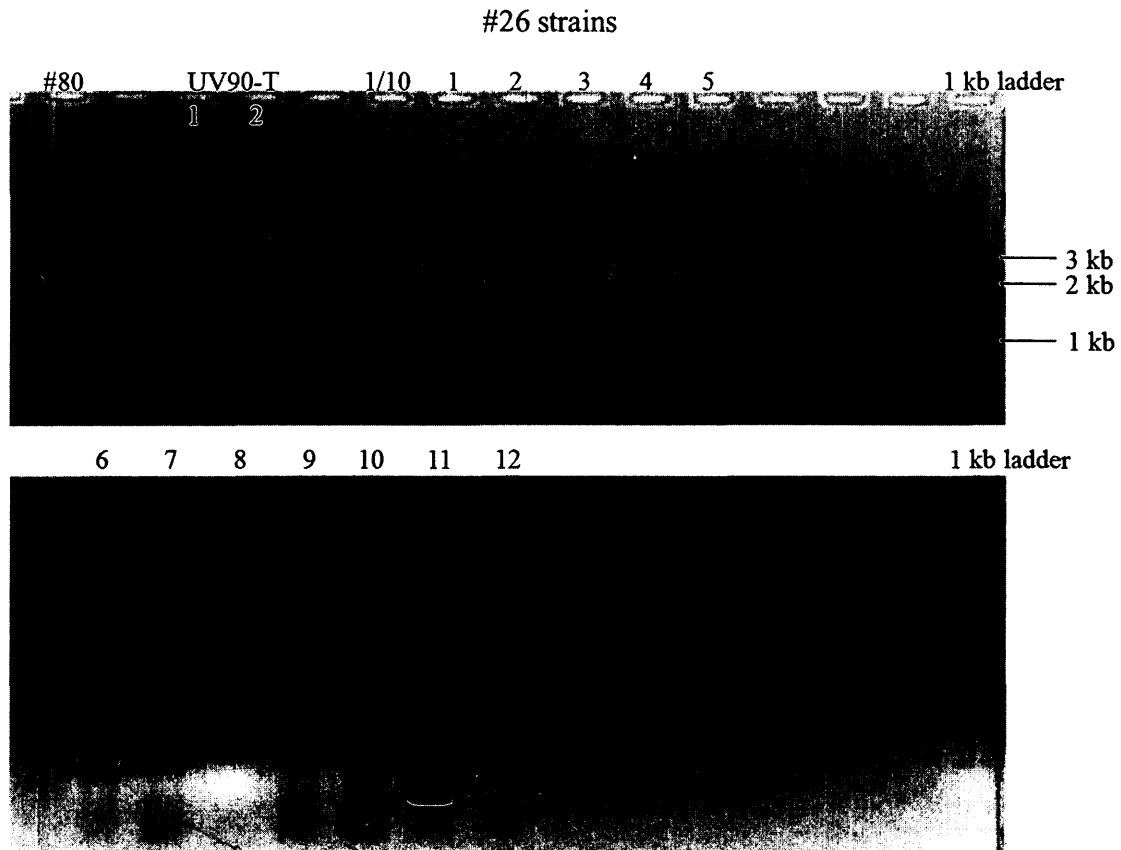
Figure 54. PCR results from *UV90* and #26 transformants using F4-R4 primers.

#80 (*csp-1; chol-1 bd; frq^{10}*) served as a control. UV90-T 1 & 2 = replicates of *csp-1;*

chol-1 bd; UV90 transformant. 26-1/10 = *csp-1; chol-1 bd* transformant from 1/10 spore

dilution. 26-1 through 26-12 are *csp-1; chol-1 bd* transformants from undiluted spores.
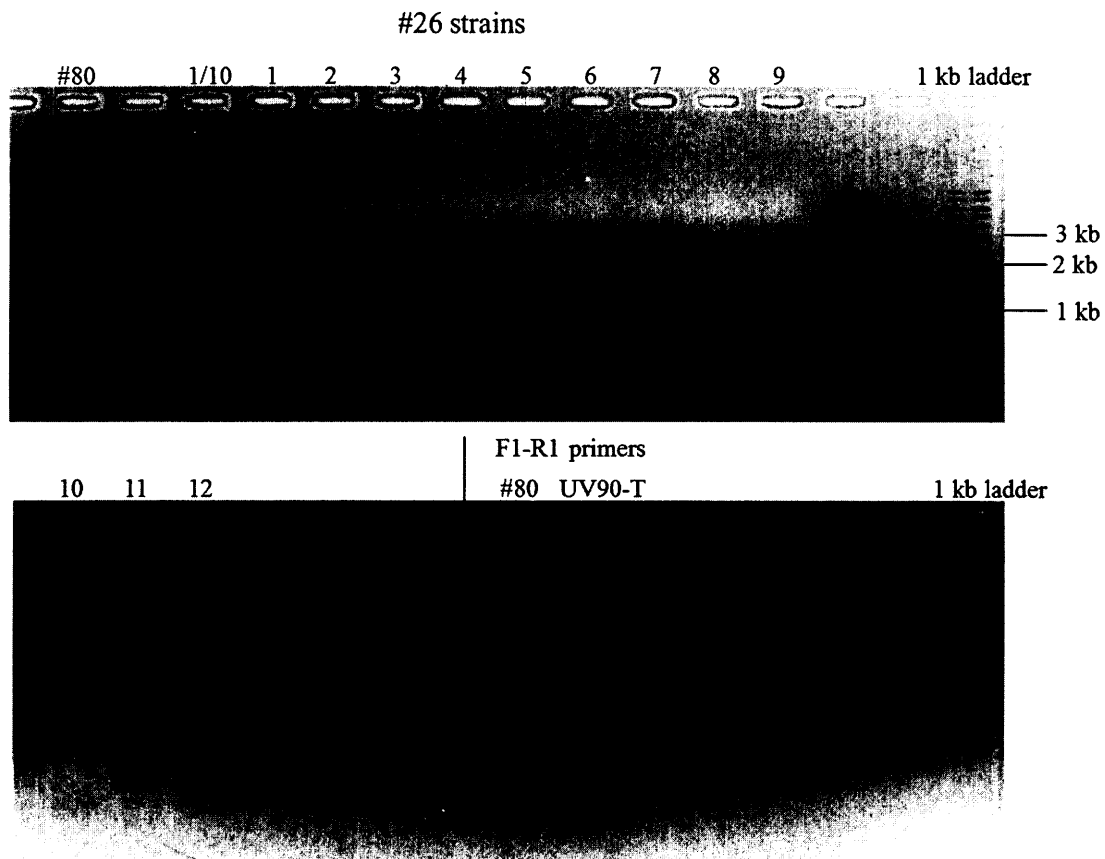
Figure 55. PCR results from *UV90* and #26 transformants cleaved with EcoRI restriction

enzyme and #80 and *UV90* transformant with F1-R1 primers.

#80 (*csp-1; chol-1 bd; frq^{10}*) served as a control. 26-1/10 = *csp-1; chol-1 bd* transformant

from 1/10 spore dilution. 26-1 through 26-12 are *csp-1; chol-1 bd* transformants from

undiluted spores. #80 and all transformants were cleaved with EcoRI restriction enzyme.

Lower half of gel: F1-R1 primers were used on #80 (*csp-1; chol-1 bd; frq^{10}*) and *csp-1;*

chol-1 bd; UV90 transformant (UV90-T).
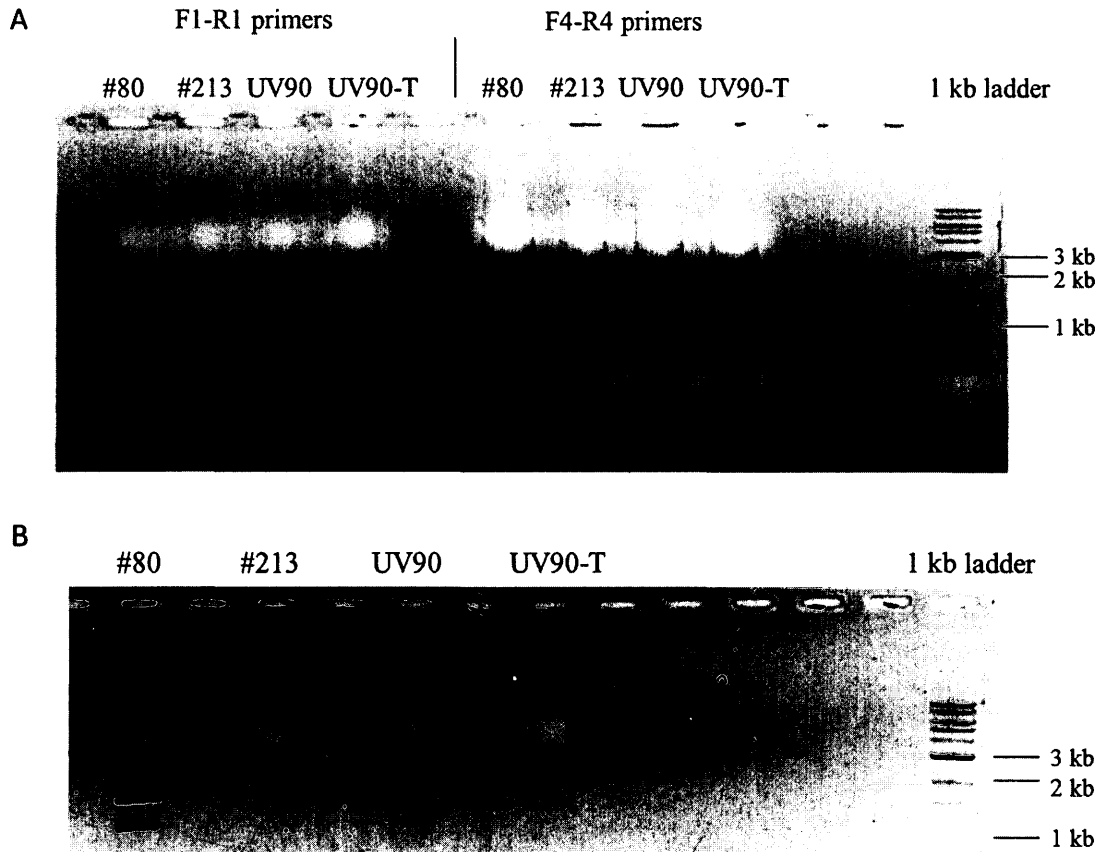
Figure 56. PCR results from controls and *UV90* transformant with F1-R1 and F4-R4

primers (A) and after EcoRI restriction enzyme digestion (B).

(A) shows #80 (*csp-1; chol-1 bd; frq^{10}*), #213 (*csp-1; chol-1 bd; UV90; frq^{10}*), *UV90*

(*csp-1; bd; UV90*), and UV90-T (*csp-1; chol-1 bd; UV90* transformant) with F1-R1 and

F4-R4 primers.

(B) shows products from F4-R4 in (A) after EcoRI restriction enzyme digestion.

3.4 Sequencing of *UV90* candidate, NCU05950

3.4.1 PCR and sequencing of NCU05950

Sequencing of the NCU05950 gene was performed to compare the sequence to

the published Oak Ridge *Neurospora* genome. This was attempted to discover the exact

nature of the *UV90* gene mutation and to confirm the identity of the gene.

Figure 57 shows a map of the primers used to sequence the putative *UV90* gene,

NCU05950. Primers were designed as described in Methods 2.2.4 and locations are

listed in Table 4 (Materials and Methods). DNA was also extracted as described in

Methods 2.2.3 from *csp-1; chol-1 bd; frq*^{10} (sg #80) and *csp-1; chol-1 bd; UV90; frq*^{10}

(sg #213) for use as controls. PCR was performed as described in Methods 2.2.6 using

F1-R1 primers on sg #213 as well as *csp-1; bd; UV90* progeny #189 from previous cross

between *csp-1; bd; UV90* and Mauriceville wild type. No PCR products were obtained

from both *UV90* strains (data not shown). The same *UV90* strains were tested with F1-

R3, F2-R2 and F3-R1 primers and no products were obtained (data not shown).

Figure 58 shows F1-R1, F2-R2, F4-R4, F5-F5 and F6-R6 primers on *csp-1; bd;*

UV90 (sg #227), Oak Ridge wild type, *csp-1; chol-1 bd; UV90; frq*^{10} (sg #213) and *csp-*

1; chol-1 bd; frq^{10} (sg #80). Only Oak Ridge and #80 strains exhibited PCR products of

the appropriate sizes. Figure 58B shows a faint product for F1-R1 primers, yet as seen in

Figure 58A, these results were often not repeatable. Figure 58C shows incorrect product

size for F5-R5 primers in all strains, suggesting these are products from non-specific

binding of primers. Figure 59 shows R3-F4, R3-F5, R3-F6, F3-R4, F3-R5 and F3-R6

150

primers with strains #227, Oak Ridge, #213 and #80. The *UV90* strains again often failed

to produce PCR products.

Some product of a slightly larger size was seen in #213 and *csp-1; bd; UV90* with

F3-R6, however, I was unable to obtain any PCR product for sequencing when it was

repeated. PCR product was also seen in #213 and *csp-1; bd; UV90* with F6-R3 primers,

and these were purified as described in Methods 2.2.6 and sent to the York University

Core Facility for sequencing. Sequences were compared to the Oak Ridge genome as

described in Methods 2.2.6. Base pair changes appearing in the first or last 20

nucleotides of the sequence were ignored due to inaccuracy. *csp-1; bd; UV90* (sg #227)

product was sent for sequencing with F6, F5, F4, F1 and R3 primers. Only F6 and F5

primers produced a sequence which was compared to Oak Ridge using LALIGN program

as described in Methods 2.2.6 (Appendix VIII). *csp-1; chol-1 bd; UV90; frq^{10}* (sg #213)

was sent for sequencing with F6, F5, F4, F1 and R3 primers. Only F6, F5 and F1 primers

produced a sequence (Appendix VIII). Any base pair changes seen in the sequences were

not repeatable and disregarded. Therefore no changes to the DNA sequence were

observed in the F6-R3 PCR product with either *csp-1; bd; UV90* or *csp-1; chol-1 bd;*

UV90; frq^{10} (Appendix VIII).

Primers F6-R7, F6-R8 and F6-R9 were tested with strains *csp-1; bd; UV90* (sg

#227), *csp-1; chol-1 bd; UV90; frq^{10}* (sg #213) and *csp-1; chol-1 bd; frq^{10}* (sg #80). No

PCR products were seen in the *UV90* strains (data not shown). Primers F1, F2 and F3

were tested with reverse primer ADRp (Table 5, Materials and Methods) on strains #227, #80 and #213. *UV90* strains again failed to produce any PCR products (data not shown).

New primers were designed as described in Methods 2.2.4 and ordered from IDT (Table 4, Materials and Methods). PCR was performed as described in Methods 2.2.6 and results are shown in Figure 60. Most PCR products were the same size as control #80 (*csp-1; chol-1 bd; frq^{10}*), with the exception of UV90AFor-R2 which produced a larger 1 kb fragment, and UV90BFor-R1 which produced a larger 500 bp fragment (Fig. 60). These larger fragments were purified and prepared as described in Methods 2.2.6 and sent for sequencing to The Centre for Applied Genomics (Hospital for Sick Children, Toronto, Canada). PCR was repeated 3 more times in an attempt to produce more DNA for the other fragments. However, not enough PCR products were obtained to submit for sequencing.

Sequences from the larger fragments were compared to the Oak Ridge genome using BLAST searches at the Broad Institute database (http://www.broadinstitute.org/ annotation/genome/neurospora/Blast.html) (Appendix VIII). The 500 bp fragment from UV90BFor-R1 primers matched a sequence on Linkage Group II, around 2.046 Mbp, for both *csp-1; bd; UV90* and *csp-1; chol-1 bd; UV90; frq^{10}* (sg #213) (Appendix VIII). The 1 kb fragment from UV90AFor-R2 primers matched a sequence on Linkage Group VI, around 2.655 Mbp, for both strains. A BLAST search of UV90BFor, UV90AFor, R1 and R2 primers against the Oak Ridge database did not produce any partial matches to these

regions on Linkage Group II or VI, ruling out the possibility of non-specific binding by the primers.

3.4.2 Protein prediction of NCU05950

In order to determine a possible function for the protein product of gene NCU05950, the amino acid sequence obtained from Broad Institute *Neurospora crassa* database (http://www.broadinstitute.org/annotation/genome/neurospora/FeatureSearch.html) was run through two programs: PHYRE2 Protein Fold Recognition Server (Kelley and Sternberg, 2009) and JPred3 Secondary Structure Prediction Server (Cole et al., 2008).

PHYRE2 protein program produced a possible model of the NCU05950 protein product (Fig. 61) with 33.3% confidence. (Confidence represents the probability of the protein product being homologous to the model). The secondary structure prediction is shown in Appendix IX, Figure A3. The top 5 protein templates which match NCU05950 are shown in Appendix IX, Figure A4. The remaining predicted protein templates had confidence values less than 11.7% (data not shown).

JPred3 protein program produced a list of similar proteins and the organisms in which they are found (Table 28). All of the similar proteins are located in fungi, yet their functions are currently unknown. The UniProt protein database entries and sequence similarities of the other proteins compared to NCU05950 are shown in Appendix IX.
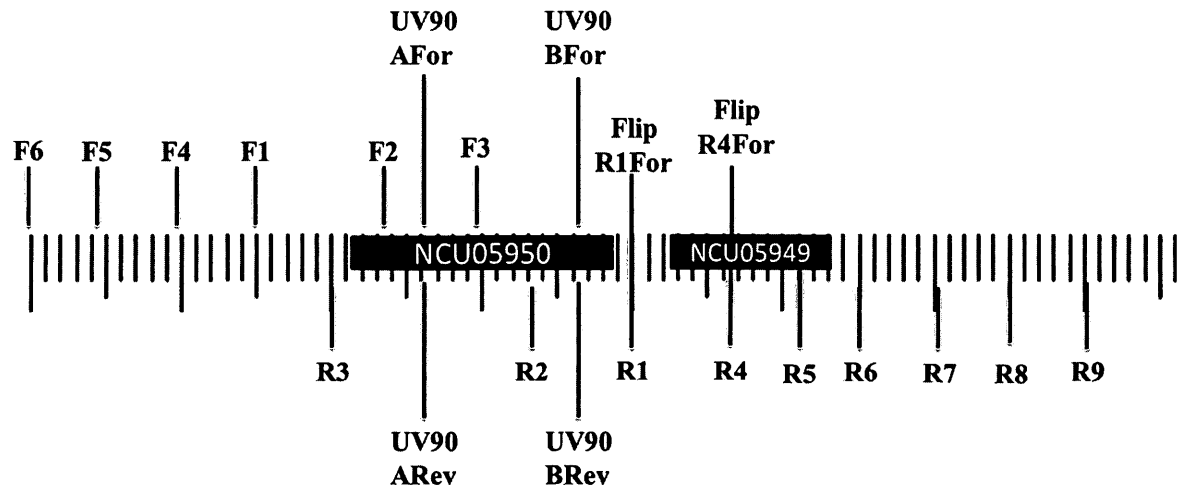
Figure 57. Schematic of primers used to sequence putative *UV90* gene, NCU05950 on

Neurospora crassa Linkage Group VI.

NCU05950 is located at 3,347,867-3,348,756. Neighbouring gene, NCU05949 is located

at 3,349,464-3,350,054. Primer locations are listed in Table 4 (Materials and Methods).
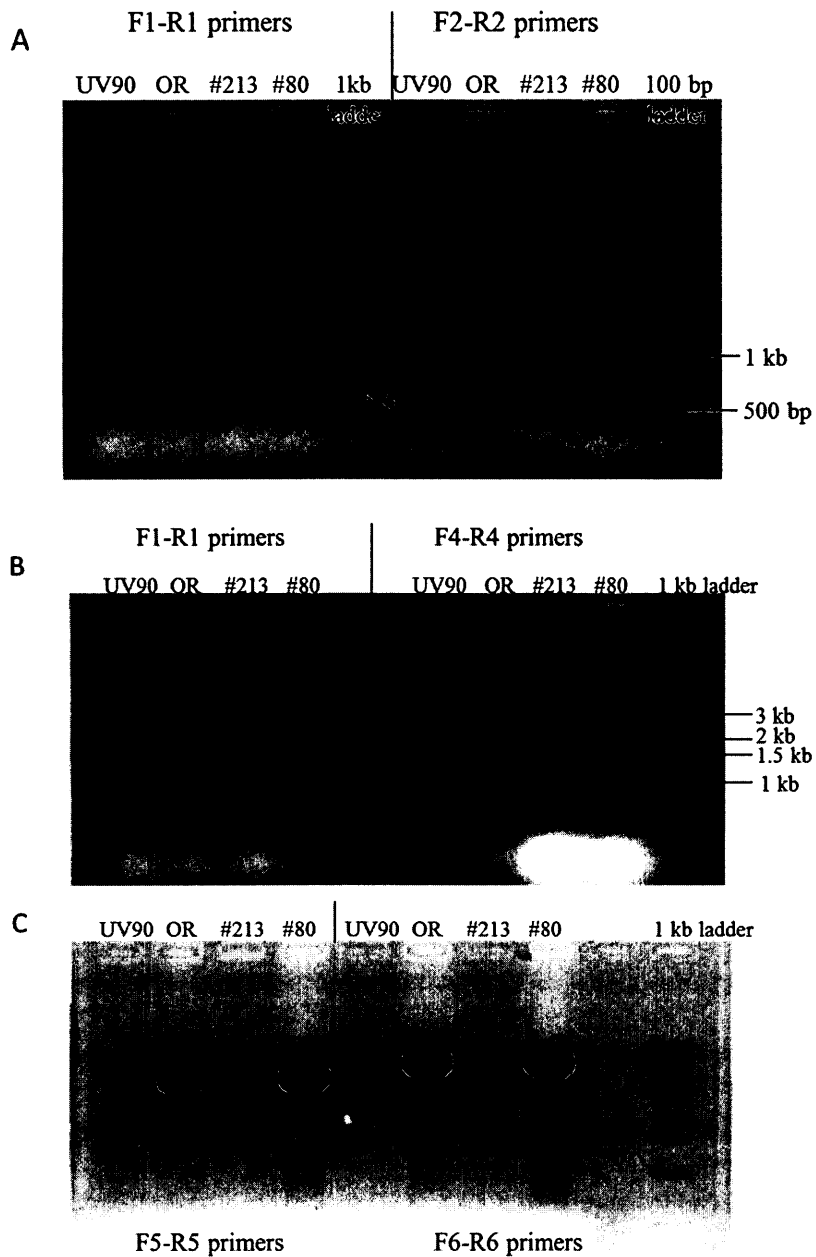
Figure 58. PCR showing attempted sequencing of NCU05950 with F1 through F6

primers. *UV90* = *csp-1; bd; UV90.* OR = Oak Ridge wild type. #213 = *csp-1; chol-1 bd;*

UV90; frq^{10}. #80 = *csp-1; chol-1 bd; frq^{10}.*
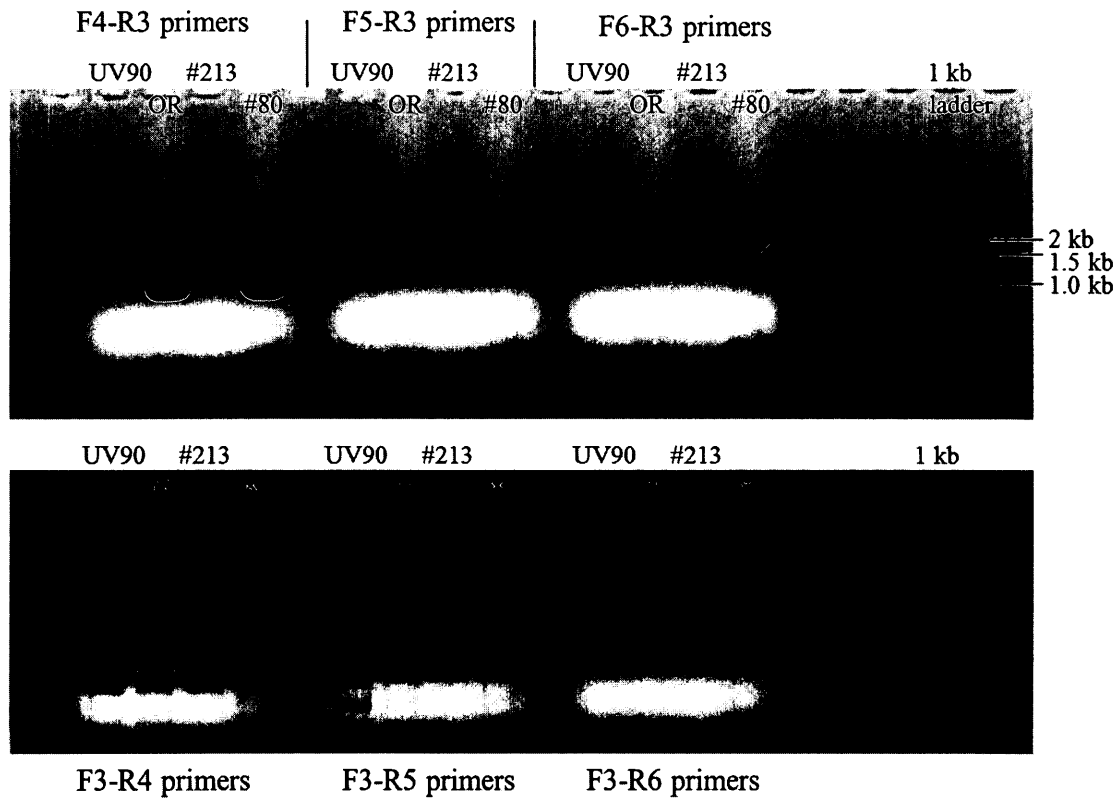
Figure 59. PCR showing attempted sequencing of NCU05950 with F4, F5, F6-R3 and

R6, R5, R4-F3 primers.

UV90 = csp-1; bd; UV90. OR = Oak Ridge wild type. *#213 = csp-1; chol-1 bd; UV90;*

frq[10]. #80 = csp-1; chol-1 bd; frq[10].
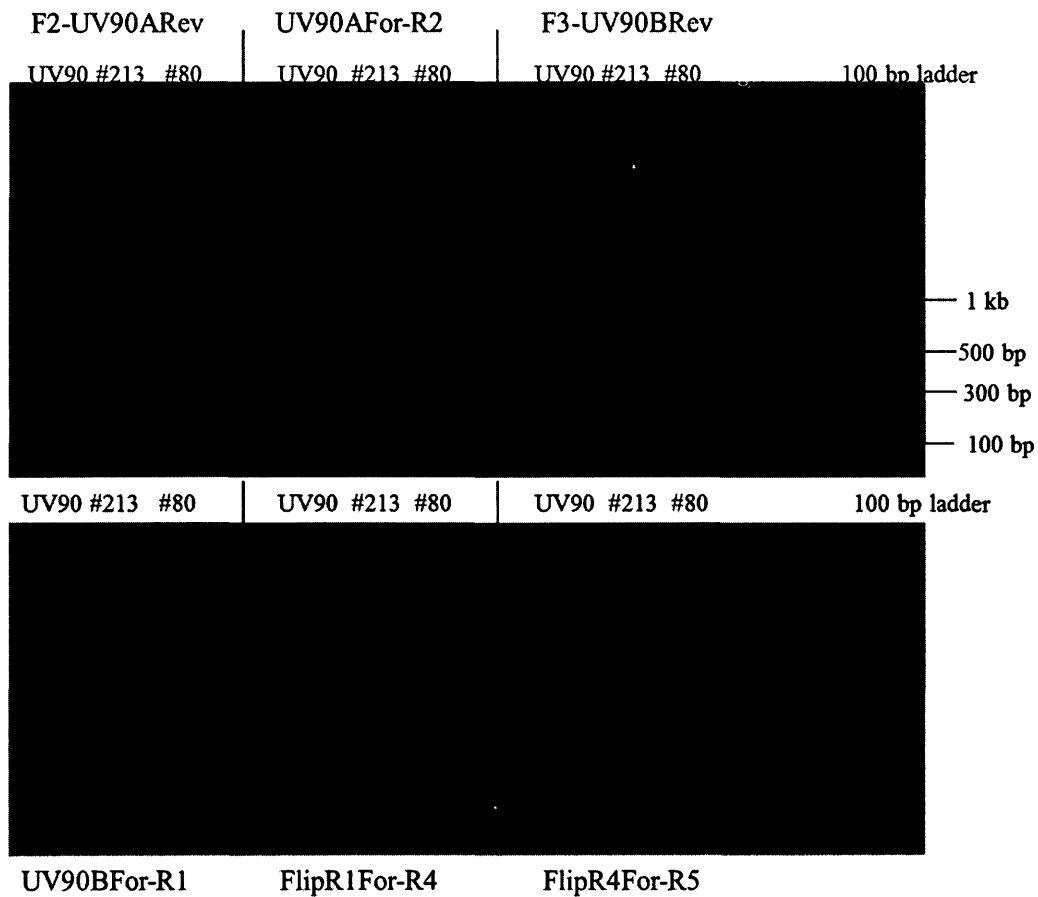
Figure 60. PCR showing attempted sequencing across NCU05950 with IDT primers.

UV90 = csp-1; bd; UV90. #213 = csp-1; chol-1 bd; UV90; frq^{10}. #80 = csp-1; chol-1 bd; frq^{10}.

(http://www.sbg.bio.ic.ac.uk/phyre2/html/page.cgi?id=index)
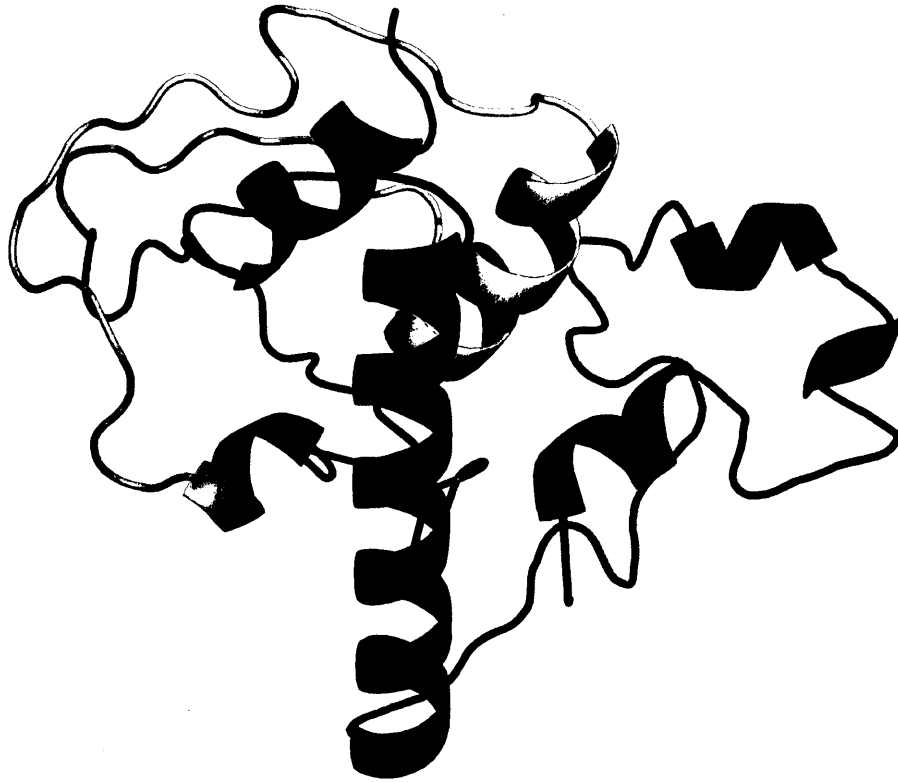
Figure 61. Predicted 3D model of protein product of *Neurospora crassa* gene

NCU05950.

Model predicted with 33.3% confidence (Appendix IX, Figs. A3 and A4).

158

Table 28. Proteins similar to protein product of *Neurospora crassa* gene NCU05950

UniProtKB/ UniRef90 Entry*	Protein Name & Function	Organism	Locus & Location (if relevant/available)
Q2GRJ7	Hypothetical protein	*Chaetomium globosum* (soil fungus)	CHGG_09407** Supercontig 6 3,364,696-3,365,347 +
I1RMZ9 (previously UPI000023E1E1)	Conserved hypothetical protein	*Fusarium graminearum* (*Gibberella zeae*; wheat head blight fungus)	FGSG_05355** Chromosome 3 1,992,968-1,994,032 +
B2AQ67	Hypothetical protein	*Podospora anserina* (filamentous fungus)	Chromosome 4, Supercontig 4 2,087,746-2,088,377
A7EA02	Hypothetical protein	*Sclerotinia sclerotiorum* (white mold)	SS1G_02132** Chromosome 4, Supercontig 3 49,801-50,485 +
B6GXY1	Hypothetical protein	*Penicillium chrysogenum* (Penicillin fungus)	Pc12g08110 1,915,643-1,916,272
A2QWY4	Hypothetical protein (weak similarity to PDZ domain protein MUPP1 - *Rattus norvegicus*)	*Aspergillus niger* (fruit & vegetable black mold)	An11g06890 183,872-184,599
Q5BCG8	Conserved hypothetical protein	*Aspergillus nidulans* (filamentous fungus)	ANID_01762.1** Chromosome 7; Contig 27 110,537-111,223 -
A1DMW4	Conserved hypothetical protein	*Neosartorya fischeri* (fungal pathogen)	NFIA_054830 2,304,209-2,304,920
Q0CI11	Conserved hypothetical protein	*Aspergillus terreus* (fungus)	ATEG_06673** Supercontig 9 1,133,008-1,133,654+

UniProtKB/ UniRef90 Entry*	Protein Name & Function	Organism	Locus & Location (if relevant/available)
B8NPB4	Conserved hypothetical protein	*Aspergillus flavus* (pathogenic fungus)	AFLA_128970 1,568,173-1,568,868
B6Q423	Conserved hypothetical protein	*Penicillium marneffei* (fungus, causes Penicilliosis in humans)	PMAA_030110 3,998,847-3,999,546
C0S031	Predicted protein	*Paracoccidioides brasiliensis* (pathogenic fungus)	PABG_01789** Supercontig 2 2,657,423-2,660,152 +
A6RA59	Predicted protein	*Ajellomyces capsulatus* (*Histoplasma capsulatum*; Darling's disease fungus)	HCAG_05847** Supercontig 7 694,509-695,321 -
B2W9B9	Hypothetical protein	*Pyrenophora tritici-repentis* (Wheat tan spot fungus)	PTRG_06577 1,073,374-1,073,951
Q0U774	Hypothetical protein	*Phaeosphaeria nodorum* (Glume blotch fungus)	SNOG_12390 254,347-255,417

*Entries searched at the UniProt Protein Database (http://www.uniprot.org/)

**Also located at the Broad Institute Database (http://www.broadinstitute.org/)

CHAPTER 4

DISCUSSION

Genetic mapping of *UV90* gene location

Mapping the *UV90* gene location was initiated following previous mapping done

on Linkage Group VI by Dr. Kamyar Motavaze and Daniel Rubinger (Fig. 18).

Recombination frequencies of progeny are typically used for genetic mapping in

Neurospora crassa (Jin et al., 2007). *Neurospora* genetic mapping is often performed

using tester strains, where the mutated strain is crossed against strains with known

mutations on specific chromosomes, and recombination frequencies are observed (Jin et

al., 2007). Genes located on different chromosomes are unlinked and will typically

segregate independently in crosses with a recombination frequency of 50%, whereas

genes closer together are linked and will segregate together in a cross with a lower

recombination frequency (Griffiths et al., 1993). The method in this study similarly uses

recombination frequencies, but instead is based on the segregation of specific regions of

DNA (CAPS markers) that distinguish between Oak Ridge and Mauriceville strains (Jin

et al., 2007). The CAPS marker method is also much faster by using DNA extraction and

PCR to analyze dozens of progeny as opposed to performing multiple test crosses which

often takes several months (Jin et al., 2007). There is the additional advantage of being

able to create the CAPS marker at any desired location in the chromosome, eliminating

the need for finding and obtaining tester strains with specific mutations near the mutated

gene of interest (Jin et al., 2007).

161

CAPS markers F3-R3 produced 20.4% recombination, whereas F6-R6 and F9-R9 produced 14.3% recombination for Dr. Motavaze (Fig. 18). The decreasing values of recombinants moving to the right on the chromosome suggested that the *UV90* gene mutation was further downstream, specifically to the right of F9-R9 marker. My progeny produced 3/29 (10.3%) recombinants with both F6-R6 and F9-R9 markers (Table 10, Fig. 18). Daniel Rubinger also tested marker 668F-668R (sequence obtained from Jin et al., 2007) with *UV+* and *UV90* progeny from the same cross and obtained 4 out of 54 (7.4%) recombinants (Fig. 18). The low recombination frequency indicated that the *UV90* gene was likely close to marker 668F-668R, yet it was unknown whether or not *UV90* was to the right or the left of the centromere (Fig. 18).

Dr. Motavaze and I both had identical recombinant progeny, and thus zero recombination, between F6-R6 and F9-R9 markers (Table 10). This initially led me to suspect that there was potentially an inversion or deletion between those markers in *UV90*, or the possibility that the PCR primers were binding to an alternate, incorrect location. To check these possibilities, I tested *prd-1* and *prd+* progeny from a cross between *csp-1; prd-1; bd* and Mauriceville wild type (previously performed by Nardin Nano) with F6-R6 and F9-R9 markers. The period (*prd-1*) mutation is a long period rhythm mutation found on Linkage Group III (Li and Lakin-Thomas, 2010). Genes located on separate chromosomes are unlinked and thus should produce recombination frequencies of approximately 50% (Griffiths et al., 1993). *prd-1* and *prd+* progeny produced 21/45 (46.7%) identical recombinants with both F6-R6 and F9-R9 markers

162

(Table 11). The recombination frequency close to 50% was expected for unlinked genes, yet zero recombination was again seen between F6-R6 and F9-R9. This eliminated the possibility of a chromosomal rearrangement specific to the *UV90* mutant, and suggested the possibility of generalized reduced recombination between these CAPS markers.

UV90 and *UV+* progeny were tested a second time on race tubes to also rule out the possibility that some progeny were misclassified. 10 progeny were disregarded after producing unclassifiable phenotypes (Fig. 15). This reduced the total number of progeny and the number of recombinants from 7/39 (17.9%) to 3/29 (10.3%) (Table 10). This resulted in a very small sample size and a drastic change in the recombination frequency.

New primers were designed downstream of marker F9-R9 in an attempt to avoid the region between F6-R6 and F9-R9 which was producing zero recombination. 6 pairs of CAPS markers were tested with parental *UV90* strains (Fig. 19). Markers LCF1-LCR1 and F10-R10 did not produce any results with either OR or MV strains and were not used further (Fig. 19).

RCF3-RCR3 and RCF4-RCR4 produced identical bands for both OR and MV after restriction enzyme digestion (Fig. 19). This was due to a fault during primer designing, where I did not check for the presence of multiple restriction enzyme sites in the CAPS marker sequence. Multiple restriction enzyme sites were found in these CAPS markers, causing the cleaved products to appear to be roughly the same size for both strains. These markers were therefore disregarded for further use. LCF2-LCR2 and F11-R11

produced different bands for OR and MV after digestion and were chosen for use in mapping (Fig. 19).

Six out of 39 (15.38%) identical *UV+* and *UV90* progeny were recombinant with both LCF2-LCR2 and F11-R11 markers (Table 12). These values were adjusted to 2 out of 29 (6.9%) after the previously disregarded race tubes were removed from the total values (Table 12). This again drastically reduced the recombination frequency. Zero recombination was also seen between LCF2-LCR2 and F11-R11. However, one recombinant was seen between F9-R9 and LCF2-LCR2 and F11-R11 markers (Fig. 36). The lower recombination frequencies to the right of F9-R9 again indicated that the *UV90* gene was further downstream, and likely to the right of the centromere.

No recombination was seen between F6-R6 and F9-R9 markers, as well as between LCF2-LCR2 and F11-R11. One possible explanation is that the total number of progeny was simply too small to be able to detect more recombinants for each CAPS marker. The corrected pool size from 39 to 29 progeny greatly reduced the number of recombinants. However, Dr. Kamyar Motavaze had 49 total progeny and also did not detect any recombination between markers F6-R6 and F9-R9 (Fig. 18). The *prd-1* and *prd+* progeny also produced identical recombinants between *prd-1* and F6 or F9, showing no recombination between F6 and F9.

It was noted on the Broad Institute *Neurospora crassa* database in March 2013 (http://www.broadinstitute.org/annotation/genome/neurospora/News.html) that a change in the orientation was made to the region left of the Linkage Group VI centromere. The

primers on the left of the centromere therefore changed locations (Table 20). The previous order of the primers used in mapping, from left to right on the chromosome, was: F3, F6, F9, F11, LCF2 (Table 20). The new order of the primers is now reversed: LCF2, F11, F9, F6, F3 (Table 20). The distances between the primers remained the same as previously. In light of this new information, it appears that the LCF2 and F11 primers are farther to the left than F9, F6, and F3, and therefore should have produced a larger number of recombinants as they moved away from *UV90*, not fewer. It is unknown why this was the case, except that there appears to be low recombination rates in that entire region.

It is also unknown whether or not there is an inversion to the left of the Linkage Group VI centromere in Mauriceville relative to Oak Ridge. An inversion could explain the low recombination frequencies in that region in our mapping crosses. Chromosomal inversions often create inversion loops during crossover events, which cause breaks in the chromosome and the loss of genes (Griffiths et al., 1993). These chromosomal breaks and gene deletions can be lethal and thus reduce the number of recombinant progeny observed (Griffiths et al., 1993). Inversions may also prevent crossover events from occurring altogether by preventing homologous pairing in the chromosome, and thus reducing the total number of recombinants (Griffiths et al., 1993).

Another explanation is that the chromosome is not inverted, however, there are little to no recombination or crossover events occurring in those regions of the chromosome. The distance between F6 and F9 primers is approximately 270,000 bp, and

between LCF2 and F11 is 170,000 bp (Table 20), and so it seems unlikely that there would be no crossover events amongst such a large chromosome fragment. There is the possibility that neighbouring genes or genes on other chromosomes are preventing recombination events (Catcheside and Corcoran, 1973). Catcheside and Corcoran (1973) discovered that certain *recombination* genes (dubbed *rec-2*+ and *rec-3*+) were responsible for reducing recombination frequencies between the *arg-3* and *his-2* genes on Linkage Group I. *rec-2*+ was found to reduce recombination by approximately half between *arg-3* and *his-2*, and *rec-3*+ nearly eliminated recombination in that region altogether (Catcheside and Corcoran, 1973). It is also interesting to note that *rec-2*+ is located in Linkage Group V, and also reduces recombination between *pyr-3* and *leu-2* in Linkage Group IV, indicating that genes on completely different chromosomes can have an effect on reducing recombination rates (Catcheside and Corcoran, 1973). Catcheside and Corcoran (1973) also noticed *rec* genes affecting non-allelic recombination.

Repetitive sequences of DNA can be responsible for non-allelic crossovers, and also a reduction in recombination frequencies (Griffiths et al., 1993). Duplications of regions of DNA can cause misaligned chromosomes during crossover events and create gene duplications or deletions, which may be lethal and reduce recombination rates (Griffiths et al., 1993). Repetitive sequences occur in approximately 10% of the *Neurospora* genome (Galagan et al., 2003). The fact that the Broad Institute reversed the orientation of the previous contig on Linkage Group VI suggests that there may be similar sequences at the beginning and end of that region. Given the large region of

DNA in Linkage Group VI which appears to have little to no recombination, it seems likely that repetitive sequences or recombination-suppressing genes may be responsible for this anomaly.

New spores from the cross between *csp-1; bd; UV90* (sg #227) and MV wild type (sg #258) were picked in order to increase the number of progeny and obtain a better sample size for mapping. *bd; UV+* progeny were distinguished from *UV90* progeny by their faster growth rates and rhythmic conidiation on the race tubes (Fig. 24). *UV90* progeny, as previously, were identified by low amplitude rhythms of conidiation (Fig. 25). *bd+* progeny exhibited faster growth rates than *bd*, and *UV90* strains were distinguished by their constant conidiation (Figs. 26 and 27). The phenotypes matched previously reported observations for *UV90* progeny (Li et al., 2011).

CAPS markers RCF5-RCR5, RCF6-RCR6 were designed to the right of the centromere to further narrow down the location of the *UV90* gene (Tables 2 and 3). The sequence of 668F-668R was obtained from Jin et al. (2007). Only RCF5-RCR5 and 668F-668R markers both produced distinct bands for each parental strain after digestion and were used for PCR (Fig. 28). 8 out of 85 progeny (9.41%) were recombinant with RCF5-RCR5, and 3 out of 85 progeny (3.53%) were recombinant with 668F-668R (Table 17). The decreasing recombination frequency indicated that the CAPS markers were moving closer to *UV90*. It was likely situated to the right of marker 668F-668R. The 3 recombinants with 668F-668R (#143, 184 and 122) were also recombinant with RCF5-

RCR5 (Table 17), indicating that the crossover event that produced recombination in both of those markers would have occurred to the right of 668F-668R (Fig. 41).

CAPS markers F15-R15 and F16-R16 were designed and tested with *UV90* parental strains (Tables 2 and 3, Fig. 33). F16-R16 was chosen for PCR as the MV product produced an uncleaved DNA product, and thus would be easier to distinguish from the cleaved OR product (Fig. 33). 8 out of 85 progeny (9.41%) were recombinant with F16-R16 (Table 18). This increase in recombination frequency indicated that the *UV90* gene was somewhere to the left of F16-R16, and likely closer to 668F-668R (Fig. 36). The *UV90* mutation therefore must be between 668F-668R and F16-R16 (Figs. 36 and 41).

One minor discrepancy occurred with the recombinant values. It was expected with 3/85 recombinants for 668F-668R and 8/85 progeny for F16-R16 that there would be a total of 11 different recombinant progeny between those two markers. However, *csp-1; bd+; UV+* progeny #143 was recombinant with both markers (Tables 17 & 18; Fig. 41). This left a total of 9 different recombinant progeny for 668F-668R and F16-R16 (Tables 17 & 18; Fig. 41). One possible explanation for this discrepancy is that progeny #143 was misclassified as *UV+* when it is actually *UV90* and therefore should not be included, leaving a total of 9 recombinants. Another possible explanation is that progeny #143 is a double recombinant, and experienced a crossover event both to the right of 668F-668R, and to the left of F16-R16. This would cause #143 to appear recombinant with both CAPS markers. In this scenario, one recombinant would need to

be added to the total for 668F-668R and one for F16-R16, leaving a total of 11 progeny. In either case, the total number of recombinants indicates the *UV90* gene is located somewhere in between those CAPS markers (Fig. 36).

The distance between CAPS markers 668F-668R and F16-R16 is approximately 190,000 bp (Table 2). It was therefore necessary to further narrow down the region in which the *UV90* gene was located. 8 CAPS markers were designed and tested with *UV90* parental strains (Tables 2 and 3, Fig. 37). Only recombinants from 668F-668R and F16-R16 (Tables 17 and 18) were chosen for PCR with these markers because they would have a recombination event in this interval (Fig. 41). The numbers of recombinants are shown in Table 19. 3 recombinants were seen with 668F-668R, 1 with 3317F-3317R, and 2 with 3368F-3368R (Table 19; Fig. 41). The recombinant frequency decreases towards 3317F-R and increases towards 3368F-R, suggesting that the *UV90* gene is located in between 668F-668R and 3368F-3368R.

FGSC Knockouts

Table 21 shows a list of *UV90* candidate genes in the region between 668F-668R and 3368F-3368R. Knockouts of these genes were ordered from the Fungal Genetics Stock Center (FGSC) (Table 1). Gene prediction software at the Broad Institute is used to predict genes based on genomic sequences and detects the presence of open reading frames (ORFs), start and stop codons.
(www.broadinstitute.org/annotation/genome/neurospora/GeneFinding.html). Expressed sequence tags (ESTs) from the cDNA sequences were aligned against the predicted

169

genome sequences and only those ESTs with high alignments (95%+) to one location were used in gene predictions (http://www.broadinstitute.org/annotation/genome/neurospora/GeneFinding.html).

FGSC knockouts were created by knocking out individual genes using a cassette containing Hygromycin B resistance (Colot et al., 2006). Only FGSC knockout #18029 produced arrhythmic, constant conidiation on the race tube which resembled *UV90* (Figs. 42-44). This corresponded with gene NCU05950 (Table 1) and was chosen as a potential *UV90* candidate. A cross was then performed between FGSC #18029 and *csp-1; chol-1 bd; UV90; frq^{10}* (sg #80) to determine if the knockout resembled *UV90* when placed through a cross.

The race tube phenotypes for knockout #18029 also looked very similar to the *UV90* phenotype. *bd+* progeny were separated from *bd* by their faster growth rates (Fig. 45). On media containing choline, *csp-1; bd; UV+* progeny exhibited clear, rhythmic conidiation, and *csp-1; bd; UV+; frq^{10}* progeny exhibited the same fluffy, arrhythmic conidiation as the control (Figs. 46 and 47). The most interesting results were seen in the *UV90* strains. *csp-1; bd; UV90; frq^{10}* was arrhythmic with constant conidiation, whereas *csp-1; bd; UV90* strains appeared to have a low amplitude rhythm at the beginning of the race tubes that tapered off to an arrhythmic pattern (Figs. 46 and 47). On media with no choline, *csp-1; bd; UV+* progeny exhibited a rhythmic pattern, yet bands were not as distinct and clear to observe (Fig. 48A). This is the result of the *chol-1* mutation which exhibits a slower growth rate and longer period when choline levels are depleted (Lakin-

Thomas, 1996). *csp-1; bd; UV90* progeny appeared arrhythmic on low choline (Fig. 48B). In the *frq^10* strains, *chol-1; UV+* progeny on low choline appear to have a long period, low amplitude rhythm, as expected (Fig. 49A). *chol-1; UV90; frq^10* strains abolish the rhythm and appear completely arrhythmic (Fig. 49B). This is identical to what was seen in the *UV90* mutants previously (Li et al., 2011). These results confirm that FGSC knockout #18029 exhibits the same allelic segregation, phenotype and growth rate as *UV90*, giving strong evidence to conclude gene NCU05950 and *UV90* are the same. It was also demonstrated in the lab via PCR analysis by Amanda Mohabeer that NCU05950 was the correct gene that was replaced with a Hygromycin B resistance cassette.

In the presence of the *frq^10* mutation, the *UV90* phenotype appears to be completely arrhythmic (Li et al., 2011). *UV90* also abolishes the rhythm found in *chol-1; frq^10* strains grown on media without choline (Fig. 49B), giving strong evidence that it is involved with, or part of, the FRQ-less oscillator (FLO) (Li et al., 2011). However, low amplitude rhythms have previously been seen in *UV90* strains that contain the *frq* gene (Li et al., 2011). This is also noticed in the progeny used for mapping from the cross between *csp-1; bd; UV90* and Mauriceville wild type. Some of the *csp-1; bd; UV90* progeny appear to have a very low amplitude rhythm, as well as *UV90* progeny from the knockout cross (Figs. 9, 25, and 46). Since the knockout resembled *UV90*, it is possible that the original *UV90* mutation is a null mutant or results in a loss of function protein.

The *UV90* mutation has been seen to dampen the amplitude of the FRQ protein (Li et al., 2011). This suggests that the *UV90* gene is likely interacting with, or possibly supporting the FRQ-WCC feedback loop. Furthermore, since *UV90* is believed to be part of the FLO, this is an indicator that the FLO may be interacting in some manner with the FRQ-WCC feedback loop (Li et al., 2011).

Transformation of *Neurospora crassa*

In order to further confirm whether the NCU05950 gene was in fact *UV90*, a complementation test was performed where the wild type copy of the NCU05950 gene was inserted into the *UV90* mutant strain in an attempt to restore the rhythm. Restoration of the rhythm would provide conclusive proof that the NCU05950 gene is in fact, *UV90*. Typically transformations in *Neurospora* are performed using the pDE1 plasmid which contains a non-functional part of the *his-3* (histidine) locus, as well as multiple restriction enzyme sites for insertion of desired genes (Ebbole, 1990). The plasmid would be transformed into a *his-3* strain, where recombination at the *his-3* locus would produce a functional histidine gene that can be selected by placing transformants on media without histidine. Unfortunately, this method was not used in this study due to the fact that the lab has been unable, for several years, to create a *his-3; UV90* double mutant. Several different crosses between *his-3* and *UV90* strains appear to be viable with the production of spores, yet germination rates have repeatedly been exceptionally low. A *his-3; UV90* double mutant has been unattainable.

It was therefore decided to transform *Neurospora* with the naked wild type copy

of the NCU05950 gene and a copy of the Hygromycin B resistance gene (*hyg*) which

would be used to select for transformants, based on the methods by Staben et al. (1989).

Strains which would receive the DNA were *csp-1; chol-1 bd; UV90* (sg #224) and *csp-1;*

chol-1 bd (sg #26). Strains *csp-1; chol-1 bd; UV90; frq^{10}* (sg #213) and *csp-1; chol-1 bd;*

frq^{10} (sg #80) were not used in this transformation due to the presence of the *frq^{10}*

mutation. This mutation is created by replacing the *frq* gene with a cassette containing

the Hygromycin resistance gene (Colot et al., 2006), making it impossible to detect if the

transformed strains contained our inserted *hyg* gene. It was expected that the NCU05950

gene would restore the rhythm in the *UV90* strain. The *csp-1; chol-1 bd* strain was

transformed to determine if there would be any phenotypic effects of having multiple

wild type copies of the *UV+* gene.

Thirteen transformants were seen with *csp-1; chol-1 bd* and 1 with *csp-1; chol-1*

bd; UV90. All transformants grew on plates and microtiter wells containing Hygromycin

B, confirming the presence of the *hyg* gene. Race tube analysis of the transformants,

however, did not show clear evidence of a successful transformation. The *UV90*

transformant showed no rhythm and very little conidiation along the length of the race

tube (Fig. 51). The *UV+* transformants showed some rhythmic conidiation for several

days before changing to an arrhythmic pattern, with the exception of transformants #26-1

and #26-6 which showed a constant rhythm (Figs. 51-53). Growth rates for the *UV90*

transformant were very slow at a mean of 0.32 (± 0.015) mm/hr (Table 27). *UV+*

transformants had a slow mean growth rate of 0.675 (± 0.035) mm/hr and a longer period of 25.07 (± 0.943) hr (Table 27). PCR and restriction enzyme digestion analysis revealed that *UV+* transformants #26-6, 26-7, 26-11, and 26-12 may have the inserted NCU05950 gene (Figs. 50 and 55). However, race tube analysis for #26-7, 26-11 and 26-12 transformants showed no clear rhythmic conidiation (Figs. 52-53). #26-6 showed the strongest evidence via PCR that it received the NCU05950 gene (Fig. 55), and race tube analysis showed a clear rhythmic pattern (Fig. 52). The *UV90* transformant did not show any PCR product (Fig. 54). One PCR product was seen at one point (Fig. 55), but this was believed to be non-specific binding of the primers as this result was not repeatable. Therefore, it could not be concluded that the *UV90* transformant obtained the wild type copy of the NCU05950 gene or whether or not NCU05950 is capable of restoring the *UV90* phenotype.

The results obtained from this transformation may be due to known difficulties in the experimental design. In *Neurospora*, sequences of DNA in transformations will usually insert themselves through non-homologous recombination at various locations in the genome (Asch et al., 1992; Case et al., 1992). It has also been discovered in *Neurospora* that during these insertion events, portions of the inserted plasmid DNA can be lost, as much as 450 bp (Asch et al., 1992). This is a plausible explanation for the results obtained. It is likely that both the *hyg* and NCU05950 genes were inserted into random locations in the genome. The loss of inserted DNA can also explain why no PCR product was seen in the *UV90* transformant, if large sections of DNA necessary for

primer binding were lost. Furthermore, Asch et al. (1992) discovered that linearized plasmid was separated into 2 fragments and inserted into different locations in the genome. If this also occurred during the *UV90* transformation, it is likely that fragments of both genes were inserted into several random DNA sequences, causing the abolishment of the rhythm seen on the race tubes.

Case et al. (1979) have experienced successful transformations with inserted linear and plasmid DNA replacing the desired gene of interest. This suggests the possibility that the transformation may work if it was repeated several more times to get more recombinants.

Sequencing of gene NCU05950

Several attempts were made to sequence the *UV90* gene candidate NCU05950. Sequencing of the gene was attempted in order to characterize the *UV90* mutation and confirm the identity of the *UV90* gene. Some PCR products were obtained for sequencing to the left of the gene for F6-R3 primers (Fig. 59; Appendix VIII). Sequences for approximately the first and last 20 basepairs were ignored for all products due to inaccuracies in the sequencing method. Some misaligned basepairs were observed in the sequences, however, these were not observed when the sequencing was repeated and were disregarded. No base pairs changes were seen in the sequence for this PCR product. The sequence produced by F6-R3 primers also falls just to the left of NCU05950 (Fig. 57), and therefore did not provide any information as to the type of gene mutation.

Some PCR products were seen along the NCU05950 gene that were larger than expected (Fig. 60). The 500 bp fragment from UV90BFor-R1 primers (Fig. 60) matched a sequence on Linkage Group II, around 2.046 Mbp (Appendix VIII). This corresponded to a region inside gene NCU06756, listed as a ubiquitin protein ligase (www.broadinstitute.org/annotation/genome/ neurospora/FeatureSearch.html). The 1 kb fragment from UV90AFor-R2 primers (Fig. 60) matched a sequence on Linkage Group VI, around 2.655 Mbp (Appendix VIII). This corresponded to a region inside gene NCU04073, currently listed as a hypothetical protein (www.broadinstitute.org/annotation/genome/neurospora/FeatureSearch.html). As with previous sequencing, the first and last 20 basepairs were ignored. Triplicates of each DNA sample were submitted for sequencing, and any mismatches were not observed more than once and were also disregarded.

It is unclear whether or not the matches to other Linkage Groups observed in sequencing are an indication of the gene function. There is the possibility that during mutagenesis, random fragments of coiled DNA were broken and reattached at various locations, causing extraneous fragments of DNA in the NCU05950 gene. The NCU05950 gene could not be sequenced, yet problems with obtaining PCR products were observed in multiple *UV90* strains. This indicates that the NCU05950 gene is disrupted in the *UV90* mutant, and helps add evidence to the hypothesis that NCU05950 is possibly the *UV90* gene.

Characterization of gene NCU05950 protein product

The hypothetical protein product of NCU05950 was compared against other proteins in an attempt to determine the function. PHYRE2 protein program produced a ferritin-like model structure for one domain of NCU05950 (Fig. 61; Appendix IX). However, the confidence in this prediction was only 33.3%, and thus it is not a definitive conclusion that the gene has a ferritin-like structure. The entire predicted structure gave no clues as to the protein function.

Other proteins were compared to NCU05950 using Jpred3 protein program (Table 28; Appendix IX). All of the similar proteins were found exclusively in fungi, specifically other fungi that live in soil and manure (Table 28). This indicates that this protein is possibly unique to fungi, yet not exclusive to *Neurospora crassa*. The match to other fungi with a highly conserved amino acid sequence (Appendix IX) suggests this gene is important and has gone through little evolutionary genetic variation even amongst different species.

It was interesting to note that one protein match discovered had a sequence similarity to PDZ domain protein MUPP1 in the brown rat (Table 28). MUPP1 protein, which contains multiple PDZ (PSD-95/*Drosophila* Disc large/ZO-1 homology) domains, has been found to bind to and regulate the signal transduction of a melatonin receptor in humans (Guillaume et al., 2008). Melatonin is known as an important feature in the mammalian circadian clock and has also recently been discovered in plants (Paredes et

al., 2009). There is a possibility that the NCU05950 protein product may have an important role in signal transduction.

FUTURE DIRECTIONS

Transformation of *Neurospora* with gene NCU05950

One of the most important experiments that needs to be repeated is the complementation test by transforming *Neurospora* with NCU05950. If performed correctly, this can provide definitive proof that this gene is responsible for the *UV90* phenotype. However, with the inability to create a *his-3; UV90* double mutant strain, one possibility would be to use another gene that can be easily targeted using a plasmid. Case et al. (1992) have successfully restored quinic acid mutants, *qa-2* and *qa-1F*, in *Neurospora* by using plasmids that contain part of a functional copy of these genes. This allowed for targeted transformations since only a homologous recombination event could produce functional copies of these genes, which can be tested for on media without aromatic amino acid supplements (Case et al., 1992).

Successful transformations have also been performed by creating a recipient *Neurospora* strain that contained the 3' end of the Hygromycin resistance gene (*hyg*) downstream from the glutamate dehydrogenase mutant (*am*) gene (Cambareri and Kinsey, 1994). The inserted plasmid contained the 5' of the *hyg* gene and also a copy of *am* (Cambareri and Kinsey, 1994). Hygromycin resistance can therefore only be observed if homologous recombination between the recipient and donor strains occurs.

178

Both recipient strains (FGSC #8071 and #8072) and plasmids used for transformations are available at the FGSC (Cambareri and Kinsey, 1994). Successful targeting of specific regions in *Neurospora* was achieved with both methods. *UV90* can be crossed with either the quinic acid mutants (*qa-2, qa-1F*) or the glutamate dehydrogenase mutant (*am*) to create a double mutant that can be used for plasmid targeting.

It is also possible that the transformation experiment can be repeated as performed, with the exception of introducing a piece of the NCU05950 gene with a large amount of flanking sequences on either direction to attempt to target the gene to the correct location. It has been noticed previously in *Neurospora* that homologous recombination in transformation events is dependent upon the length of the inserted fragment (Asch et al., 1992).

Another possibility is to repeat the experiment performed, but with placing the wild type NCU05950 gene directly into the Hygromycin resistance plasmid (pCSN44), and then transform the entire plasmid into *Neurospora*. This may prevent issues with non-homologous recombination since an entire plasmid will be inserted as opposed to two lone fragments of DNA that will almost certainly recombine at various locations. The recipient strain that uptakes the entire plasmid (including the wild type gene) will be also resistant to Hygromycin.

Sequence and gene function of *UV90*

Another experiment which failed after repeated attempts was the sequencing of NCU05950. PCR and sequencing should be repeated with new primers to confirm if the

179

previous sequencing results matching fragments of NCU05950 to Linkage Groups II and VI can be repeated. PCR will also need to be repeated on the regions of NCU05950 that showed a normal sized PCR product yet were unable to be sequenced. Sequencing may provide clues as to the nature of the mutation and possibly the gene function of *UV90*. If there is a mutation in the promoter region of the gene, this may prevent transcription and translation of a protein product. A mutation in the amino acid sequence of the protein may provide clues as to the affect this has on the final protein sequence and structure. Knowing the sequence of the *UV90* mutation will also provide information as to the nature of the protein product: specifically, does the *UV90* mutant protein have any function or is it completely abolished?

Characterize protein product of *UV90*

The protein product and the function of gene NCU05950 are currently unknown. One method of determining the function is to identify which other proteins the desired protein is interacting with. Typically, target proteins are tagged with an epitope tag which can then be detected using an antibody specific for that epitope (Honda and Selker, 2009). Epitope tags may interfere with protein folding, processing, modification, or function unless a polypeptide linker (made up of 10-glycines) is placed between the epitope tag and the protein (Honda and Selker, 2009). Interacting tagged proteins can then be co-immunoprecipitated from cell extracts and identified using mass spectrometry (Honda and Selker, 2009).

Other protein tags that have previously been used are Myc-6xHis tandem affinity purification (TAP) tag and FLAG-6xHis TAP tag (Honda and Selker, 2009). A green fluorescent protein (GFP) tag may also be added to the *UV90* gene and inserted using an appropriate vector. GFP tag is particularly useful due to the fact that it produces green fluorescence under UV light (Honda and Selker, 2009). This can be used in detecting the movement and localization of the *UV90* protein product in the cell using live-cell confocal microscopy.

It will also be useful to determine if the gene transcription of *UV90* is rhythmic. Northern blotting and quantitative reverse transcription PCR (qRT-PCR) can be used to detect mRNA levels at regular intervals to determine the nature of the gene transcription. *UV90* protein rhythms can similarly be observed using Western blotting of the tagged protein. If either *UV90* mRNA or protein levels are rhythmically expressed, it can be determined if the rhythms are necessary for their function by expressing the genes using a promoter that is constantly induced and non-rhythmic. In addition, continuing to compare the predicted protein product with those in other fungi may reveal information if the function of a similar protein is discovered.

REFERENCES

Aronson, B.D., Johnson, K.A., Loros, J.J., and Dunlap, J.C. 1994a. Negative feedback defining a circadian clock: autoregulation of the clock gene *frequency*. *Science* **263**:1578-1584.

Aronson, B.D., Johnson, K.A., and Dunlap, J.C. 1994b. Circadian clock locus frequency: protein encoded by a single open reading frame defines period length and temperature compensation. *Proc Natl Acad Sci USA* **91**:7683-7687.

Asch, D.K., Frederick, G., Kinsey, J.A., and Perkins, D.D. 1992. Analysis of junction sequences resulting from integration at nonhomologous loci in *Neurospora crassa*. *Genetics* **130**:737-748.

Avivi, A., Albrecht, U., Oster, H., Joel, A., Beiles, A., and Nevo, E. 2001. Biological clock in total darkness: the *Clock/MOP3* circadian system of the blind subterranean mole rat. *Proc Natl Acad Sci USA* **98(24)**:13751-13756.

Brunner, M. and Schafmeier, T. 2006. Transcriptional and post-transcriptional regulation of the circadian clock of cyanobacteria and *Neurospora*. *Genes Dev* **20**:1061-1074.

Cambareri, E.B., and Kinsey, J.A. 1994. A simple and efficient system for targeting DNA to the *am* locus of *Neurospora crassa*. *Gene* **142**:219-224.

Case, M.E., Geever, R.F., and Asch, D.K. 1992. Use of gene replacement transformation to elucidate gene function in the *qa* gene cluster of *Neurospora crassa*. *Genetics* **130**:729-736.

Case, M.E., Schweizer, M., Kushner, S.R., and Giles, N.H. 1979. Efficient transformation of *Neurospora crassa* by utilizing hybrid plasmid DNA. *Genetics* **76(10)**:5259-5263.

Cashmore, A.R., Jarillo, J.A., Wu, Y.-J., and Liu, D. 1999. Cryptochromes: blue light receptors for plants and animals. *Science* **284**:760-765.

Catcheside, D.G., and Corcoran, D. 1973. Control of non-allelic recombination in *Neurospora crassa*. *Aust J Biol Sci* **26**:1337-1353.

Ceriani, M.F., Darlington, T.K., Staknis, D., Mas, P., Petti, A.A., Weitz, C.J., Kay, S.A. 1999. Light-dependent sequestration of TIMELESS by CRYPTOCHROME. *Science* **285**:553-556.

Cheng, P., Yang, Y., and Liu, Y. 2001. Interlocked feedback loops contribute to the robustness of the *Neurospora* circadian clock. *Proc Natl Acad Sci USA* **98(13)**:7408-7413.

Christensen, M.K., Falkeid, G., Loros, J.J., Dunlap, J.C., Lillo, C., and Ruoff, P. 2004. A nitrate-induced *frq*-less oscillator in *Neurospora crassa*. *J Biol Rhythms* **19(4)**:280-286.

Cole, C., Barber, J.D., and Barton, G.J. 2008. The Jpred3 secondary structure prediction server. *Nucl Acids Res* **36(suppl 2)**:W197-W201.
< http://www.compbio.dundee.ac.uk/www-jpred/index.html>

Colot, H.V., Park, G., Turner, G.E., Ringelberg, C., Crew, C.M., Litvinkova, L., Weiss, R.L., Borkovich, K.A., and Dunlap, J.C. 2006. A high-throughput gene knockout procedure for *Neurospora* reveals functions for multiple transcription factors. *Proc Natl Acad Sci USA* **103(27)**:10352-10357.

Correa, A., Lewis, Z.A., Greene, A.V., March, I.J., Gomer, R.H., and Bell-Pedersen, D. 2003. Multiple oscillators regulate circadian gene expression in *Neurospora*. *Proc Natl Acad Sci USA* **100(23)**:13597-13602.

Crosthwaite, S.K., Dunlap, J.C., and Loros, J.J. 1997. Neurospora *wc-1* and *wc-2*: Transcription, photoresponses, and the origins of circadian rhythmicity. *Science* **276**:763-769.

Davis, R.H. 2000. *Neurospora*: Contributions of a model organism. Oxford University Press, New York. pp. 283-302.

de Paula, R.M., Lewis, Z.A., Greene, A.V., Seo, K.S., Morgan, L.W., Vitalini, M.W., Bennett, L., Gomer, R.H., and Bell-Pedersen, D. 2006. Two circadian timing circuits in *Neurospora crassa* cells share components and regulate distinct rhythmic processes. *J Biol Rhythms* **21(3)**:159-168.

Dong, G., Kim, Y.-I., and Golden, S.S. 2010. Simplicity and complexity in the cyanobacterial circadian clock mechanism. *Curr Opin Genet Dev* **20(6)**:619-625.

Dunlap, J.C., and Loros, J.J. 2004. The *Neurospora* circadian system. *J Biol Rhythms* **19(5)**:414-424.

Dunlap, J.C., and Loros, J.J. 2006. How fungi keep time: circadian system in *Neurospora* and other fungi. *Curr Opin Microbiol* **9**:579-587.

Dvornyk, V., Vinogradova, O., and Nevo, E. 2003. Origin and evolution of circadian clock genes in prokaryotes. *Proc Natl Acad Sci USA* **100(5)**:2495-2500.

Eban-Rothschild, A., Shemesh, Y., and Bloch, G. 2012. The colony environment, but not direct contact with conspecifics, influences the development of circadian rhythms in honey bees. *J Biol Rhythms* **27(3)**:217-225.

Ebbole, D.E. 1990. Vectors for construction of translational fusions to β-galactosidase. *Fungal Genet Newslett* **37**:15-16.

Ellman, D., Fuller, C., Moore-Ede, M.C., Sulzman, F.M., and Wassmer, G. 1984. *Neurospora* circadian rhythms in space: a re-examination of the endogenous-exogenous question. *Science* **225**:232.

Froehlich, A.C., Liu, Y., Loros, J.J., and Dunlap, J.C. 2002. White collar-1, a circadian blue light photoreceptor, binding to the *frequency* promoter. *Science* **297**:815-819.

Froehlich, A.C., Loros, J.J., and Dunlap, J.C. 2003. Rhythmic binding of a WHITE COLLAR-containing complex to the *frequency* promoter is inhibited by FREQUENCY. *Proc Natl Acad Sci USA* **100**:5914-5919.

Fincham, J.R.S., Day, P.R., and Radford, A. 1979. Fungal Genetics: Botanical Monographs Volume 4. Blackwell Scientific Publications, California. pp. 180.

Fuller, P.M., Lu, J., and Saper, C.B. 2008. Differential rescue of light- and food-entrainable circadian rhythms. *Science* **320**:1074-1077.

Galagan, J.E., Calvo, S.E., Borkovich, K.A., Selker, E.U., Read, N.D., Jaffe, D., Fitzhugh, W., Ma, L.-J., Smirnov, S., Purcell, S., Rehman, B., Elkins, T., Engels, R., Wang, S., Nielsen, C.B., Butler, J., Endrizzi, M., Qui, D., Ianakiev, P., Bell-Pedersen, D., Nelson, M.A., Werner-Washburne, M., Selitrennikoff, C.P., Kinsey, J.A., Braun, E.L., Zelter, A., Schulte, U., Kothe, G.O., Jedd, G., Mewes, W., Staben, C., Marcotte, E., Greenberg, D., Roy, A., Foley, K., Naylor, J., Stange-Thomann, N., Barrett, R., Gnerre, S., Kamal, M., Kamvysselis, M., Mauceli, E., Bielke, C., Rudd, S., Frishman, D., Krystofova, S., Rasmussen, C., Metzenberg, R.L., Perkins, D.D., Kroken, S., Cogoni, C., Macino, G., Catcheside, D., Li, W., Pratt, R.J., Osmani, S.A., Desouza, C.P.C., Glass, L., Orbach, M.J., Berglund, J.A., Voelker, R., Yarden, O., Plamann, M., Seiler, S., Dunlap, J., Radford, A., Aramayo, R., Natvig, D.O., Alex, L.A., Mannhaupt, G., Ebbole, D.J., Freitag, M., Paulsen, I., Sachs, M.S., Lander, E.S., Nusbaum, C., and Birren, B. 2003. The genome sequence of the filamentous fungus *Neurospora crassa*. *Nature* **422**:859-868.

Glickman, G. 2010. Circadian rhythms and sleep in children with autism. *Neurosci Biobehav Rev* **34**:755-768.

Granshaw, T., Tsukamoto, M., and Brody, S. 2003. Circadian rhythms in *Neurospora crassa*: farnesol or geraniol allow expression of rhythmicity in the otherwise arrhythmic strains *frq*^{10}, *wc-1*, and *wc-2*. *J Biol Rhythms* **18**:287-296.

Green, R.M. and Tobin, E.M. 1999. Loss of the circadian clock-associated protein 1 in *Arabidopsis* results in altered clock-regulated gene expression. *Proc Natl Acad Sci USA* **96**:4176-4179.

Griffiths, A.J.F., Miller, J.H., Suzuki, D.T., Lewontin, R.C., and Gelbart, W.M. 1993. An Introduction to Genetic Analysis: Fifth Edition. W.H. Freeman and Company, New York. pp. 74-79, 118-135, 215-219, 580-585.

Guillaume, J-L., Daulat, A.M., Maurice, P., Levoye, A., Migaud, M., Brydon, L., Malpaux, B., Borg-Capra, C., and Jockers, R. 2008. The PDZ protein Mupp1 promotes G_i coupling and signaling of the Mt_1 melatonin receptor. *J Biol Chem* **283**:16762-16771.

Hardin, P.E. 2009. Molecular mechanisms of circadian timekeeping in *Drosophila*. *Sleep Biol Rhythms* **7**:235-242.

Harmer, S.L. 2009. The circadian system in higher plants. *Annu Rev Plant Biol* **60**:357-377.

Hasler, B.P., Smith, L.J., Cousins, J.C., and Bootzin, R.R. 2012. Circadian rhythms, sleep, and substance abuse. *Sleep Med Rev* **16**:67-81.

Heckman, K.L., and Pease, L.R. 2007. Gene splicing and mutagenesis by PCR-driven overlap extension. *Nat Protoc* **2(4)**:924-932.

Honda, S., and Selker, E.U. 2009. Tools for fungal proteomics: Multifunctional *Neurospora* vectors for gene replacement, protein expression and protein purification. *Genetics* **182**:11-23.

Jin, Y., Allan, S., Baber, L., Bhattarai, E.K., Lamb, T.M., and Versaw, W.K. 2007. Rapid genetic mapping in *Neurospora crassa*. *Fungal Genet Biol* **44**:455-465.

Johnson, C.H., Mori, T., and Xu, Y. 2008. A cyanobacterial circadian clockwork. *Curr Biol* **18**:R816-825.

Kelley, L.A., and Sternberg, M.J.E. 2009. Protein structure prediction on the web: a case study using the Phyre server. *Nat Protoc* **4**:363-371. <http://www.sbg.bio.ic.ac.uk/phyre2/html/page.cgi?id=index>

Kondo, T., Mori, T., Lebedeva, N.V., Aoki, S., Ishiura, M., and Golden, S.S. 1997. Circadian rhythms in rapidly dividing cyanobacteria. *Science* **275**:224-227.

Lakin-Thomas, P.L. 1996. Effects of choline depletion on the circadian rhythm in *Neurospora crassa*. *Biol Rhythm Res* **27(1)**:12-30.

Lakin-Thomas, P.L. 2006a. New models for circadian systems in microorganisms. *FEMS Microbiol Lett* **259**:1-6.

Lakin-Thomas, P.L. 2006b. Transcriptional feedback oscillators: Maybe, maybe not... *J Biol Rhythms* **21(2)**:83-92.

Lakin-Thomas, P.L., Bell-Pedersen, D., and Brody, S. 2011. The genetics of circadian rhythms in *Neurospora*. *Adv Genet* **74**:55-103.

Lakin-Thomas, P.L., and Brody, S. 2000. Circadian rhythms in *Neurospora crassa*: lipid deficiencies restore robust rhythmicity to null *frequency* and *white-collar* mutants. *Proc Natl Acad Sci USA* **97**:256-261.

Lambreghts, R., Shi, M., Belden, W.J., deCaprio, D., Park, D., Henn, M.R., Galagan, J.E., Baştürkmen, M., Birren, B.W., Sachs, M.S., Dunlap, J.C. and Loros, J.J. 2009. A high-density single nucleotide polymorphism map for *Neurospora crassa*. *Genetics* **181**:767-781.

Leloup, J.-C., Gonze, D., and Goldbeter, A. 1999. Limit cycle models for circadian rhythms based on transcriptional regulation in *Drosophila* and *Neurospora*. *J Biol Rhythms* **14(6)**:433-448.

Levine, J.D., Funes, P., Dowse, H.B., and Hall, J.C. 2002. Resetting the circadian clock by social experience in *Drosophila melanogaster*. *Science* **298**:2010-2012.

Li, S., and Lakin-Thomas, P. 2010. Effects of *prd* circadian clock mutations on FRQ-less rhythms in *Neurospora*. *J Biol Rhythms* **25(2)**:71-80.

Li, S., Motavaze, K., Kafes, E., Suntharalingam, S., Lakin-Thomas, P. 2011. A new mutation affecting FRQ-less rhythms in the circadian system of *Neurospora crassa*. *PLoS Genet* **7(6)**:e1002151.

Lim, C., and Allada, R. 2013. ATAXIN-2 activates PERIOD translation to sustain circadian rhythms in *Drosophila*. *Science* **340**:875-879.

Lindegren, C.C. 1932. The genetics of *Neurospora*-II. Segregation of the sex factors in asci of *N. crassa*, *N. sitophila*, and *N. tetrasperma*. *Bull Torrey Bot Club* **59(3)**:119-138.

Liu, Y., and Bell-Pedersen, D. 2006. Circadian rhythms in *Neurospora crassa* and other filamentous fungi. *Eukaryot Cell* **5(8)**:1184-1193.

Loros, J.J. and Feldman, J.F. 1986. Loss of temperature compensation of circadian period length in the *frq-9* mutant of *Neurospora crassa*. *J Biol Rhythms* **1**:187-198.

Markowitz, M., Rotkin, L., and Rosen, J.F. 1981. Circadian rhythms of blood minerals in humans. *Science* **213(4508)**:672-674.

Metzenberg, R.L., and Glass, N.L. 1990. Mating type and mating strategies in *Neurospora*. *BioEssays* **12(2)**:53-59.

Mohawk, J.A., Green, C.B., and Takahashi, J.S. 2012. Central and peripheral circadian clocks in mammals. *Annu Rev Neurosci* **35**:445-462.

Nagel, D.H., and Kay, S.A. 2012. Complexity in the wiring and regulation of plant circadian networks. *Curr Biol* **22(16)**:R648-R657.

Nakajima, M., Imai, K., Ito, H., Nishiwaki, T., Murayama, Y., Iwasaki, H., Oyama, T., and Kondo, T. 2005. Reconstitution of circadian oscillation of cyanobacterial KaiC phosphorylation in vitro. *Science* **308**:414-415.

O'Neill, J.S., and Reddy, A.B. 2011. Circadian clocks in human red blood cells. *Nature* **469**:498-504.

Paredes, S.D., Korkmaz, A., Manchester, L.C., Tan, D.-X., and Reiter, R.J. 2009. Phytomelatonin: a review. *J Exp Bot* **60(1)**:57-69.

Pickard, G.E., Kahn, R., and Silver, R. 1984. Splitting of the circadian rhythm of body temperature in the golden hamster. *Physiol Behav* **32**:763-766.

Pickard, G.E., and Turek, F.W. 1982. Splitting of the circadian rhythm of activity is abolished by unilateral lesions of the suprachiasmatic nuclei. *Science* **215(4536)**:1119-1121.

Plautz, J.D., Kaneko, M., Hall, J.C., and Kay, S.A. 1997. Independent photoreceptive circadian clocks throughout *Drosophila*. *Science* **278**:1632-1635.

Pomraning, K.R., Smith, K.M., and Freitag, M. 2010. An improved SNP map for *Neurospora crassa* Mauriceville.
<http://www.fgsc.net/Neurospora/SNPs/SNP_map.htm>

Portaluppi, F., Tiseo, R., Smolensky, M.H., Hermida, R.C., Ayala, D.E., and Fabbian, F. 2012. Circadian rhythms and cardiovascular health. *Sleep Med Rev* **16**:151-166.
Reddy, A.B., and O'Neill, J.S. 2010. Healthy clocks, healthy body, healthy mind. *Trends Cell Bio* **20(1)**:36-44.

Salomé, P.A., and McClung, C.R. 2004. The *Arabidopsis thaliana* clock. *J Biol Rhythms* **19(5)**:425-435.

Staben, C., Jensen, B., Singer, M., Pollock, J., Schechtman, M., Kinsey, J., and Selker, E. 1989. Use of a bacterial Hygromycin B resistance gene as a dominant selectable marker in *Neurospora crassa* transformation. *Fungal Genet Newslett* **36**:79-81.

Swann, J.M., and Turek, F.W. 1985. Multiple circadian oscillators regulate the timing of behavioral and endocrine rhythms in female golden hamsters. *Science* **228**:898.

Tapp, W.N., and Holloway, F.A. 1981. Phase shifting circadian rhythms produces retrograde amnesia. *Science* **211(4486)**:1056-1058.

Tomita, J., Nakajima, M., Kondo, T., and Iwasaki, H. 2005. No transcription-translation feedback in circadian rhythm of KaiC phosphorylation. *Science* **307**:251-254.

Tsuchiya, Y., Akashi, M., Matsuda, M., Goto, K., Miyata, Y., Node, K., Nishida, E. 2009. Involvement of the protein kinase CK2 in the regulation of mammalian circadian rhythms. *Sci Signal* **2(73)**:ra26.

Van Gelder, R.N., Herzog, E.D., Schwartz, W.J., and Taghert, P.H. 2003. Circadian rhythms: In the loop at last. *Science* **300**:1534-1535.

Zhang, E.E., and Kay, S.A. 2010. Clocks not winding down: unravelling circadian networks. *Nature Rev Mol Cell Biol* **11**:764-776.

APPENDIX

Appendix I

4% agar:

2 g Difco Bacto-Agar

50 mL dd H_2O

Mix together agar and water, sterilize and pour contents into two sterile small (8.5 cm) Petri plates.

Minimal agar medium:

2 mL 50x/Vogel's stock

2 g D-glucose

2 g Difco Bacto-agar

100 mL dd H_2O

Several drops green food colouring

1 mL choline (10 mM), final concentration 100 μM*

Mix all ingredients together. For baby tubes, use 1 mL of media per tube, cover with cotton plugs, sterilize and lean tubes on their sides to produce slants. For stock tubes, use 3 mL per large test tube, cover with plastic caps, sterilize and slant.

*Added if *Neurospora* strain contains choline (*chol-1*) mutation.

Appendix I

50x/Vogel's Stock:

Add the following in succession to a 250 mL flask:

188 mL dd H_2O, stir with heat

32.8 g Na_3-citrate $\cdot$ $2H_2O$, let dissolve

62.5 g KH_2PO_4 anhydrous, let dissolve

25.0 g NH_4NO_3 anhydrous, let dissolve

Turn off heat and add water to 250 mL. Add the following while stirring:

2.5 g $MgSO_4$ $\cdot$ $7H_2O$, let dissolve

1.25 g $CaCl_2$ $\cdot$ $2H_2O$ dissolved in 5 mL water, let dissolve (Add calcium mixture slowly with a pasteur pipette submerged below the solution surface to avoid precipitation)

1.25 mL trace elements solution

0.625 mL biotin solution (make fresh)

Allow solution to cool completely, add 2 mL chloroform and cap tightly. Store at room temperature.

Biotin solution:

1 mg biotin per 10 mL of 50/50 ethanol/water

Weigh a small amount (close to 1 mg) of biotin and add 50/50 ethanol/water for a final concentration of 0.1 mg/mL.

Appendix I

Trace elements solution:

Add in succession to 9.5 mL water (dd H_2O), while stirring:

0.5 g citric acid $\cdot$ H_2O

0.5 g $ZnSO_4$ $\cdot$ $7H_2O$

0.1 g $Fe(NH_4)_2(SO_4)_2$ $\cdot$ $6H_2O$

0.025 g $CuSO_4$ $\cdot$ $5H_2O$

0.066 g $MnSO_4$ $\cdot$ $4H_2O$ (or 0.05 g $MnSO_4$ $\cdot$ $H2O$)

0.005 g H_3BO_3 anhydrous

0.0037 g $(NH_4)_6Mo_7O_{24}$ $\cdot$ $4H_2O$ (ammonium molybdate hydrate)

Keep refrigerated and wrapped in foil to keep dark.

Maltose-arginine (MA) medium:

2 mL 50x/Vogel's stock

0.5 mL L-arginine (2% or 20 mg/mL), final concentration 0.01%

0.5 g maltose

2 g Difco Bacto-agar

100 mL dd H_2O

Several drops green or blue food colouring**

1 mL choline (10 mM), final concentration 100 μM, optional*

Mix all ingredients together. Sterilize media separately from race tubes sealed with

cotton plugs at both ends. For short (30 cm) race tubes, use 6 mL per tube. For long (40

cm) race tubes, use 8 mL per tube.

*May be added if *Neurospora* strain contains choline (*chol-1*) mutation.

**Blue food colouring is typically added to media containing choline; green without

choline

Appendix II

Liquid minimal medium:

2 mL 50x/Vogel's stock

2 g D-glucose

100 mL water

Several drops blue or green food colouring, optional

Mix all ingredients together and sterilize.

DNA Extraction Buffer:

1.21 g Tris (final concentration 100 mM)

1.86 g EDTA (final concentration 50 mM)

1 mL 10% SDS

Dissolve Tris and EDTA with stirring in 80 mL dd H_2O. Adjust pH to 8.0. Add water

for a total volume of 100 mL. Store at room temperature.

To make DNA extraction buffer with 1% SDS, measure 1 mL 10% SDS with 9 mL DNA

extraction buffer.

RNase A:

0.121 g Tris (final concentration 10 mM)

500 µL glycerol

10 mg RNase powder

192

Dissolve Tris in 80 mL dd H_2O. Adjust pH to 8.0. Add water for a total volume of 100

mL. Place 500 μL glycerol into 1.5 mL screw-cap conical tube. (If glycerol is too dense

to pipette, measure 500 μL in grams, 1 mL = 1.26 g). Add 500 μL of Tris-HCl solution

and RNase powder. Vortex to mix and store in fridge.

TE Buffer:

0.121 g Tris (final concentration 10 mM)

0.0372 g EDTA (final concentration 1 mM)

Dissolve Tris and EDTA with stirring in 80 mL dd H_2O. Adjust pH to 8.0. Add water

for a final volume of 100 mL. Can be sterilized in 1.5 mL screw-cap conical tubes and

frozen.

Appendix III

CAPS marker: Right Side of Centromere – RCF5 & RCR5

(Linkage Group VI; Supercontig 6)

>N. crassa OR74A (NC10) supercont10.6 of Neurospora crassa (OR74A) [DNA]

3,102,391 – 3,102,921 +

██████████████████████TCACCAAGAGCATGACTTCATTGCACACCA
GACTGAAGTCAGCAGAGAATCCGTTCACAAAGCCGACTGTCACTGGGCCTGG
GATTGGAGCCCATCCCACTGACTTACGAACCTTGGCCACC██████GTGTAGCG
AGCCAAGGTTGAAAACTTTCAATATAAAGGATGAGTTGAATTGGGGAACTGA
GGGAATGGCGACATCGGGTCATGTCGTGGTCTCGGCAGATACA█████GAGCC
ACCGAATGTATTCAGGAGTCTGTTTAATGATGTTACTACACCCAATACCTTCC
TGATGCCAACATGAGTAAGGCAGTCAGGGTTGGAAGGCAAACTAAGTGTGTC
CGTGGATAGCCTTGGGCTTATACATCTCCTCCAAATACTTCTCCTCCTCCACC
GTTAAAACCTTGCCTCTAGCGGTGATTGCTTCTTCCAAACGCTCAACGCTGCT
AAAACCAATGATTGGACTGATGACGCGCTTAGCAATCC██████████████████
█████████

(http://www.broadinstitute.org/annotation/genome/neurospora/Regions.html)

Forward Primer (RCF5): GCGAATTGGAAATCTCCAAGGG

Reverse Primer (RCR5): ATCTCCCACGTAGCCTTGGCTT (reverse & complement of

green)

FORWARD: 22nt, GC: 50%, Tm: 69.62

REVERSE: 22nt, GC: 54.55%, Tm: 69.08

SNP location: 3,102,537

Taqα1 enzyme cuts at **TCGA**: cut in OR (TCGA); uncut in MV (TCAA)

Size of OR sequences: 146, 107, 278 bp; Size of MV sequences: 253, 278 bp

Total CAPS marker size: 531 bp

Polymerase Chain Reaction (PCR):

<u>**Primer Preparation:**</u>

Centrifuge primer tubes several times to collect primers (about 10 sec. x 2 times). Use

"nmoles" amount on Invitrogen or IDT invoice that arrives with primers, add this amount

(in μL) of sterile TE Buffer (nmole concentration). Mix well and centrifuge to collect

primers. Dilute primers to 10 pmol concentration for PCR (99 μL dd H_2O + 1 μL of

primer = 10 pmol).

<u>**PCR recipes:**</u>

Table A1.
PCR recipe using *Taq* DNA polymerase.

PCR Recipe	More than ~12 samples	Less than ~12 samples
Taq 10X Thermopol Buffer	2 μL	2 μL
Water (sterile, dd H_2O)	14.52 μL	13.8 μL
dNTP Mix (from NEB)	0.4 μL	0.4 μL
Taq Polymerase	0.08 μL	0.8 μL (diluted*)
Forward primer (10 pmol)	1 μL	1 μL
Reverse primer (10 pmol)	1 μL	1 μL
DNA template (50 ng/μL concentration)	1 μL	1 μL
	20 μL total	**20 μL total**

*diluted *Taq* Polymerase: If using a small number of samples, it is difficult to measure

out 0.08 μL per tube. Dilute 1 μL of 10X Buffer + 9 μL water = 10 μL of 1X Buffer.

Take 1 μL *Taq* Polymerase + 9 μL of 1X Buffer = 10 μL of Diluted *Taq* Polymerase.

Appendix IV

Mix first 4 ingredients in this order: water, *Taq* Buffer, dNTP, and *Taq* Polymerase. Add

1 μL each of Forward primer, Reverse primer and DNA template to each sample, mix

gently.

Table A2.
PCR recipe using *Takara LA Taq* polymerase.

PCR Recipe	
LA Taq 10X Buffer	5 μL
Water (sterile, dd H₂O)	15 μL
LA dNTP	8 μL
Takara LA Taq Polymerase	1 μL
Forward primer (10 pmol)	10 μL
Reverse primer (10 pmol)	10 μL
DNA template (stock concentration; should be at least 50 ng/μL)	1 μL
	50 μL total

Mix first 4 ingredients in this order: water, *LA Taq* Buffer, *LA* dNTP, and *LA Taq*

Polymerase. Add Forward primer, Reverse primer and DNA template to each sample,

mix gently.

PCR conditions:

Table A3.
PCR conditions using *Taq* DNA Polymerase. Conditions are based on NEB "*Taq*
Polymerase" PCR Manual.

	Step	Temperature	Time
Initial DNA denaturing	Step 1	94 °C	3 min
DNA denature (26-35 cycles)	Step 2: i)	94 °C	15 sec (for a DNA fragment less than 1000

			bp; for 1 kb or more use 30 sec - 1 min)
Primer annealing	ii)	Varies*	15 sec (for fragment less than 1000 bp; for 1 kb or more use 30-45 sec)
Strand extension	iii)	72 °C	1 min (typically 1 min per 1 kb; use minimum 1 min for smaller fragments)
Final extension	Step 3	72 °C	5 min (for less than 1000 bp, for more use 10 min)
Storage	Step 4	4 °C	infinitely

*Step 2 annealing temperature: Use the actual "Tm, 50 mM Na+/NaCl" value in the

Invitrogen or IDT invoice from both primers (not the calculated Tm). Optimal annealing

temperature is 3-5 °C less than the primer with the lowest Tm.

Table A4.
PCR conditions using *Takara LA Taq* polymerase. Conditions are based on Takara "*LA Taq* Polymerase" PCR Manual

	Step	Temperature	Time
Initial DNA denaturing	Step 1	94 °C	3 min
DNA denature (26-35 cycles)	Step 2: i)	94 °C	15 sec (for a DNA fragment less than 1000 bp; for 1 kb or more use 30 sec - 1 min)
Primer annealing and extension*	ii)	Varies**	1 min (for "2-step" PCR, use 1 min per kb)
Final extension	Step 3	72 °C	5 min (for less than 1000 bp, for more use 10 min)
Storage	Step 4	4 °C	infinitely

Appendix IV

*Primer annealing and extension are combined in one step, as recommended by *Takara LA Taq* PCR manual. "3-step" PCR using a 72 °C extension (see Table A3) will also work.

**Step 2 annealing temperature: Use the actual "Tm, 50 mM Na+/NaCl" value in the Invitrogen or IDT invoice from both primers (not the calculated Tm). Optimal annealing temperature is 3-5 °C less than the primer with the lowest Tm.

Restriction Enzymes:

Table A5.
Restriction enzymes used in digestion of *UV90* progeny

Restriction Enzyme Recipe	Restriction Enzymes				
	EcoRI	Taqα1	HaeIII	MspI	MseI
Water (sterile, dd H₂O)	14.5 μL	14.3 μL	14 μL	14.5 μL	13.8 μL
Restriction Enzyme Buffer*	2 μL	2 μL	2 μL	2 μL	2 μL
Restriction Enzyme**	0.5 μL	0.5 μL	1 μL	0.5 μL	1 μL
DNA – PCR product	3 μL	3 μL	3 μL	3 μL	3 μL
BSA (optional)	--	0.2 μL	--	--	0.2 μL
Incubation temperature (°C)	37	65	37	37	37
	20 μL	20 μL	20 μL	20 μL	20 μL

Appendix IV

*All enzymes used Buffer #4 with the exception of EcoRI, which uses EcoRI Buffer.

**Restriction Enzyme amount depends on enzyme concentration. For a concentration of 10,000 units/mL (U/mL), use 1 μL per sample, for 20,000 U/mL, use 0.5 μL per sample.

Mix first 4 ingredients in this order: Water, Restriction Enzyme Buffer, Restriction Enzyme, and BSA (optional). Add 3 μL of PCR product to each sample, mix gently. Incubate samples in a water bath at incubation temperature for 1.5 hours.

Gel Electrophoresis:

10X TAE Buffer:

48.4 g Tris

3.72 g EDTA, disodium salt, dihydrate

11.4 mL acetic acid

Measure out ~ 600 mL dd H_2O into a beaker. Add, with stirring: Tris, EDTA, and acetic acid one at a time. Make sure each is dissolved fully before adding the next. Adjust pH to 8.0. Pour into a graduated cylinder and add water for a final volume of 1 L.

Gel Preparation:

Table A6.
Recipes for preparation of agarose gels

Small Gel (30 mL)		Large Gel (150 mL)	
1X TAE Buffer	3 mL 10X TAE buffer + 27 mL water	1X TAE Buffer	15 mL 10X TAE buffer + 135 mL water

Agarose (1.5%)	0.45 g	Agarose (1.5%)	2.25 g
Ethidium Bromide (3%) **OR** Gel Red*	EB: 0.9 µL Gel Red: 3 µL	Ethidium Bromide (3%) **OR** Gel Red*	EB: 4.5 µL Gel Red: 15 µL

*Gel Red is strongly preferred as it is not a carcinogen

Mix appropriate amount of 10X TAE buffer and water to get 1X TAE buffer and add agarose.

Heat in microwave, swirling often, until agarose is well dissolved. Let cool until warm and add Gel Red. Swirl gently until thoroughly combined and pour into gel mold with combs. Let stand for 20-30 min until set.

Running Buffer:

Prepare 1X TAE Running Buffer and pour into electrophoresis box with prepared gel. Ensure entire gel is submerged and covered approximately 0.5 cm. Small gel boxes (30 mL gels) use approximately 250 mL 1X TAE buffer (25 mL 10X TAE + 225 mL water). Large gel boxes (150 mL gels) use approximately 1000 mL 1X TAE buffer (100 mL 10X TAE + 900 mL water).

Preparing & Loading Samples:

Table A7.
Recipes for gel electrophoresis loading with PCR and restriction enzyme products

Small Gel – undigested samples		Small Gel – digested samples		Small Gel – Ladder	
6X Loading Dye	2 µL	6X Loading Dye	3 µL	6X Loading Dye	1 µL

(NEB)					
PCR product	10 µL	PCR product	15 µL	Ladder*	1 µL
-	-	-	-	Water (sterile, dd H_2O)	4 µL
Total	12 µL		18 µL		6 µL
Large Gel – undigested samples		**Large Gel – digested samples**		**Large Gel – Ladder**	
6X Loading Dye (NEB)	2 µL	6X Loading Dye	4 µL	6X Loading Dye	1 µL
PCR product	10 µL	PCR product	20 µL	Ladder*	1 µL
-	-	-	-	Water (sterile, dd H_2O)	4 µL
	12 µL		24 µL		6 µL

*Use either 100 bp ladder or 1 kb ladder (NEB), depending on size of DNA fragment

For each sample, mix 6X Blue Loading Dye (NEB), PCR product, and water (optional) together in a PCR eppendorf tube. PCR product amounts can be altered from the above values as long as 6X loading dye is diluted to a final concentration of 1X.

Load samples and dye into agarose gel wells (covered with 1X TAE running buffer) closest to the negative (black) anode. Attach electrodes and run until loading dye has moved about halfway down the agarose gel. Small gels (30 mL) use 70 Volts for ~ 30 minutes. Large gels (150 mL) use 80-100 Volts for 45-60 minutes.

Sequence of NCU05950 and primers for creation of "AD" CAPS marker for

Neurospora **transformation**

CCGGATGACTTCATCTTCCCTGTTGAACTCGTGGTCCGTTCCTGATGATTCAA
TCCTTGTAGTGTACATATACCTAGGTACATAGGTAGTTGAAGGTGTTTTTGGT
TGGGTGATCAACCACTGATCGATGTGAGTGACAGACTCGTGCGACTGACAGA
TCACTGTACATAGCGCACATTAGCGACCAAACAAGGTTAAAATGGCGTATAA
GTGCGCATTGACCAACTGTTTCTACCACCCACCAGGACAGCAGCGCCTTGGT
AGGCTGATGAGGCTAGAGGCTAGAGGTAGTCTGGATAGCCGCACGTGCACTC
GCGCCTGCTGTTCAGCCCCAGGGCCACACAGCACACACAGGGTTCGCTAGAG
TTCGTTGGGCTCTGGCGCCTGTACACTAGCAAAAGTTTTGCCGGAGGCGGCTG
AATAAGGCACGAGCAAGGATGAACCAACCAGATGACCGCTCCAAATCTTGC
GTCGGTGGATTTTTAGCCGCACATGGCAGGCGCATTGAA
CCGTGACACATTTGTTGCTGCAATCACCAATTCAATTCAATACGCGACCGAGA
AGACCTTGTGCTGGGCTCCAGTTGCGGGAAGGAACGCCTGGAAATGAGTCGG
GGCGCGTTGAAATTTGGAAACAGCGACGACGACGATCGATATCGATAAGGAC
AACTTTCCCTAGGTTCCTTGGGTTCCCTTATCCCGTCATTCATCCCTACCTAGG
TCCTGCCTCACCTCGCGCAATCATCGCCCGATTCCAAGCCGACGGCCGACCA
CATTTCGGGACACTGCAGCAAGTCCATCGCGACACATTCCTTCCTTTGCCTGA
TGAACCGACCTCGCTAGCAGTCCCCTCCCCCGCGGGCACCCGACAGAAGCCG
AAGCAACTCGACTAAACCAGCACCACAAGCCATTTTCACGACGGGACCCAAC
TTTTTTTTTTTTTTTTTTTGGTTTTTTTTTTGTCGGTCTGATCTCATTTCGTCAT
CGATCGAGTTTCATCTCTTC<u>GCGACGGTCTTTTCTCCCAACTTTACTTCGA</u>
<u>CGACGTCTGGCTTCAAGACGAGACTTTTTCTTGTCGCTTCGCGC</u>GAATTC
<u>CAATTGACAAACGTCATCCGACGACTTGATACCGACCGACCGACCGACC</u>
<u>ACCATCCGACTGGCGACACGGCACATAAAGAAGGGAGGACAAGATAACA</u>
<u>AGATGGGCAACTTTTGCTCAACCTGCTTCGGCGGTAGGAGGAGCGATGA</u>
<u>CTACGATGAGGTAGGTTTCGGCATAGCGGCCACAGTCCGATGACATGGC</u>
<u>CATCAAAAGAGGCATTCGACGGAACAAGAGAACTGACGTGGACTGTTGC</u>
<u>GTGACACAGGAGGACGAGGCCCAGCATCTCTTCGACGAGAACAACATGC</u>
<u>ACTACGGGAGCTTTGATCAGCAACACATGATGAACCAGGAAGATCCCCA</u>
<u>AGAGACAGAAAGGGAAATTGCGGCTCTGCAGGGCGTGGTGGAACGCAC</u>
<u>ATCAAAGTATGCCCTCCCACCTGAAATGTCTCCCATCCAAGATCTAGTCC</u>
<u>GAGACCCAAGTCCACGGAGCCGGTAGAGCGAATAACTGA</u>
GGTCGACATCTATGATATGGTCCCGCATGATAAACCCA
TGCAGGACGCTCCTGCTCCCTACGGCTTTGCCAACCAGCGCTACAATGC
CCTGCTTTCCAAGCTCTCAACCCACGATGACATGGCCGCCGTTGCACGG
GTTGACTGGGGCACCCCTGAGGACGACAGCATGGAGATGCTGCGCAAA
GCTTCCTTGCCAACCATCCCCATCAAGGCTGAAGGAGGCGAGGCCCTCG

<u>**TCGGTAACTTTACCGATGCCGCTGCCGCCATGCGCTGAAACCATACCAC**</u>
<u>**GACACCAAAACCATGACTTGCTGTCT**</u>ATACCCTATCCACCTGATGCCGACA
GCAACATGACAGAACATCCACAGTATCCTCCGACCCAGAATATACCACACCA
TACGTTCATCAAACCAGAACCATCTGACACAACAATAACTCCGGGACTCCTT
GGCCATGCCGATACGAGGTGGCATGCCCAAGTTCGCTTGGCCGGTTTCCCCC
ATCATATTTTCCTTTTGTAATTTCTCGTCTTTCCTGATGCTGTTCCGGAAACAG
CGGGCGTTCAGC▉GATTC▉GATAGGTCTGCGGCCAGAGACAACGTGGCATGGC
AGGATGTTATGTTGATGAGTTGTCGATACCCGTCGAGGTGGGATACAGCATC
CATTCGTCTCATACATCACCGCTTCGTATGCCCAAGTTGTTGGATAAGGCCAA
GGATAGGCTTAAAAACGGCGTGTCTGGGGGTATGTATGCGTTGTACAGCAAC
AATCCAATTTAATGCTTTCCTTTGTTCAATGACTGGATCAGTGCTGTTTGGAC
CAACCCATGGTGGTGTAGTCCTCCGGCCCCCAACAAACAAAATGTTGACAAG
GCGCGCGCCCACTAAATGTCAGCCACGTTCATCAAGTTCCGTTTTCTTGCCCA
TTGTCAAAGATATAAA▉▉▉▉▉▉▉▉▉▉▉▉▉▉▉▉▉TCCCTTTGCACAAA
ACTGACCCTTGTTTAATGCTTGTATAGAAACACCGCGTTTCCATCGGTGGTGG
ACATGATCCGAGATGCGACCACAGCCATTT
(http://www.broadinstitute.org/annotation/genome/neurospora/Regions.html)

<u>Bold, underlined</u> area = location of NCU05950 (putative *UV90* gene): 3,347,867-3,348,756

Existing EcoRI restriction enzyme site: ▉GAATTC▉

Extra adenine (A) will be inserted at ▉GATTC▉ into the primer sequence to create a second EcoRI restriction enzyme size

1) Two pieces: "AB" and "CD" created using overlapping primers with an extra adenine

F4 ->   **"AB"**

_____

                                  <- Rev2B-NCU05950

                                  For2C-NCU05950 ->

_____

                                          "CD"   **<-R4**

2) Final "AD" piece created with the extra adenine using "AB" and "CD" as templates

F4 -> ——————————————————————————————— **<-R4**

GAATTC

Overlapping primers with extra adenine (A):

Forward (For2C-NCU5950):
TCAGCGAATTCGATAGGTCTGCGGCCAG
27nt; GC = 59.26%; Tm = 79.48

Reverse (Rev2B-NCU5950):
CTGGCCGCAGACCTATCGAATTCGCTGA
27nt; GC = 59.26%; Tm = 79.48

Wild type *csp-1; chol-1 bd; frq*[10] (#80):   1081 bp, 1550 bp (with EcoRI digestion)
With mutagenic primers: 1081bp, 1062bp, 488bp (with EcoRI digestion)

Additional overlapping primers designed which were unsuccessful and not used in the transformation:

Forward (ForC-NCU5950):
GCGTTCAGCGAATTCGATAGGT
21nt; GC = 52.38%; Tm = 67.6

Reverse (RevB-NCU5950):
ACCTATCGAATTCGCTGAACGC
21nt; GC = 52.38%; Tm = 67.6

Forward (For3C-NCU5950)
CTTTCCTGATGCTGAATTCCGGA
21nt; GC = 52.38%; Tm = 68.76

Reverse (Rev3B-NCU5950):
TCCGGAATTCAGCATCAGGAAAG
21nt; GC = 52.38%; Tm = 68.76

Appendix V

Extra primers to test for presence of "AD" CAPS marker after transformation:

F3: █████████████████████████
21 nt; GC = 52.38%; Tm = 68.38

AD-Rp: █████████████████████████
21 nt; GC = 52.38%; Tm = 67.91

Entire piece: 968bp; After EcoRI digestion: 577, 391 bp

Appendix VI

Neurospora **transformation:**

Minimal medium for transformation:

2 mL 50X/Vogel's stock

1.5 mL choline (2 mg/mL)

1.5 g sucrose

1.5 g agar

100 mL dd H_2O

Green or blue food colouring, optional

Mix all ingredients together and sterilize. Use 100 mL per flask. Swirl flask after

sterilizing to encourage growth on the sides of the flask.

Sorbitol (1M):

182.17 g sorbitol

Dissolve sorbitol in ~700 mL of dd H_2O. Add water to make 1 L and sterilize.

Bottom agar:

91 g sorbitol

10 mL 50X/Vogel's stock

7.5 mL choline (2 mg/mL)

14 g agar

Appendix VI

50 mL FIGS

2 mL Hygromycin B (50 mg/mL), final concentration 0.2 mg/mL (Invitrogen)

Dissolve sorbitol, 50X and choline in ~350 mL dd H_2O and top up to 450 mL. Add agar and autoclave. Add FIGS and hygromycin B. Use 20 mL per small (8.5 cm) Petri plate.

Top agar:

50 mL dd H_2O

2 mL 50X/Vogel's stock

1.5 mL choline (2 mg/mL)

1.8 g sorbitol

0.5 g agar

10 mL FIGS

Mix water, 50X, choline and sorbitol. Top up to 90 mL. Add agar and autoclave. Add FIGS. Use 5 mL per small (8.5 cm) Petri plate.

FIGS:

10 g sorbose

0.25 g fructose

0.25 g glucose

50 mL water

Appendix VI

Mix all ingredients together, autoclave and cool.

Recovery medium:

0.2 mL 50X/Vogel's stock

1.82 g sorbitol

9 mL dd H_2O

150 μL choline (2 mg/mL)

1 mL FIGS

Mix together 50X, sorbitol, water and choline. Autoclave, cool and add FIGS.
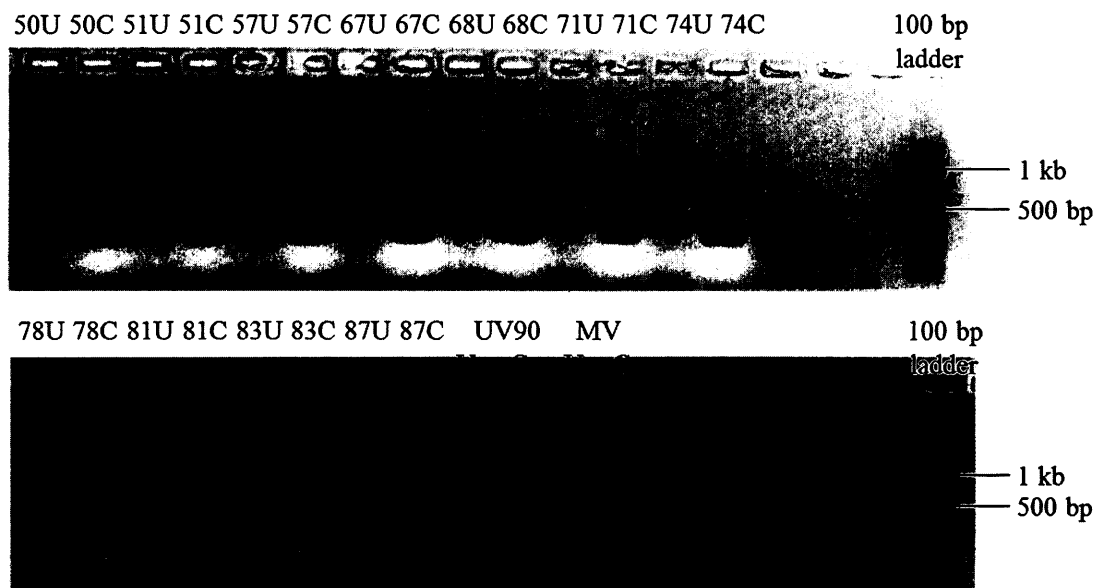
Figure A1. PCR results from *csp-1; bd; UV90* progeny #50-87 using F9-R9 primers.

U = "uncut", undigested DNA; C = "cut", DNA digested with Taqα1 restriction enzyme.

"Cut" OR DNA exhibits two overlapping bands, each ~250 bp in size. "UV90" (*csp-1;*

bd; UV90) and "MV" (Mauriceville, *csp+; bd+; UV+*) served as controls.

#83 and #87 resembled MV, and were determined to be recombinants.

Appendix VII

A

B
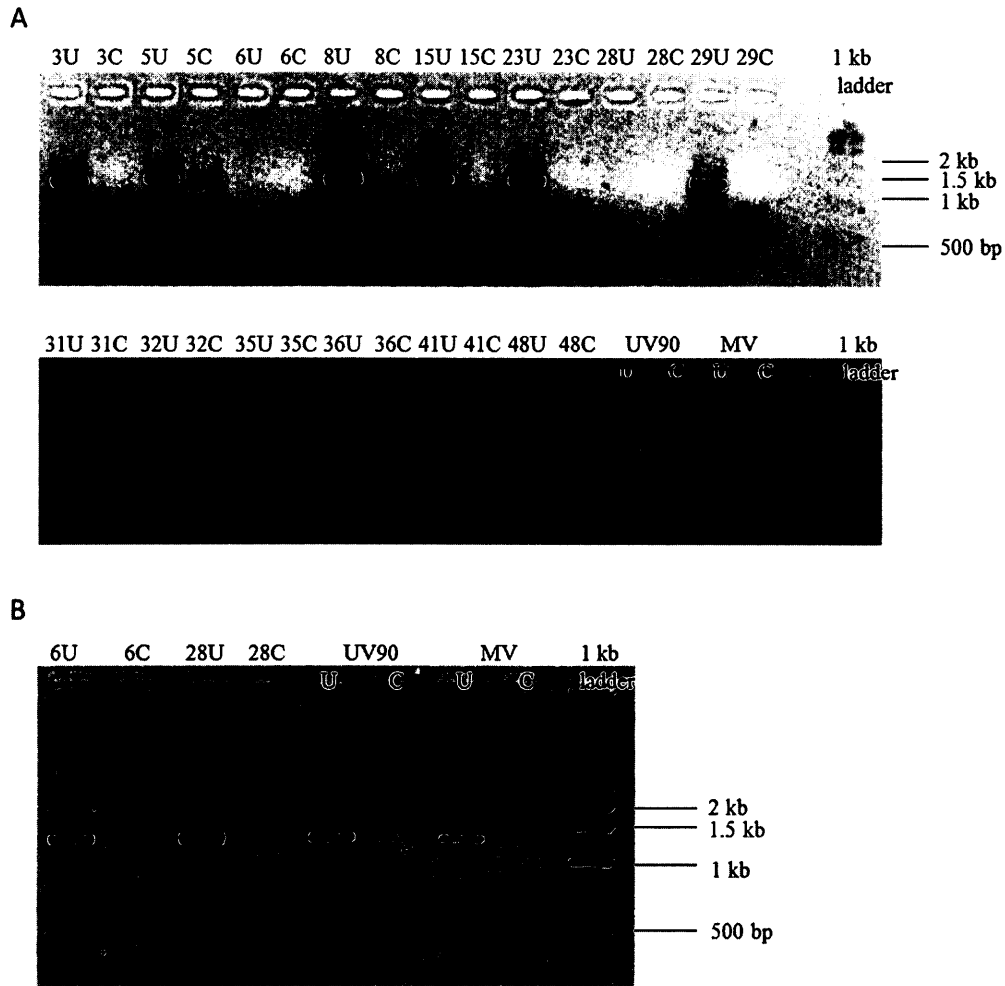
Figure A2. PCR results from *csp-1; bd; UV90* progeny #3-48 using F6-R6 primers.

U = "uncut", undigested DNA; C = "cut", DNA digested with EcoRI restriction enzyme.

"UV90" (*csp-1; bd; UV90*) and "MV" (Mauriceville, *csp+; bd+; UV+*) served as

controls. Most progeny resembled *UV90* control after digestion with the exception of #5,

#6 and #31 which resembled MV, and thus were determined to be recombinants. #6 and

#28 were repeated in (B).

LALIGN Outputs for *Neurospora crassa* NCU05950 sequencing
(http://embnet.vital-it.ch/software/ LALIGN_form.html)

lalign output for Oak Ridge wt vs. UV90 F6 primer

LALIGN finds the best local alignments between two sequences version 2.1u09
December 2006 Please cite: X. Huang and W. Miller (1991) Adv. Appl. Math. 12:373-381 resetting to DNA matrix alignments < E(0.05):score: 65 (50 max)

```
 Comparison of:
(A) ./wwwtmp/.3903.1.seq Oak Ridge wt 506 bp                              -
506 nt
(B) ./wwwtmp/.3903.2.seq UV90 F6 primer 206 bp                           -
206 nt
 using matrix file: DNA (5/-4), gap-open/ext: -14/-4 E(limit)    0.05

100.0% identity in 204 nt overlap (54-257:3-206); score: 1020 E(10000):
1.3e-77


            60        70        80        90       100       110
Oak    AGGGCCACGGTGTATTATCCGAGGCATACGGTCGATCAGTCGGTCGATCATAATGGTGTG
       ::::::::::::::::::::::::::::::::::::::::::::::::::::::::::::::
UV90   AGGGCCACGGTGTATTATCCGAGGCATACGGTCGATCAGTCGGTCGATCATAATGGTGTG
            10        20        30        40        50        60

           120       130       140       150       160       170
Oak    CGCCCGGGGACAGCGCTGTAGTGAGTTGGTGCACGATTTTGAGAAGGAACAGGAACACCT
       ::::::::::::::::::::::::::::::::::::::::::::::::::::::::::::::
UV90   CGCCCGGGGACAGCGCTGTAGTGAGTTGGTGCACGATTTTGAGAAGGAACAGGAACACCT
            70        80        90       100       110       120

           180       190       200       210       220       230
Oak    CTCGTATAACAAACAAGAGGATTGGGGACTAAGGATTTACGGTCGACGAGCTACACAGAG
       ::::::::::::::::::::::::::::::::::::::::::::::::::::::::::::::
UV90   CTCGTATAACAAACAAGAGGATTGGGGACTAAGGATTTACGGTCGACGAGCTACACAGAG
           130       140       150       160       170       180

           240       250
Oak    GCTCTTTTTTCTTTATACGTTTTC
       ::::::::::::::::::::::::
UV90   GCTCTTTTTTCTTTATACGTTTTC
           190       200
```

lalign output for Oak Ridge wt vs. UV90 F5 primer

LALIGN finds the best local alignments between two sequences version 2.1u09
December 2006 Please cite: X. Huang and W. Miller (1991) Adv. Appl. Math. 12:373-
381 resetting to DNA matrix alignments < E(0.05):score: 76 (50 max)
```
 Comparison of:
(A) ./wwwtmp/.31701.1.seq Oak Ridge wt 966 b                           -
966 nt
(B) ./wwwtmp/.31701.2.seq UV90 F5 primer 709 bp                        -
709 nt
 using matrix file: DNA (5/-4), gap-open/ext: -14/-4 E(limit)    0.05


 99.6% identity in 710 nt overlap (33-742:1-709); score: 3509 E(10000):
2.7e-284


              40        50        60        70        80        90
Oak     GTTCCCCGCAAAAAAGATGCCAATCTCGGCTGTGACACTCGTCGACTTGAACGAGTTCCA
        ::::  ::::::::::  :::::::::::::::::::::::::::::::::::::::::::::
UV90    GTTCGCCGCAAAAA-GATGCCAATCTCGGCTGTGACACTCGTCGACTTGAACGAGTTCCA
              10        20        30        40        50


             100       110       120       130       140       150
Oak     GCCCTGATGTTGATGGTAAAGCTCCATTTTCGCAGTCTCCGATAGCAGCACGTATCATTT
        ::::::::::::::::::::::::::::::::::::::::::::::::::::::::::::::::
UV90    GCCCTGATGTTGATGGTAAAGCTCCATTTTCGCAGTCTCCGATAGCAGCACGTATCATTT
           60        70        80        90       100       110


             160       170       180       190       200       210
Oak     ATCGCAACATGTTTCCATGTTTTCGCCATGTGCAGACGTTGCAACGTGAAAATATAACCC
        ::::::::::::::::::::::::::::::::::::::::::::::::::::::::::::::::
UV90    ATCGCAACATGTTTCCATGTTTTCGCCATGTGCAGACGTTGCAACGTGAAAATATAACCC
        120       130       140       150       160       170


             220       230       240       250       260       270
Oak     GAGTCGACGGGAACCCGACGAGATGGAACTCCATGATGGGCATCGGCATGGACCCAAGTC
        ::::::::::::::::::::::::::::::::::::::::::::::::::::::::::::::::
UV90    GAGTCGACGGGAACCCGACGAGATGGAACTCCATGATGGGCATCGGCATGGACCCAAGTC
        180       190       200       210       220       230


             280       290       300       310       320       330
Oak     ACAGTGGGACTTCCAGGGCAATAGTGTACCGCAAAGTCGGGTCGCTTCCACTATCAGGGC
        ::::::::::::::::::::::::::::::::::::::::::::::::::::::::::::::::
UV90    ACAGTGGGACTTCCAGGGCAATAGTGTACCGCAAAGTCGGGTCGCTTCCACTATCAGGGC
        240       250       260       270       280       290
```

Appendix VIII

```
           340        350        360        370        380        390
Oak     AGTAAGTCCGAAGTCCGGTGAGCTCCGCACCGGGGCTTCCTTGTCTAGAACACTCATCAA
        ::::::::::::::::::::::::::::::::::::::::::::::::::::::::::::::
UV90    AGTAAGTCCGAAGTCCGGTGAGCTCCGCACCGGGGCTTCCTTGTCTAGAACACTCATCAA
           300        310        320        330        340        350


              400        410        420        430        440        450
Oak     TCAGCAAGTTGAGACGTTTCAGCAGAAATGATGACGGGACATTTCCGGATGACTTCATCT
        ::::::::::::::::::::::::::::::::::::::::::::::::::::::::::::::
UV90    TCAGCAAGTTGAGACGTTTCAGCAGAAATGATGACGGGACATTTCCGGATGACTTCATCT
           360        370        380        390        400        410


           460        470        480        490        500        510
Oak     TCCCTGTTGAACTCGTGGTCCGTTCCTGATGATTCAATCCTTGTAGTGTACATATACCTA
        ::::::::::::::::::::::::::::::::::::::::::::::::::::::::::::::
UV90    TCCCTGTTGAACTCGTGGTCCGTTCCTGATGATTCAATCCTTGTAGTGTACATATACCTA
           420        430        440        450        460        470


           520        530        540        550        560        570
Oak     GGTACATAGGTAGTTGAAGGTGTTTTTGGTTGGGTGATCAACCACTGATCGATGTGAGTG
        ::::::::::::::::::::::::::::::::::::::::::::::::::::::::::::::
UV90    GGTACATAGGTAGTTGAAGGTGTTTTTGGTTGGGTGATCAACCACTGATCGATGTGAGTG
           480        490        500        510        520        530


           580        590        600        610        620        630
Oak     ACAGACTCGTGCGACTGACAGATCACTGTACATAGCGCACATTAGCGACCAAACAAGGTT
        ::::::::::::::::::::::::::::::::::::::::::::::::::::: :::::::::
UV90    ACAGACTCGTGCGACTGACAGATCACTGTACATAGCGCACATTAGCGACCAAGCAAGGTT
           540        550        560        570        580        590


           640        650        660        670        680        690
Oak     AAAATGGCGTATAAGTGCGCATTGACCAACTGTTTCTACCACCCACCAGGACAGCAGCGC
        ::::::::::::::::::::::::::::::::::::::::::::::::::::::::::::::
UV90    AAAATGGCGTATAAGTGCGCATTGACCAACTGTTTCTACCACCCACCAGGACAGCAGCGC
           600        610        620        630        640        650


           700        710        720        730        740
Oak     CTTGGTAGGCTGATGAGGCTAGAGGCTAGAGGTAGTCTGGATAGCCGCAC
        ::::::::::::::::::::::::::::::::::::::::::::::::::::
UV90    CTTGGTAGGCTGATGAGGCTAGAGGCTAGAGGTAGTCTGGATAGCCGCAC
           660        670        680        690        700
```

Appendix VIII

lalign output for Oak Ridge wt vs. 213 F6 primer

LALIGN finds the best local alignments between two sequences version 2.1u09
December 2006 Please cite: X. Huang and W. Miller (1991) Adv. Appl. Math. 12:373-
381 resetting to DNA matrix alignments < E(0.05):score: 76 (50 max)
```
 Comparison of:
(A) ./wwwtmp/.25499.1.seq Oak Ridge wt 964 bp                    -
964 nt
(B) ./wwwtmp/.25499.2.seq 213 F6 primer 703 b                    -
703 nt
 using matrix file: DNA (5/-4), gap-open/ext: -14/-4 E(limit)    0.05

  99.7% identity in 704 nt overlap (46-749:1-703); score: 3488
E(10000): 1.5e-282


          50        60        70        80        90       100
Oak     ATCCGTCAAGGGCCACGGTGTATTATCCGAGGCATACGGTCGATCAGTCGGTCGATCATA
        :::::::: ::::::::::::::::::::::::::::::::::::::::::::::::::::::
213     ATCCGTCA-GGGCCACGGTGTATTATCCGAGGCATACGGTCGATCAGTCGGTCGATCATA
                 10        20        30        40        50


         110       120       130       140       150       160
Oak     ATGGTGTGCGCCCGGGGACAGCGCTGTAGTGAGTTGGTGCACGATTTTGAGAAGGAACAG
        ::::::::::::::::::::::::::::::::::::::::::::::::::::::::::::::::
213     ATGGTGTGCGCCCGGGGACAGCGCTGTAGTGAGTTGGTGCACGATTTTGAGAAGGAACAG
           60        70        80        90       100       110


         170       180       190       200       210       220
Oak     GAACACCTCTCGTATAACAAACAAGAGGATTGGGGACTAAGGATTTACGGTCGACGAGCT
        ::::::::::::::::::::::::::::::::::::::::::::::::::::::::::::::::
213     GAACACCTCTCGTATAACAAACAAGAGGATTGGGGACTAAGGATTTACGGTCGACGAGCT
          120       130       140       150       160       170


         230       240       250       260       270       280
Oak     ACACAGAGGCTCTTTTTTTCTTTATACGTTTTCAAGCTTCATGTATCAAAGATTTGCATGT
        ::::::::::::::::::::::::::::::::::::::::::::::::::::::::::::::::
213     ACACAGAGGCTCTTTTTTTCTTTATACGTTTTCAAGCTTCATGTATCAAAGATTTGCATGT
          180       190       200       210       220       230


         290       300       310       320       330       340
Oak     CTTATGGTGTTGGCGTGGGTGTTGAAAGGAAGGAATGGGATGAGATTGGAGCATTTATGT
        ::::::::::::::::::::::::::::::::::::::::::::::::::::::::::::::::
213     CTTATGGTGTTGGCGTGGGTGTTGAAAGGAAGGAATGGGATGAGATTGGAGCATTTATGT
          240       250       260       270       280       290
```

Appendix VIII

```
     350           360        370        380        390        400
Oak      AAAGTTAGGATATACCCCTTAATGTTTTATCTCGTCATTCTTCTCAGTCGTAAATGTCAAA
         ::::::::::::::::::::::::::::::::::::::::::::::::::::::::::::::::
213      AAAGTTAGGATATACCCCTTAATGTTTTATCTCGTCATTCTTCTCAGTCGTAAATGTCAAA
         300        310        320        330        340        350


         410        420        430        440        450        460
Oak      AATCGAAGTGGCCTCATCACTCTGATATGCTTGCGACAAGAGCCGAGTGCAGTGTGTAGT
         :::::::::::::::::::::::::::::::::::::::::::::::::::::::::::::::
213      AATCGAAGTGGCCTCATCACTCTGATATGCTTGCGACAAGAGCCGAGTGCAGTGTGTAGT
         360        370        380        390        400        410


         470        480        490        500        510        520
Oak      AGAGGGCCGTGAAGCCCGAGGAACCTCCGAAGAAAGGAAGGAAAGCCCAGACCGTCACCT
         :::::::::::::::::::::::::::::::::::::::::::::::::::::::::::::::
213      AGAGGGCCGTGAAGCCCGAGGAACCTCCGAAGAAAGGAAGGAAAGCCCAGACCGTCACCT
         420        430        440        450        460        470


         530        540        550        560        570        580
Oak      GTGGAGTTTAAAGGTTCCCCGCAAAAAAGATGCCAATCTCGGCTGTGACACTCGTCGACT
         :::::::::::::::::::::::::::::::::::::::::::::::::::::::::::::::
213      GTGGAGTTTAAAGGTTCCCCGCAAAAAAGATGCCAATCTCGGCTGTGACACTCGTCGACT
         480        490        500        510        520        530


         590        600        610        620        630        640
Oak      TGAACGAGTTCCAGCCCTGATGTTGATGGTAAAGCTCCATTTTCGCAGTCTCCGATAGCA
         :::::::::::::::::::::::::::::::::::::::::::::::::::::::::::::::
213      TGAACGAGTTCCAGCCCTGATGTTGATGGTAAAGCTCCATTTTCGCAGTCTCCGATAGCA
         540        550        560        570        580        590


         650        660        670        680        690        700
Oak      GCACGTATCATTTATCGCAACATGTTTCCATGTTTTCGCCATGTGCAGACGTTGCAACGT
         :::::::::::::::::::::::::::::::::::::::::::::::::::::::::: :::
213      GCACGTATCATTTATCGCAACATGTTTCCATGTTTTCGCCATGTGCAGACGTTGCAGCGT
         600        610        620        630        640        650


         710        720        730        740
Oak      GAAAATATAACCCGAGTCGACGGGAACCCGACGAGATGGAACTC
         ::::::::::::::::::::::::::::::::::::::::::::::
213      GAAAATATAACCCGAGTCGACGGGAACCCGACGAGATGGAACTC
         660        670        680        690        700
```

----

lalign output for Oak Ridge wt vs. 213 F5 primer

LALIGN finds the best local alignments between two sequences version 2.1u09
December 2006 Please cite: X. Huang and W. Miller (1991) Adv. Appl. Math. 12:373-
381 resetting to DNA matrix alignments < E(0.05):score: 75 (50 max)

```
 Comparison of:
(A) ./wwwtmp/.9973.1.seq Oak Ridge wt 966 bp                              -
966 nt
(B) ./wwwtmp/.9973.2.seq 213 F5 primer 626 bp                            -
626 nt
 using matrix file: DNA (5/-4), gap-open/ext: -14/-4 E(limit)    0.05

  99.8% identity in 627 nt overlap (19-645:1-626); score: 3112
E(10000): 3e-251


          20        30        40        50        60        70
Oak     TGTGGAGTTTAAAGGTTCCCCGCAAAAAAGATGCCAATCTCGGCTGTGACACTCGTCGAC
        ::::::::::::  :::::::::::::::::::::::::::::::::::::::::::::::::
213     TGTGGAGTTTAA-GGTTCCCCGCAAAAAAGATGCCAATCTCGGCTGTGACACTCGTCGAC
               10        20        30        40        50


          80        90       100       110       120       130
Oak     TTGAACGAGTTCCAGCCCTGATGTTGATGGTAAAGCTCCATTTTCGCAGTCTCCGATAGC
        ::::::::::::::::::::::::::::::::::::::::::::::::::::::::::::::
213     TTGAACGAGTTCCAGCCCTGATGTTGATGGTAAAGCTCCATTTTCGCAGTCTCCGATAGC
         60        70        80        90       100       110


         140       150       160       170       180       190
Oak     AGCACGTATCATTTATCGCAACATGTTTCCATGTTTTCGCCATGTGCAGACGTTGCAACG
        ::::::::::::::::::::::::::::::::::::::::::::::::::::::::::::::
213     AGCACGTATCATTTATCGCAACATGTTTCCATGTTTTCGCCATGTGCAGACGTTGCAACG
        120       130       140       150       160       170


         200       210       220       230       240       250
Oak     TGAAAATATAACCCGAGTCGACGGGAACCCGACGAGATGGAACTCCATGATGGGCATCGG
        ::::::::::::::::::::::::::::::::::::::::::::::::::::::::::::::
213     TGAAAATATAACCCGAGTCGACGGGAACCCGACGAGATGGAACTCCATGATGGGCATCGG
        180       190       200       210       220       230


         260       270       280       290       300       310
Oak     CATGGACCCAAGTCACAGTGGGACTTCCAGGGCAATAGTGTACCGCAAAGTCGGGTCGCT
        ::::::::::::::::::::::::::::::::::::::::::::::::::::::::::::::
213     CATGGACCCAAGTCACAGTGGGACTTCCAGGGCAATAGTGTACCGCAAAGTCGGGTCGCT
        240       250       260       270       280       290
```

Appendix VIII

```
320         330        340        350        360        370
Oak    TCCACTATCAGGGCAGTAAGTCCGAAGTCCGGTGAGCTCCGCACCGGGGCTTCCTTGTCT
       :::::::::::::::::::::::::::::::::::::::::::::::::::::::::::::::
213    TCCACTATCAGGGCAGTAAGTCCGAAGTCCGGTGAGCTCCGCACCGGGGCTTCCTTGTCT
       300        310        320        330        340        350


       380        390        400        410        420        430
Oak    AGAACACTCATCAATCAGCAAGTTGAGACGTTTCAGCAGAAATGATGACGGGACATTTCC
       :::::::::::::::::::::::::::::::::::::::::::::::::::::::::::::::
213    AGAACACTCATCAATCAGCAAGTTGAGACGTTTCAGCAGAAATGATGACGGGACATTTCC
       360        370        380        390        400        410

       440        450        460        470        480        490
Oak    GGATGACTTCATCTTCCCTGTTGAACTCGTGGTCCGTTCCTGATGATTCAATCCTTGTAG
       :::::::::::::::::::::::::::::::::::::::::::::::::::::::::::::::
213    GGATGACTTCATCTTCCCTGTTGAACTCGTGGTCCGTTCCTGATGATTCAATCCTTGTAG
       420        430        440        450        460        470

       500        510        520        530        540        550
Oak    TGTACATATACCTAGGTACATAGGTAGTTGAAGGTGTTTTTGGTTGGGTGATCAACCACT
       :::::::::::::::::::::::::::::::::::::::::::::::::::::::::::::::
213    TGTACATATACCTAGGTACATAGGTAGTTGAAGGTGTTTTTGGTTGGGTGATCAACCACT
       480        490        500        510        520        530

       560        570        580        590        600        610
Oak    GATCGATGTGAGTGACAGACTCGTGCGACTGACAGATCACTGTACATAGCGCACATTAGC
       :::::::::::::::::::::::::::::::::::::::::::::::::::::::::::::::
213    GATCGATGTGAGTGACAGACTCGTGCGACTGACAGATCACTGTACATAGCGCACATTAGC
       540        550        560        570        580        590

       620        630        640
Oak    GACCAAACAAGGTTAAAATGGCGTATA
       :::::::::::::::::::::::::::::
213    GACCAAACAAGGTTAAAATGGCGTATA
       600        610        620
```

217

lalign output for Oak Ridge wt vs. 213 F1 primer

resetting to DNA matrix alignments < E(0.05):score: 70 (50 max)

```
 Comparison of:
(A) ./wwwtmp/.31701.1.seq Oak Ridge wt 609 bp                    -
609 nt
(B) ./wwwtmp/.31701.2.seq 213 F1 primer 398 bp                   -
398 nt
 using matrix file: DNA (5/-4), gap-open/ext: -14/-4 E(limit)   0.05
99.2% identity in 398 nt overlap (31-428:1-398); score: 1963 E(10000):
7.5e-156
                40        50        60        70        80        90


Oak     GAAGACCTTGTGCTGGGCTCCAGTTGCGGGAAGGAACGCCTGGAAATGAGTCGGGGCGCG
        :::::::::::::::::::::::::::::::::::::::::::::::::: ::::::::::::
213     GAAGACCTTGTGCTGGGCTCCAGTTGCGGGAAGGAACGCCTGGAAATGAGCCGGGGCGCG
                10        20        30        40        50        60


                100       110       120       130       140       150
Oak     TTGAAATTTGGAAACAGCGACGACGACGATCGATATCGATAAGGACAACTTTCCCTAGGT
        ::::::::::::::::::::::::::::::::::::::::::::::::::::::::::::::::
213     TTGAAATTTGGAAACAGCGACGACGACGATCGATATCGATAAGGACAACTTTCCCTAGGT
                70        80        90        100       110       120


                160       170       180       190       200       210
Oak     TCCTTGGGTTCCCTTATCCCGTCATTCATCCCTACCTAGGTCCTGCCTCACCTCGCGCAA
        ::::::::::::::::::::::::::::::::::::::::::::::::::::::::::::::::
213     TCCTTGGGTTCCCTTATCCCGTCATTCATCCCTACCTAGGTCCTGCCTCACCTCGCGCAA
                130       140       150       160       170       180


                220       230       240       250       260       270
Oak     TCATCGCCCGATTCCAAGCCGACGGCCGACCACATTTCGGGACACTGCAGCAAGTCCATC
        ::::::::::::::::::::::::::::::::::::::::::::::::::::::::::::::::
213     TCATCGCCCGATTCCAAGCCGACGGCCGACCACATTTCGGGACACTGCAGCAAGTCCATC
                190       200       210       220       230       240


                280       290       300       310       320       330
Oak     GCGACACATTCCTTCCTTTGCCTGATGAACCGACCTCGCTAGCAGTCCCCTCCCCCGCGG
        ::::::::::::::::::::::::::::::::::::::::::::::::::::::::::::::::
213     GCGACACATTCCTTCCTTTGCCTGATGAACCGACCTCGCTAGCAGTCCCCTCCCCCGCGG
                250       260       270       280       290       300


                340       350       360       370       380       390
Oak     GCACCCGACAGAAGCCGAAGCAACTCGACTAAACCAGCACCACAAGCCATTTTCACGACG
        ::::::::::::::::::::::::::::::::::::::::::::::::::::::::::::::::
213     GCACCCGACAGAAGCCGAAGCAACTCGACTAAACCAGCACCACAAGCCATTTTCACGACG
                310       320       330       340       350       360
```

```
400        410        420
Oak     GGACCCAACTTTTTTTTTTTTTTTTTTTTGGTTTTTTT
        :::::::::::::::::::::::::::::  :::::::
213     GGACCCAACTTTTTTTTTTTTTTTTTTTTTTTTTTTTT
                370        380        390
```

BLAST searches at Broad Institute *Neurospora crassa* database
(http://www.broadinstitute.org/annotation/genome/neurospora/Blast.html)

500 bp piece – #213 with R1 primer

Target	Score (Bits)	Expect	Alignment Length	Identities	Positives

▼ N. crassa OR74A (NC12): Supercontig 2: 2046700-2046934 -
Score = 451.752 (227), Expect=0.0
Identities=234/235 (99%), Positives=234/235 (99%)

```
Query  GGCAAACTTTCCTTTTTTCGACTCCCATGTTTCAAAATCCGCCACGAGGTCGGAGTCGTC
       ||||||||||||||||||||||||||||||||||||||||||||||||||||||||||||
Sbjct  GGCAAACTTTCCTTTTTTCGACTCCCATGTTTCAAAATCCGCCACGAGGTCGGAGTCGTC

Query  AAGAAGAGTGGTGTAGAAATCGCTTGTGGCAAGAATTTGCCCGCGCATTTGGACCCGATC
       ||||||||||||||||||||||||||||||||||||||||||||||||||||||||||||
Sbjct  AAGAAGAGTGGTGTAGAAATCGCTTGTGGCAAGAATTTGCCCGCGCATTTGGACCCGATC

Query  CCTTGTGCTCGCCACGGGTCCATCCGTAAGATTGGCGAGGCTGCGCCGTGAATGTCCCGT
       ||||||||||||||||||||||||||||||||||||||||||||||||||||||||||||
Sbjct  CCTTGTGCTCGCCACGGGTCCATCCGTAAGATTGGCGAGGCTGCGCCGTGAATGTCCCGT

Query  GTTGTTGGCGGCGAAAATCAGCGCAAGAACCTGCGCCGAGGC-TTGATCTGCCAG
       ||||||||||||||||||||||||||||||||||||||||||| |||||||||||
Sbjct  GTTGTTGGCGGCGAAAATCAGCGCAAGAACCTGCGCCGAGGCTTTGATCTGCCAG
```

219

Appendix VIII

500 bp piece – #213 with UV90BFor primer

Target	Score (Bits)	Expect	Alignment Length	Identities	Positives

▼ N. crassa OR74A (NC12): Supercontig 2: 2046531-2046681 +
Score = 295.723 (147), Expect=0.0
Identities=149/151 (98%), Positives=149/151 (98%)

```
Query  CCAGGCAATCCCGACGAACATCTAACACCAGGTGCTGCTGGATAACACGATGAGTCAAGA
       ||||||||||||||||||||||||||||||||||||||||||||||||||||||||||||
Sbjct  CCAGGCAATCCCGACGAACATCTAACACCAGGTGCTGCTGGATAACACGATGAGTCAAGA

Query  TGCTGTTGAAAAAGGCGTCTCTTGCCTTGTCCTCCATCTGCCGCTTCGCGTCATATTCAA
       ||||||||||||||||||||||||||||||||||||||||||||||||||||||||||||
Sbjct  TGCTGTTGAAAAAGGCGTCTCTTGCCTTGTCCTCCATCTGCCGCTTCGCGTCATATTCAA

Query  GGATTTGGATCTTGGCGCCTATGCTRASAAG
       |||||||||||||||||||||||||| | |||
Sbjct  GGATTTGGATCTTGGCGCCTATGCTGAGAAG
```

500 bp piece – *UV90* with R1 primer

Target	Score (Bits)	Expect	Alignment Length	Identities	Positives

▼ N. crassa OR74A (NC12): Supercontig 2: 2046766-2046899 -
Score = 239.874 (116), Expect=0.0
Identities=126/134 (94%), Positives=126/134 (94%)

```
Query  AGKGGTGTAGAAATKSCTTGTGGCAAGAATTTGCCCGCGCATTTGGACCCGATCCCTTGT
       || |||||||||||   |||||||||||||||||||||||||||||||||||||||||||
Sbjct  AGTGGTGTAGAAATCGCTTGTGGCAAGAATTTGCCCGCGCATTTGGACCCGATCCCTTGT

Query  GCTCGCCACGGGTCCATCCGTAAGATTGGCGAGSCTGCGCCGYGAATGTCCCGTSYTGTT
       ||||||||||||||||||||||||||||||||| ||||||||| ||||||||||   ||||
Sbjct  GCTCGCCACGGGTCCATCCGTAAGATTGGCGAGGCTGCGCCGTGAATGTCCCGTGTTGTT

Query  GGCGGCGAAMATCA
       |||||||||| ||||
Sbjct  GGCGGCGAAAATCA
```

220

Appendix VIII

500 bp piece – *UV90* with UV90BFor primer

Target	Score (Bits)	Expect	Alignment Length	Identities	Positives

▼ N. crassa OR74A (NC12): Supercontig 2: 2046535-2046750 +
Score = 412.154 (202), Expect=0.0
Identities=209/216 (96%), Positives=209/216 (96%)

```
Query  GCAATCCCGACGARCATCTAACACCAGGTGCTGCTGGATAACACGATRAGTCAAGATGCT
       |||||||||||||| |||||||||||||||||||||||||||||||||| ||||||||||||
Sbjct  GCAATCCCGACGAACATCTAACACCAGGTGCTGCTGGATAACACGATGAGTCAAGATGCT

Query  GTTGAAAAAGGCGTCTCTTGCCTTGTCCTCCATCTGCCGCTTCGCGTCATATTCAAGGAT
       |||||||||||||||||||||||||||||||||||||||||||||||||||||||||||||||
Sbjct  GTTGAAAAAGGCGTCTCTTGCCTTGTCCTCCATCTGCCGCTTCGCGTCATATTCAAGGAT

Query  TTGGATCTTGGCGCCTATGCTGASAAGGAAGGSAAACTGACAAAAGGCAAACTTTCCTTT
       |||||||||||||||||||||||| |||||||| |||||||||||||||||||||||||||
Sbjct  TTGGATCTTGGCGCCTATGCTGAGAAGGAAGGGAAACTGACAAAAGGCAAACTTTCCTTT

Query  TTTCGACTCCCMTGTTWCAAAATCCRCCACGAGGTC
       ||||||||||| |||| ||||||||| ||||||||||
Sbjct  TTTCGACTCCCATGTTTCAAAATCCGCCACGAGGTC
```

Appendix VIII

1 kb piece - #213 with R2 primer

▼ N. crassa OR74A (NC12): Supercontig 6: 2654898-2655137 +
Score = 463.295 (232), Expect=0.0
Identities=237/240 (98%), Positives=237/240 (98%)

```
Query  CAGGTATTCGACCACGTACCTGGTATCCGCAGGGGCATGGTCTAAAGTTACGATCAGAGA
       ||||||||||||||||||||||||||||||||||||||||||||||||||||||||||||
Sbjct  CAGGTATTCGACCACGTACCTGGTATCCGCAGGGGCATGGTCTAAAGTTACGATCAGAGA

Query  GATCAAACTCCTCGATACAGAGGGGGCTATAGTATACTAGTTAGTCTGATGTGTTCTTGT
       ||||||||||||||||||||||||||||||||||||||||||||||||||||||||||||
Sbjct  GATCAAACTCCTCGATACAGAGGGGGCTATAGTATACTAGTTAGTCTGATGTGTTCTTGT

Query  GGACGGCCGAGGGCGTTGTGACAGGGGGTCGGCTCGAGGCTGAGGAAGGCGGAGAGAGCA
       ||||||||||||||||||||||||||||||||||||||||||||||||||||||||||||
Sbjct  GGACGGCCGAGGGCGTTGTGACAGGGGGTCGGCTCGAGGCTGAGGAAGGCGGAGAGAGCA

Query  GGCATGACRAGGCCATGGAGGGGCAGGGGCAGTCGTCATGGATTCGGCTGGAGRWAGGTC
       ||||||||  |||||||||||||||||||||||||||||||||||||||||||||  |||||
Sbjct  GGCATGACGAGGCCATGGAGGGGCAGGGGCAGTCGTCATGGATTCGGCTGGAGAGAGGTC
```

▼ N. crassa OR74A (NC12): Supercontig 6: 2654808-2654871 +
Score = 128.16 (64), Expect=3.5233E-29
Identities=64/64 (100%), Positives=64/64 (100%)

```
Query  AACAGAACTGGCATATCTGGGGTGGGGCGGCGGCGTTAGCGCTCAGGTTGAGCCAAAAGA
       ||||||||||||||||||||||||||||||||||||||||||||||||||||||||||||
Sbjct  AACAGAACTGGCATATCTGGGGTGGGGCGGCGGCGTTAGCGCTCAGGTTGAGCCAAAAGA

Query  AAAA
       ||||
Sbjct  AAAA
```

222

Appendix VIII

1 kb piece - #213 with UV90AFor primer

Target	Score (Bits)	Expect	Alignment Length	Identities	Positives

▾ N. crassa OR74A (NC12): Supercontig 6: 2655229-2655646 -
Score = 783.319 (393), Expect=0.0
Identities=409/418 (97%), Positives=409/418 (97%)

```
Query  GCGTTGGGAGTGACGGCAAGCTGGAGGCTGCTCCCAGGTAAACGGGGACGACTGTGAGGT
       ||||||||||||||||||||||||||||||||||||||||||||||||||||||||||||
Sbjct  GCGTTGGGAGTGACGGCAAGCTGGAGGCTGCTCCCAGGTAAACGGGGACGACTGTGAGGT


Query  GTCGGGTCGAATACGGATKGATGGAATCCTTTTCCMCTTGTCGGTAAGGTAGGTATTAAA
       |||||||||||||||||| |||||||||||||||| ||||||||||||||||||||||||
Sbjct  GTCGGGTCGAATACGGATGGATGGAATCCTTTTCCACTTGTCGGTAAGGTAGGTATTAAA


Query  AGGGCCGTAAACTAGCGGCGCGAAAATTGGTCTATGGTAGAAAGAAGCAAAGGAGGACCT
       ||||||||||||||||||||||||||||||||||||||||||||||||||||||||||||
Sbjct  AGGGCCGTAAACTAGCGGCGCGAAAATTGGTCTATGGTAGAAAGAAGCAAAGGAGGACCT


Query  GATAATAACGCCCGTGGTAATGTAAGATACAGAGAATAGAGGGTCGGTGCCTCTTCNNNN
       |||||||||||||||||||||||||||||||||||||||||||||||||||||||||
Sbjct  GATAATAACGCCCGTGGTAATGTAAGATACAGAGAATAGAGGGTCGGTGCCTCTTCTTTT


Query  NNNGAGGGGTTGTGCTCGTGTCAACAAATGGGGGATTATTAGAGAGAACAAAGTTGGCCG
          ||||||||||||||||||||||||||||||||||||||||||||||||||||||||||
Sbjct  TTTGAGGGGTTGTGCTCGTGTCAACAAATGGGGGATTATTAGAGAGAACAAAGTTGGCCG


Query  GATGTGGGTGGAAAGGAACTGCGTGGACGGGATGCGGGTGCAGGCAAGTTTGAGCACAGG
       ||||||||||||||||||||||||||||||||||||||||||||||||||||||||||||
Sbjct  GATGTGGGTGGAAAGGAACTGCGTGGACGGGATGCGGGTGCAGGCAAGTTTGAGCACAGG


Query  TGGAAGCGAGCGAAACGCAGAGCCTTCCAGCAAAACGTCCTCGGCTGAGCGCTAGTCC
       ||||||||||||||||||||||||||||||||||||||||||||||||||||||||||
Sbjct  TGGAAGCGAGCGAAACGCAGAGCCTTCCAGCAAAACGTCCTCGGCTGAGCGCTAGTCC
```

Appendix VIII

1 kb piece – *UV90* with R2 primer

Target	Score (Bits)	Expect	Alignment Length	Identities	Positives

▼ N. crassa OR74A (NC12): Supercontig 6: 2654898-2655047 +
Score = 284.512 (142), Expect=0.0
Identities=147/150 (98%), Positives=147/150 (98%)

```
Query CAGGTATTCGACCACGTACCTGGTATCCGCAGGGGCATGGTCTAAAGTTACGATCAGAGA
      ||||||||||||||||||||||||||||||||||||||||||||||||||||||||||||
Sbjct CAGGTATTCGACCACGTACCTGGTATCCGCAGGGGCATGGTCTAAAGTTACGATCAGAGA

Query GATCAAACTCCTCGATACAGAGGGGGCTATAGTATACTAGTTAGTCTGATGTGTTCTTGT
      ||||||||||||||||||||||||||||||||||||||||||||||||||||||||||||
Sbjct GATCAAACTCCTCGATACAGAGGGGGCTATAGTATACTAGTTAGTCTGATGTGTTCTTGT

Query GGACGGCCGAKGGCRTTWTGACAGGGGGTC
      ||||||||| ||| || |||||||||||
Sbjct GGACGGCCGAGGGCGTTGTGACAGGGGGTC
```

▼ N. crassa OR74A (NC12): Supercontig 6: 2654808-2654871 +
Score = 128.499 (64), Expect=1.98258E-29
Identities=64/64 (100%), Positives=64/64 (100%)

```
Query AACAGAACTGGCATATCTGGGGTGGGGCGGCGGCGTTAGCGCTCAGGTTGAGCCAAAAGA
      ||||||||||||||||||||||||||||||||||||||||||||||||||||||||||||
Sbjct AACAGAACTGGCATATCTGGGGTGGGGCGGCGGCGTTAGCGCTCAGGTTGAGCCAAAAGA

Query AAAA
      ||||
Sbjct AAAA
```

224

1 kb piece – *UV90* with UV90AFor primer

Target	Score (Bits)	Expect	Alignment Length	Identities	Positives

▼ N. crassa OR74A (NC12): Supercontig 6: 2655323-2655646 -
Score = 587.444 (293), Expect=0.0
Identities=312/324 (96%), Positives=312/324 (96%)

```
Query  CACTTGTYGGTAAGGTAGGTATTAAAAGGGCCGTAAAMTAGSGGCGCGAAAAWTGGTCTA
       |||||||  |||||||||||||||||||||||||||||| ||| |||||||||| |||||||
Sbjct  CACTTGTCGGTAAGGTAGGTATTAAAAGGGCCGTAAACTAGCGGCGCGAAAATTGGTCTA

Query  TGGTAGAAAGAAGCAAAGGAGGACCTGATAATAACGCCCGTGGTAATGTAAGATACAGAG
       ||||||||||||||||||||||||||||||||||||||||||||||||||||||||||||||
Sbjct  TGGTAGAAAGAAGCAAAGGAGGACCTGATAATAACGCCCGTGGTAATGTAAGATACAGAG

Query  AATAGAGGGTCGGTGCCTCTTCNNNNNNNNGAGGGGTTGTGCTYGTGTCAACAAATGGGGG
       ||||||||||||||||||||||          |||||||||||| |||||||||||||||||
Sbjct  AATAGAGGGTCGGTGCCTCTTCTTTTTTTTGAGGGGTTGTGCTCGTGTCAACAAATGGGGG

Query  ATTATTAGAGAGAACAAAGTTGGCCGGATGTGGGTGGAAAGGAACTGCGTGGACGGGATG
       ||||||||||||||||||||||||||||||||||||||||||||||||||||||||||||||
Sbjct  ATTATTAGAGAGAACAAAGTTGGCCGGATGTGGGTGGAAAGGAACTGCGTGGACGGGATG

Query  CGGGTGCAGGCAAGTTTGAGCACAGGTGGAAGCGAGCGAAACGCAGAGCCTTCCAGCAAA
       ||||||||||||||||||||||||||||||||||||||||||||||||||||||||||||||
Sbjct  CGGGTGCAGGCAAGTTTGAGCACAGGTGGAAGCGAGCGAAACGCAGAGCCTTCCAGCAAA

Query  ACGTCCTCGGCTGAGCGCTAGTCC
       ||||||||||||||||||||||||
Sbjct  ACGTCCTCGGCTGAGCGCTAGTCC
```

Appendix IX

Confidence Key
High(9) ▮▮▮▮▮▮▮▮▮ Low (0)
? Disordered
ᴧᴧ Alpha helix
➡ Beta strand

(http://www.sbg.bio.ic.ac.uk/phyre2/html/page.cgi?id=index)

Figure A3. PHYRE2 secondary structure and disorder prediction for protein product of

Neurospora crassa gene NCU05950.

Confidence Key = represents the probability of NCU05950 protein product being

homologous to the template.

Appendix IX

Detailed template
Information

#	Template	Alignment Coverage	3D Model	Confidence	% I.d.	Template Information
1	d2gtsa1	Alignment			20	Fold:Ferritin-like Superfamily:HP0062-like Family:HP0062-like
2	c2kmB_	Alignment			21	PDB header:toxin Chain: B: PDB Molecule:putative membrane antigen; PDBTitle: bipd - an invasion prtein associated with the type-III2 secretion system of burkholderia pseudomallei.
3	c4kixB_	Alignment			24	PDB header:protein binding Chain: B: PDB Molecule:slr1964 protein; PDBTitle: structure of the fluorescence recovery protein from synechocystis sp2 pcc 6803
4	c4diaA_	Alignment				PDB header:lyase Chain: A: PDB Molecule:photolyase; PDBTitle: crystal structure of a prokaryotic (6-4) photolyase phrb from2 agrobacterium tumefaciens with an fe-s cluster and a 6,7- dimethyl-8-3 ribityllumazine antenna chromophore at 1.45a resolution
5	d1xp8a_	Alignment			29	Fold:Thioredoxin fold Superfamily:Thioredoxin-like Family:YuzD-like

(http://www.sbg.bio.ic.ac.uk/phyre2/html/page.cgi?id=index)

Figure A4. PHYRE2 top 5 protein templates matching *Neurospora crassa* gene

NCU05950 protein product.

Confidence (%) = represents the probability of NCU05950 protein product being

homologous to the template.

Appendix IX

Jpred3 protein sequence alignments with *Neurospora crassa* NCU05950 protein product

(http://www.compbio.dundee.ac.uk/www-jpred/index.html)

```
                       1          10         20         30         40
QUERY                  M G N F C S T C F G G R R S D D Y D E E D E A Q H L F D E N N M H Y G S F D Q Q
UniRef90_Q2GRJ7        M G N   C S S C L G N R R R D E Y D E E E D A R H L F D D N N L N Y N S F D Q Q
UniRef90_UPI000023E1E1     G A C A S C L G R A D G N S Y D E E E E S R L L Y D E N G M Q Y G S F G D Q
UniRef90_B2AQ67        M G N   C A S C L G S R R R D D Y D E D D E A Q H L F D D N N L Q Y G S F E Q Q
UniRef90_A7EA02        M G N   C S S C L G L D R D R D S S D E G E D Q R L L D A H P H H Y G S F D Q N
UniRef90_A4RIX4            G V C A S C L G N N R S E Q Y E E                                       Q
UniRef90_B6GXY1                C R R A Q L S D L S S V K P E S S R L L E E D G Y G Y G A L N H A
UniRef90_A2QWY4        G I C A S C L G R N R Q E P H D P H P E S S R L L D E D G Y G Y G A L H Q S
UniRef90_Q5BCG8        G V C S S C L G G G R R D S T D   P E S S R L L E D D G Y S Y G A L N H N
UniRef90_A1DMW4        G V C A S C L G L N R R E S H D A E   S S R L L D D D G Y G Y G A L N H A
UniRef90_Q0CI11        G V C A S C L G H A R R D S P E P E S S R L L E E Y Q S G Y G Y G A L N H A
UniRef90_B8NPB4        G V C A S C L G V G R R D S Q D S E S S Q R L L I Y Q P G Y G Y G A L N N S
UniRef90_B6Q423        G A C Q S C L G I R R R E D H E S E   H A R L I D D D L Y P G G Y G Y G S I
UniRef90_C0S031        G V C A S C L G R G G R D S H D S E   S S R L L D D E L Y Q S G Y G Y G S
UniRef90_A6RA59        G I C A S C L G R S A R D S H D S E S S R L L D D Y Q S S Y G Y G A V G S V
UniRef90_B2W9B9        G I C S S C L G G R A S E     D Q S D T S H L L G D Q Y Q P N Y G T S S S N
UniRef90_Q0U774                            Q S D T S H L L H D P Y Q P N Y G T N N G S

lupas_21
lupas_14
lupas_28
jnet
conf                   9 8 6 2 4 7 0 0 0 1 5 7 8 8 8 7 7 6 4 3 0 0 0 0 0 0 1 4 6 7 7 7 7 7 7 7 6 6 6
sol25                     B B B B B B B B B                       B   B B           B B B B
sol5                        B B   B B
sol0                        B
jhmm
jpssm
```

```
                       50         60         70         80
QUERY                  H M M N Q E D P Q E T E R E I A A L Q G V V E R T S N N M V D I Y D M V P H D K
UniRef90_Q2GRJ7        H M M G Q E D P Q E V Q R E L E A L Q R V V A R T S D A M V D I Y E I V P Q D K
UniRef90_UPI000023E1E1 A L N G E N D T L E A Q R E N E A L Q R V I A K T S D N M V D I F D I A P Q E N
UniRef90_B2AQ67        Q M M G P E D P Q E V Q R E L E A L Q R V V A R T S D N M V D I Y D I A P S N H
UniRef90_A7EA02        S N L I Q A D P L E V Q R E T E A L Q K V V A Q T S N H L V D I F A L V P P N A
UniRef90_A4RIX4        Q L T G Q E D P L E T Q R E L E A L Q R V V A R T S D N M V D I F E I T P Q D
UniRef90_B6GXY1        H Q A S Q P D S E Y V R R E R E A L E S I C Q R T S D S V I D I W S I Q P Q P H
UniRef90_A2QWY4        T Q G N H P D P S Y L K R E R E A L E A I C Q R T S D S V I D I W S L Q P Q P H
UniRef90_Q5BCG8        Q Q A N Q P D P G Y V R R E R E A L E A I C Q R T S D S V I D I W S L Q P Q P H
UniRef90_A1DMW4        N Q I N N P D P E N I K R E R E A L E A I C Q R T S E S V I D I W S L Q P Q P H
UniRef90_Q0CI11        S Q V N Q P D S G Y V R R E R E A L E A I C Q R T S E S V I D I W S L Q P Q P H
UniRef90_B8NPB4        T Q G N H P D T G Y L K R E R E A L E A I C Q R T S D S V I D I W S L Q P Q P H
UniRef90_B6Q423        N N A N Q Q D P E D L K R E R E A L E A I C Q R A S D T V I D I W A L Q P Q P N
UniRef90_C0S031        V G S V Q R D P E Y L K R E R E A L E A I C Q R T S D S V V D I W A L Q P H Q S
UniRef90_A6RA59        H R Q G   P D P E Y L K Q E R E V L E A I C Q R T S D S V I D I W A L Q S S Q L
UniRef90_B2W9B9        H N V P Q P D P E E L R R Q R E N L E R I C A E T N E Q L I P       V S Q P S
UniRef90_Q0U774        H N A P Q P D P E E L R R Q R E T L L E R I C A E T S E Q L L P V A T I P P E V S

lupas_21
lupas_14
lupas_28
jnet
conf                   6 7 7 7 7 6 5 0 7 9 9 9 9 9 9 9 9 9 9 9 9 9 9 9 8 6 0 5 8 7 1 0 0 8 8 6 1 5 7 7 7 7
sol25                               B       B             B B       B B       B       B B   B B   B   B
sol5                                                           B               B
sol0                                                               B
jhmm
jpssm
```
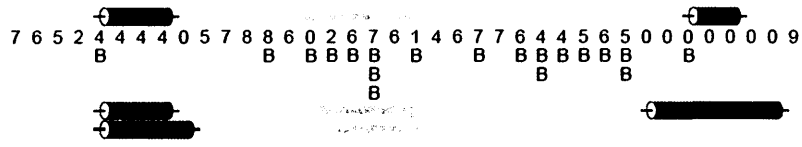
228

Appendix IX

```
                                   90             100            110            120
QUERY                    P M Q D A P A P Y G F A N Q R Y N A L L S K L S T H D D M A A V A R V D W G T P
UniRef90_Q2GRJ7          A A Q T A P G P Y V Y V G Q R Y Q T L L S K L S S H D D L P S V A R V D W G T P
UniRef90_UPI000023E1E1   G N R G T T T P F A Y A G Q R Y Q H L V A K L S N Q G D N A P V S K V D W L P
UniRef90_B2AQ67          A A P D S P E M P Y A Y P A R Y H N L L S K L S S H D D L A A V A R V D W G T P
UniRef90_A7EA02          D L A           P V T M Y N L R Y Q E V L A K M P S Q D K S S N T K P T D G W L S
UniRef90_A4RIX4            T R A A P K Q Y D V E G E R Y Q S L L S K L S E D A S S T A S T K V D W V P W
UniRef90_B6GXY1          P Q A T L H T P T S V P S Q R T D T T T P A V S T H R T S P P S R P T S G
UniRef90_A2QWY4          L Q P R A T L
UniRef90_Q5BCG8          L Q P Q A T L
UniRef90_A1DMW4          L Q P R A T L
UniRef90_Q0CI11          L Q P R A T L R G S V S P S           T S R P E S H D G A P
UniRef90_B8NPB4          L Q P R A T G P V S P A S S R
UniRef90_B6Q423          F Q P R A T L P
UniRef90_C0S031          G
UniRef90_A6RA59          P
UniRef90_B2W9B9          A L P E V S E Q      P K N D E Y A H L
UniRef90_Q0U774          E Q P T N D A E Y A L F N E R F A T L


lupas_21
lupas_14
lupas_28
jnet
conf    7 7 7 7 7 7 7 7 7 7 7 7 6 0 1 6 7 7 7 6 3 2 6 7 7 7 7 7 7 7 7 7 7 7 7 7 7 7 7
sol25           B       B   B           B       B B       B                 B       B     B     B
sol5                                              B B       B
sol0
jhmm
jpssm


                                  130            140            150
QUERY                    E D D S M E M L R K A S L P T I P I K A E G G E A L V G N F T D A A A A M R
UniRef90_Q2GRJ7          D D D T I E M Q Q G V M P I K V E G G D S L V G N F A D A A A A M
UniRef90_UPI000023E1E1   E D E T I E M Q K N G P A S I K T I E S D D G P L V G T F A D A A A A M Q
UniRef90_B2AQ67          D D D T I E M Q Q N T A I P I K L E G A E G P L V G N F A D A A A A M R
UniRef90_A7EA02          D D E D V E E M K K Y K P V K S E D V G P L L G G F A D A E S A M E
UniRef90_A4RIX4          D E D N I E M H N G A I V P P L K I E A A E P F V G T F
UniRef90_B6GXY1
UniRef90_A2QWY4
UniRef90_Q5BCG8
UniRef90_A1DMW4
UniRef90_Q0CI11
UniRef90_B8NPB4
UniRef90_B6Q423
UniRef90_C0S031
UniRef90_A6RA59
UniRef90_B2W9B9
UniRef90_Q0U774


lupas_21
lupas_14
lupas_28
jnet
conf    7 6 5 2 4 4 4 4 0 5 7 8 8 6 0 2 6 7 6 1 4 6 7 7 6 4 4 5 6 5 0 0 0 0 0 0 0 0 9
sol25         B             B   B B B B     B       B B B B B B     B
sol5                                  B
sol0                                  B
jhmm
jpssm
```
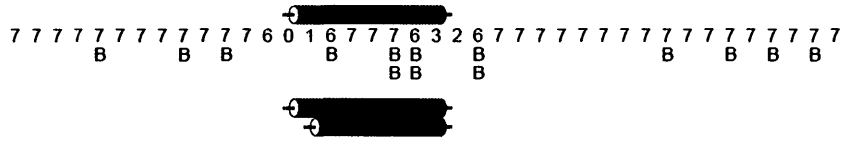
229

Appendix X

<u>Chi-square tests:</u>

χ^2 = (observed − expected)^2/expected

Degrees of freedom (df) = (# of classes − 1)

p **values obtained from Microsoft Excel, 2010**

First group of progeny: *csp-1; bd; UV90* **(sg #227) x Mauriceville wild type (Table 8):**

	UV90	*UV+*
Observed: 44 total	25	14
Expected:	22	22
χ^2	0.409	2.9

Total: χ^2 = 3.318; df = 1; *p* = 0.0685

Second group of progeny: *csp-1; bd; UV90* **(sg #227) x Mauriceville wild type (Table 14):**

	bd; UV90	*bd; UV+*	*bd+; UV90*	*bd+; UV+*
Observed: 100 total	21	19	25	21
Expected:	25	25	25	25
χ^2	0.64	1.44	0	0.64

Total: χ^2 = 2.72; df = 3; *p* = 0.4368

Progeny from cross: FGSC Knockout #18029 x *csp-1; chol-1 bd; UV90; frq^{10}* **(Table 24):**

	bd; UV+	*bd; UV90*	*bd; frq^{10}*	*bd; UV90; frq^{10}*
Observed: 55 total	18	8	16	7
Expected:	13.75	13.75	13.75	13.75
χ^2	1.31	2.40	0.368	3.31

Total: χ^2 = 7.39; df = 3; *p* = 0.0601